EC Nuclear Fission Safety Programme, 1995-99

Contract No. F14P-CT95-0035

Final Report

Radioecological Assessment of the Consequences of Contamination of Arctic Waters: Modelling the Key Processes Controlling Radionuclide Behaviour Under Extreme Conditions (ARMARA)

Department of Experimental Physics
University College Dublin

December 1999

EC Nuclear Fission Safety Programme, 1995–99
Contract No. F14P–CT95–0035

Radioecological Assessment of the Consequences of Contamination of Arctic Waters: Modelling the Key Processes Controlling Radionuclide Behaviour Under Extreme Conditions (ARMARA)

Prof. P.I. Mitchell
University College Dublin (UCD), Ireland

Prof. E. Holm
University of Lund (LUND), Sweden

Dr. H. Dahlgaard
Risø National Laboratory (RISØ), Denmark

Dr. D. Boust
Institut de Protection et de Sûreté Nucléaire (IPSN), France

Dr. K.S. Leonard
The Centre for Environment, Fisheries and Aquaculture Science (CEFAS), United Kingdom

Dr. C. Papucci
Ente per le Nuove Tecnologie, l'Energia e l'Ambiente (ENEA), Italy

Prof. B. Salbu
Agricultural University of Norway (AUN)

Dr. G. Christensen
Institute for Energy Technology (IFE), Norway

Dr. P. Strand
Nowegian Radiation Protection Authority (NRPA), Norway

Dr. J.A. Sánchez-Cabeza
Universitat Autònoma de Barcelona (UAB), Spain

Dr. K. Rissanen
Finnish Centre for Radiation and Nuclear Safety (STUK), Finland

Dr. D. Pollard
Radiological Protection Institute of Ireland (RPII), Ireland

Dr. C. Gascó
Centro de Investigaciones Energéticas Medioambientales y Tecnológicas (CIEMAT), Spain

Introduction – Objectives of the ARMARA project

The European Commission's ARMARA project was initiated in late-1995 as a co-ordinated effort to address the issue of radioactive contamination of the Arctic environment in response to revelations about the disposal of large quantities of radioactive waste in the Barents and Kara Seas by the former Soviet Union. The project had a duration of 3½ years and was carried out under the EC's Nuclear Fission Safety research and training initiative (Fourth Framework Programme, 1995–99). The collaboration comprised ten institutions from eight countries within the European Union (Denmark, Finland, France, Ireland, Italy, Spain, Sweden, United Kingdom) and a further three institutions from Norway.

The overall goal of the ARMARA project was to assess the potential radiological consequences of anthropogenic radionuclide contamination of the Arctic marine environment. To this end, model-directed sampling campaigns were undertaken in the Arctic, and extensive data on radionuclide contamination and transfer mechanisms were collected, interpreted and used to refine and validate an advanced compartmental model of radionuclide dispersal, with a view to (a) predicting likely short- and long-term doses to man, and (b) providing clear scientific guidelines for policy and decision makers.

In order to facilitate the achievement of these objectives, the project was divided into ten distinct work-packages, each of them sub-divided into a set of relevant research activities. The work packages included • an assessment of the scope of the Arctic database, including models, • the design of model-directed sampling campaigns and experiments, • an evaluation of the short-term reactivity of radionuclides upon their input into the Arctic, • an examination of radionuclide reactivity within the Arctic water column (shelf seas and deep ocean), • an examination of radionuclide reactivity at the freshwater/sea water interface (estuaries), • an investigation of the key processes controlling reactivity at the sediment/sea water interface (post-depositional processes), • a quantification of fluxes, mixing layer processes and advective transport, • an evaluation of transfer processes to living species, including man, • the refinement and validation of the RISØ-NRPA compartmental model for the north-east Atlantic and the Arctic, and prediction of the likely consequences of Arctic contamination, and • the publication and dissemination of results, preparation of tec-docs, interim and final reports, and archiving of all data.

Here, we present our final report on the scientific progress made in each of these work-packages, followed by a summary of the main achievements and deliverables. This is followed by a set of conclusions and recommendations. Finally, a listing of the publications that have issued as a result of the project is also given.

1. Assessment of the scope of the Arctic database, including models

1.1. Evaluation of existing data on radionuclide concentrations (including temporal evolution) in the Arctic and transfer mechanisms in extreme environments

An extensive bibliography on Arctic pollution and radioecology has been assembled by the collaboration covering the period up to 1999. The bibliography includes papers presented at conferences on pollution and radioactivity in the Arctic held in Anchorage (May 1993), Kirkenes (August 1993), Oslo (August 1995) and Tromsø (June 1997), as well as relevant papers presented at a two–part symposium on *Radionuclides in the Oceans* held in Cherbourg–Octeville (RADOC–1, October 1996) and Norwich (RADOC–2, April 1997), and at an international symposium *on Marine Pollution* organised by the IAEA and held in Monaco (October 1998). This bibliography has been extended to include the substantial information on radionuclide concentrations (especially ^{137}Cs and ^{90}Sr) available from the AMAP database (AMAP, 1998), as well as data gathered from the Russian–Swedish Tundra '94 Expedition, the Canadian 1994 Arctic Ocean Section and Danish monitoring around Greenland. In addition, bibliographies of key publications on Arctic oceanography, hydrodynamical fluxes, Arctic trophic chains, biological processes and the role of benthic fauna in actinide biokinetics and actinide transfer through the food chain have been compiled by various partners in the collaboration as part of their contribution to this work-package.

The main conclusion to be extracted from all the available data is that present radionuclide concentrations in the Arctic Seas are dominated by fallout from nuclear weapons testing, riverine discharges and land run-off of radionuclides originating from global fallout and releases from nuclear installations located along the drainage areas of the large Siberian rivers (Ob, Yenisey), marine transport of radionuclides discharged from European reprocessing plants and run-off from land areas contaminated by fallout from the Chernobyl accident (there is now a net export of ^{137}Cs from the Baltic Sea). For those nuclides for which enough temporal and spatial measurement exist (^{137}Cs, ^{90}Sr), time-trends and present distributions reflect the evolution of the above-mentioned source-terms when coupled to water circulation patterns and transport processes. To illustrate, we consider the case of ^{137}Cs, for which a considerable body of data has been accumulated over the years. The spatial distribution of ^{137}Cs concentrations in surface Arctic waters for 1994, as determined from a number of separate studies (Ellis *et al.*, 1995; Joseffson *et al.*, 1995; Persson *et al.*, 1995; Aarkrog *et al.*, 1996), are shown in Figure 1. The highest ^{137}Cs concentrations were measured in the vicinity of the North Pole, over the Lomonosov Ridge. A slight increase in the ^{137}Cs levels was also observed in the Laptev Sea compared with the Kara and Barents Seas. When combined with the results of similar studies carried out in the early 1980s, which showed the highest concentrations in the Barents and Kara Sea, this is consistent with the transport pattern of ^{137}Cs derived from the reprocessing plant at Sellafield (Cumbria, UK) and indicates that maximum releases from this plant in the 1970s are now reflected in the vicinity of the North Pole and the Laptev Sea. East of the outlets of the large Siberian rivers (Ob, Yenisey and Lena), ^{137}Cs concentrations were found to decrease, reflecting dilution of ^{137}Cs derived from riverine sources. This is further confirmed by the increase in ^{90}Sr concentrations and ^{90}Sr/^{137}Cs ratios observed in the low-salinity waters of the north-eastern Kara Sea. In the vicinity of Greenland, the highest ^{137}Cs levels were found along the east coast. The lowest measured ^{137}Cs concentrations were found in the East Siberian Sea and over the south-eastern area of the Makarov Basin.

The influence of Sellafield on ^{137}Cs concentrations in Arctic waters is further evidenced by the temporal evolution of ^{137}Cs concentrations in the Barents Sea (Figure 2), which clearly reflect the pattern of the ^{137}Cs releases from Sellafield, allowing for an advection transport lag time of 4–5 years.

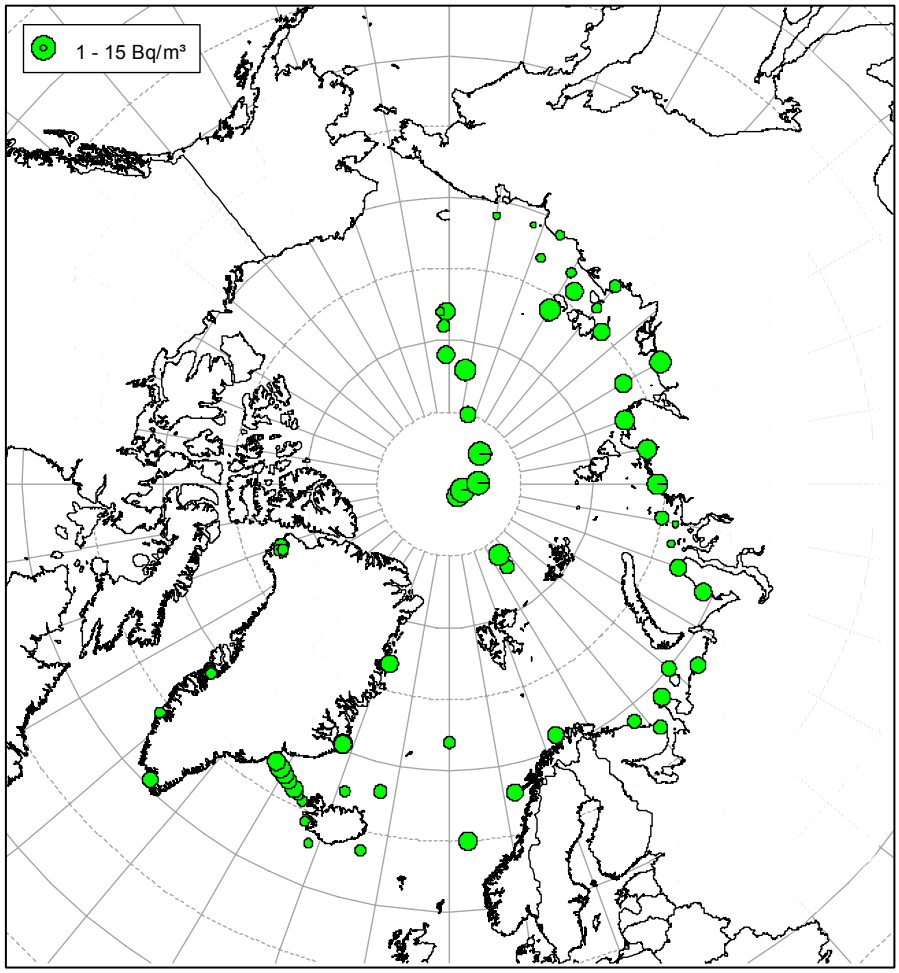

Figure 1. ^{137}Cs concentrations in Arctic surface waters in 1994 (*from:* Strand et al. 1996)

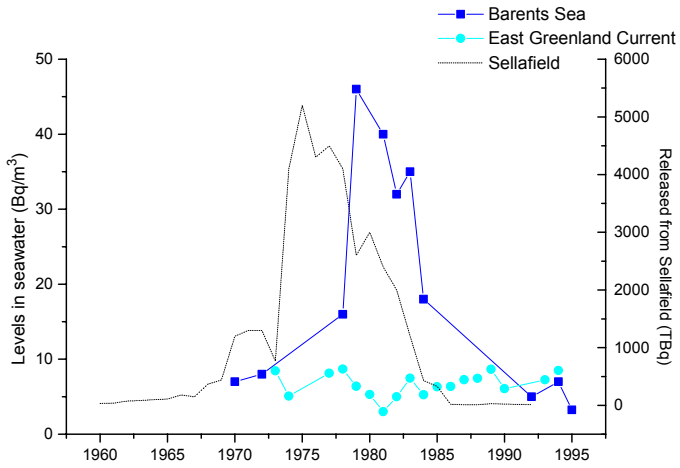

Figure 2. Temporal evolution of ^{137}Cs concentrations in surface waters in the Barents Sea (*from:* Strand et al. 1996)

Also shown in Figure 2 are the ^{137}Cs concentrations in surface waters of the East Greenland Current. Although up to 1995 concentrations appeared to be rather constant, more recent studies have shown increased concentrations in waters of polar origin. These can be attributed to the transport back into the Atlantic of waters labelled with Sellafield-sourced ^{137}Cs after circulation in the Arctic interior.

In addition to the above mentioned sources, which have led to wide-spread contamination of Arctic waters, localised sources such as underwater weapons tests, accidents involving nuclear weapons and dumping of solid and liquid radioactive wastes have led to local perturbations in distributions and levels of radionuclides at locations such as Thule (Greenland), the Abrosimov and Stepovogo fjords at Novaya Zemlya, and Kola Bay.

1.2. Identification of knowledge gaps in the Arctic database

In spite of the increasing database of radionuclide concentrations in the Arctic Seas, careful scrutiny of the published literature at the commencement of the project identified a number of significant gaps in knowledge and understanding of Arctic radioecology. Gaps in the temporal and spatial distributions of radionuclides other than ^{137}Cs and ^{90}Sr were particularly notable, with few data available on, for example, transuranium nuclides or ^{99}Tc concentrations. Even for ^{137}Cs and ^{90}Sr, concentration levels in biota were quite scarce and time-series data were limited to a few studies carried out in Greenland. Further, few if any studies had been published on the basic mechanisms governing the physico-chemical speciation, mixing, advective transport, residence time, biological uptake and sedimentation processes of the more important long-lived radionuclides within this unique and sensitive ecosphere. As an understanding of these processes is considered an essential pre-requisite to the development of a process-oriented model, the actions of the collaboration were mainly directed to the remediation of this information deficit.

Other important information gaps related to the role of river/sea ice in the transport of radionuclides and the significance of the large Siberian rivers as a source of radionuclides.

Regarding the transfer of radionuclides from contaminated water and sediments into the food chain, it quickly emerged, following inter-group consultation and feedback particularly from the modelling groups, that *in situ* data relevant to uptake of radionuclides and transfer into the food chain were of more immediate concern. Focus was given to six bio-kinetic parameters: sea water–animal concentration factors; sediment–animal concentration ratios; radionuclide assimilation efficiencies; radionuclide tissue distribution; radionuclide elimination and chemical and physical speciation.

1.3. Examination of the conceptual basis of a compartmental model for the Arctic

The conceptual basis of the RISØ–NRPA compartmental model, used to simulate the dispersion and transfer of radionuclides in the Arctic marine environment, was revised at the outset of the project and some significant refinements incorporated to ensure a better representation of the real system. The original model, covering the Arctic Ocean and the north-east Atlantic (Nielsen *et al.*, 1997), had been tested and validated within the framework of other international projects (IASAP and EC/DGXI Kara Sea Project) and its predictions compared with those of other advanced models. These comparisons showed that the model included all the features considered essential for the reliable estimation of future doses to man at both individual and population level. The main drawback in the application of the model to the assessment of doses arising from potential discharges of radioactivity from dumped nuclear waste in the Kara Sea was related to the model's coarse spatial resolution and the effects that this could have on the predicted doses to critical groups. Although comparison of the results obtained using this compartmental model with those derived from a high-resolution hydrodynamic model of the Kara Sea showed that estimated doses were generally in good agreement, elements of local/regional modelling were incorporated into the original model in order to improve its

predictive capability and evaluate the contribution of specific locations (e.g., rivers, estuaries) to estimated doses (Iosjpe *et al.*, 1997).

In addition, the general assumption for box modelling about instantaneous mixing in all boxes (which leads in practical calculations to instantaneous mixing in the whole ocean space) was altered to include the dispersion of radionuclides over time by defining a 'time lag' between radionuclide releases and their incorporation into a given compartment. This gives a better and more realistic/physical approach compared to traditional box modelling, as radionuclides do not spread instantaneously through all the boxes (Iosjpe *et al.*, 1997). Calculations of radionuclide dispersion comparing the new approach with traditional box modelling identified differences in radionuclide concentrations of up to an order of magnitude over the short time scale.

The model was further improved by describing the sediment compartment as a two-phase system (sub-model) with the incorporation of reversible and irreversible radionuclide interactions with the sediment phase. This refinement enables the dynamics of radionuclide interactions in sediment to be accounted for within the transport model proper. Relevant data for tuning this sub-model were derived and are presented in WP6.

2. Design of model-directed campaigns and experiments, incl. QA/QC

A number of research expeditions to the Arctic were undertaken by the collaboration in the course of the project. Such expeditions are seen as a key element in the overall success of the ARMARA initiative. Each of these operations required the most detailed advanced planning on both the scientific and logistic fronts, and involved extensive environmental sampling and *in situ* chemical processing. In each case, the sampling campaigns were designed to satisfy the most pressing requirements of the modellers, i.e., to fill gaps in the Arctic database such as the absence of concentration values for specific boxes and compartments of the model, or uncertainties in the values of key parameters such as sediment-water distribution coefficients, sedimentation rates or transfer coefficients.

In particular, eight major sampling campaigns to the Central Arctic Ocean and its surrounding seas took place during the duration of the project. The areas covered by these expeditions included the Kara Sea continental break (crossing the St Anna and Voronin Troughs), the Nansen, Amundsen and Makarov Basins, the Lomonosov Ridge, the continental slopes of the Laptev and the East Siberian Seas, the continental shelf surrounding Spitsbergen and the western coast of Greenland (including the Thule accident area). The expeditions to the Central Arctic Ocean aboard the *F.S. Polarstern* (Germany) and *I.B. Oden* (Sweden) were part of the Arctic '96 Expedition, jointly organised by the *Alfred-Wegener Institute for Polar and Marine Research* (Bremerhaven) and the *Swedish Polar Research Secretariat* (Stockholm). The four expeditions to the western Spitsbergen continental shelf and fjords were organised by the *Geophysical Institute of the University of Bergen* and carried out aboard the *R.V. Håkon Mosby*. The Thule '97 expedition aboard the Greenland Home Rule Fisheries Investigation Vessel *Adolf Jensen* was financed by Danish funds under the Arctic Monitoring and Assessment Project (AMAP), and provided an opportunity to bring a team from five of the ARMARA participating laboratories right into the Bylot Sound area, where a US B-52 bomber carrying four plutonium-bearing weapons crashed on sea-ice in January 1968.

In the course of these expeditions, particular emphasis was placed on the determination of high-resolution vertical profiles of radionuclide concentrations in the water column and the partition of radionuclides between the dissolved and solid phases. Specifically, the physico-chemical speciation of plutonium and americium was examined with a view to establish the kinetics of transuranium (and other particle-reactive radionuclides) within the water column and how these are influenced by their chemical speciation and association with suspended particulate and colloidal matter. Scavenging rates and residence times of particle-reactive radionuclides were also investigated in the water column of the Svalbard continental shelf using ^{238}U – ^{234}Th

parent-daughter disequilibrium. In addition, a large number of large-volume surface and sub-surface water samples were also collected throughout the Central Arctic and its surrounding seas for ^{90}Sr, ^{129}I, ^{137}Cs, ^{226}Ra, ^{228}Ra, ^{238}Pu, ^{239}Pu, ^{240}Pu and ^{241}Am analysis in order to investigate the advection of radionuclides by shelf water and ice into the Arctic interior along the Lomonosov Ridge (with the Transpolar Drift) towards the Fram Strait. Work was completed by the collection of a considerable number of sediment cores for the determination of inventories, sedimentation rates and mixing processes. Sediment studies were given particularly emphasis during the Thule '97 expedition, and were complemented by the analysis of significant quantities of benthic fauna and a limited number of phytoplankton and zooplankton samples for transfer coefficient determination. Detailed accounts of the routes taken and the sampling programmes during these expeditions can be found elsewhere.

The above expeditions were augmented throughout the duration of the project by a number of successful joint campaigns in non-Arctic regions. These included:

- INTERPRO 6/96, *R.V. Thalia*, Seine Estuary/River, June 1996, speciation and desorption studies;
- BELTRA 8/96, *R.V. Lough Beltra*, western Irish Sea, August 1996, studies of behaviour in the water column including phyto- and zoo-plankton, and the sediment compartment with emphasis on deep cores;
- CIROLANA 12/96, *R.V. Cirolana*, Irish Sea, December 1996, water column and sediment/benthos;
- IRMA 12/96, western approaches to the English Channel, water and sediment;
- PO 3/97, Po River/Estuary, sedimentation processes and stability of sedimentary deposits;
- MARINA 4/97, *R.V. Thalia*, Seine Estuary/River, April 1997, studies on colloidal association of natural and anthropogenic radionuclides at the fresh water/sea water interface;
- ATMARA 7/98, R.V. *Surôit*, North Atlantic, water column and sediment cores.
- CELTIC VOYAGER 9/97, *R.V. Celtic Voyager*, western Irish Sea, water columns and sediment cores.

Additional information was extracted from the analysis of samples gathered by members of the ARMARA collaboration in the course of major sampling campaigns carried out before the commencement of the project, covering important zones such as the Norwegian, Greenland, Petshora, White, Kara, Barents and Laptev Seas, the Kola Peninsula, the Ob and Yenisey estuaries, Novaya Zemlya and the Siberian shelf. Analysis of these samples proved vital to the completion of the project's objectives, as access to sensitive Russian Arctic zones was denied to the collaboration for the duration of the project. As an example, the location of sediment and biota samples collected by members of the ARMARA collaboration (in collaboration with the Murmansk Marine Biological Institute) in the period 1993–96 are shown in Figures 3 and 4.

Regarding QA/QC, the Group has carried out a number of initiatives, principal amongst them being the decision by all the contractors/associated contractors to participate in the analysis of a very large sample of sea water from the North Sea for intercomparison purposes. Drs Hartmut Nies and Jurgen Herrmann (Hamburg) undertook the collection and distribution of this intercomparison sample, for which we are grateful. Each laboratory received 600 litres of a surface sea water sample collected from aboard the *R.V. Gauss* on the 3rd of November 1996 at 55°23.0′N, 04°30.0′E. The well-mixed character of the North Sea at the season of sampling, together with precautions taken during collection ensured the homogeneity of the sample. The radionuclides analysed included ^{90}Sr, ^{99}Tc, ^{137}Cs, ^{238}Pu, ^{239,240}Pu and ^{241}Am. The means submitted by the participants were tested for outliers using the Dixon test. Median (and mean) values were then calculated for all of the results passing the test. These values were considered to be the most reliable estimates of the unknown true values. Confidence intervals were taken from a non-parametric sample population and represent a two-sided interval at a significance level of 0.05. To illustrate, the results for ^{137}Cs, ^{239,240}Pu and ^{238}Pu are shown in Figure 5.

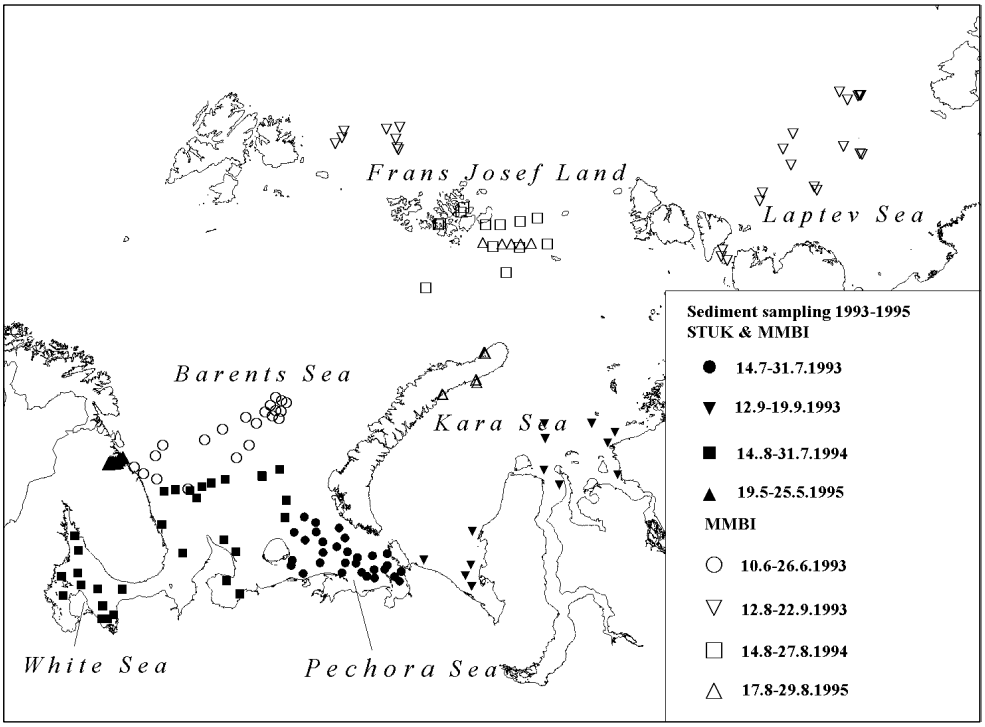

Figure 3. Location of sediment samples collected in Russian waters over the period 1993–95
(Black symbols represent joint STUK–MMBI sampling; open symbols sampling by MMBI)

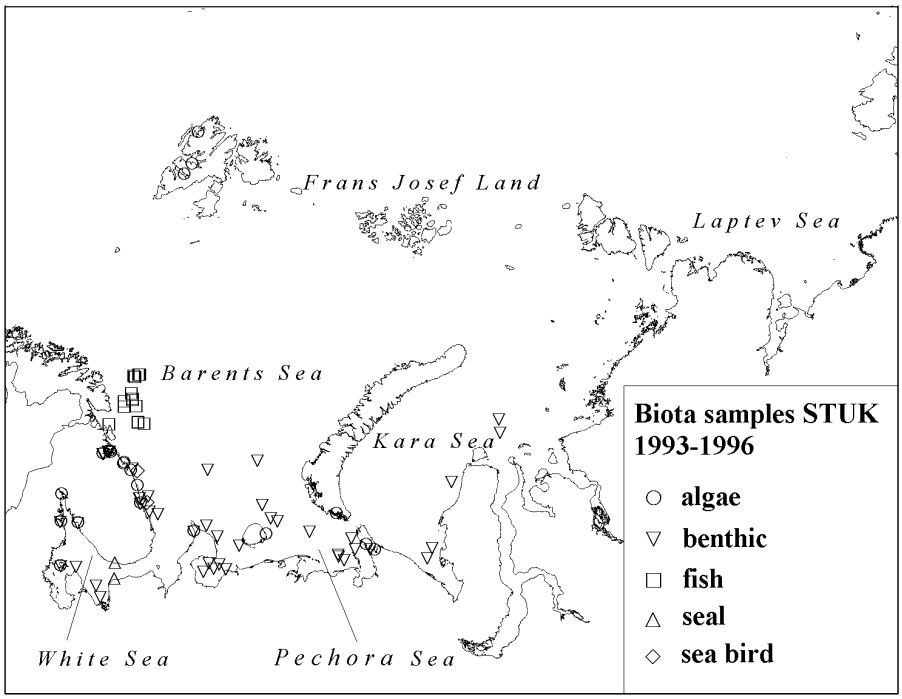

Figure 4. Location of biota (algae, benthic organisms, fish, seals, sea birds) samples collected in Russian waters over the period 1993–95

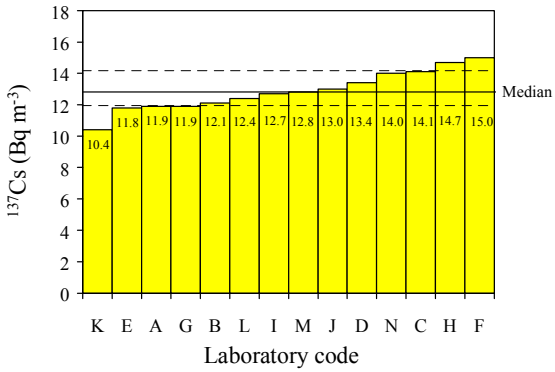

Code	^{137}Cs (Bq m^{-3})
K	10.4 ± 1.0
E	11.8 ± 0.5
A	11.9 ± 0.5
G	11.9 ± 0.6
B	12.1 ± 0.9
L	12.4 ± 0.3
I	12.7 ± 0.8
M	12.8 ± 1.1
J	13.0 ± 0.4
D	13.4 ± 0.5
N	14 ± 2
C	14.1 ± 1.4
H	14.7 ± 0.7
F	15.0 ± 0.6

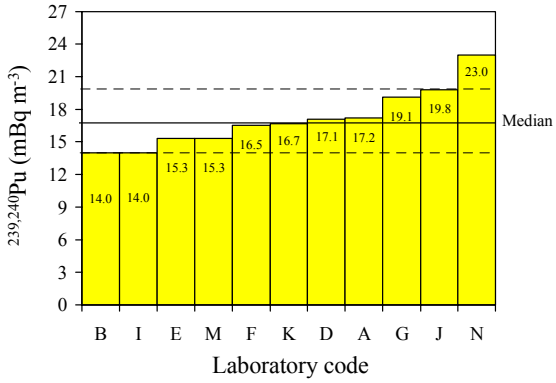

Code	^{239,240}Pu (mBq m^{-3})
B	14.0 ± 1.2
I	14.0 ± 1.4
E	15.3 ± 1.0
M	15.3 ± 2.8
F	16.5 ± 1.4
K	16.7 ± 1.1
D	17.1 ± 1.0
A	17.2 ± 1.3
G	19.1 ± 1.0
J	19.8 ± 0.8
N	23 ± 5

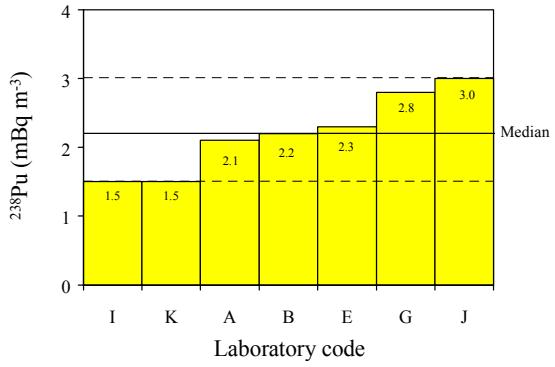

Code	^{238}Pu (mBq m^{-3})
I	1.5 ± 0.3
K	1.5 ± 0.4
A	2.1 ± 0.4
B	2.2 ± 0.4
E	2.3 ± 0.2
G	2.8 ± 0.4
J	3.0 ± 0.3

Figure 5. Reported ^{137}Cs, ^{239,240}Pu and ^{238}Pu concentrations for the ARMARA sea water intercomparison. Dashed lines indicate the 95% confidence intervals of the medians

Of the fourteen values reported for ^{137}Cs, none was rejected as an outlier. The range of accepted laboratory means was 10.4 – 15.0 Bq m^{-3}; the median was 12.75 Bq m^{-3}, with a confidence interval of 11.9 – 14.1 Bq m^{-3}. In the case of ^{239,240}Pu, eleven laboratories reported their results. All passed the outliers test. The range of laboratory means was 14.0 – 23.0 mBq m^{-3}, and the median was 16.7 mBq m^{-3}, with a confidence interval of 14.0 – 19.8 mBq m^{-3}. For ^{238}Pu, seven results were reported, all passing the outlier test. The range of laboratory means was 1.5 – 3.0 mBq m^{-3}, the median was 2.2 mBq m^{-3} with a confidence interval of 1.5 – 3.0 mBqm^{-3}. For all three data-sets, the mean of the reported values was very similar to the median, indicating a near-symmetrical probability distribution of the parent population.

The agreement between the results submitted by the participants in this internal exercise is considered to be satisfactory, given the low activity concentrations involved. We are, thus, confident that data being reported by collaborating laboratories within the framework of the ARMARA project are consistent and that an appropriate level of intra-laboratory quality control is in place. An indication of the overall quality of the data can be obtained from the widths of the confidence intervals around the respective medians. Comparison of our values with those obtained in IAEA-organised intercomparison runs shows our results to be comparable with those generally considered to reflect good quality data.

In addition to this initiative, ongoing QA/QC programmes between members of the collaboration continued throughout the programme. For example, analysis of ^{90}Sr concentrations in replicate samples taken at seven different locations throughout the Irish Sea in the course of the *Cirolana 10/95* research expedition by two of the participating laboratories established their intercomparability for this particular radionuclide. The results, presented in Figure 6, show the good agreement between the two sets of data over a wide range of environmental ^{90}Sr concentrations. This agreement is of particular importance when, as in the ARMARA programme, sets of independent data gathered by different laboratories are combined to study the long-term dispersion of radionuclides over large geographical areas.

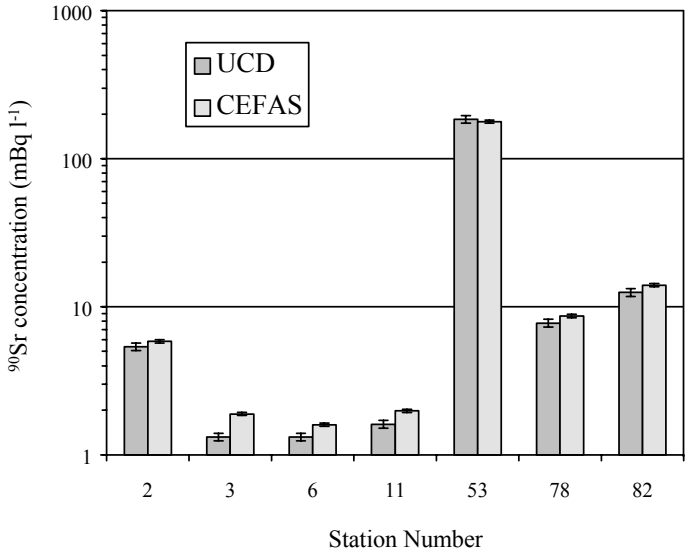

Figure 6. Comparison of ^{90}Sr concentrations measured in filtered sea water samples collected aboard *R.V. Cirolana* in December 1995

3. Short-term reactivity of radionuclides upon input into the Arctic

3.1. Physico-chemical characterisation of radionuclides at input

The group recognises that in any assessment of the long-term behaviour of radionuclides in the Arctic marine environment, it is of fundamental importance to have a clear understanding of the species formed under different conditions, together with the biogeochemical cycles. Although in the short term, behaviour may be dominated by the physical/chemical form of the radionuclide upon release, the prevalence of source-dependent species will diminish with time and, ultimately, behaviour will be controlled largely or completely by source-independent forms. The nature of the later will be determined by the chemistry of the element in question and the properties of the receiving milieu, in our case, the Arctic Seas. Accurate data on the speciation of radio-elements, particularly those exhibiting multivalent behaviour, is an essential pre-requisite when attempting

to model the transfer of radio-contaminants in the environment and predict their likely radiological impact on man.

We have already signalled the virtual absence of field data on the chemical speciation of radionuclides in the Arctic Seas at the outset of this project and how this important knowledge gap was addressed by the group in studies on radionuclide reactivity (i) at the fresh water/sea water interface (estuaries), (ii) within the water column (shelf seas and deep ocean), and (iii) at the sediment/sea water interface. In addition, there now exists an extensive knowledge base on this subject derived from studies carried out in more temperate zones. Indeed, the group included contractors with considerable practical expertise in marine speciation analysis, who have accumulated extensive data on the speciation of a number of key radio-elements (including technetium, caesium, strontium, plutonium and americium) in the NE Atlantic waters feeding into the Arctic. This understanding is based on numerous analyses conducted in the waters of the Irish Sea, English Channel, Baltic Sea and North Sea by these contractors in the course of previous projects funded by the Commission.

3.2. Review of transformation processes post-input, including dissolution of 'hot' particles

Detailed studies on effluent samples taken from the Sellafield and La Hague reprocessing plants carried out by the collaboration in the course of the present and past programmes have enabled us to have a clear understanding of the transformation processes which are likely to take place upon release of (reprocessed) radionuclides to the marine environment. Hollow-fibre ultrafiltration and on-line ion-exchange chromatography studies carried out on La Hague effluents in January 1997 showed that a major fraction of the γ-emitting radionuclides was associated with particulate material (>0.45 μm) and that a significant fraction of the dissolved component was, in fact, in a colloidally-bound form (>3kDa). Similar results had previously been obtained for Sellafield effluents, where a significant fraction of the ^{90}Sr, ^{137}Cs, ^{239,240}Pu(V), ^{239,240}Pu(IV) and ^{241}Am was found to be in a colloidal form (>3 kDa). Despite the presence of a significant colloidal fraction in the effluent, further experiments by Leonard *et al.* (1995), following dilution of Sellafield effluent into sea water under laboratory conditions, indicated that ^{90}Sr, ^{137}Cs and ^{239,240}Pu(V) colloidal forms did not persist in sea water. On the other hand, the same researchers did find evidence to suggest that colloidal forms of ^{239,240}Pu(IV) and ^{241}Am do persist in sea water. The latter observation is supported by chemical speciation and enhanced sorption analyses carried out under field conditions by Mitchell *et al.* (1995) on samples of ultrafiltered water from the north-eastern Irish Sea. These confirmed that some of the Pu(IV) present in sea water is in a colloidal form and that the size of the colloidal particles or aggregates involved is generally much smaller than that observed in, for example, rivers and lakes.

Using transmission electron microscopy (TEM), electron dense structures of variable size (corresponding to so-called 'hot' particles) were identified in the La Hague effluent and Sellafield effluents. Similar structures have been found in contaminated sediments in the close vicinity of dumped objects in the Abrosimov and Stepovogo Fjords at Novaya Zemlya using scanning electron microscopy (Figure 7). Clearly, knowledge of the weathering rate of the matrix of these particles is an essential parameter in order to determine the rate of future release of mobile radionuclides from dumped wastes and their dissolution into the water column. Indeed, 'hot' particles in the Sellafield effluent have been shown to persist in the marine environment for at least several months before dissolving, with some being preserved in accreting estuarine sediments (Hamilton *et al.*, 1991). In Thule, where weapons-grade plutonium was dispersed in the form of plutonium oxide particles with a median diameter of 2 μm, hot particles are still present 30 years after the accident. Currently, the properties of radioactive 'hot' particles from La Hague and Chernobyl are being studied by the group using radiometric, radiochemical and microscopy methods, while transformation processes (i.e., weathering and dissolution) upon contact with sea water are being followed over time.

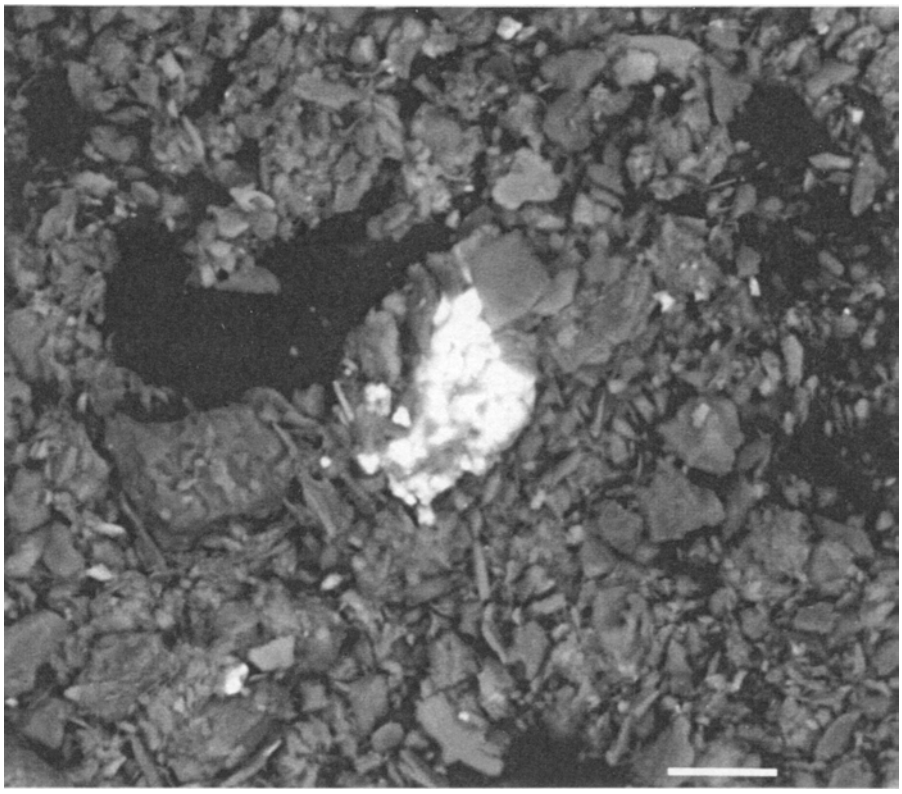

Figure 7. Scanning electron microscopy (BEI-mode imaging) of a radioactive particle sampled in Stepovogo Fjord. The corroded particle (about 10-20 μm), containing Co, Fe, Mn and Cr, is evident as a bright area in the centre of the image

3.3. Corrosion rates and radionuclide leakage rates from encapsulations containing radioactive wastes

Detailed data on the release rates of radionuclides from dumped objects in the Arctic Seas are available from a number of sources. Lynn *et al.* (1996) have predicted radionuclide release rates to the year 3000 from nuclear reactors, some containing their spent nuclear fuel, which have been dumped in the Kara Sea. These release rates are based on the best available predictions for corrosion rates in an Arctic environment and have been calculated for the fission product, activation product and actinide inventories in the different types of reactors that were dumped. Using inventory and construction data, corrosion rates were applied to computer models of the reactors to produce radionuclide release rates for scenarios ranging from no effective containment to all containment barriers being fully effective. Suffice to say that, in the latter scenario, the predicted release rate from all the units dumped in Abrosimov Bay, summed over all radioactive isotopes, is predicted to rise to 1.5×10^{13} Bq y^{-1} by about the year 2005, falling to 7.4×10^{9} Bq y^{-1} by 2400, and ending by the year 2660, when all the units should have corroded away. Data on release rates have also been provided by the IASAP project of the IAEA and the Kara Sea Project organised by EC/DGXI. Both of these projects were completed in 1997 and their results were available to the ARMARA programme. A summary of the time-integrated releases for fission products, actinides and corrosion products from the dumped objects in the Kara Sea is given in Table 1.

Table 1. Time-integrated release from dumped objects in the Kara Sea estimated by the EC/DGXI Kara Sea Project

Nuclide	Release (TBq)
^{238}Pu	1.1×10^{-3}
^{239}Pu	8.3×10^{0}
^{240}Pu	2.3×10^{0}
^{241}Pu	1.1×10^{-11}
^{241}Am	1.3×10^{0}
^{90}Sr	3.8×10^{-5}
^{137}Cs	6.6×10^{-4}
^{151}Sm	1.0×10^{-2}
^{99}Tc	1.1×10^{-1}
^{129}I	3.8×10^{-4}
^{55}Fe	2.5×10^{1}
^{60}Co	3.5×10^{-1}
^{59}Ni	4.9×10^{0}
^{63}Ni	4.7×10^{0}

4. Radionuclide reactivity within the water column

4.1. Radionuclide distribution within the water column

The main objective of this work-package was to examine the kinetics of radiologically-important radionuclides within the Arctic and how such kinetics are influenced by the chemical speciation of these nuclides and their association with suspended particulate and colloidal matter. In the first two years of the programme particular emphasis was given to the determination of high resolution vertical profiles of transuranium an other radionuclides in the shelf seas and the Central Arctic Ocean, the partition of these radionuclides between filtered and suspended particulate phases, the fractions in colloidal form and the size and composition of the latter. The aim was to obtain a reliable database on (a) radionuclide concentrations, and (b) representative values for the parameters controlling the transfer rates between the water and sediment compartments.

Samples were collected in the course of the Arctic Ocean ’96 expeditions along the Kara Sea continental break (between Franz-Josef-Land and Severnaya Zemlya), in the Nansen, Amundsen and Makarov Basins, along the Lomonosov Ridge, and over the continental slopes in the Laptev and East Siberian Seas.

The section between Franz-Josef-Land and Severnaya Zemlya (Figure 8) was considered to be of particular importance, connecting as it does the Barents and Kara Seas with the central Arctic Basin, and representing one of the main pathways by which water-borne radionuclides released from the dump sites in the shelves could be transported to the Central Arctic Ocean. Exchange between these shelf seas and the deep basins of the Central Arctic is through the St. Anna and Voronin Troughs, canyons of ~600 m and ~400 m in the deepest parts, respectively, separated by a submarine plateau of depth ~50 m or less.

Measured $^{239,240}Pu$ (and ^{238}Pu) concentrations in filtered sea water sampled along this transect, extending from 065^{o}E to almost 090^{o}E, confirm that $^{239,240}Pu$ concentrations in the dissolved phase in this region of the Arctic are extremely low, being in the range 2.0 – 8.2 mBq m^{-3} (Figure 9a). Concentrations in the surface mixed layer were lowest of all, being < 4 mBq m^{-3} in most cases. The data confirm the presence of a sub-surface maximum in the plutonium

concentration at several hundred metres depth, with concentrations being typically double those observed in both the surface and near-bottom layers. Within surface and sub-surface waters highest concentrations were observed at the most westerly stations. This is consistent with the established pattern of water circulation in the vicinity of this zone and the surrounding seas, as modified Atlantic water (MAW), labelled with higher ^{239,240}Pu concentrations, advectively intrudes in a N-S direction through the western half of the St. Anna Trough. The injection of MAW is evident from the potential temperature and salinity data recorded at the same stations and plotted in Figure 9b and 9c. These can be compared with the ^{239,240}Pu data depicted in Figure 9a; the correspondence is very satisfactory given that the total number of plutonium measurements is by no means large (n = 23).

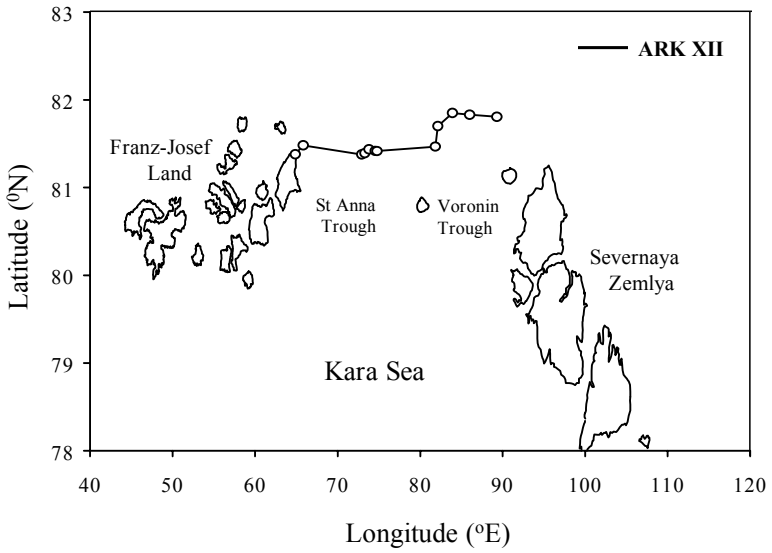

Figure 8. Sampling stations in the St. Anna/Voronin Troughs (July-August, 1996)

In the Central Arctic (Figure 10), vertical profiles showed a distinct sub-surface maximum in the plutonium concentration at several hundred metres (Figure 11). The Lomonosov Ridge and north Makarov Basin profiles (Stn. 9, 15 31 and 34) were rather similar, with the highest concentrations (17–22 mBq m^{-3}) observed at the temperature maximum in the Atlantic layer (at depths between 200 and 350 m), and slightly lower values (14–17 mBq m^{-3}) in deep Atlantic layer samples (800–1000 m). In comparison, plutonium concentrations in the Atlantic layers were lower in the Nansen Basin (Stn. 5), but in level at Stn. 40 in the western Amundsen Basin. It is worth to compare these concentration profiles with those observed by Herrmann *et al.* (1998) in the Western Spitsbergen Current (WSC) in 1995. Here, an activity maximum was observed in the top 100 m of the water column, followed by a slow decrease in concentrations with increasing depth. When the WSC enters the Arctic Ocean, it sinks below the Arctic surface water and the maximum plutonium concentrations move to lower depths. The major Atlantic Ocean inflow across the Barents Sea enters the Nansen basin mainly below the surface layer. North of Svalvard and Franz Josef land, Atlantic water is observed to penetrate down to approximately 500 metres, while the inflow through the St Anna Trough distributes the Atlantic water down to 1000 m (Schauer *et al.*, 1997). The combined WSC and Barents Sea inflow will result in a plutonium maximum deeper than 100 m but above 1000 m.

Our measurements on plutonium concentrations in the Central Arctic and surrounding seas complement the extensive set of measurements on plutonium made in the Norwegian, Barents and Greenland Seas in 1995 by Herrmann *et al*. (1998), and a similarly impressive set extending across the Arctic Ocean in 1994 by Ellis *et al*. (1995).

Figure 9. (a) ^{239,240}Pu concentration, (b) temperature and (c) salinity in a section across the St Anna/Voronin Troughs (July–August 1996)

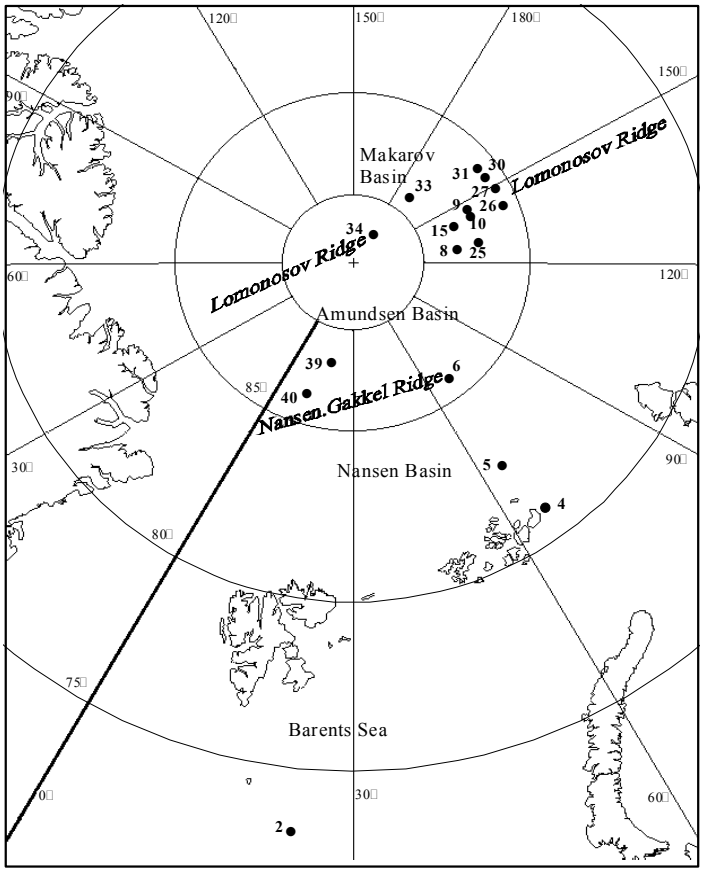

Figure 10. Sampling stations in the Central Arctic Ocean (Arctic '96)

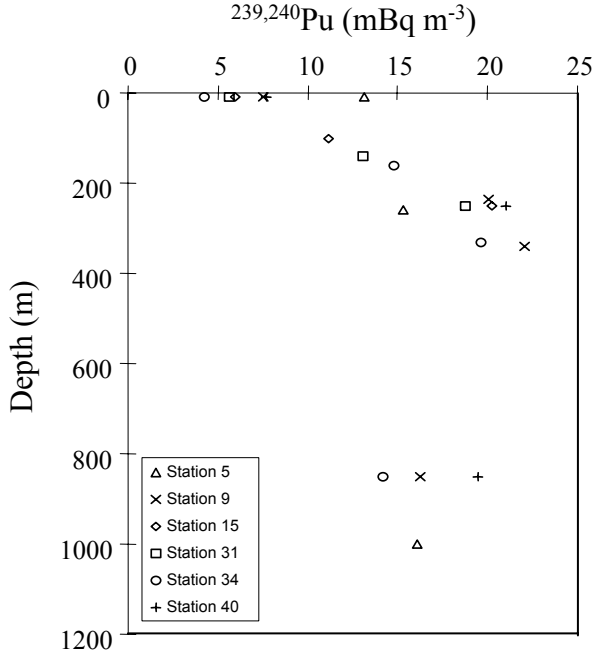

Figure 11. ^{239,240}Pu vertical profiles at stations in the Central Arctic Ocean

In their survey, Herrmann *et al*. (1998) observed a clear trend of decreasing plutonium (and americium) concentrations along the transport route represented by the Norwegian Coastal Current (NCC), the West Spitsbergen Current (WSC) and the East Greenland Current (EGC). They attributed this to the influence of discharges from European reprocessing plants, a point reinforced by their observation of an elevated $^{238}Pu/^{239,240}Pu$ activity ratio, particularly in the sub-surface layer, almost everywhere throughout their sampling area. However, their measurements did not extend beyond 040°E. Close to this meridian in the Barents Sea, they reported concentrations in the surface and sub-surface layers of ~7–9 and ~12–18 mBq m^{-3}, respectively. These are clearly higher than the corresponding concentrations observed by us along the St. Anna and Voronin Troughs which, of course, are situated much farther to the east along one of the transport routes to the Central Arctic Ocean. We were unable to detect any significant elevation in the $^{238}Pu/^{239,240}Pu$ ratio, our values being < 0.07 in all cases. This is consistent with measurements reported for seabed sediments sampled in the open Kara and Barents Seas in recent years.

Across the Central Arctic, reported concentrations in surface waters were similar to those observed in surface waters of the St. Anna and Voronin Troughs. However, concentrations at the level of the sub-surface maximum throughout the Central Arctic were significantly higher than at the equivalent depth in the St. Anna and Voronin Troughs. These higher levels have been explained by Ellis *et al*. as an advective feature caused by inputs of Atlantic water contaminated by $^{239,240}Pu$ from both global fallout and reprocessing plant discharges, modified by adsorption of $^{239,240}Pu$ onto particles, followed by particle sinking and redissolution at depth. These mechanisms will be further discussed in WP 7.

It is evident from the database on plutonium concentrations in the Arctic Seas that a fraction of the measured plutonium within the water column has been advected over distances exceeding several thousand kilometres. Although plutonium in a reduced chemical form is highly particle-reactive and is rapidly scavenged from the water column by sinking particles, most of the plutonium in the filtered phase in north-east Atlantic waters is in an oxidised and fully soluble form, as shown by experiments using ultrafiltration (Mitchell *et al.*, 1995). Presumably it is mainly oxidised plutonium that is transported over long distances by the prevailing currents, rather than particulate-bound plutonium.

For the more conservative ^{137}Cs, ^{90}Sr and ^{129}I, the highest surface concentrations were found in a band stretching from north of the Lomonosov Ridge and its close vicinity across the North Pole and south along 15°E in the Amundsen Basin. Lower activity concentrations were found in the Nansen and eastern Amundsen Basins. In contrast to the plutonium distribution, vertical profiles (0–1000 m) for ^{137}Cs, ^{90}Sr and ^{129}I at 15 separate profiles throughout the Central Arctic Ocean showed a general decrease in concentrations with increasing depth (Figure 12). The only exception to this trend were the ^{137}Cs concentrations measured in the lower halocline layer at stations above the Lomonosov Ridge and the northern Makarov basin, which were higher than those at either the surface or Atlantic layers (see Stn. 34 profile). This is not seen in the halocline sample at Stn. 40, nor in the ^{129}I and ^{90}Sr profiles at any of the stations.

The origin of the waters in the lower halocline is still the object of debate, with some author suggesting that it is originated in the Barents Sea shelf and others suggesting that it mainly evolves from the surface layers as the result of multiple years of ice freezing/melting cycles. The estimated mean residence times for the surface layer are 2–6 years, while that of the halocline is up to 15 years. This is compatible with the ^{129}I signal and the measured $^{129}I/^{137}Cs$ ratios in the halocline, which are significantly lower than in the surface layer. A temporary input of higher activity to both the surface and the halocline layers would traverse the surface layer much faster than the halocline and result in enhanced concentrations being measured in the latter. The lack of a corresponding peak in the ^{129}I and ^{90}Sr concentrations exclude Sellafield and global fallout as the source and point to the Chernobyl activity (mainly ^{137}Cs) introduced into the Central Arctic Ocean around 1990.

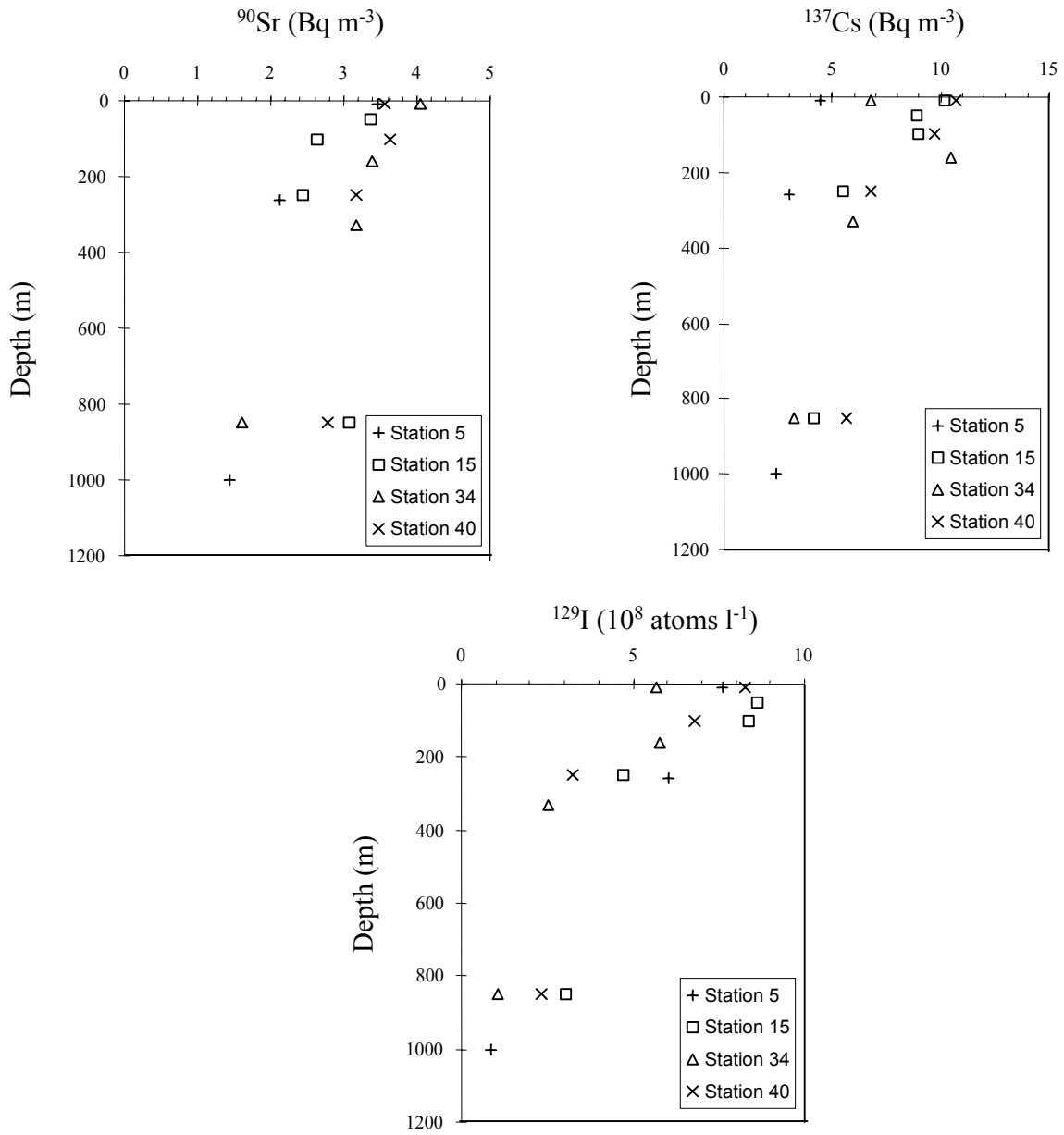

Figure 12. ^{90}Sr, ^{137}Cs and ^{129}I profiles at selected stations in the Central Arctic Ocean

Atlantic layer circulation is reflected in the ^{137}Cs and ^{90}Sr distributions, with activities increasing along the path as an effect of the decreasing inputs from European reprocessing and fallout. The lowest ^{137}Cs and ^{90}Sr concentrations are found in the Nansen Basin north of Franz Josef Land, with higher concentrations above the Lomonosov Ridge and highest above the Gakkel Ridge. ^{129}I concentrations also follow the Atlantic water circulation, but with concentrations decreasing along the path as the result of increasing Sellafield and La Hague discharges.

4.2. Chemical speciation

The mobility and bioavailability of a radioelement in a natural water system is heavily influenced by its physical and chemical form. Of no element is this more true than for plutonium, which, in solution, can exist in at least four distinct oxidation states simultaneously. In sea water, oxidation states IV and V have been shown to predominate as the reduced ($Pu(OH)_4$) and

oxidised (PuO_2^+) forms, respectively. Plutonium can be thought of as being present in two distinct forms: reduced plutonium, Pu(IV), which is highly particle-reactive and is thus quickly scavenged by particles, sediments and colloids; and oxidised plutonium, Pu(V), which is relatively soluble and can be transported over long distances within the dissolved phase. These two forms of plutonium exhibit very different sediment-water distribution coefficients (K_d), with reduced plutonium possessing a K_d approximately two orders of magnitude higher than oxidised plutonium, i.e., 10^6 compared to 10^3–10^4. Clearly, accurate data on the speciation of plutonium is essential if it is desired to model its transport in the environment and predict its likely effect on man.

Accordingly, the oxidation state distribution of plutonium in filtered sea water under Arctic conditions was examined in the course of the programme during a collaborative research expedition to NW Greenland in August 1997. Specifically, the chemical speciation of plutonium was studied in waters collected in the marine zone close to the Thule air base (Figure 13), where a B-52 bomber carrying four plutonium-bearing weapons crashed on ice in 1968, causing the release of kilogram quantities of insoluble plutonium oxide to the snow-pack and underlying sediments. For comparison purposes, the oxidation state distribution of plutonium was also examined at a reference site (Upernavik) remote from the accident zone (Figure 13).

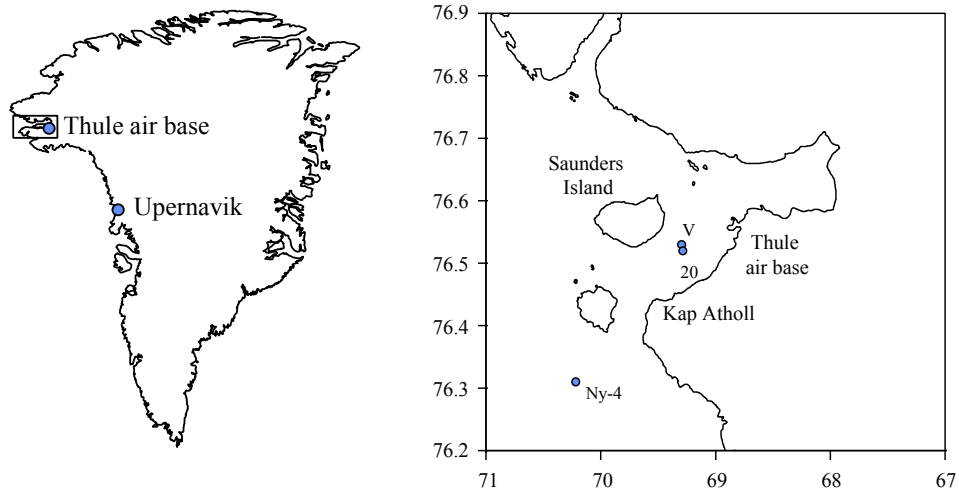

Figure 13. Locations at which plutonium chemical speciation analyses were carried out (Thule '97 expedition)

The oxidation state distribution of plutonium in the dissolved phase was determined using a technique based on the sequential co-precipitation of reduced plutonium species with small amounts of ferric hydroxide. Briefly, two isotopic tracers in different oxidation states, ^{242}Pu(IV) and ^{236}Pu(VI), were added to each sample, which was then made 0.3M in HCl. A small amount of Fe^{3+} (0.1 mg l^{-1}) was added and subsequently precipitated in hydroxide form following neutralisation with ammonia. By using such a small amount of iron, only reduced (III, IV) plutonium species were co-precipitated, leaving oxidised (V,VI) species in solution. The ferric hydroxide precipitate was collected by filtration and retained for the analysis of the reduced fraction. Following reacidification of the sample and a further addition of Fe^{3+}, reduction of the oxidised species of plutonium was accomplished by the addition of appropriate reducing agents prior to precipitation.

Plutonium was recovered from both fractions (precipitates) separately using routine radio-chemical separation techniques based on selective sorption on ion-exchange resins, followed by electrodeposition onto stainless-steel discs. Tracer cross-over was monitored carefully throughout and was found to be less than ~6% in all cases. The resulting data are summarised in Table 2.

Table 2. Oxidation–state distribution of ^{239,240}Pu in sea water sampled off the NW coast of Greenland (August 1997). Uncertainties are given to ±1σ

Location	Station depth (m)	Depth (m)	%^{239,240}Pu(V,VI) in filtrate	^{239,240}Pu (total) (mBq m^{-3})
Thule:				
Stn Ny-4 (76°18'N, 70°13'W)	290	2	75 ± 8	5.8 ± 0.5
		280	68 ± 5	10.8 ± 0.5
Stn V (76°32'N, 69°18'W)	187	2	67 ± 4	6.6 ± 0.3
		100	65 ± 4	11.2 ± 0.4
		177	59 ± 3	17.6 ± 1.0
Stn 20 (76°31'N, 69°17'W)		2	76 ± 7	9.3 ± 0.6
Upernavik:				
Stn 1(72°49'N, 56°12'W)		2	77 ± 10	7.5 ± 0.4
	Mean (*n*=7)		*70 ± 7*	

The data show that most of the plutonium in the dissolved phase at all four Greenland stations is in an oxidised form, i.e., Pu(V,VI), highlighting the well-oxygenated character of these cold shelf waters. Further, there appears to be no difference between the oxidation state distribution measured at stations close to the Thule accident site and that at a reference station remote from this site (i.e., Upernavik). Overall, the percentage of oxidised ^{239,240}Pu in surface waters near Thule is similar to that observed at lower latitudes (see Table 3), suggesting that the underlying processes controlling plutonium speciation are, to first order, insensitive to temperature over the range 0–25°C. Unfortunately, there appears to be no published data on the oxidation-state distribution of plutonium in Arctic waters with which to compare results, with the exception of a single measurement by Pentreath *et al.* (1986), who reported a value of 55% for oxidised plutonium at an unspecified location in the Arctic (understood to be somewhere within the Norwegian Sea).

Table 3. Oxidation–state distribution of plutonium in filtered sea water from shallow coastal waters in more temperate environments

Location	^{239,240}Pu(V,VI) (%)	Source
Irish Sea	80–94	Mitchell *et al.*(1995)
English Channel	76–79	Boust *et al.* (1996)
Western Mediterranean Sea	63–71	Mitchell *et al.*(1995)
Gulf of Vera (Palomares)	68	Mitchell *et al.*(1995)
Enewetok and Bikini Atolls	92	Noshkin and Wong (1981)

Measurement of the ^{238}Pu/^{239,240}Pu ratio in the water column (dissolved phase) at Thule yielded a mean value of 0.06 ± 0.02 (*n*=10) which, being similar to the global fallout ratio at these latitudes of about 0.04, suggests that there is virtually no weapons-grade plutonium in the Thule water column at the present time. This is in sharp contrast to the seabed sediments, which show considerable inhomogeneities in their plutonium content, with ratios in some samples as low as 0.01–0.02, characteristic of weapons-grade plutonium (Aarkorg *et al.*, 1987; Mitchell *et al.*, 1997; Dahlgaard *et al.*, 1999). Statistically there was no difference in ratios recorded in

surface and sub-surface waters, suggesting that even in near-bottom waters (dissolved phase) global fallout plutonium now predominates. This is consistent with observations made in the early 1990s in the vicinity of the coastal village of Palomares (Spain), where a similar accident involving nuclear weapons occurred in 1966 (Mitchell *et al.*, 1995).

In the case of suspended particulate, the only sample in which it proved possible to determine the $^{238}Pu/^{239,240}Pu$ activity ratio with reasonable precision gave a value of 0.006 ± 0.003, consistent with the isotopic signature of the plutonium released in the Thule accident. This sample was taken at the actual accident site (Stn. V), some few metres above the seabed, and the very low ratio more than likely reflects the presence of some accident-contaminated fine sediment resuspended into the water column.

4.3. Association with suspended particulate – Sediment/water distribution coefficients

The partitioning of plutonium between filtered (<0.45 μm) sea water and suspended particulate was examined at a number of selected locations in the Central Arctic and surrounding shelf seas in the course of the Arctic'96 expedition (Table 4). The extremely low suspended particulate loads of these waters (found to be typically 0.1–0.3 mg l^{-1}) required the filtration of large water volumes (500–1000 l). The use of pre-filters (>20 μm) permitted the separation of large (>20 μm) particles, usually biogenic, from those in the range 0.45–20 μm.

Table 4. Partitioning of $^{239,240}Pu$ (± 1σ) between filtered sea water and suspended particulate in the Central Arctic Ocean and surrounding shelf seas (July–August 1996)

Location	Fraction	$^{239,240}Pu$ (mBq m^{-3})
St. Anna Trough	<0.45 μm	3.1 ± 0.9
	>0.45 μm	0.44 ± 0.04
	Total	3.5 ± 0.9
Stn. 24	<0.45 μm	2.6 ± 0.3
81°42.0'N 82°09.2'E	0.45–20 μm	<0.1
	>20 μm	0.33 ± 0.06
	Total	3.0 ± 0.3
Stn. 70	<0.45 μm	4.7 ± 0.4
86°21.5'N 148°07.0'E	0.45–20 μm	0.23 ± 0.03
	>20 μm	0.13 ± 0.03
	Total	5.0 ± 0.4
Stn. 84	<0.45 μm	3.5 ± 0.3
82°31.2'N 132°58.3'E	0.45–20 μm	<0.1
	>20 μm	<0.1
	Total	3.6 ± 0.3
Stn. 98	<0.45 μm	3.8 ± 0.3
79°39.5'N 148°40.7'E	0.45–20 μm	<0.1
	>20 μm	0.13 ± 0.02
	Total	3.9 ± 0.3

In general, the percentages of plutonium in a particulate form (>0.45 μm) in sea water throughout the Arctic Ocean were found to lie in the range 3–12%. These percentages are quite similar to those observed in more temperate environments such as the western Mediterranean (1–

14%) and the western Irish Sea (2–32%). It is also very similar to those reported by other workers in the Atlantic Ocean and the Norwegian Sea. Representative sediment–water distribution coefficients (K_ds) determined from these measurements gave a mean value of (2.8 ± 1.6) × 10^5 (n=5), identical to K_d values reported for ^{239,240}Pu in Atlantic, Pacific and Mediterranean waters. Again, this would seem to suggest that under field conditions, at least after long equilibration periods, the underlying processes controlling plutonium physico–chemical speciation are insensitive to temperature changes over the range 0 – 25°C.

4.4. Association with colloidal matter

The migration of particle-reactive radionuclides in the ocean is primarily governed by the transfer and equilibrium processes controlling their distribution between the dissolved and solid phases. Although a substantial body of data has been collated on the partitioning of naturally-occurring and anthropogenic radionuclides between these phases on the basis of operationally defined particle-size cut-offs (typically 0.45 μm), there is now good evidence to suggest that a significant fraction of conventionally defined dissolved radionuclides in estuarine, coastal and open waters are, in fact, associated to colloidal matter. To examine the extent and size fractionation of the colloidal plutonium, large volumes of water collected in the Lomonosov Ridge and the Laptev and Kara Seas continental breaks in the course of the Arctic '96 expedition were micro-filtered *in situ* through a 0.45 μm screen filter prior to subdivision and tangential flow ultrafiltration using a selection of polysulphone membrane cassettes corresponding to molecular weight limits (NMWLs) of 100, 10 and 1 kDa (1 kDa ≈ 1.2 nm). The results of these experiments, summarised in Table 5, reveal that in the Laptev Sea (Stn. 98) and the Lomonosov Ridge (Stn. 70) zones, a significant fraction (24 ± 9%; *n*=5) of the plutonium in the operationally-defined dissolved phase is actually in colloidal form. In contrast, no retention was observed in the Kara Sea continental break (Stn. 24), even with a 1 kDa ultrafilter.

Table 5. ^{239,240}Pu concentrations (±1σ) in different size fractions upon ultrafiltration with membranes of various NMWLs at selected stations in the Central Arctic

Location	Size Fraction	^{239,240}Pu (mBq m^{-3})	Retention (%)
Stn. 24 (Kara Sea)	x < 0.45 μm	2.6 ± 0.3	
81°42.0'N 82°09.2'E	1 kDa < x < 0.45 μm	5.6 ± 0.3	0
	x <1 kDa	5.5 ± 0.3	
Stn. 70 (Lomonosov Ridge)	x < 0.45 μm	4.7 ± 0.4	
86°21.5'N 148°07.0'E	10 kDa < x < 0.45 μm	6.9 ± 0.4	39 ± 2
	x <10 kDa	3.0 ± 0.3	
	1 kDa < x < 0.45 μm	6.0 ± 0.4	24 ± 3
	x <1 kDa	3.7 ± 0.3	
Stn. 98 (Laptev Sea)	x < 0.45 μm	3.8 ± 0.3	
79°39.5'N 148°40.7'E	100 kDa < x < 0.45 μm	4.6 ± 0.3	18 ± 3
	x <100 kDa	3.2 ± 0.3	
	10 kDa < x < 0.45 μm	4.2 ± 0.3	17 ± 3
	x <10 kDa	3.0 ± 0.3	
	1 kDa < x < 0.45 μm	5.4 ± 0.6	21 ± 4
	x <1 kDa	3.5 ± 0.4	

As the colloidal particles/aggregates present in the sample taken at St. 98 appear to be of high molecular weight (≥100 kDa), it is not unreasonable to suggest that some of this colloidal matter may be of riverine origin, particularly considering the relative contribution of riverine

input to the water column in these areas (Table 6). If this the case, riverine colloidal material could play an important role in the transport of particle-reactive contaminants from the shelves to the Arctic interior.

Table 6. Percentage contribution of river runoff to the water column for the Arctic Seas (Östlund, 1993)

Arctic Sea	River runoff inventory (%)
Barents Sea	0
SW Kara Sea	1
NE Kara Sea	5–9
Laptev Sea	11

Similar measurements in the vicinity of Thule revealed that little, if any, of the plutonium in these waters is associated to colloidal entities (Table 7). This observation is consistent with results reported recently for more temperate environments, where virtually all of the plutonium, including the fraction in a reduced chemical form, was found to be present as fully dissolved species (Mitchell *et al.*, in press). That in waters relatively unaffected by riverine discharges the association of radionuclides to the colloidal phase is negligible has been confirmed by laboratory contact experiments carried in the Kara Sea and Stepovogo Fjord using a 10 kDa membrane, which show that nearly all the ^{90}Sr and most of the $^{239,240}Pu$ in Arctic sea water is present as low molecular weight species. In contrast, dynamic tracer experiments in which $^{60}Co^{2+}$ ions were mixed with the colloidal and particulate fractions of Stepovogo Fjord sediments (i.e., resuspended fraction) suggest strong interactions between this nuclide and the resuspended solid phase.

Table 7. $^{239,240}Pu$ concentrations ($\pm 1\sigma$) in different size fractions upon ultrafiltration with membranes of various NMWLs at Thule (Greenland)

Location	Size Fraction	$^{239,240}Pu$ (mBq m^{-3})	Retention (%)
Stn. A	$x < 0.45$ μm	6.8 ± 0.4	
	10 kDa $< x <$ 0.45 μm	5.3 ± 0.7	-
	$x <$10 kDa	6.2 ± 0.9	
	1 kDa $< x <$ 0.45 μm	4.2 ± 0.8	-
	$x <$1 kDa	5.7 ± 0.9	
Stn. P2	$x < 0.45$ μm	3.2 ± 0.4	
	10 kDa $< x <$ 0.45 μm	2.3 ± 0.2	-
	$x <$10 kDa	2.9 ± 0.3	
	1 kDa $< x <$ 0.45 μm	2.7 ± 0.3	-
	$x <$1 kDa	2.9 ± 0.3	

4.5. Scavenging processes and residence times

Accurate data on scavenging rates and residence times of particles in the water column are essential requirements when modelling the long-term behaviour of particle-reactive radionuclides in a marine ecosystem. However, prior to this study, values for these parameters in the Arctic environment had been reported at only a few sites. As part of the ARMARA commitments to remedy this important information gap, the W-Spitsbergen coastal environment was selected as a

key site for the study of scavenging and sedimentation processes. In particular, studies were carried out in two fjords (Van Mijen and Kongsfjord) and in the adjacent continental shelf. A total of five oceanographic expeditions were conducted within the framework of the ARMARA project. Three of them were carried out in summer conditions (August 96 and 97, and September 98) in collaboration with the University of Bergen. A research agreement with UNIS (University Studies at Svalvard) and with the Italian Scientific base in Ny Aalesund allowed the organisation of two winter field expeditions (in 1998 and 1999).

Specific objectives of these expeditions included:

- determination of scavenging rates and residence times of particles in the water column of the continental shelf and in the fjords, using disequilibrium between ^{234}Th and ^{238}U in the water column,
- determination of ^{137}Cs and ^{210}Pb vertical profiles and inventories in sediment cores from shelf and fjord areas, and
- estimation of sedimentation rates.

The disequilibrium between ^{234}Th and ^{238}U in the water column was used to trace scavenging processes. Thorium-234 is a particle-reactive, naturally-occurring radionuclide, produced in the water column by the decay of its soluble parent ^{238}U. After production, thorium is scavenged onto suspended particles and removed from the water column in association with these particles. The extent of the disequilibrium between ^{234}Th and ^{238}U is a measure of how active these scavenging processes are and allows particle residence times to be determined in coastal waters and in the upper ocean layers. Due to its short half-life (24.1 days), ^{234}Th can be used to trace scavenging processes on time scales varying from a few days to about 100 days.

Thorium fluxes and residence times were estimated at different locations of the W-Spitsbergen shelf and fjords (Figures 14 and 15). Particulate and dissolved ^{234}Th were pre-concentrated by filtration of large volumes of water (700–1000 l) using battery-powered in situ pumps. Sea water was pumped at a rate of 8–10 l min^{-1} through a pre-filter (1 μm, polypropylene) and two identical polypropylene MnO_2-impregnated cartridges arranged in series, to extract dissolved thorium. The cartridges were ashed at 450^{o}C and the ash obtained packed in a sealed container for gamma counting. U-238 concentrations were estimated from salinity measurements.

A box model was used to estimate the rate of thorium scavenging and removal by sinking particles assuming that (i) thorium profiles are in steady state, and (ii) advection and diffusion are negligible (Buesseler *et al.*, 1992). Under this conditions, the flux of dissolved thorium onto particles, J_{th}, and the flux of particulate thorium, P_{Th}, can be written as

$$J_{Th} = \lambda \cdot \left(A_U - A^{d}_{Th} \right)$$
$$P_{Th} = \lambda \cdot \left(A_U - A^{d}_{Th} - A^{p}_{Th} \right)$$

where $A_U, A^{d}_{Th}, A^{p}_{Th}$ are the activities of ^{238}U, ^{234}Th in the dissolved form and ^{234}Th in the particulate form, respectively, and λ is the decay constant of ^{234}Th (0.0288 d^{-1}). From these fluxes, the residence time of dissolved (τ_{diss}) and particulate (τ_{part}) ^{234}Th with respect to scavenging onto particles and particle sinking are then calculated using the following expressions:

$$\tau_{diss} = \frac{A^{d}_{Th}}{J_{Th}} \quad \text{and} \quad \tau_{part} = \frac{A^{p}_{Th}}{P_{Th}} \ .$$

The vertical profiles of salinity, ^{238}U, dissolved and total ^{234}Th for all the stations are shown in Figures 16 to 18.

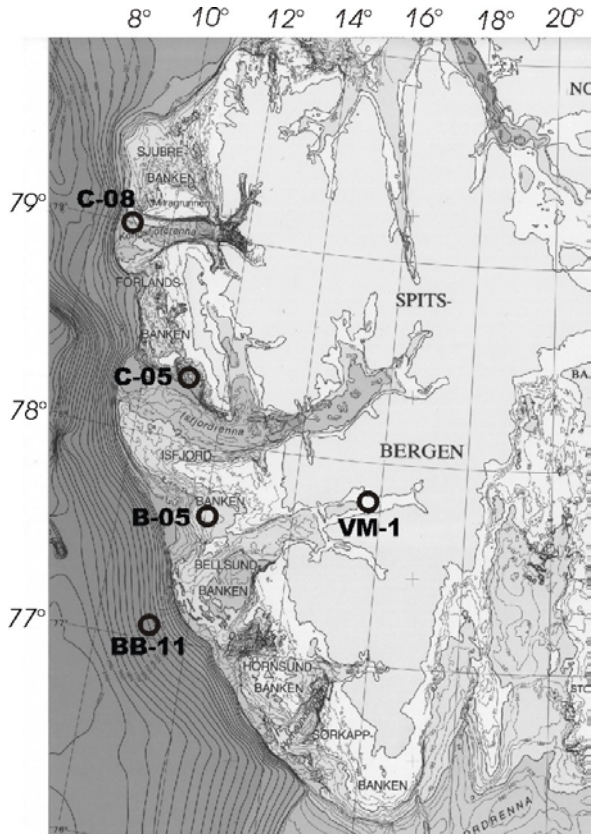

Figure 14. Sampling sites in the W-Spitsbergen shelf and in Van Mijen Fjord

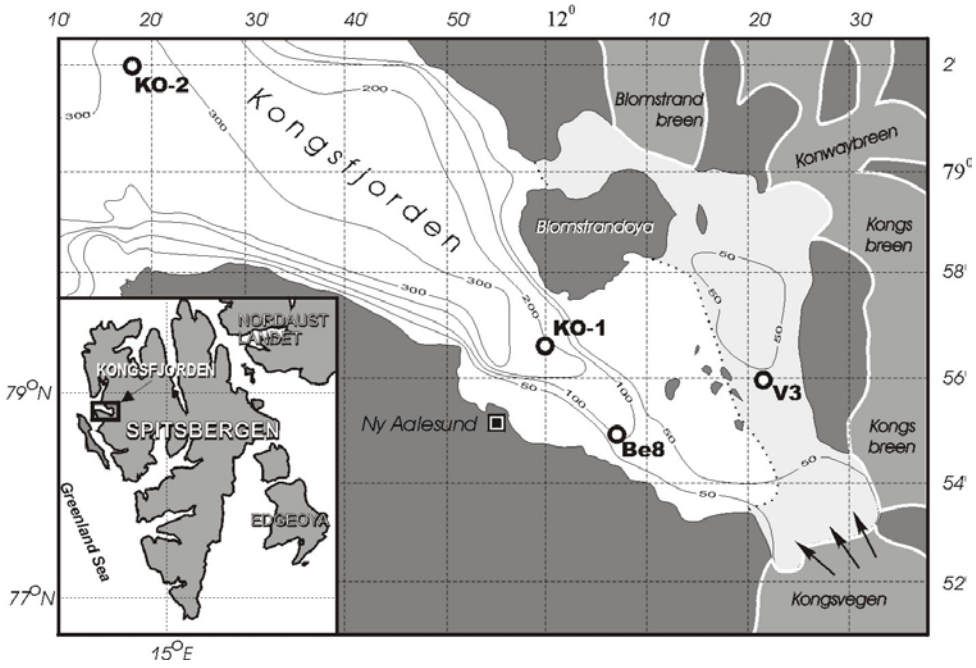

Figure 15. Sampling sites in Konsfjord

4.5.1. Shelf stations

Four sites were examined on the continental shelf of the Western Spitsbergen in summer situation. The sampling area is influenced by northward flowing currents having different characteristics: the East Spitsbergen Current, close to the coast, carrying a substantial amount of terrigenous material, and the West Spitsbergen Current, offshore, that transfers heat, water and radionuclides from the mid-latitudes along the western Svalbard into the polar region. The bathymetry of the study area is characterised by two troughs, corresponding to the exit of Isfjord and Kongsfjord. Samples were taken in 1996 on the Isfjord Bank (St. B-05), near the margin of Isfjord trough (St C-05) and on Sjubre Bank, on the limit of the Kongsfjord trough (St. C-08). In summer 1997 the sampling was repeated at Station C-05 and a station near the shelf-break (St. BB-11), on the path of the Western Spitsbergen current was also examined.

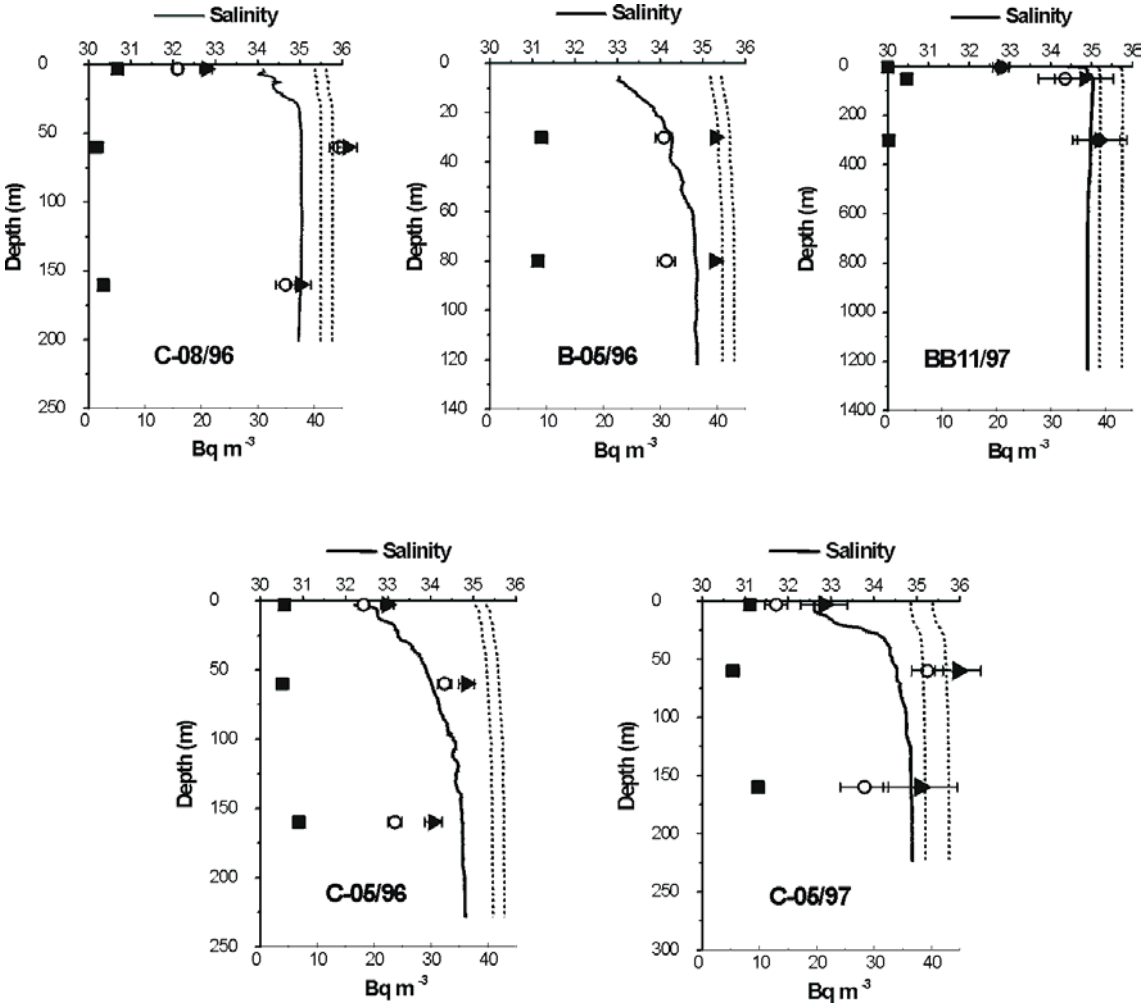

Figure 16. Vertical profiles of salinity, ^{238}U (----) and ^{234}Th (■ particulate; ● soluble; ▲ total) in the W-Spitsbergen continental shelf

At all stations, a marked disequilibrium between ^{234}Th and ^{238}U was present only near the surface, while equilibrium conditions were usually established below 60 m. The layer 0–60 m corresponds to the euphotic zone at these latitudes, in summer. Thus it is likely that biogenic particle production and cycling are the dominant processes controlling thorium scavenging.

Only at Station C-05, in 1996, total ^{234}Th concentration was far from equilibrium with ^{238}U at 160 m, probably not only in relation to vertical transport, but also to particle resuspension inside the Isfjord trough. Sampling at this station was repeated in summer 1997: again, a marked ^{238}U/^{234}Th disequilibrium was present near the surface, but equilibrium was established all along the water column, below 60 m.

4.5.2. Fjord areas

Kongsfjord, located in the North-western part of Spitsbergen, is divided by a sill about 50 m deep into two main basins: the inner one, with a maximum depth of about 90 m and strongly influenced by the inputs of two glaciers (Kongsvegen and Kongsbreen); the outer one, deeper (up to 300 m), which communicates directly with the Greenland Sea through Kongsfjordrenna, a depression which crosses the continental shelf and terminates on the slope. Three stations were examined in Kongsfjord: two of them, KO-1 and KO-2 are situated in the outer fjord at water depths of 250 m and 320 m; the third one (KO-4) is in the inner fjord, near Kongsbreen front. At all stations the suspended particle load increases from surface to the bottom and is lower at Station KO-2 than at station KO-1, probably in relation to the major distance from the glaciers. In both cases, scavenging processes are quite efficient, as a disequilibrium between ^{238}U and ^{234}Th is observed at all depths.

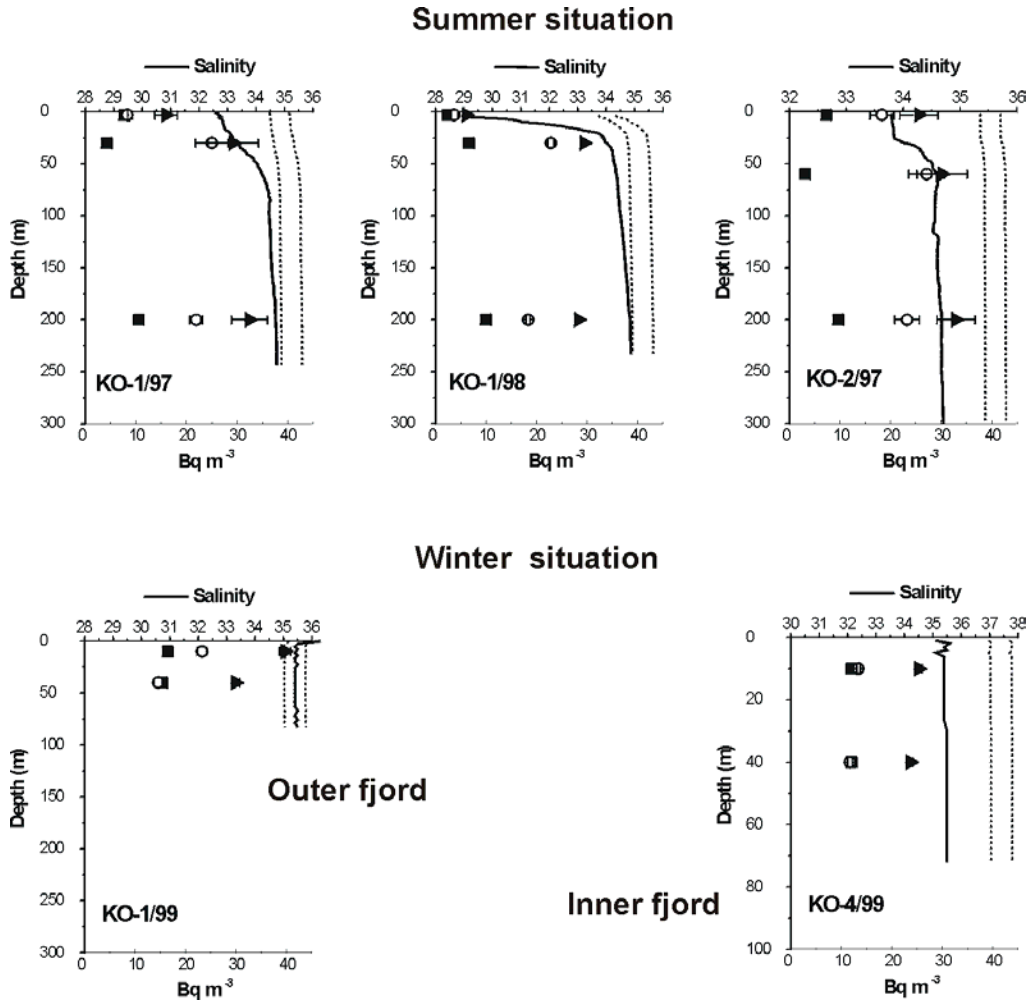

Figure 17. Vertical profiles of salinity, ^{238}U (----) and ^{234}Th (■ particulate; ● soluble; ▲ total) in Kongsfjord

Station VM-1 is located in the inner part of Van Mijen Fjord at a water depth of 75 m, in an area characterised by the input of freshwater and particulate matter coming from rivers and directly from glacier ice melting. Also in this station ^{234}Th is far from equilibrium with ^{238}U all along the water column.

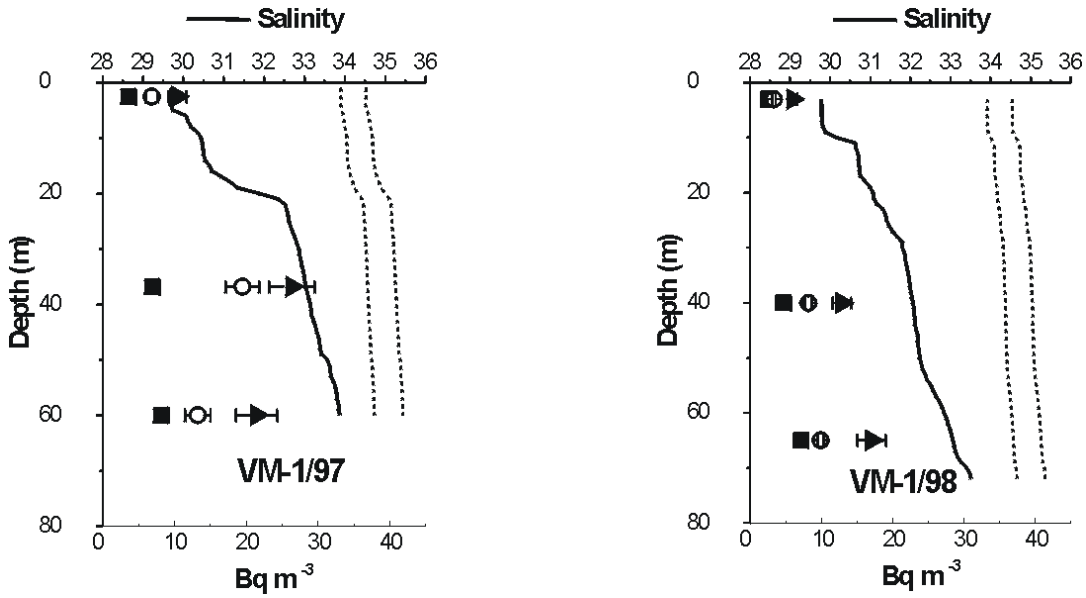

Figure 18. Vertical profiles of salinity, ^{238}U (----) and ^{234}Th (■ particulate; ● soluble; ▲ total) in Van Mijen Fjord

The sampling was repeated at Stations KO-1 and VM-1 in late summer 1998: again, at both stations, a disequilibrium was present all along the water column. However, the extent of the disequilibrium was higher in 1998, in relation to higher particle population near the surface, with respect to the summer of 1997.

The measurements carried out in the winter situation (1999) show that in Kongsfjord, despite the ice covering, scavenging processes on short time scales are active, particularly near the glacier front (St. KO-4/99), where suspended particle population is relatively high and a disequilibrium between ^{234}Th and ^{238}U is present all along the water column.

4.5.3. Thorium fluxes and residence times

In the shelf stations, fluxes and residence times have been calculated in the depth layer 0 to 60 m, corresponding to the limit of the euphotic zone, assuming that thorium scavenging in this environment is mainly due to association with biogenic particles. For the fjord stations, where particle supply from land is significant, the data were integrated over the whole water column (300 m in Kongfjord and 60 m in Van Mijen Fjord). The results are reported in Table 8.

Thorium removal from the water column is more efficient in the fjords than on the continental shelf. In fact, when considering the same depth interval (0–60 m), thorium fluxes from solution onto particles (J_{Th}) and particulate thorium fluxes from the water column to the sediment (P_{Th}) are about double in Van Mijen Fjord than in the shelf stations. Consequently, thorium residence times in soluble and particulate form are much shorter in the fjord area. Thorium fluxes are even higher in Kongsfjord, but this is mainly related to the deeper water layer (0–300 m) we have considered.

Sampling has been repeated at selected stations in different years both in the fjord and on the shelf. The characteristics of uranium and thorium vertical profiles are usually very similar also in different years: disequilibrium in the upper 60 m on the shelf and all along the water column in the fjords. However, in summer 98, the disequilibrium in the surface layer in both fjords was more pronounced than in 1997, and consequently thorium fluxes were 20–30% higher. This is likely related to the suspended particle load that was indeed about double in 1998.

These results indicate that the particles exported from land can effectively scavenge particle-reactive radionuclides inside the fjords. These particles are mainly deposited in the fjord area and do not reach the continental shelf, where scavenging processes appear to be controlled mainly by the cycling of biogenic particles.

Table 8. Thorium scavenging rates and residence times in the W-Spitsbergen continental shelf and fjords

Sampling site	J_{Th} (Bq m^{-2} d^{-1})	P_{Th} (Bq m^{-2} d^{-1})	τ_{diss} (d)	τ_{part} (d)	Reference
Svalvard shelf†	23–25	13–19	60–95	14–30	This work
VanMijen Fjord†	41–55	30–48	8–21	6–12	This work
East Greenland shelf†	6–23	4–16	52–293	6–52	Cochran *et al.* (1995)
Kongsfjord‡	93–120	59–76	32–52	20–23	This work
Arctic Ocean‡		1–45			Moran *et al.* (1997)

Svalvard shelf	Chlorophyll-a biomass residence time measured by sediment traps	18–29

† depth interval: 0–60 m
‡ depth interval: 0–300 m
Note: J_{Th} is the rate of removal of dissolved Th onto particles; P_{Th} is the rate of removal of particulate Th due to particle sinking; τ_{diss} and τ_{part} are the residence times of dissolved and particulate ^{234}Th with respect to scavenging onto particle and particle sinking, respectively

4.6. Sedimentation rates

Sedimentation rates in a number of different Arctic environments were determined in the course of the programme by the analysis of radionuclide profiles and inventories in selected sediment cores. The results reported relate to the following environments:

- the continental shelf of western Spitsbergen, at the same locations as those at which scavenging rates and particle residence times were estimated, as well as inside Kongsfjord (SVA ’96, ’97 and ’98 expeditions)
- the Russian Arctic continental shelf (Tundra ’94 expedition) and the Central Arctic
- the Stepovogo, Tsivolky and Abrosimov Fjords, Novaya Zemlya Trough, north-east Kara Sea and Yenisey Estuary.

4.6.1. Svalvard shelf and fjords

The vertical profiles of ^{137}Cs and unsupported ^{210}Pb in cores from the W-Spitsbergen shelf and fjords are shown in Figures 19 and 20. In the shelf cores (Figure 19), ^{137}Cs is only present in the upper 8–10 cm and its concentration usually decreases from surface values of 2–10 Bq kg^{-1}

to undetectable values below 10 cm. The inventories (Table 9) range from 40 Bq m^{-2} at Station C-08, the deepest one, to 400 Bq m^{-2} at Stations C-05, located in Isfjord trough. Unsupported ^{210}Pb is also only present in the upper 8–10 cm. Its concentration in the surface layers varies from 60 Bq kg^{-1} at stations B-05 and C-08 to maximum values of 250 Bq kg^{-1} at station C-05. The inventories of excess ^{210}Pb in the shelf range from 1.3 kBq m^{-2} at St. C-08 to 7.5 kBq m^{-2} at St. C-05.

Among the shelf stations, Stn. C-05 shows the highest inventory of both ^{137}Cs and unsupported ^{210}Pb. This is probably due to the fact that this station is located at the margin of a trough, where slumping processes can transport surface sediment from elsewhere, thus enhancing the total quantity of both radionuclides. Moreover, as discussed above, at this station a marked disequilibrium between ^{234}Th and ^{238}U indicates that scavenging processes are active in the deeper water layer, probably in relation to bottom morphology, that favours particle resuspension in the trough. Pb-210, being particle reactive, can also be effectively scavenged from the water column, thus leading to the observed high concentrations and inventory.

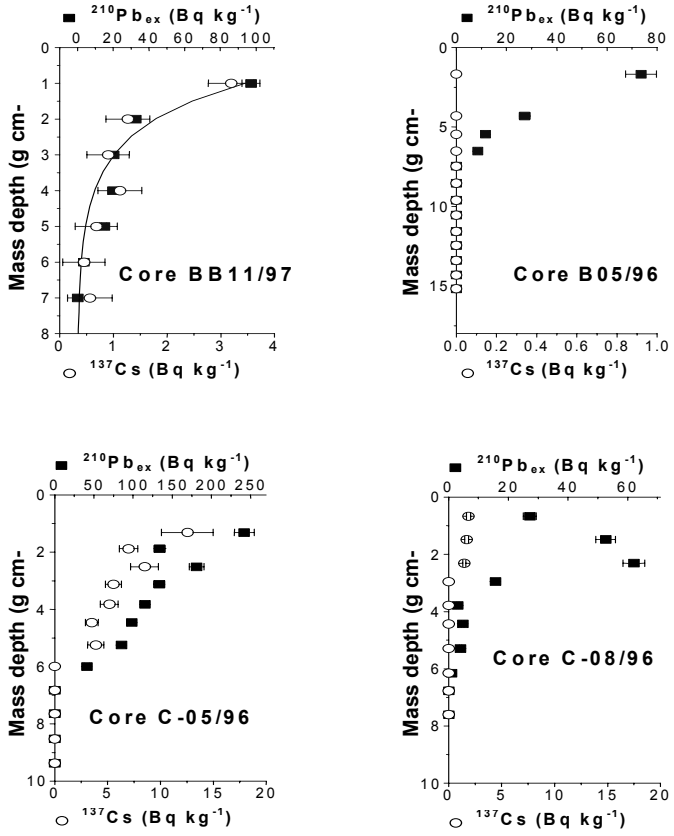

Figure 19. Vertical profiles of ^{137}Cs and $^{210}Pb_{excess}$ in sediment cores from the W-Spitsbergen shelf

In general, the vertical radionuclide profiles on the W-Spitsbergen shelf seem to be mainly controlled by mixing processes, as:

(1) radionuclide penetration into the sediment is relatively low: it never exceeds 10 cm, which is a depth compatible with physical and/or biological mixing;

(2) the vertical profiles of ^{137}Cs and unsupported ^{210}Pb have usually the same shape, including subsurface maxima. As the two radionuclides have different input functions (constant input for ^{210}Pb and maximum in 1963 for ^{137}Cs), this feature clearly points

to low sedimentation rate and penetration into the sediment mainly controlled by mixing.

Table 9. ^{137}Cs and $^{210}Pb_{excess}$ inventories in sediment cores of W-Spitsbergen and estimated accumulation rates

Station	Maximum penetration length (cm)		Inventory (kBq m^{-2})		Accumulation rate (g cm^{-2} y^{-1})
	^{137}Cs	$^{210}Pb_{excess}$	^{137}Cs	$^{210}Pb_{excess}$	
Svalvard Shelf					
C-08/96	5	10	0.04 ± 0.02	1.3 ± 0.3	<0.15
C-05/96	10	11	0.4 ± 0.2	7.5 ± 0.9	<0.15
B-05/96	6	7	0.2 ± 0.1	2.9 ± 0.6	<0.15
BB-11/97	4	6	0.10 ± 0.05	4.9 ± 0.9	<0.15
Svalvard Fjords					
V3A/98	>60	>60	>1.9	>10.3	-
Be8/98	>30	26	2.0 ± 0.4	3.3 ± 0.6	-
KO-1/96	8	28	0.4 ± 0.2	10.1 ± 1.2	0.14 – 0.25
KO-2/97	5	6	0.11 ± 0.05	3.2 ± 0.6	<0.1
VM-1/97	20	>21	>2.4	>4.6	0.12 – 0.33

The situation is different inside the fjords: relatively large amounts of terrigenous particles are present, due to ice melting, and the hydrodynamics of the area allows particle settling. This is clearly reflected in the vertical profiles of ^{137}Cs and of the excess ^{210}Pb (Figure 20). In Van Mijen Fjord ^{137}Cs is detectable down to 20 cm and shows a subsurface maximum at a mass depth of 12 g cm^{-2}. This indicates an average sediment accumulation rate in the order of 0.33 g cm^{-2} y^{-1}. However, the vertical profile of excess ^{210}Pb is quite disturbed all along the core, reflecting changes in sedimentation rate. To determine this parameter we have then used the CRS (constant rate of supply) hypothesis. The average sediment accumulation rate derived from ^{210}Pb in this way is about 1/3 that estimated by ^{137}Cs subsurface maximum. This may be partly due to downward transport of caesium, but could also be related to the assumption of constant supply of ^{210}Pb that, in this highly dynamic environment, could be inappropriate.

In Kongsfjord, sediment cores have been collected along a transect, with two samples in the inner fjord, near the glaciers front (Cores V3 and Be8), and two in the outer fjord (KO-1 and KO-2), where also scavenging processes have been studied.

In the inner fjord, ^{137}Cs and excess ^{210}Pb are present in all layers (down to 60 cm), without a clear trend, indicating fast sediment accumulation and mixing processes.

In the central Kongsfjord (station KO-1), $^{210}Pb_{ex}$ exponentially decreases from surface to depth. At this station the sediment accumulation rate has been estimated using two different models: the constant flux-constant sedimentation rate and the constant rate of supply (CRS) model. In the first case, we estimate a sediment accumulation rate of 0.18 g cm^{-2} y^{-1}. This sedimentation rate is also in good agreement with the profile of ^{137}Cs, whose penetration into the sediment is 8 cm. When calculating the age of each sediment layer, using the CRS model, we obtain two layers, characterised by different accumulation rates: 0.14 g cm^{-2} y^{-1} in the deeper layers and 0.25 g cm^{-2} y^{-1} in the last 60 years.

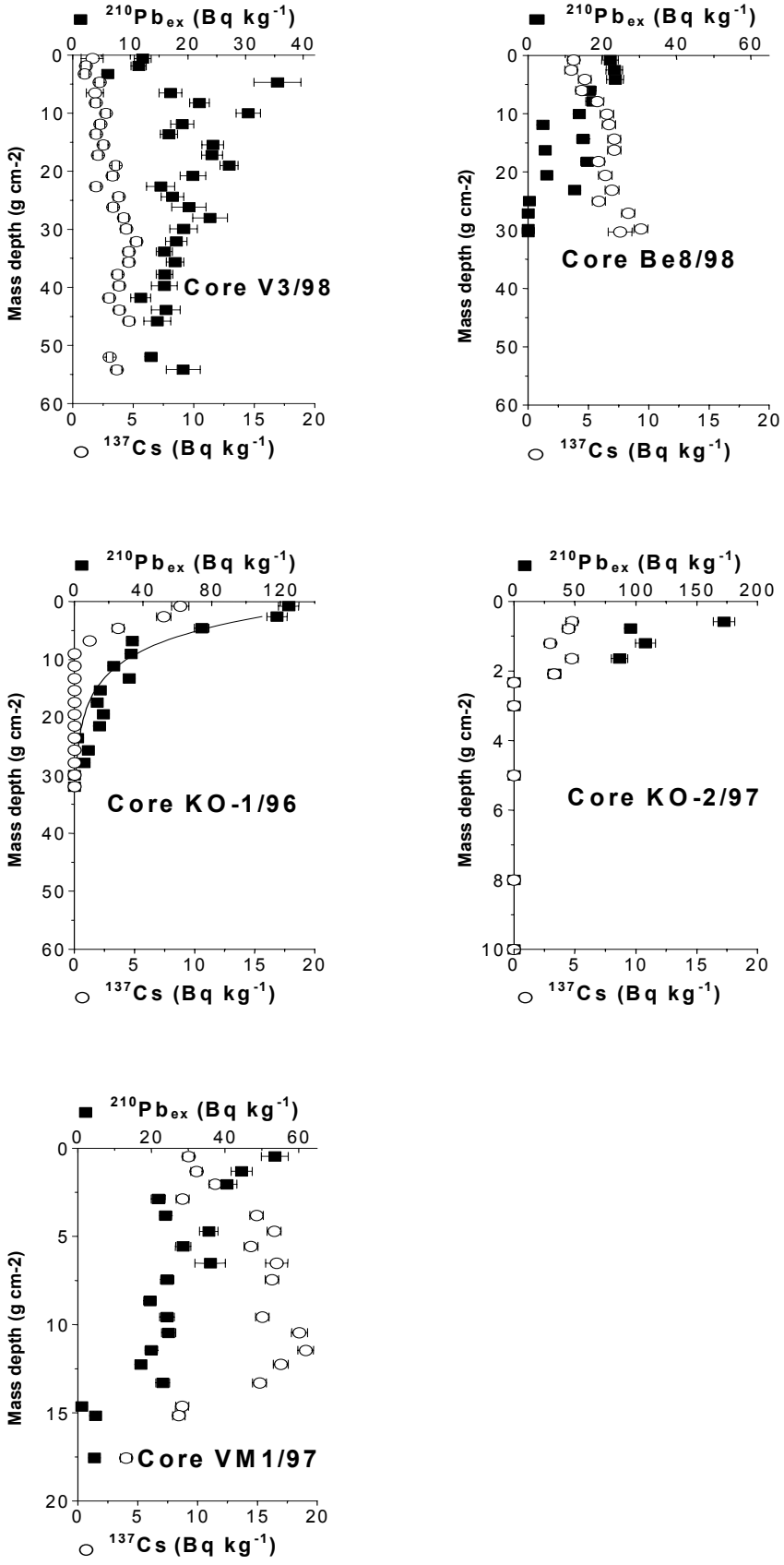

Figure 20. Vertical profiles of ^{137}Cs and $^{210}Pb_{excess}$ in sediment cores from two W-Spitsbergen Fjords: KO = kongsfjord; VM = Van Mijen Fjord

The vertical radionuclide profiles at station KO-2, in the outer fjord, are very similar to those characterising the shelf. ^{137}Cs and excess ^{210}Pb are present in the upper 5 cm, show exactly the same trend and are mainly controlled by mixing processes.

4.6.2. The Russian Arctic continental shelf and the Central Arctic Ocean

In the course of the Tundra '94 and the Arctic '96 expeditions, a large number of sediment cores were collected for the determination of radiocaesium and plutonium inventories along the Eurasian Arctic shelf and throughout the Central Arctic Ocean. The integrated ^{137}Cs and ^{239,240}Pu inventories, together with the co-ordinates, water column depth and radionuclide penetration depth are given in Table 10. Although 15 cores from the Eurasian shelf were analysed, it only proved feasible to estimate radionuclide inventories for five of these cores, as radionuclide penetration beyond the sampling depth occurred for the remainder. The variability in depth penetration and the presence of radionuclides deep in the sediment column indicates intense sediment mixing in the shelf seas. Based on the calculated inventories for the five complete cores (T94), radionuclide deposition inventories in the Kara, Laptev and East Siberian Seas are estimated to be in the range 100–800 Bq m^{-2} and 5–35 Bq m^{-2} for ^{137}Cs and ^{239,240}Pu, respectively. In contrast, the corresponding figures for the Central Arctic Ocean (AO96) are much smaller, at 15–100 Bq m^{-2} and 0.2–1.3 Bq m^{-2}, respectively. The larger deposition on the shelf reflects the higher sedimentation rates prevailing on these shallow zones. Comparison of sediment column inventories with time-integrated water column inventories estimated from reported sea water profiles (Table 11) indicate that approximately 10% of the ^{137}Cs and 75% of the ^{239,240}Pu which have entered the shelf seas have been deposited on the shelf sediment, while the corresponding figures in the Central Arctic are 0.3% and 0.9%. These figures indicate that while the Arctic shelf acts as a sink for particle-reactive elements, only a very small fraction of the total inventory is deposited on the sea-floor of the Central Arctic during the time it takes the water to pass through the basin.

Table 10. Sampling stations and estimated ^{137}Cs and ^{239,240}Pu inventories in sediment cores from the Russian continental shelf (T94) and the Central Arctic Ocean (AO96)

Station	Co-ordinates	Water depth (m)	Activity penetration depth (cm)	^{137}Cs (Bq m^{-2})	^{239,240}Pu (Bq m^{-2})
(T94) 9	70°14'N 66°17'E	20	19	556 ± 67	29 ± 3
(T94) 14	76°11'N 93°34'E	55	8	217 ± 11	
(T94) 18	75°08'N 129°50'E	58	9	393 ± 17	
(T94) 21	74°50'N 137°32'E	20	14	836 ± 60	34 ± 3
(T94) 28	70°16'N 170°26'E	30	7	119 ± 8	4.9 ± 0.4
(AO96) A6	85°34'N 72°17'E	3780	1	17 ± 3	0.42 ± 0.03
(AO96) A8	87°05'N 129°30'E	3762	3	21 ± 2	
(AO96) A9	86°23'N 144°20'E	995	4	89 ± 5	1.32 ± 0.07
(AO96) A23	87°11'N 144°34'E	980	4	79 ± 6	
(AO96) A24	86°28'N 130°55'E	4150	3	33 ± 3	
(AO96) A27	85°21'N 149°15'E	1110	4	104 ± 8	0.96 ± 0.07
(AO96) A30	85°32'N 156°29'E	2388	2	31 ± 2	
(AO96) A31	85°39'N 160°35'E	3586	1	15 ± 2	
(AO96) A35	88°49'N -178°42'E	1113	2	33 ± 4	0.24 ± 0.04
(AO96) A37	89°00'N 179°55'E	2271	3	35 ± 3	0.35 ± 0.04
(AO96) A39	87°17'N 22°28'E	4180	0.5	41 ± 5	
(AO96) A40	85°31'N 12°03'E	2360	2	44 ± 6	
(AO96) A41	84°02'N 11°18'E	3270	2	24 ± 6	0.30 ± 0.04

Table 11. Fraction of the time-integrated water inventory deposited on the Arctic shelf and the Central Arctic Ocean

	^{137}Cs			^{239,240}Pu		
	Kara Sea	Laptev Sea	Central Arctic	Kara Sea	Laptev Sea	Central Arctic
Time-integrated water inventory (Bq m^{-2})	3900	6000	8800	8	12	46
Mean sediment inventory (Bq m^{-2})	400	800	43	30	34	0.6
Fraction deposited	9%	12%	0.5%	79%	74%	1.3%

The ^{238}Pu/^{239,240}Pu activity ratio in both water and sediment indicate that global fallout is the main source of plutonium to the shelf. Variations in plutonium inventories along the shelf most likely relate to differences in sedimentation rates, although water circulation effects can also contribute to the observed differences. For example, the low inventory in the East Siberian Sea (Stn. 28) agrees well with the low ^{137}Cs, ^{134}Cs and ^{129}I water concentrations recorded in the course of the same expedition. The sharp decrease in low ^{137}Cs, ^{134}Cs and ^{129}I concentrations between the Laptev and East Siberian Seas is due to the influence of Pacific waters (carrying only the fallout signal) to the East Siberian Sea. On the other hand, the large river outflow into the Laptev Sea, mainly from the river Lena, provides large quantities of sedimentary material onto which dissolved radionuclides may attach before settling, leading to higher inventories.

In the Central Arctic Ocean, the highest inventories of both radiocaesium and plutonium are found at the shallow (~1000 m) stations of the Lomonosov Ridge, and significantly lower in the Eurasian Basin. From ^{230}Th sediment distributions, the annual sediment deposition flux has been determined to be 10–20 g m^{-2} in the Nansen Basin and below 5 g m^{-2} in the Gakkel Ridge (Bohrmann, 1991). Sedimentation rates are estimated to be ~3 mm Ky^{-1} in the Nansen Basin, 3–6 mm Ky^{-1} in the Gakkel Ridge, and 3 mm Ky^{-1} in the eastern Lomonosov Ridge at 85°N (Bohrmann, 1991; Somayajulu *et al.*, 1989). Thus, the variations in inventories observed throughout the Central Arctic stations can not be explained on the basis of difference in sedimentation rates but are more likely related to the circulation pathway of surface and Atlantic waters within the Arctic interior.

4.6.3. Other Arctic environments

Sediment cores were also taken from the Stepovogo, Tsivolky and Abrosimov Fjords, the Novaya Zemlya Trough, the NE Kara Sea and the Yenisey Estuary. Sedimentation rates, derived from the measured ^{210}Pb$_{excess}$ profiles (Figure 21), are given in Table 12.

Table 12. Estimated sedimentation rates in a selection of Arctic environments

Location	Sample Code	Sedimentation rate (mm y^{-1})
North east Kara Sea	Karex'94 Stn. 32	0.6
Yenisey Estuary	Karex'94 Stn. 84	0.5
Novaya Zemlya Trough	Stn. 8–1–7	-
Abrosimov Fjord	Stn. 10	1.1
Stepovogo Fjord	Stn. 12	0.6
Tsivolky Fjord	Stn. 3–1–6	0.6

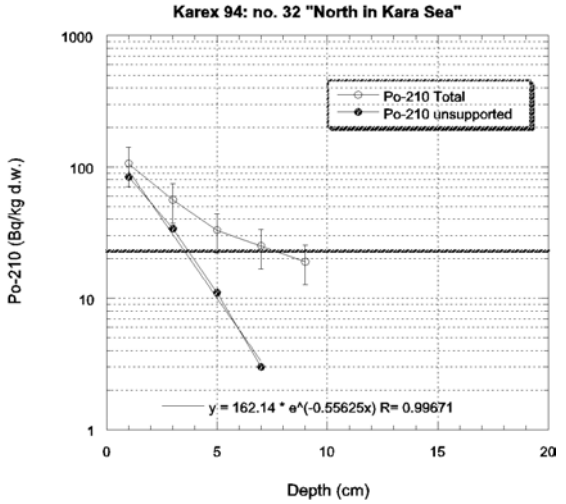

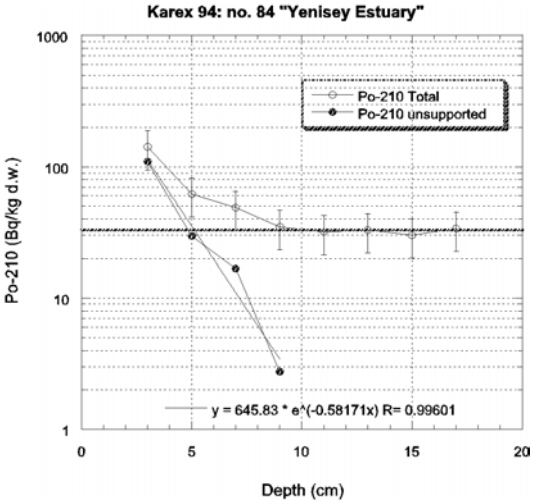

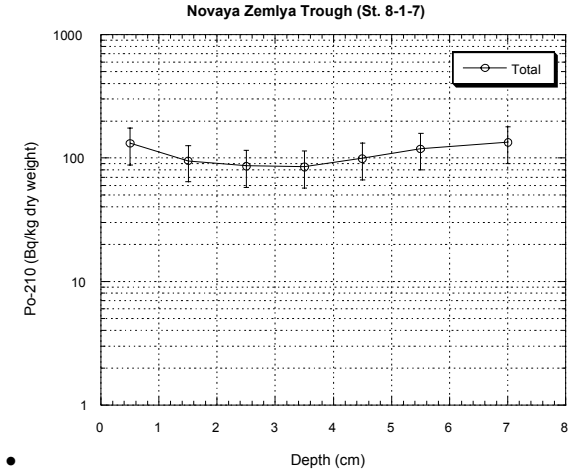

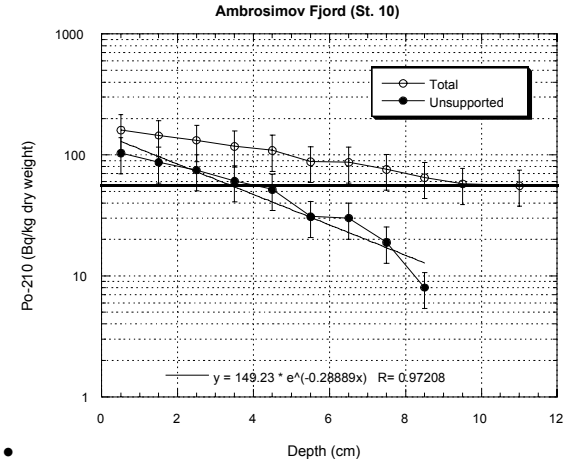

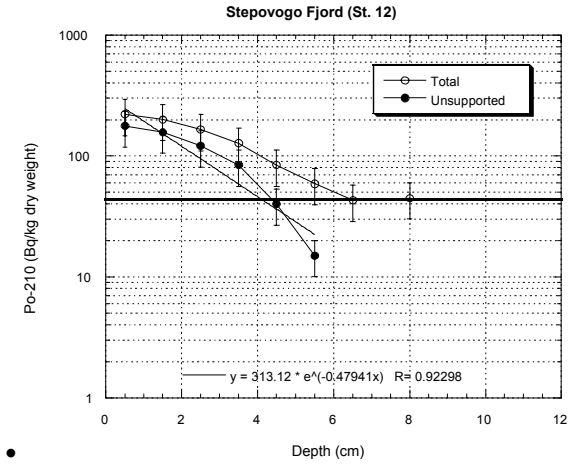

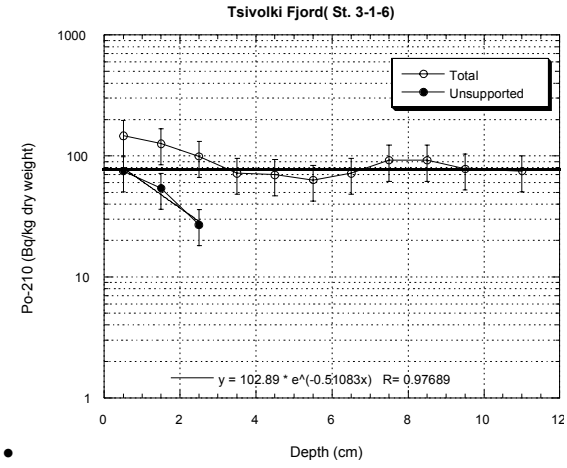

• **Figure 21.** $^{210}Pb_{excess}$ profiles at selected Arctic sites

4.7. Role of speciation on biological uptake

Laboratory experiments were undertaken in the course of the programme with a view to examining the influence of speciation and solid partition of radionuclides on biological uptake. Filtering (*Mytilus edulis*, blue mussel) and non-filtering (*Scopthalmus maximum*, turbot) organisms were exposed to ^{134}Cs in both ionic and particulate forms. The results suggest that for *Mytilus edulis* the initial concentration factor (CF, Bq kg^{-1} biota per Bq l^{-1} water) is higher (factor >10) following exposure to contaminated particles compared to ionic uptake. After about 48 hours, however, most of the particles have passed through the gut of the blue mussel and the undigested sediment has been excreted (Figure 22). For turbot, the results indicate that the uptake of ^{134}Cs is a factor of 3 higher following exposure to the ionic form as opposed to contaminated particles. Thus, CF will vary depending on the speciation of the radionuclide and the nature of the organism.

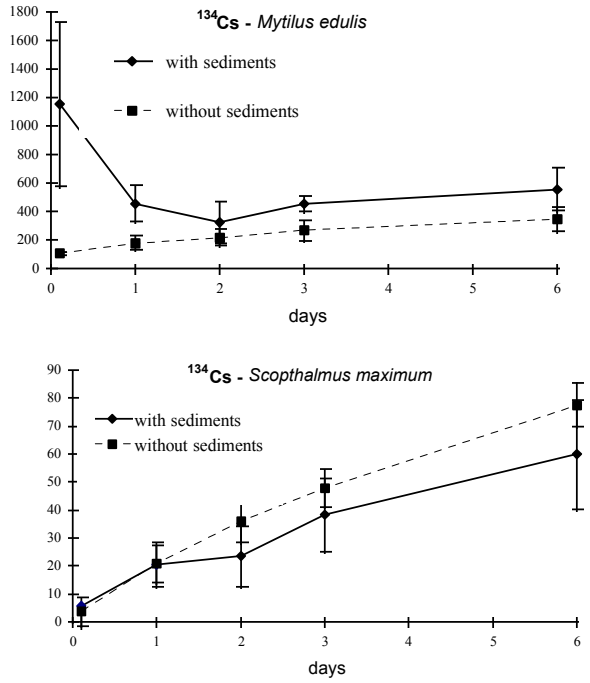

Figure 22. Comparative uptake of ^{134}Cs in *Mytilus edulis* and *Scopthalmus maximum* exposed to ^{134}Cs tracer added to sea water in ionic and particulate form (n = 5; ± 1 S.D.). The vertical axis has a relative scale of arbitrary units that is corrected for organism weight and makes the figures comparable

5. Reactivity at the fresh water/sea water interface

In natural environments, interfaces are privileged locations for the study of reactive processes yielding drastic changes in radionuclide physical and chemical forms. Interfaces are characterised by strong gradients, which can lead to important changes in the solid/liquid partitioning of certain radionuclides, altering their mobility and bioavailability. It is for this reason that special attention was paid by the ARMARA collaboration to two interfaces considered to be of great importance for the radiological assessment of the consequences of contamination of Arctic waters: the fresh water/sea water interface and the sediment/sea water interface. In the following sections, we present the results obtained in a number of studies carried out at the fresh water/sea water interface. The results for the sediment/sea water interface are discussed in WP6.

5.1. Particulate/colloidal/dissolved radionuclide partitioning along salinity gradients

Most of land-derived radionuclides are brought by the rivers to the open ocean through complex mixing zones (estuaries and deltas). In response to changing environmental parameters (salinity, DOC, suspended particulate load, etc.), radionuclides undergo a number of reactions such as dissolution, complexation, precipitation, etc. These reactions involve particulate, colloidal and dissolved phases, and yield changes in the solid-liquid radionuclide partitioning between these phases. Since sampling along the estuaries of the big Siberian rivers was denied by Russian authorities during the duration of the programme, our studies on radionuclide reactivity at the fresh water/sea water interface, from which to infer probable transformations in the estuaries of the Ob, Yenisey and other Siberian rivers, were focused on more readily accessible estuarine environments, namely the Seine and the Rhône estuaries (France).

5.1.1. The non-conservative behaviour of plutonium in the Seine estuary

The reactivity of plutonium at low salinities in the Seine estuary had already been demonstrated in previous studies (Garcia, 1996; Garcia *et al.*, 1996). Consequently, plutonium was chosen as a marker for the processes taking place at the fresh water/sea water interface, with emphasis on the role of colloids in the partitioning of this element between solid and 'dissolved' (<0.45 μm) fractions.

Water samples were collected in the estuary from aboard the R.V. *Thalia* during a week-long expedition in April 1997. Large-volume (100–300 l) surface samples were collected across the full salinity gradient (salinities 30, 15, 10, 4, 1.4, 0.8 and 0‰) using the ship's deck pump. The samples were immediately filtered through glass microfibre pre-filters connected in series to large area, 0.45 μm cellulose nitrate filters. At four of the stations (salinities 30, 4, 1.4 and 0.8‰), tangential flow ultrafiltration of the (nominally) dissolved phase was carried out *in situ* using 10 kDa membranes.

The plutonium concentrations in filtered water samples were found to be very low, being in the range 0.1–1.8 and 0.3–4.5 for ^{238}Pu and ^{239,240}Pu, respectively. The ^{238}Pu/^{239,240}Pu ranged from 0.3 (at the fresh water end-member) to 0.7 (close to the sea water end-member) and are typical of mixing between riverine inputs and sea water masses labelled by the La Hague reprocessing plant. The evolution of 'dissolved' plutonium concentrations versus salinity (Figure 23) clearly indicates that plutonium behaves non-conservatively in the Seine estuary, with low-salinity waters being substantially enriched in plutonium and intermediate-salinity waters being depleted in plutonium relative to the theoretical dilution line. This departure from the mixing or dilution line is indicative of solution loss or gain relative to the particulate phase, a feature already reported for the Seine Estuary (Garcia *et al.*, 1996) and the Esk Estuary (Cumbria, UK), the latter affected by discharges from the Sellafield reprocessing plant (Eakins *et al.*, 1985; Assinder *et al.*, 1984).

Experiments conducted by these and other workers have demonstrated that the presence of excess dissolved plutonium at low salinities is related to the rapid desorption of plutonium from suspended particles and sediments when exposed to fresh water during the tidal cycle. The loss of plutonium from the dissolved phase at intermediate salinities in the Seine Estuary has been shown to be due to the rapid reduction of Pu(V,VI) upon contact with riverine water and the subsequent sorption of the resulting reduced species onto suspended particles (Garcia *et al.*, 1996).

The partitioning of plutonium between colloidal and dissolved phases in the micro-filtered (<0.45 μm) fraction at different stations along the salinity gradient is shown in Figure 24. At high salinity (30‰), the percentage of plutonium in colloidal form was found to be ~8%. This low value appears to be similar to that reported in certain other coastal environments (Mitchell *et al.*, 1995) and supports the view that the bulk of the filtered plutonium entering the estuary is in an oxidised, fully dissolved form. Indeed, measurements carried out by our laboratory at two

stations in the open waters of the English Channel during 1994 showed the bulk (77 ± 2%) of the plutonium to be in oxidised form (León Vintró, 1997). At low salinities, the percentages of colloidally-bound plutonium increased, reaching a maximum at a salinity of 1.4‰, where the maximum in excess plutonium was also observed. A plot of the dissolved and colloidal concentrations in the filtered fractions (Figure 24) shows that while dissolved plutonium is progressively removed towards lower salinities as a result of dilution and removal by particles, the colloidal component would appear to be responsible for most of the observed plutonium excess at these low salinities.

This means either that plutonium is being directly released from the sediment in a colloidally-bound form, or that it is being released as species that can readily associate with riverine colloidal material. We favour this last explanation, as laboratory experiments based on sequential leaching have demonstrated that the remobilised plutonium is being desorbed from the sediment oxy-hydroxide fraction as a result of the dissolution of weakly-bound iron and manganese oxides (Garcia, 1996).

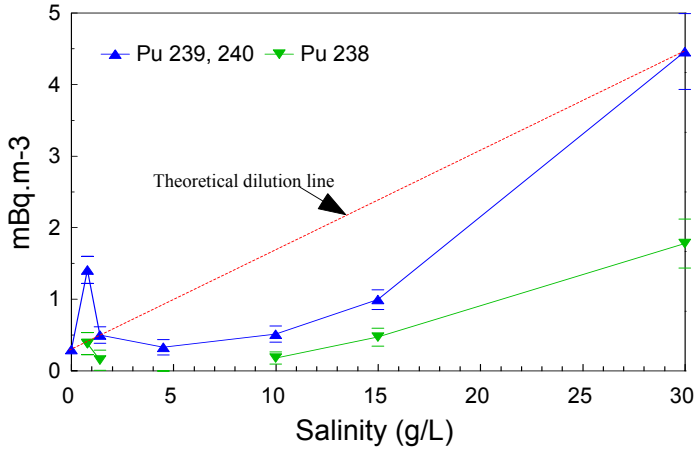

Figure 23. Plutonium concentrations in filtered water across the Seine estuary salinity gradient (April 1997)

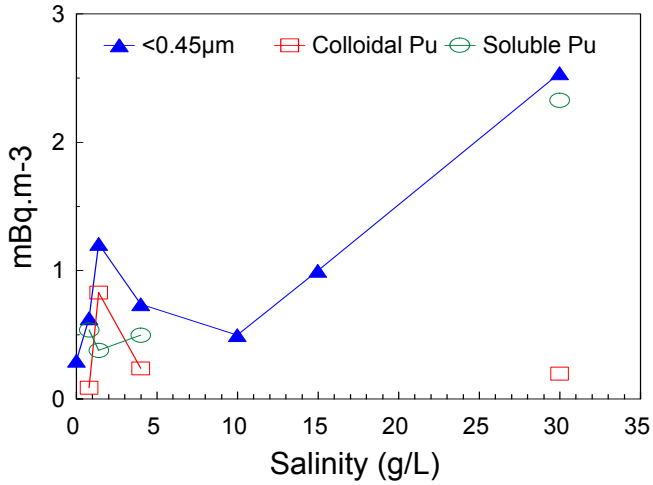

Figure 24. Soluble (<10 kDa), colloidal (10 kDa – 0.45µm) and 'dissolved' (<0.45 µm) ^{239,240}Pu concentrations in waters sampled across the salinity gradient in the Seine estuary

5.1.2. Evidence of colloidal radionuclides in the Rhône estuary

The partition of radionuclides between particles, colloids and true solution was also studied within the fresh water/sea water interface of the Rhône Estuary (affected by direct radionuclide discharges from the Marcoule reprocessing plant) using a large volume sequential ultrafiltration system. About 80 fractionated subsamples collected in the course of four separate expeditions were analysed for organic content, major elements and anthropogenic radionuclides (^{60}Co, ^{106}Ru and ^{137}Cs). The results indicate that, under low river discharges (900 and 1500 m^3 s^{-1}), 11–15% of the total organic carbon is present in the colloidal phase (>2 nm). While ^{137}Cs is not significantly transferred by colloidal compounds, up to 25% of both ^{60}Co and ^{106}Ru is associated with organic and inorganic colloids. At higher salinities (31‰), colloidal iron and aluminium constitute 40% of the dissolved (>0.45 μm) phase and 15% of the total concentrations. These percentages are lower at depth (37‰). With the exception of ^{137}Cs, present as a truly dissolved species, no other anthropogenic radionuclides were detectable at these higher salinities. These results indicate that flocculation and sedimentation of colloidal substances in the Rhône Estuary may be a multi-step mechanism governed by vertical and lateral profiles, and underline the non-conservative behaviour of colloidal substances (in terms of surface properties) under fresh water/sea water mixing.

5.1.3. Behaviour of ^{137}Cs and ^{106}Ru in the Rhône estuary

The partitioning of ^{137}Cs and ^{106}Ru between the dissolved (<0.45 μm) and particulate phases was investigated at the Rhône river – Mediterranean Sea mixing zone. The Rhône river is one of the major rivers flowing into the Mediterranean Sea, with a large catchment area, an annual flowrate of 1700 m^3 s^{-1}, an annual liquid flow nearing 50 billion m^3 and an annual solid load of around 10^7 tonnes. It thus represents an ideal test-site to study processes governing the behaviour of artificial radionuclides at the fresh water/sea water interface. Besides, until 1997, the whole nuclear fuel cycle was represented with the facilities laying along the Rhône River. These industries were allowed to release in compliance with the legislation low activity liquid effluent into the Rhône River. The major part of the releases came from the Marcoule reprocessing plant which constituted 76.7% of beta gamma emitters input in the North Western Mediterranean Sea.

The mixing zone is highly stratified, with a deep salt wedge intrusion into the lower river course and a thin unstable surface plume extending several kilometres seaward according to wind stress and river discharge. Most of the particulate Rhône input settles on a relatively small area close to the river mouth. For instance, about two-thirds of the solid discharge accumulate over an area of 4000 km^2, representing only 17% of the total surface of the continental shelf in the Gulf of Lions, and a large fraction of the remaining input does not significantly escape the shelf area.

A sampling cruise was carried out in September 1997 in the Rhône River mouth in order to assess the radionuclide contents and their solid partition within the water column at the fresh water/sea water interface. The sampling locations are shown in Figure 25. At the Roustan Buoy station, an Eulerian sampling was achieved during 10 days during which the river flow rate was around 1200 m^3 s^{-1}. Samples were taken at depths of 1.5 and 5.5 m below the surface.

In the Grand Rhône river waters, the total (unfiltered) ^{137}Cs activities were correlated with the river flow rate in contrast with the total ^{106}Ru-Rh activities, which may mainly depend on the Marcoule reprocessing plant releases (Figure 26a). Beyond 1000 m^3 s^{-1}, the total ^{137}Cs activity swiftly tended to 2.0 $\pm$ 0.5 Bq m^{-3} which is the activity generally encountered in the North Western Mediterranean Sea. These trends were observed as well at the river mouth (Roustan Buoy station, surface samples): Under quasi-constant river flow rate (1200 m^3 s^{-1}), and for salinities ranging from 11 to 35 psu, the total ^{137}Cs activity was constant (2.0 $\pm$ 0.5 Bq m^{-3}) while the total ^{106}Ru-Rh activity was more varying, showing its probable dependence on the Marcoule releases (Figure 26b).

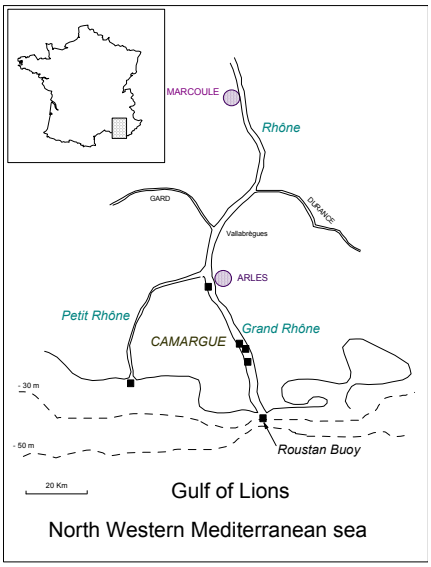

Figure 25. Sampling locations in the Rhône estuary (1997)

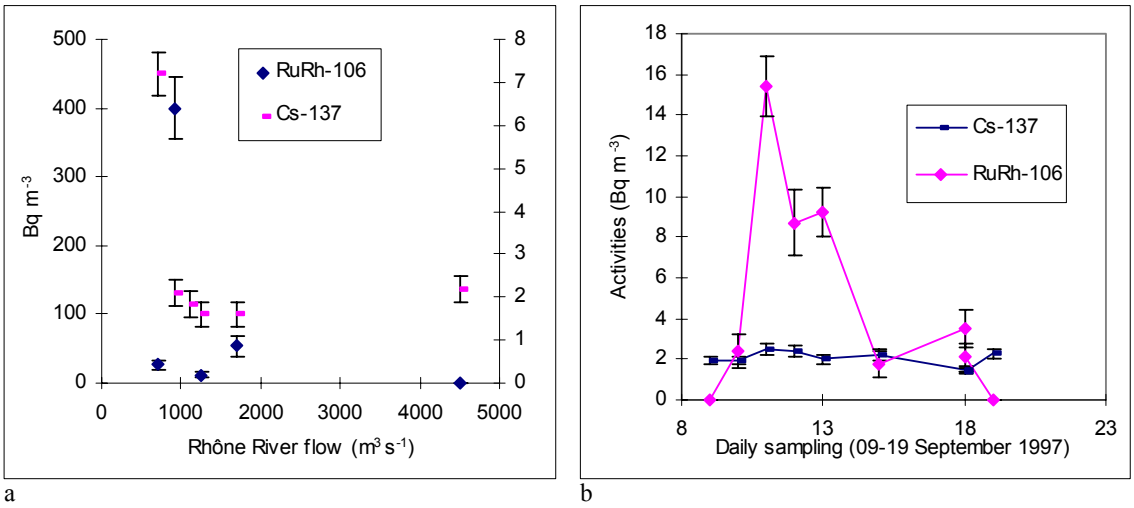

Figure 26. (a) Variation of the ^{137}Cs and ^{106}Ru-Rh total activities (Bq m^{-3}) with river flow; (b) daily measurements of ^{137}Cs and ^{106}Ru-Rh total activities (Bq m^{-3}) at the freshwater/sea water interface (Roustan Buoy Station)

The *in situ* solid-solution partitioning coefficient (K_d) for ^{137}Cs and ^{106}Ru-Rh were measured at different salinities. A plot of log K_d values versus salinity is shown in Figure 27. In the case of ^{137}Cs, the log K_d values show a general trend to decrease from 5.0 to 4.4 as the salinity rises from 0 to 35 psu, indicating a remobilisation of almost 65% of particulate caesium in the whole mixing zone. For ^{106}Ru-Rh, a 'particle concentration' effect, as first described by Honeyman *et al.* (1988), may explain the increasing log K_d values along the salinity gradient. Indeed, in the mixing zone the decrease of suspended particulate matter (SPM) concentrations, as shown in Figure 28, may bring the partitioning coefficient to its 'true' value. These observations are consistent both with the lowering of log K_d values with increasing SPM concentrations, observed only in the case of ruthenium, and the significant colloidally-bound ruthenium observed in the Rhône River waters. The results underline the uptake of ruthenium by colloidal substances present in the Rhône River and its estuary.

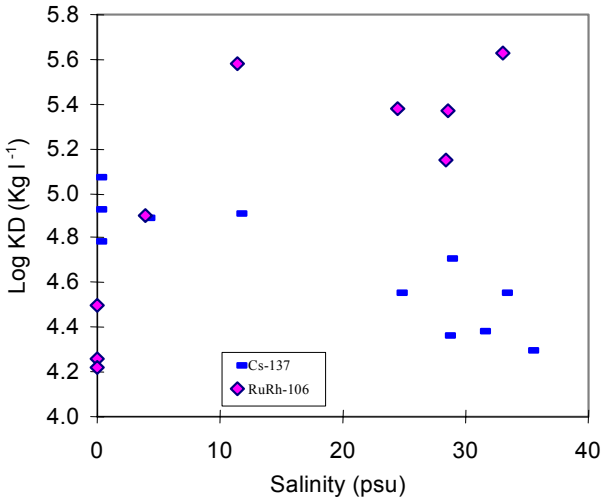

Figure 27. Distribution coefficient (K_d) for ^{137}Cs and ^{106}Ru-Rh as a function of salinity within the Rhône river mouth

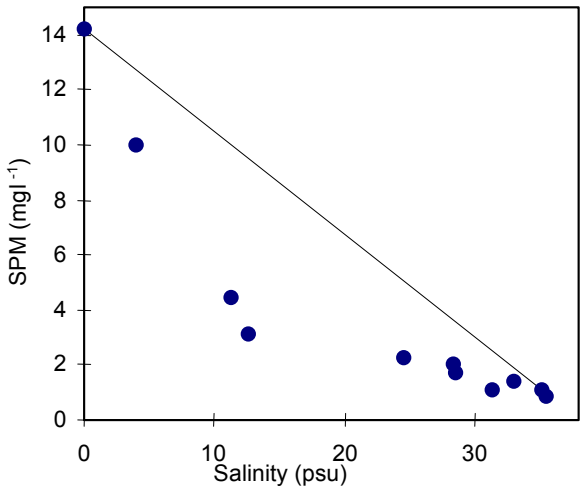

Figure 28. Variation of SPM concentration with salinity at the Rhône river mouth

5.2. Land-derived plutonium in the estuaries of Russian Arctic rivers

The Eurasian shelves are strongly influenced by riverine discharges from the large Siberian rivers. The main contributions are from the Ob and Yenisey rivers, which annually discharge 400 and 630 km^3 of fresh water into the Kara Sea, respectively, and the Lena river, with an annual discharge of 520 km^3 into the Laptev Sea. Most of the Siberian rivers draining into the Arctic Ocean pass wetlands over the tundra region. In such mire-like areas, concentrations of dissolved/colloidal organic carbon are elevated, enhancing the mobility of actinides. During spring run-off, these wetlands are flushed and the mobile fraction of actinides transported down the river. In the course of the Tundra '94 expedition, comparatively high plutonium concentrations were observed outside the mouths of the Yenisey, Lena and Yana rivers at salinities around 1–8 g l^{-1}. Time did not permit sampling in individual estuaries, but combination of all plutonium data along the shelves reveal a trend of increasing concentrations at lower salinities (Figure 29). From this graph, it is tempting to conclude that, as in the Seine and other more temperate estuaries, plutonium behaves non-conservatively at the fresh water/sea water interface. However, the mixing of water masses on the Arctic shelf is too complex to confidently consider just a simple two point end-member system.

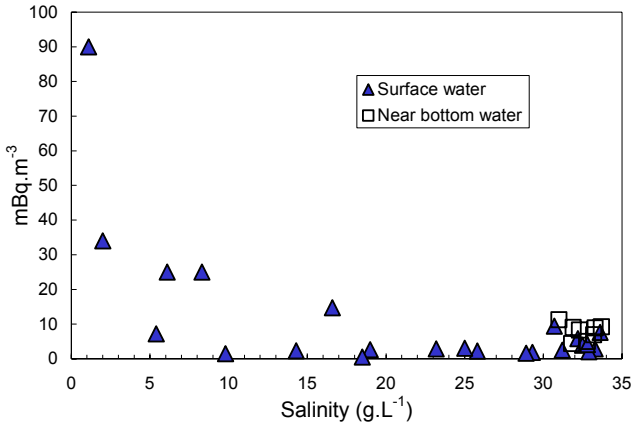

Figure 29. Plutonium concentration versus salinity in surface water from along the Siberian shelf

5.3. Sedimentation processes at the freshwater/sea water interface

The importance of sediment mixing in the redistribution of radionuclides within the sediment column in the Arctic shelf has already been signaled in Section 4.6.2. The same appears to be true for estuarine sediments affected by discharges from the large Siberian rivers. Radionuclide analysis of sediment cores collected in the estuaries of the Dvina river (flowing into the White Sea) and the Yenisey river (flowing into the Kara Sea) in 1993–94 show ^{137}Cs and ^{239,240}Pu profiles which are characteristic of mixing. The effect of riverine transport on these sediments is evidenced by an increase in the measured ^{137}Cs/^{239,240}Pu ratios, which is indicative of the presence of excess radiocaesium carried by the rivers from the large catchment areas in Siberia (Figure 30).

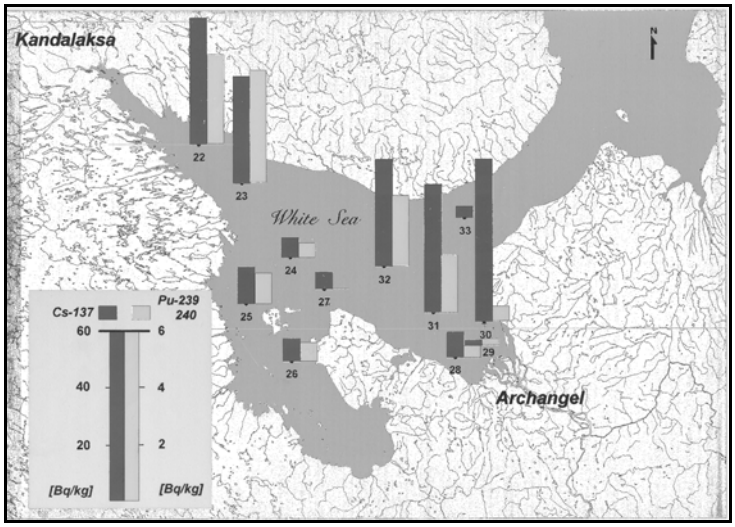

Figure 30. ^{239,240}Pu and ^{137}Cs concentrations in surface (0–2 cm) sediments in the White Sea in 1994. Note the difference in the relative proportions of these elements at Station 30, affected by the Dvina river discharge

During the White Sea expedition in 1994, samples were taken at eleven locations (Figure 30) using Van Veen grab, box corers or Niemistö cores. Undisturbed cores were only observed at Stns. 22 and 32. In Kandalskha Bay (Stn. 22; depth 290 m), ^{137}Cs concentrations decreased from 45 Bq kg^{-1} in the surface to undetectable levels below 15 cm. Plutonium isotopes were detectable

in the top 25 cm of the core. In the open White Sea (Stn. 32; depth 127 m), ^{137}Cs concentrations decreased from 38 Bq kg^{-1} in the surface layer to undetectable levels below 20 cm, and the ^{239,240}Pu and ^{238}Pu concentrations from 2.5 and 0.14 Bq kg^{-1} in the surface layer to undetectable values below 20 cm. Sedimentation rates at these two locations, determined using ^{210}Pb$_{excess}$, yielded values of 0.28 and 0.26 mm y^{-1} for Stns. 22 and 32, respectively, similar to those obtained in other Arctic shelf Seas (see Section 4.6.3). Excluding Stn. 30, ^{137}Cs inventories were found to be in the range 420–600 Bq m^{-2}, while the corresponding figures for ^{239,240}Pu were 30–65 Bq m^{-2}. For Stn. 30, a much higher ^{137}Cs inventory was observed (5800 Bq m^{-2}), reflecting the riverine contribution of the Dvina river. In contrast, the ^{239,240}Pu inventory, at 59 Bq m^{-2}, was similar to the rest of the stations.

Radionuclide profiles in sediment cores collected in the Kara Sea and the Yenisey estuary in 1993 showed a similar pattern to that observed in the White Sea. At locations in the vicinity of the estuary, ^{137}Cs and ^{239,240}Pu profiles were totally mixed to depths in excess of 20 cm, and ^{137}Cs inventories as high as 10000 Bq m^{-2} were measured. Interestingly, ^{60}Co was also present down to depths in excess of 20 cm, with inventories ranging between 150–260 Bq m^{-2}. In sampling locations outside the estuary, the maximum depth penetration of ^{137}Cs (10–20 cm) was lower than in the estuary and the profiles showed a progressive decrease in concentrations with increasing depth. The ^{137}Cs inventories were found to decrease with increasing distance from the estuary to levels typical of the Arctic continental shelf, again highlighting the influence of riverine inputs to sediment inventories in the Arctic shelf.

5.4. Mobilisation of radionuclides from freshwater contaminated sediment

The Ob and Yenisey rivers discharge about one third of the freshwater input to the Arctic Basin through the Kara Sea. Furthermore, it has been estimated that about 20–30 million tonnes of sediments are transported annually by these rivers. Since sediments contaminated by discharges from nuclear facilities situated upstream of the large Siberian rivers may eventually reach the estuarine zones, knowledge of the possible interactions between contaminated fresh water sediment and marine water in estuaries is clearly essential to an evaluation of the impact of such discharges on the marine environment. Two different processes are of particular importance:

- the mobilisation of low molecular species from sediment particle surfaces upon contact with the high ionic strength sea water (decreases in K_d); and
- the polymerisation of low molecular species followed by aggregation and sedimentation in the coastal zone (decrease in water concentration).

The sediment/water interactions of some radionuclides in relation to the above processes have been studied in various laboratory experiments where fresh water and sea water have been exposed to contaminated riverine sediments. Tracer experiments using sediments from the Ob river have demonstrated that ^{134}Cs and ^{85}Sr may be substantially mobilised in the estuarine mixing zone. Indeed, the relatively high distribution coefficients (K_ds) for ^{85}Sr and ^{134}Cs in fresh water systems have been shown to decrease by a factor of ~100 for ^{85}Sr and 20–50 for ^{134}Cs upon contact with sea water (Oughton *et al*., 1996).

Similar experiments have been carried out by exposing both fresh and sea water to contaminated sediment cores collected in the Nitelva River (affected by discharges from a uranium reprocessing pilot plant shut down in 1968). In one set of experiments, the water covering the sediments was agitated for 3000 hours in such a way as to leave the sediment undisturbed (passive diffusion). In a second set, sediments and water were thoroughly shaken (turbulent diffusion) for 24 hours to ensure complete exchange. The results from a passive diffusion experiment using Oslo Fjord sea water with a salinity of 34.3‰ at 15°C are shown in Figure 31. As in the tracer experiments, a significant desorption of ^{137}Cs from the sediments was observed, with sea water concentrations reaching values up to 27 times higher than those in the

original fresh water. Desorption took place according to a logarithmic function, with concentrations approaching equilibrium after about 3000 hours.

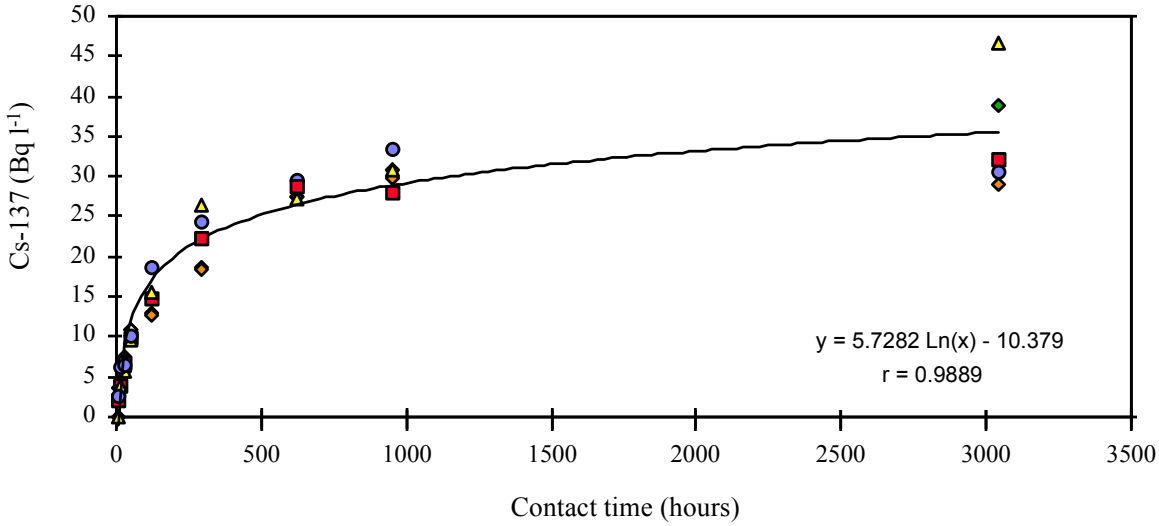

Figure 31. Evolution of ^{137}Cs concentrations in sea water in a 'passive diffusion' experiment using contaminated riverine sediment from the Nitelva River and sea water from Oslo Fjord

Analysis of sediment pore waters after this contact time revealed ^{137}Cs concentrations in excess of those observed in the overlying sea water. The same was true for fresh water experiments, where comparatively high ^{137}Cs concentrations in pore waters were also observed. Concentrations in pore waters corresponding to the lower sections of the cores were found to be even higher. These enhanced ^{137}Cs concentrations may be indicative of the anoxic character of the sediments (somewhat more pronounced in the deeper layers), with production of ammonium species which can easily replace caesium ions bound to illite. Measurement of ammonium profiles in the cores supports this hypothesis. A summary of the results is given in Table 13.

Table 13. Summary of ^{137}Cs results in passive and turbulent diffusion experiments

Experiment type	Sea water	Fresh water	Ratio sw/fw
Sediment concentration (Bq kg^{-1})	1.03×10^5	1.03×10^5	1
Passive diffusion (3000 h)			
Water concentration after 3000 h (Bq l^{-1})	35 ± 9	1.3 ± 0.3	27
K_d (sediment/overlying water) (l kg^{-1})	2900	68000	0.043
Pore water concentration 0–2.5 cm (Bq l^{-1})	67 ± 10	10 ± 5	7.0
K_d (sediment/pore water upper 2.5 cm) (l kg^{-1})	1500	11000	0.14
Pore water concentration 2.5–5 cm (Bq kg^{-1})	73 ± 4	18 ± 9	4.1
K_d (sediment/pore water lower 2.5 cm) (l kg^{-1})	1400	5700	0.25
Turbulent diffusion (24 h)			
Water concentration (Bq l^{-1})	50 ± 4	8 ± 2	6.2
K_d (sediment/shaking water) (l kg^{-1})	2100	13000	0.16

With regard to the 'turbulent diffusion' experiments, ^{137}Cs extraction by sea water was much higher than for fresh water, indicating that an ion exchange mechanism is responsible for most of

the desorption of caesium species. This mechanism is probably also dominant for the desorption of ^{137}Cs into sea water in the 'passive diffusion' experiment. The main conclusion to be derived from these experiments is that riverine sediments contaminated by discharges by an upstream nuclear facility will lead to a significant release of ^{137}Cs upon contact with even low salinity water.

6. Reactivity at the sediment/sea water interface

6.1. Fixation and remobilisation of radionuclides in sediments

Radionuclides are not necessarily fixed permanently to the sediments, but may be recycled *via* biological and chemical agents both in the sedimentary compartment and in the water column. Indeed, sediments are increasingly recognised not only as a sink but also as a possible source of contaminants in aquatic systems. This seems to be the case for the sediments in the Irish Sea which, as a result of the decline in the Sellafield discharges by at least one order of magnitude since their peak in the early- to mid-1970s, have now become the principal source of radiocaesium and transuranic nuclides to the north-eastern Irish Sea, the western Irish Sea and beyond. As a large proportion of the long-lived radionuclides from historical Sellafield discharges reside in the muddy seabed sediments in the eastern Irish Sea, it is important to determine the redistribution of radionuclides released from this temporary sink in order to assess the continuing impact and transport of radionuclides from the Irish Sea to the waters of the north-west European shelf and the Arctic. Consequently, a comprehensive programme of laboratory experiments and field surveys was carried out to in order to assess the sorption/desorption behaviour of different radionuclides from seabed sediments and to study the conditions which may affect the rate and extent of radionuclide remobilisation.

In a first set of experiments, the rate and extent of ^{137}Cs remobilisation at room temperature (~20^{o}C) was examined using two different suspended load concentrations. Contaminated sediment (~1 Bq g^{-1}) was added to 10 litres of relatively uncontaminated filtered sea water (~20 mBq l^{-1}) to give final suspended loads of ~50 mg l^{-1} or 500 mg l^{-1}. After contact times ranging from one hour to one week, the dissolved and particulate phases were separated by 0.45 μm filtration. Results from these experiments are shown in Figure 32.

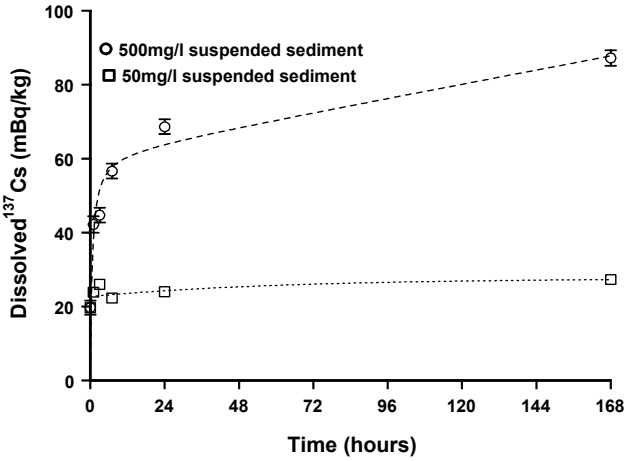

Figure 32. Remobilisation of ^{137}Cs from sedimentary material suspended in coastal sea water

Adding particulate material to a concentration of 50 mg l^{-1}, levels of dissolved ^{137}Cs increased from ~20 mBq l^{-1} up to 24 mBq l^{-1} after a contact time of one hour. The extent of

remobilisation after one week (168 hours) was essentially the same as that observed after one hour, indicating further remobilisation was slow. The use of mass balance equations to monitor the activity levels throughout each experiment indicated that typical recoveries of ~95% were found in the combined dissolved and particulate phases. The K_d value calculated from these results was ~3.6×10^4, which is somewhat higher than that observed in previous surveys of the Irish Sea ($K_d = 4.3 \pm 2.1 \times 10^3$). Using the higher concentration of particulate material (i.e., 500 mg l^{-1}), levels of dissolved ^{137}Cs were somewhat higher (~43.4 mBq l^{-1} after 3 hours, increasing to 82 mBq l^{-1} after one week).

Subsequently, a further investigation was undertaken to assess the influence of temperature upon the rate and extent of sorption and remobilisation of ^{137}Cs using the higher suspended load concentration. Experiments were carried out at 4°C and 25°C to adequately cover the temperature range observed in the Irish Sea. Results from these experiments are collectively given in Figure 33.

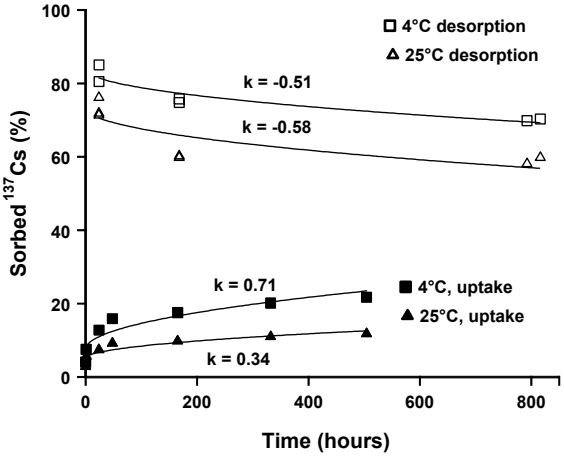

Figure 33. ^{137}Cs sorption to, and desorption from, sedimentary material suspended in coastal sea water. Suspended load concentrations were ~500 mg l^{-1}. Curves represent best fit to a transport controlled dissolution model (Stumm, 1992): % sorbed $^{137}Cs = kt^{1/2} + Cs_{(0)}$

The data in Figure 33 shows that rapid initial sorption was followed by further slow uptake over the remainder of the experiment at both temperatures. This feature is similar to that previously noted for the desorption process (Figure 32). A marked hysteresis was evident between sorption and desorption processes (i.e., a steady-state distribution between phases was not attained within the timescale of these experiments), and appears to be a characteristic in other aquatic systems (e.g., Knapinska-Skiba *et al.*, 1994). This behaviour was suggested to be due to uptake of ^{137}Cs by a number of different binding sites resulting from the heterogeneous nature of natural sediment. Although the extent of uptake was greater at the lower temperature, the converse was true with respect to remobilisation. Differences in behaviour between experiments are therefore ascribed to experimental variation rather than the effect of temperature (i.e., to a first approximation, the influence of temperature upon the rate of attainment of a steady-state distribution of ^{137}Cs between dissolved and particulate phases was not significant).

In addition, a mesocosm was designed and constructed to determine the long-term desorption behaviour of ^{137}Cs from seabed sediment under controlled laboratory conditions. Two laboratory experiments were carried out to provide an estimate of the diffusive flux of ^{137}Cs from 'contaminated' seabed sediment to the water column whilst maintaining a constant suspended particulate concentration. The second experiment was carried out over a longer timescale and involved the use of stable Br tracer to simultaneously assess the rate and extent of diffusion of

^{137}Cs from pore water into the overlying sea water. The results of these experiments are shown in Figure 34.

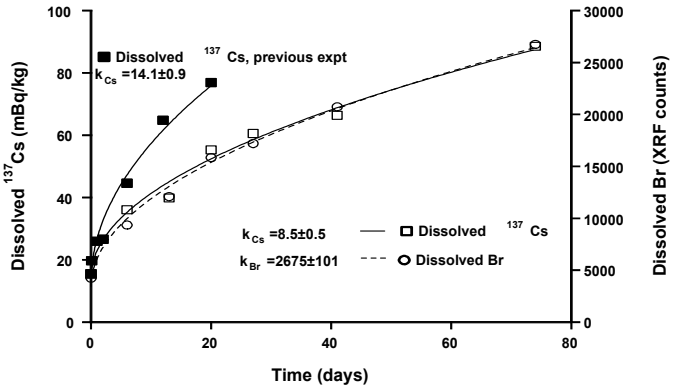

Figure 34. Temporal evolution of the desorption of ^{137}Cs from contaminated mud, and diffusion of Br from pore water into overlying sea water. Curves represent best fit to a transport controlled dissolution model (Stumm, 1992): $[^{137}Cs_{(aq)}]$ or $[Br_{(aq)}] = k_d\, t^{1/2}$ + resid

As in the previous experiments, the rate of release of ^{137}Cs appeared to decrease with time. In the short-term experiment, the concentration of dissolved ^{137}Cs at time t = 0 was ~20 mBq kg^{-1} and levels increased by an average value of ~3 mBq kg^{-1} d^{-1} over the duration of the experiment. Results from the second experiment, carried out over a longer timescale, indicate that over the first 20 days levels increased by ~2 mBq kg^{-1} d^{-1}. Over the remainder of the experiment the average rate of increase was ~0.6 mBq kg^{-1} d^{-1}. Presumably, this is because ^{137}Cs is bound to a number of sites on the sediment with different binding energies, and labile material is desorbed most rapidly. Data from the second experiment also indicate that the rate of ^{137}Cs remobilisation was similar to that of Br diffusion from the sediment box. Consequently, under the conditions of these experiments, physical processes appear to govern the release of ^{137}Cs into the water column.

Field surveys were carried out to assess the extent of remobilisation of ^{137}Cs from the Irish Sea seabed. Results of calculations to assess the inventory of ^{137}Cs in the water column and the contribution arising from the flux from the seabed of the Irish Sea are listed in Table 14. In 1995, the predicted inventory without remobilisation was just 13 TBq compared to a value of 66 TBq calculated from the survey data, indicating that the predominant contribution (~80%) to ^{137}Cs in the water column of the Irish Sea arises from the flux from the seabed. Moreover, the magnitude of this contribution is similar to that predicted for 1987, two years after the commencement of operation of the SIXEP plant to reduce discharges of ^{137}Cs. Estimates of the flux from the seabed as a percentage of the ^{137}Cs sediment inventories are listed below (Table 15).

Table 14. Inventory of ^{137}Cs in the water column of the Irish Sea and the contribution arising from the flux from the seabed

Expedition	Annual discharge (Bq)	Sea water inventory (Bq)	Remobilised activity (Bq)	Historic contribution (%)
Flux into water column				
Clione 5/87	1.20×10^{13}	2.69×10^{14}	1.98×10^{14}	74
Cir 12/94	1.38×10^{13}	8.36×10^{13}	6.79×10^{13}	81
Cir 10/95	1.22×10^{13}	6.64×10^{13}	5.32×10^{13}	80

Between 1988 and 1995, the inventory in the sediments of the Irish Sea decreased by 573 TBq (i.e., by 37% or ~6.5% per annum). This figure is remarkably similar to the estimate obtained from a consideration of the inventory in the water column predicted to be due to remobilisation (flux from seabed estimated to be 5.5% in 1995). However, it is interesting to note that the flux from the seabed in 1995 (~5.5% per annum) is lower than that estimated for 1987 (~13% per annum). It is tempting to conclude, on the basis of the above laboratory experiments, that this is caused by changes in the susceptibility of sorbed Cs (i.e., labile Cs being rapidly remobilised whilst that remaining bound to inter-lattice sites being less susceptible to dissolution). However, other possible explanations for these differences, including transport of contaminated sediment to intercoastal areas and burial of contaminated surface sediment as a result of bioturbation must be taken into account.

Table 15. Effect of the relative ^{137}Cs flux from the seabed in the Irish Sea

Year	Sediment inventory (Bq)	Remobilised activity (Bq)	Flux from seabed as percentage of inventory (%)
1987	$>1.53 \times 10^{15}$	1.98×10^{14}	~13
1995	9.59×10^{14}	5.32×10^{13}	~5.5

Separate experiments were carried out to establish and quantify the effects of two key environmental variables (light and temperature) upon the sorption/desorption behaviour of ^{239,240}Pu and ^{241}Am. Information obtained from irradiation experiments (Figure 35) indicate little, if any, change in ^{241}Am desorption behaviour after 1 hour, in both irradiated and control samples, although there is limited evidence to suggest that ^{241}Am remobilisation was marginally greater in samples exposed to natural sunlight. The extent of ^{241}Am desorption under both conditions was, however, relatively small (<2%). Partitioning between dissolved and particulate phases is often characterised by a distribution coefficient and the percentage remobilised under the conditions of these experiments corresponds to a K_d value of $\approx 1 \times 10^6$. Under dark conditions remobilisation of $^{239+240}$Pu was also very low (<1.2%). In contrast, under irradiation from sunlight $^{239+240}$Pu desorption was markedly greater and increased with time, from ≈5% after 1 hour up to ≈15% after 7 hours. Therefore, photochemical reactions produced an enhancement in the amount of dissolved ^{239,240}Pu by > 1 order of magnitude (≈14 fold). The percentages of ^{239,240}Pu remobilised at the end of this experiment correspond to K_d values of $\approx 1.6 \times 10^6$ and $\approx 1.1 \times 10^5$ under dark and light conditions, respectively. The magnitude of ^{54}Mn desorption was considerably more than observed for ^{239,240}Pu or ^{241}Am, under both experimental conditions. Significant remobilisation occurred under dark conditions, although the extent of desorption into seawater irradiated by sunlight was notably greater (≈53% after a period of 7 hours, compared with ≈19%). These percentages correspond to K_d values of $\approx 1.7 \times 10^4$ and $\approx 8.5 \times 10^4$ under light and dark conditions, respectively. The magnitude of increase in ^{54}Mn desorption resulting from irradiation by sunlight was less than that observed for ^{239,240}Pu (≈3 fold compared with ≈14 fold).

Dissolved ^{239,240}Pu can exist in at least two valence states in seawater (predominantly as Pu(IV) and Pu(V)); data showing the increase in concentration of the individual species of dissolved ^{239,240}Pu with time is provided in Table 16.

Concentrations of dissolved ^{239,240}Pu(IV) were similar, within experimental error, under light and dark conditions. In contrast, levels of dissolved ^{239,240}Pu(V) were markedly greater for samples irradiated by natural sunlight. Moreover, since concentrations of dissolved ^{239,240}Pu(IV) remained fairly constant with time, these results indicate that a near steady state distribution between sorbed and dissolved ^{239,240}Pu(IV) was achieved within 1 hour. Levels of ^{239,240}Pu(V) species consistently increased over the period of these experiments for samples irradiated by natural sunlight. The total activity of ^{239,240}Pu initially bound to the suspended particulate material was ≈650mBq l^{-1} and the proportion existing in the pentavalent state was likely to have been

<2% (Nelson and Lovett, 1981). In samples irradiated by natural sunlight, the concentration of ^{239,240}Pu(V) in solution after just 1 hour (≈30 mBq l^{-1}) was more than double the amount of ^{239,240}Pu(V) estimated to have been initially present on the suspended material (<13mBq l^{-1}). In contrast, under dark conditions the concentration of dissolved ^{239,240}Pu(V) after seven hours (≈4mBq l^{-1}) was less than half that initially present on the particulate material. Consequently, the order of magnitude increase in remobilisation of ^{239,240}Pu under light conditions (Figure 35) was a result of photooxidation of sorbed ^{239,240}Pu(IV).

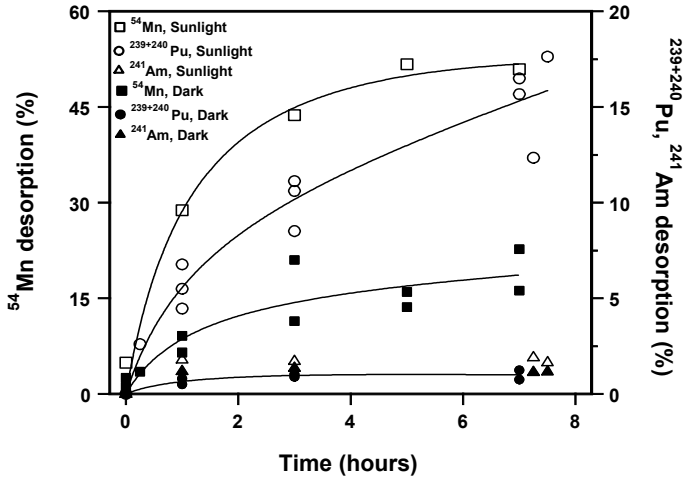

Figure 35. Effect of irradiation by natural sunlight upon radionuclide desorption behaviour in filtered sea water with time

Using artificial light sources, experiments were carried out to assess the effect of light intensity upon the rate and extent of remobilisation. Samples were irradiated with light from 15W 'True-lite' fluorescent tubes (Duro-lite International). These aquarium lamps have an output which notionally simulates that of natural sunlight and includes visible and near-UV light. Light is emitted at an intensity of 140 μE $m^{-1}s^{-1}$, a value approximately 5% of full noon sunlight. Results for ^{54}Mn and ^{239,240}Pu behaviour under these conditions are provided in Figure 36.

Table 16. Effect of irradiation by natural sunlight upon desorption of ^{239,240}Pu in filtered sea water with time

Time (h)	^{239,240}Pu (IV) (mBq kg^{-1})	^{239,240}Pu (V) (mBq kg^{-1})
	Dark conditions	
1	2.0 ± 0.1	1.9 ± 1.1
3	2.9 ± 0.2	2.7 ± 1.0
7	2.7 ± 0.2	3.7 ± 1.8
	Irradiated by sunlight	
1	4.7 ± 2.0	30 ± 5
3	2.6 ± 1.0	65 ± 9
7	5.2 ± 1.5	103 ± 11

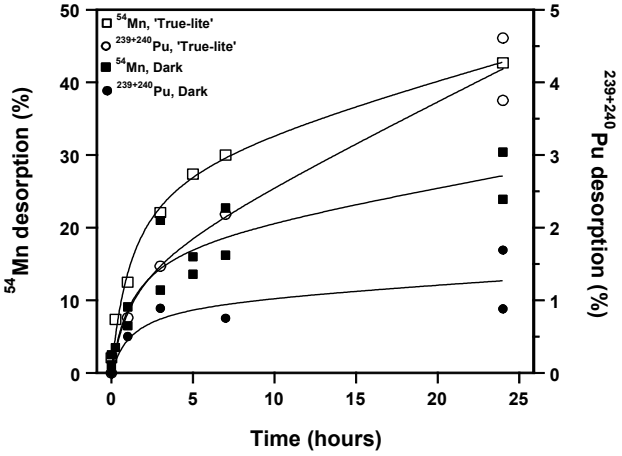

Figure 36. Effect of irradiation by artificial sunlight using 'True-lite' fluorescent tubes upon radionuclide desorption behaviour in filtered sea water with time. Lines represent best fit curves using Equation: % desorption = [A * t / (t + B)] + C * t

Remobilisation of $^{239+240}$Pu consistently increased with time. Under dark conditions desorption of ^{239,240}Pu grew from 0.5% after 1 hour up to 1.3% after 24 hours. The extent of remobilisation was significantly greater in solutions irradiated by artificial sunlight (4.2% after 24 hours). Consequently, enhancement of ^{239,240}Pu desorption observed using 'True-lite' lamps was about 3-fold compared to ≈14 fold using natural sunlight. Desorption of ^{54}Mn was also observed to be greater in the irradiated suspension (43% after 24 hours, compared to 27% in the dark) and therefore the increase produced using artificial sunlight (≈1.6 fold) was noticeably less than that using natural sunlight (≈3 fold). Since the intensity of light emitted from 'True-lite' fluorescent tubes is only ≈5% of the intensity of full noon sunlight, it is likely that the influence of photochemical reactions upon ^{239,240}Pu and ^{54}Mn remobilisation behaviour was less under the conditions of these experiments. This is because the total irradiation from the artificial light source was less than that from natural sunlight over the whole 7 hour period.

Further experiments were carried out using artificial light sources to evaluate the effect light wavelength (hence energy) upon the radionuclide desorption behaviour. A contact time of 24 hours, between particulate and dissolved phases, was allowed for these experiments and the results obtained are shown in Figure 37. The data show that the extent of ^{241}Am desorption was small and ranged from 1.2% up to 2.0%, which is similar in magnitude to that observed previously (Figure 35). Consequently, the influence of light wavelength upon ^{241}Am remobilisation was not significant and confirms that its desorption behaviour is not sensitive to photochemical reactions in natural waters. The desorption behaviour of ^{239,240}Pu was more complex. The extent of ^{239,240}Pu remobilisation ranged from 1.3% in the dark up to 18.4% using the UV lamp (mainly 254 nm). Using the 'Whitelight' (400–700 nm) and 'True-lite' lamps (predominantly 400–700 nm), desorption of $^{239+240}$Pu was fairly similar and more than double that observed under dark conditions. The spectral output of the 'Blacklight' (320–400 nm) and UV lamps consists of shorter wavelength light than the 'Whitelight' and 'True-lite' sources and desorption of ^{239,240}Pu was about 9 and 14 fold greater, respectively, compared to that observed under dark conditions. Consequently, it is reasonable to suggest that the extent of ^{239,240}Pu remobilisation is inversely dependent upon wavelength in the range 254–700 nm.

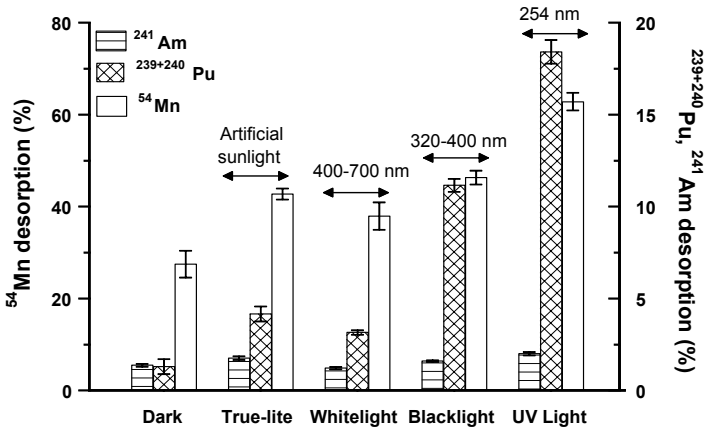

Figure 37. Effect of light wavelength upon radionuclide desorption in filtered sea water

Long-term experiments (400 h) to assess the influence of temperature upon desorption behaviour were also carried out. The extent of remobilisation of ^{241}Am (under dark conditions) and Pu(IV) species (under dark and light conditions) was very small, being always below 2%. Similar long-term experiments studying the Pu(V) behaviour at different water temperatures during dark and light conditions indicated that remobilisation of $^{239, 240}$Pu(V) species increased with temperature under both light and dark conditions. More specifically, at equivalent contact times and under dark conditions, the extent of $^{239, 240}$Pu (V) desorption was between 2 to 6 fold greater at 25°C compared with that observed at 4°C. Plutonium(V) uptake by Irish Sea sediments was also studied under the same conditions. The results showed increasing uptake with temperature and under light conditions.

In conclusion, information obtained from the present laboratory studies demonstrated indicate that the rate and extent of Pu(V) remobilisation from, and uptake of dissolved Pu(V) by, suspended particulate material are concurrently enhanced by increases in temperature and light irradiation. The behaviour of ^{137}Cs and ^{241}Am appears to be largely unaffected by these parameters. In the environment, processes other than surface chemical reactions may be equally important in governing the rate and extent of remobilisation/uptake. These include diffusion of radionuclides from pore water into the overlying water column, physical resuspension of contaminated sediment and biological mixing. Physical resuspension processes are likely to be greatly enhanced during storms which are episodic events whose frequency is likely to be greatest in the winter. Conversely, the rate of chemical reactions at the particle surface are likely to be least during this season because of low water temperature and light irradiation.

6.2. Post-depositional (reactive) processes in estuarine anoxic sediments

An experimental device was built in order to investigate estuarine post-depositional processes affecting radionuclide speciation in interstitial waters and, consequently, their export to the open ocean upon resuspension. The device consists of a 50 litre Plexiglass container in which spiked water and estuarine sediments can be stirred and equilibrated with the tracers. After settling of the sediment, sub-cores can be collected periodically and extruded in a nitrogen-flushed glove-box, avoiding alterations due to contact with air.

A 10–month experiment was performed with anoxic sediments collected in the Seine estuary. Seven kilograms of anoxic sediments were spiked with ^{54}Mn and ^{59}Fe, as the behaviour of these elements in anoxic sediment is well established. Indeed, in the Seine Estuary, alkalinity

and sulphide concentrations have been demonstrated to control the behaviour of iron and manganese, respectively, in anoxic interstitial waters. In addition, ^{57}Co, ^{65}Zn, ^{125}Sb, ^{109}Cd and ^{134}Cs were added in order to investigate their solid partitioning in anoxic sediments. Five sub-cores were collected 3, 35, 72, 133 and 307 days after the sediment column reconstruction. They were extruded in the above-mentioned glove-box and sliced at in 8 sub-samples at 1-cm depth intervals. Interstitial waters were then separated by centrifugation, and aliquots were used for radioactivity and alkalinity measurements. The specific activity of the remaining sediment was determined together with water content and particulate sulphide concentrations. The results of these experiments confirmed the validity of the experimental approach used, with sulphide, alkalinity and radionuclide profiles tending towards those observed in anoxic sediments in the Seine Estuary, after an appropriate 'incubation' period (Figure 38).

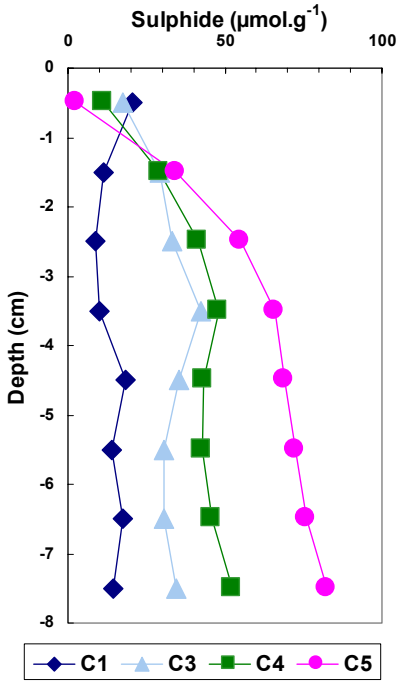

Figure 38. Vertical distribution of freshly precipitated sulphides (AVS) in an anoxic sediment monolith reconstructed in the laboratory; the measurements have been done 3 (C1), 72 (C3), 133 (C4) and 307 (C5) days after the sediment reconstruction

At the commencement of the experiment, the sediment column was homogeneous. The acid volatile sulphide (AVS) concentrations were low (10–20 µmol g^{-1}) and showed no trend with depth. The AVS concentrations progressively increased with time to 60–80 µmol g^{-1} after 10 months. In the upper layers of the sediment column, the sulphide precipitation was much lower because of the inhibition of sulphate-reducing bacterial activity and the upwards diffusion of sulphates. The sulphide precipitation is thus a very active process with production rates of 0.7 – 1 mmolS.Kg^{-1}.d^{-1} during the first month of incubation. Their potential role as carrier phases for radionuclides was then investigated by chemical leaching techniques using nitrogen flushed reagents and wet sediments under inert atmosphere to prevent coprecipitation of redox sensitive species onto the sediment residues.

A three-step chemical leaching procedure (carbonate/oxy-hydroxides/organic-sulphides) was applied to sediments from the anoxic layer of a fifth core retrieved 300 days after labelling and evolution toward anoxia. The leaching was carried out under both standard (atmosphere) and inert conditions to identify possible artifacts arising from the contact of the sediments with air during the chemical leaching extractions. The carbonate fraction was extracted with a mixture of

acetic acid and sodium acetate at pH 5. The oxy-hydroxide fraction was extracted with acetic acid and hydroxylamine hydrochloride at pH 2.5, with sodium-citrate as a complexing agent to prevent readsorption. Finally, organic matter and sulphides were solubilised (drastically in this case) with hydrogen peroxide (30%) and nitric acid at pH 2. Kinetic experiments demonstrated that the extractions were completed in 5, 3 and 1 hours for steps 1, 2 and 3, respectively. In all cases, a solid-to-liquid ratio of 1:150 was employed.

The prominent conclusion of these experiments is that under standard (atmospheric) conditions, sulphide compounds (and associated radionuclides) readily dissolve during the first step due to contact with air, and are partially re-adsorbed onto remaining particles, yielding an erroneous solid partition. The main artifact is and overestimation of the carbonate fraction due to the dissolution of acid volatile sulphides, which is also observed when these anoxic sediments are resuspended in oxic sea water. This highlights the need to adopt the most stringent precautions when applying any chemical leaching technique to sub-oxic or anoxic sediments.

Under inert conditions, very high proportions of cobalt, zinc, cadmium and antimony were found to be associated to the organic-sulphides (OS) fraction (Figure 39). As expected, manganese was found to be incorporated in the carbonate fraction in anoxic sediments, while a large proportion of the ^{134}Cs was associated to the residual fraction, probably clay materials.

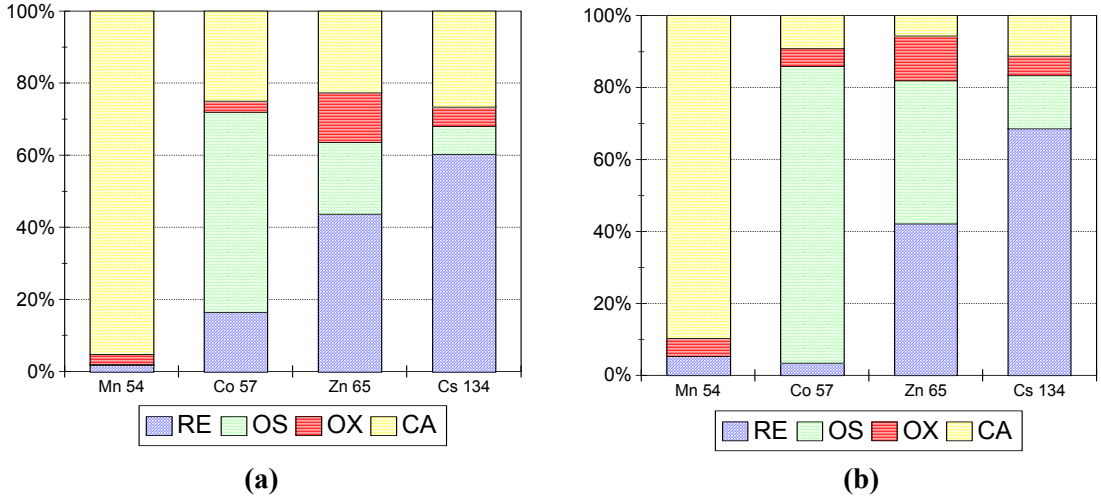

Figure 39. Comparison of the solid partition of some radionuclides in 300–day old labelled anoxic sediments under oxic conditions (a) and under inert atmosphere (b) ; CA : carbonate fraction ; OX : oxy-hydroxide fraction ; OS : organic-sulphide fraction ; RE : residual fraction

As sulphides are known to be highly sensitive to oxidation, a set of laboratory experiments were carried out in order to study the behaviour of different radionuclides (^{54}Mn, ^{57}Co, ^{125}Sb, ^{134}Cs) upon resuspension of bottom anoxic sediments and, in particular, the kinetics of their release and/or uptake by the resuspended particles.

The resuspension experiments were carried out with air contact or without air contact, in a nitrogen flushed glove bag. A known amount of sediment particles (2 to 3 g l^{-1}) were mixed in a brackish water obtained by dissolving NaCl in distilled water (5 g l^{-1}). The sediments were continuously stirred throughout the experiment, which was carried out using sediment samples from two different depths in an anoxic sediment column.

In both cases, the particulate sulphides, supposed to be major sinks for a number of trace elements in anoxic sediments, were measured before and after resuspension. The results are given in Table 17, for acid volatile sulphides (AVS) and acid reducible sulphides (ARS). Two main conclusions are derived from these data:

- with air contact, and after 72 hours, AVS sulphides are totally destroyed as are 40 to 55% of the ARS sulphides; and
- more unexpectedly, AVS and ARS sulphides are significantly affected even under nitrogen; this implies that these freshly precipitated mineral species are prone to solubilise upon stirring or contact with oxidative species.

That most of the AVS and ~50% of the ARS are destroyed after 72 hours does not mean that such a long time is required: it is indeed likely that most of AVS sulphides are dissolved in the very first hours of the experiment, especially with air contact. This is clearly observed by the discoloration of the particles (black to pale green). More recent experiments showed that 90% of the AVS was destroyed after only 1 hour of contact with oxic water.

Table 17. Concentration of AVS and ARS sulphides in the sediments before and after resuspension experiments

	Depth (cm)	AVS sulphides $\mu mol.g^{-1}$	ARS sulphides $\mu mol.g^{-1}$	Total sulphides $\mu mol.g^{-1}$
Before resuspension				
Level 1	14	62.3 ± 1.7	63.0 ± 1.7	125.4 ± 3.4
Level 2	4-7	84.7 ± 1.8	78.0 ± 1.8	162.7 ± 3.5
After 72 hours of stirring with air contact				
Level 1	1-4	-	28.1 ± 2.8	28.1 ± 2.8
Level 2	4-7	-	47.8 ± 1.4	47.8 ± 1.4
After 143 hours of stirring under nitrogen				
Level 1	1-4	15.0 ± 1.4	40.4 ± 1.1	55.4 ± 2.3
Level 2	4-7	3.6 ± 1.3	36.5 ± 1.3	40.8 ± 2.6

The percentages of radionuclides released into solution with time are shown in Figure 40. In all cases, contribution from dissolved radionuclides in interstitial pore water was negligible. The following comments can be made from the results:

- *^{54}Mn :* the amount of ^{54}Mn released into solution (2–3 % of the total) decreases sharply with air contact; under nitrogen, up to 10% of the total remains in solution during at least 3 days.
- *^{57}Co:* the amount of ^{57}Co released into solution with air contact is very low (*ca.* 1.5%) but the increase of the concentration is very steep; under nitrogen, ^{57}Co release is low (less than 0.3%) and displays no significant evolution versus time. This suggests that a little amount of ^{57}Co is associated with the sulphide phase.
- *^{125}Sb:* the release of ^{125}Sb to solution with air contact is very important (20–30% of the total activity). Under nitrogen, the released amount does not exceed 15%. These observations can be interpreted as the result of the dissolution of Sb-rich sulphides: the Sb-sulphides are highly insoluble and readily precipitate when sulphide ions appear in solution. Furthermore, the ^{125}Sb thus released is stable at dissolved state in oxic conditions as $Sb(OH)_6^-$.
- *^{134}Cs:* the amount of ^{134}Cs released into solution in rather low, being 2–3% in oxic conditions and 1–2% in anoxic conditions. There is no evidence that the behaviour observed can be related to a release from sulphides.
- *^{65}Zn:* this radionuclide is not significantly released from the sediment upon resuspension in both oxic (<0.1%) or suboxic conditions (<0.15%); the results have not been plotted.

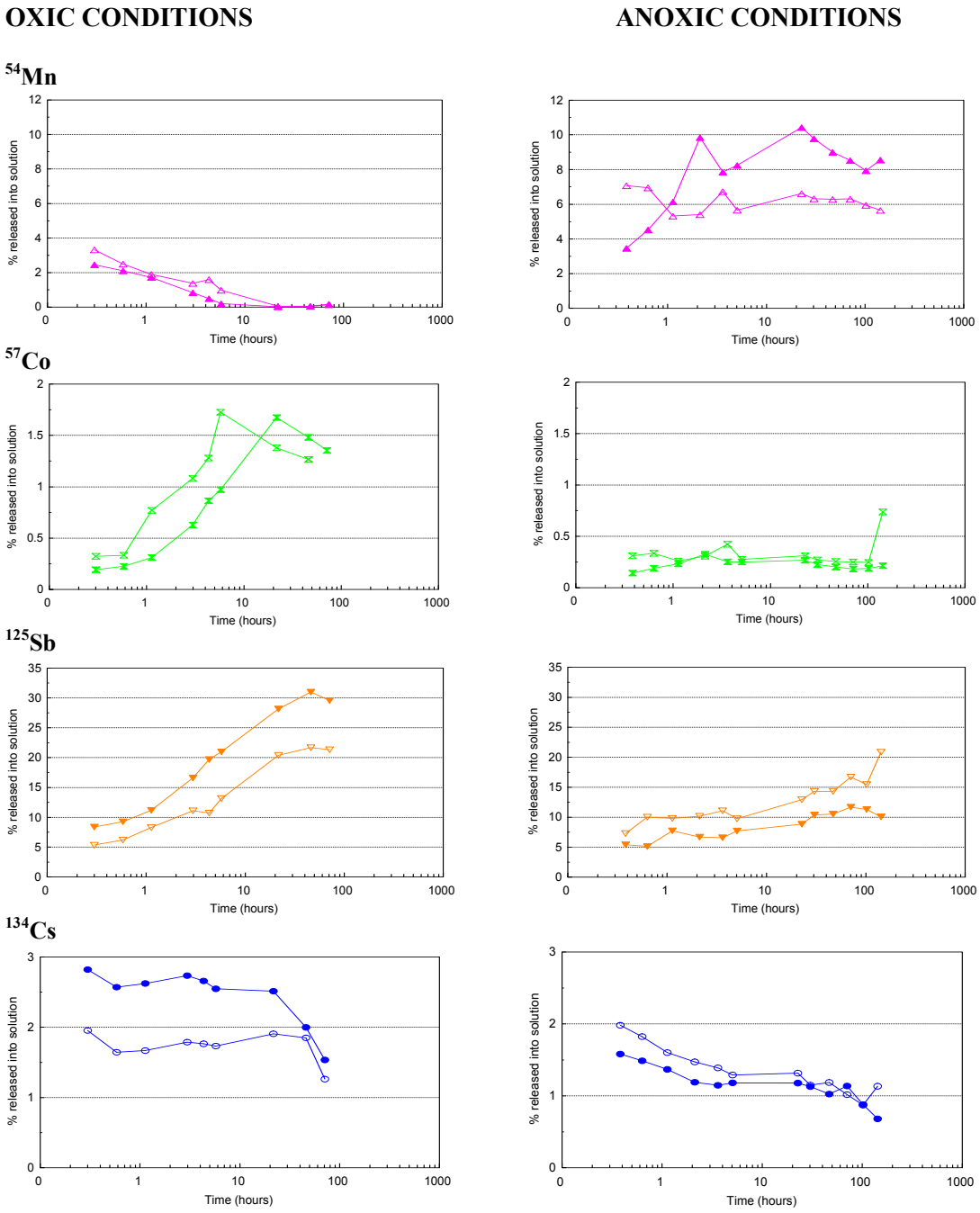

Figure 40. Remobilisation of ^{54}Mn, ^{57}Co, ^{125}Sb and ^{134}Cs upon resuspension of anoxic sediments under oxic and anoxic conditions, at a salinity of 5 g l^{-1} ; open and closed symbols refer to level 1 and 2, with suspended loads of 1.7 and 2.9 g l^{-1}, respectively ; relative 2σ error is about 5%

Even if the amount released into overlying water may seem relatively low, these processes can play a major role in the export of land-derived radionuclides to the open ocean, in estuarine environments undergoing periodic (tides) or paroxystic (high river flows, storms) events.

6.3. Solid phase speciation of transuranium nuclides in oxic and anoxic sediments (Arctic)

A series of sequential chemical leaching experiments were carried out on sediment samples collected on the western coast of Spitsbergen with a view to determine the solid phase speciation of transuranium nuclides. The results were compared with those observed in other coastal environments (Mediterranean, Baltic Sea) in order to identify any possible differences in the geochemical association of transuranium nuclides under extreme conditions. The geochemical partitioning of plutonium and americium was examined by applying the sequential leaching protocol developed by Cook *et al*. (1984). This protocol separates the activity into five operationally-defined geochemical fractions: readily available, exchangeable, bound to organic matter, bound to oxides and residual.

Arctic sediment samples were collected during the 1996 summer campaign to Svalvard at two locations inside Kongsfjord and Isfjord. Samples of oxic and anoxic sediments were collected in a zone of relatively high sedimentation rate (Stn. SVA-G-1; 78°59.42'N, 11°38.51'E; depth = 281 m) inside Kongsfjord. The high sedimentation rate observed (0.25 g cm^{-2} y^{-1}) is the result of the large amounts of terrigenous particles transported to the fjord during ice melting and to the prevailing hydrodynamic conditions in this zone, which allows particle settling. Samples were also taken in a trough near the margin of Isfjord (Stn. SVA-C-05; 78°14.96'N, 11°14.03'E; depth = 252 m), where slumping processes can transport surface sediments from elsewhere, enhancing radionuclide accumulation.

In Kongsfjord, ^{239,240}Pu was found to be mainly associated to the organically bound phase (72%) in the oxic layer, with the remainder distributed between the oxide (23%) and the residual (23%) fractions. In the anoxic layer, ^{239,240}Pu also appeared to be mainly associated to organic matter, although the percentage was somewhat smaller (55%), likely due to a higher content of organic matter of biogenic origin (the extractant employed is highly specific for organic matter of terrigenous origin, such as humic and fulvic acids). A similar partitioning was observed in the Isfjord samples, with 52% of the ^{239,240}Pu in the oxic layer (0–2 cm) associated to organic matter and 39% associated with the oxide phase. Again, the percentage of ^{239,240}Pu associated to organic matter in the anoxic layer (7–8 cm) was smaller than in oxic layer. In all cases, the amount of ^{239,240}Pu in fractions considered most mobile (readily available, exchangeable) were below the limits of detection. Americium was also found to be predominantly associated to organic matter in both oxic and anoxic layers (66% and 69%, respectively).

Mediterranean samples were collected in 1992 from aboard the R.V. *Urania* (Italy) off the coasts of Barcelona (41°26.02'N, 02°20.50'E; depth = 53 m) and Tarragona (41°45.11'N, 01°04.92'E; depth = 90 m), affected by terrigenous inputs from the Besós and Ebro rivers, respectively, as well as off the coasts of Alicante (38°10.64'N, 00°05.74'E; depth = 200 m) and Malaga (36°14.50'N, 05°07.07'W; depth = 360 m), located in an area with predominantly biogenic sediments. In sediments from areas affected by terrigenous inputs of rivers (enriched in fulvic and humic acids), plutonium was found to be mainly associated to the organic phase (54–56%), a percentage almost identical to that observed in the Svalvard fjords. In sediments of biogenic origin, the percentage associated to the organic phase was much lower (33–37%), with most of the plutonium being associated to the oxide phase (40–60%).

Baltic sediments were kindly provided by BSH (Germany) , having been collected close to the continental margin (57°45'N, 08°00'E; depth = 470 m), in a zone unaffected by riverine inputs. In this case, plutonium was mainly associated to the oxide phase (54%) and, to a lesser extent, to the organic phase (40%), while americium was mainly associated to the organic (38%) and residual (35%) fractions.

Overall, the sequential leaching experiments indicate that plutonium and americium are associated to stable phases in all the areas studied, with little if any of the transuranium inventory in a readily available, exchangeable form. A higher proportion of the americium appears to be associated to the residual fraction.

6.4. Solid phase speciation in sediment from the Thule accident zone

The solid phase speciation of ^{239}Pu and ^{241}Am in sediments from the Thule accident zone was examined using a sequential extraction protocol recommended by NIST (Schultz *et al.*, 1998). The protocol used separates the activity into six operationally-defined geochemical fractions: exchangeable, bound to carbonates, bound to Fe-Mn oxides, bound to organic matter, acid soluble and residual.

The data (Figure 41) clearly show that, even thirty years after the accident, a substantial proportion of the plutonium in the sediments is in a non-exchangeable form. This is consistent with the observation that virtually no weapons-grade plutonium is present in the overlying water column (dissolved phase), while the measured ^{238}Pu/^{239,240}Pu activity ratios suggest weapons-grade plutonium as the main source of contamination to the sediments. Although less than 2% of the plutonium was found to be in an exchangeable in two replicate samples, significant differences were observed in the partitioning of plutonium between the organic, oxide and acid-soluble fractions in these samples. This is not unexpected, considering the heterogeneous distribution of the accident plutonium. This heterogeneity was reflected in the measured total ^{239}Pu concentration, with one of the replicate samples having twice the activity concentration of the other. Nevertheless, the importance of the oxide and organic fractions in the context of scavenging and fixation of plutonium is evident from the observed distribution, and consistent with observations in sediments contaminated by reprocessing waste discharges (Cook *et al.*, 1984; Ledgerwood *et al.*, 1999).

In the case of ^{241}Am, mainly arising from the decay of ^{241}Pu contained in the weapons, the activity was found to be distributed rather evenly between the carbonate, organic and acid-soluble fractions (Figure 41). The observed association with the carbonate and organic fraction is consistent with those reported by Shanbag and Morse (1982) and Chester and Aston (1981), and supports the extensive evidence already available of the importance of these phases in the scavenging and removal of actinides to seabed sediments.

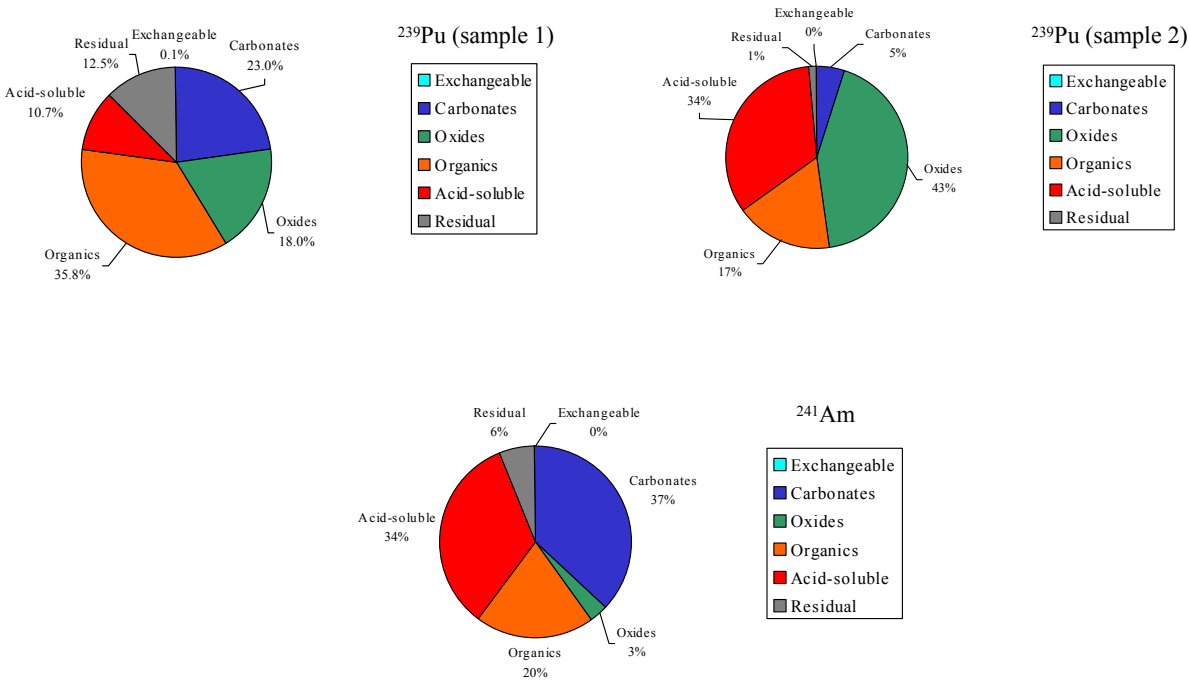

Figure 41. Solid phase speciation of plutonium and americium in contaminated sediment samples from Thule

6.5. Dynamic of the sediment-water distribution coefficient

A number of experiments were carried out in order to investigate the dynamics of sediment-water distribution coefficients (K_ds) using ^{137}Cs, ^{85}Sr and ^{236}Pu tracers. For ^{85}Sr and ^{134}Cs, experiments were repeated on sediments from different locations. In all cases, K_d values were shown to follow first order kinetics, but endpoints were found to vary over more than an order of magnitude depending on the sediments (Figure 42).

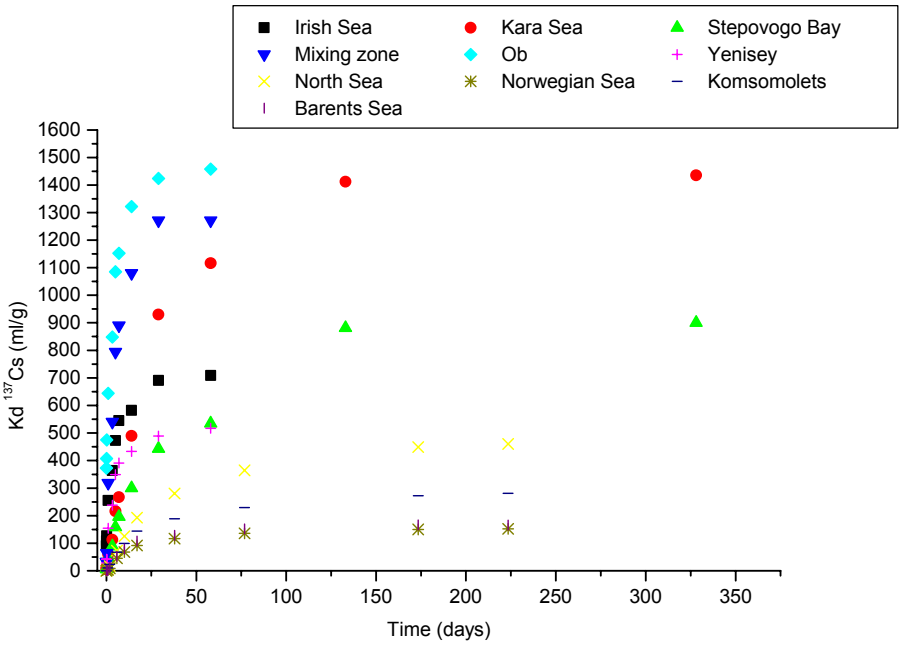

Figure 42. Dynamic K_d values for ^{137}Cs in different sediment-water systems

The K_d kinetics for different species of plutonium were also studied in order to determine the influence of speciation on measured distribution coefficients. To this end, plutonium in reduced [Pu(III,IV)], oxidised [Pu(V,VI)] and complexed [Pu(III,IV)-organic] forms was used in a series of laboratory experiments involving sediment and water from Stepovogo Fjord. As in the previous experiments, K_d values were found to follow first order kinetics in all cases. The association of ^{236}Pu(III,IV) with sediment components occurred rapidly and retention by sediments after one month's contact time was one order of magnitude higher than for ^{236}Pu(V,VI) and ^{236}Pu(III,IV)-organic. The time-dependent interaction of ^{236}Pu(III,IV)-organic was very similar to that of ^{236}Pu(V,VI) and an oxidising effect of the organic agents on ^{236}Pu(III,IV) can not be excluded. The K_ds obtained for ^{236}Pu(III,IV) were, however, about two orders of magnitude lower than the accepted K_d of ~10^5 for plutonium in the Arctic (see §4.3), and demonstrate that the time required for equilibration to be attained must be carefully considered when K_ds are chosen for modelling purposes (WP 9).

The dynamics of binding mechanisms were further studied in tracer experiments in which labile, reversible interactions, were distinguished from inert, irreversible binding using sequential extraction. By defining the sediment as a two-phase system, experimental data were modelled and operational rate constants estimated using a simple box model (Figure 43).

For $^{60}Co^{2+}$ ions, the reversible and irreversible interactions with sediments were found to occur relatively rapidly (high k_1 and k_3) and the mobile fraction became negligible after about 4 days (Figure 44). For $^{134}Cs^{+}$ ions, reversible and especially irreversible interactions took place shortly after contact (high k_3).

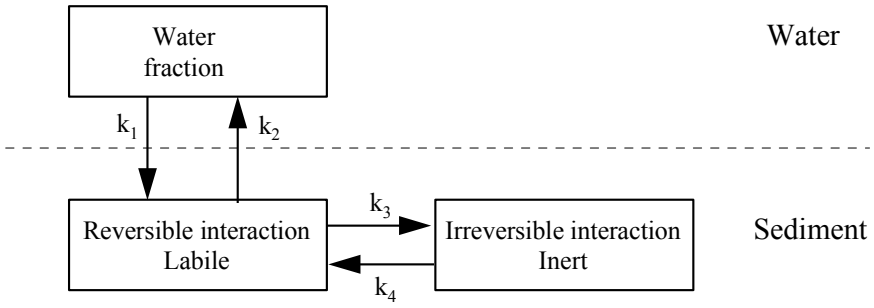

Figure 43. Box model used to study dynamics of radionuclide binding in sediment

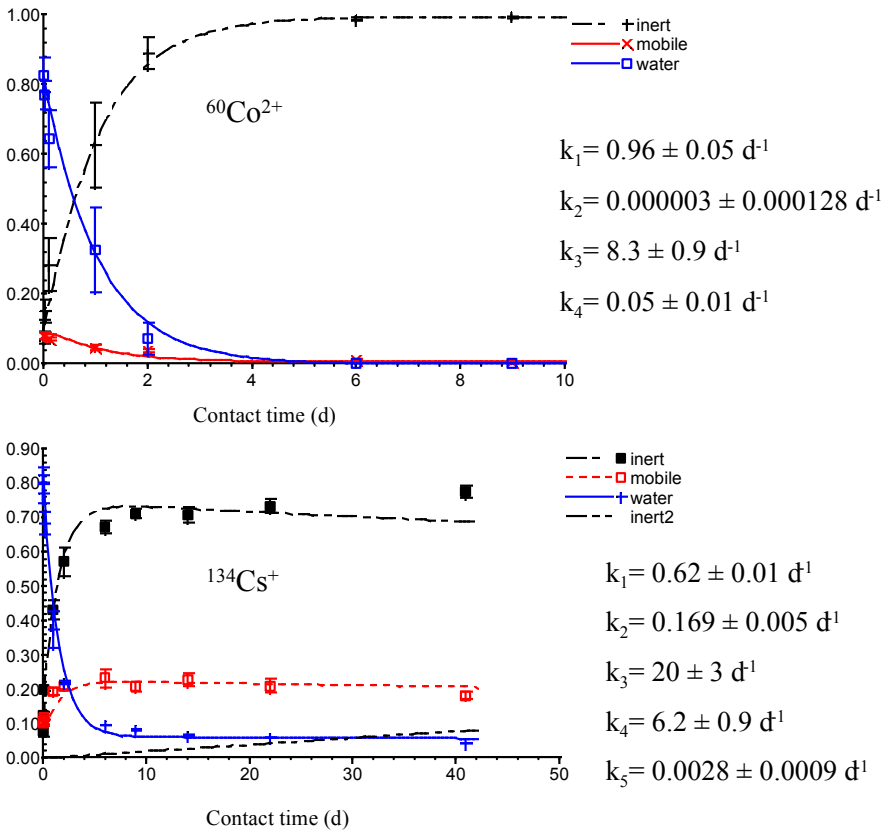

Figure 44. Binding dynamics for $^{60}Co^{2+}$ and $^{134}Cs^{+}$

6.6. Bio-availability and the role of marine invertebrates in actinide bio-kinetics and transfer through the food chain

The group recognised from the outset that to formulate a satisfactory dose-prediction model for the Arctic, the behaviour of radionuclides within the Arctic marine food-chain would have to be examined in detail. An obvious starting point in such a study is the role marine invertebrates play in relation to the distribution of radionuclides within the sediment and their potential for remobilising these radionuclides from sediments, particularly into the primary food-chain.

To this end, dedicated sampling campaigns were carried out at three locations in the western Irish Sea, the eastern Irish Sea and Thule (North-west Greenland). In the western Irish Sea, benthos was collected, together with a sediment core and top and bottom water samples, with a view to determining *in situ* actinide concentration factors (CFs) for invertebrates, as well as for deposition and suspension feeders. Similarly, benthos was collected in the eastern Irish Sea together with representative sediments from the area and a further surface water sample.

In Thule, a significant amount of ship time was given over to the performance of an experiment designed to study in detail the transfer of plutonium and americium from sediments to invertebrates at Thule. Twelve sediment cores were collected from a location approximately 1 km from the point of impact of the aircraft (coded station 20). The cores were taken from an intersecting transect in the area between co-ordinates 76°30.738' N, 69°15.029' W and 76°30.880' N, 69°20.089' W in a mean water depth of 222 m (Figure 45). The coring device used was a twin coring *Gemini* corer. It delivered two cores at each site generally to equal depth with minimal observable disturbance to the surface layer. Six coring locations (Stn. 201–206) were selected with a view to assessing the vertical and horizontal distribution of plutonium, americium and caesium, the comparability of adjacent cores and the variation on the estimate of transfer efficiency to invertebrates. These 12 cores were sliced into 5 cm sections and each core and section was analysed separately. An additional set of twin cores was taken at station 20 (76°30.789 N; 69°17.121 W) for high resolution profile analysis and sedimentation rate determination. These cores were divided into 1 cm sections and adjacent sections were combined.

The animals were sampled following the retrieval of cores by towing a *Sigsbee* dredge across the longest transect (approximately 1 km). A grab sampler was also used to collect animals at this location and 23 samples were collected in total. There was a good variety of invertebrates found in the Thule sediments with some overlap in terms of species with those collected in the Irish Sea holding out the attractive prospect of useful comparisons between both zones.

6.6.1. Invertebrate pre-treatment

Invertebrates retrieved from the sediment in both zones were divided into their respective taxonomic groups and were washed thoroughly in sea water. The animals were allowed to depurate for 24 hours in fresh sea water and were again washed thoroughly. They were drained on tissue paper, weighed and then dried to a constant weight at 80°C. For samples collected in the Irish Sea, whole animals were used in the radiometric analysis i.e. tubes, animal houses or shells were analysed together with the animal soft parts. For the samples collected in Thule, animal soft parts were separated from tubes or shells and each portion was analysed individually.

6.6.2. Invertebrates in the western and eastern Irish Sea

Invertebrate samples taken from the western Irish Sea were found to have ^{239,240}Pu activity concentrations which varied between 0.35±0.12 Bq kg^{-1} (dry) in the composite mollusc sample of *Tellina* and *Ensis* to 8.38±0.39 Bq kg^{-1} (dry) in the polychaete *Owenia*. The mean ^{238}Pu/^{239,240}Pu ratio for the western Irish Sea, excluding one significant outlier, was 0.25 which is clearly indicative of the Sellafield source term. The ^{241}Am/^{239,240}Pu ratio ranged between 0.61 and 3.09.

Invertebrate samples taken from the eastern Irish Sea were found to have ^{239,240}Pu activity concentrations up to 35 times higher than those found in samples from the western Irish Sea site. These varied between 28±1 Bq kg^{-1} (dry) for the brittle stars to 251±4 Bq kg^{-1} (dry) for the polychaete *Owenia*. The mean ^{238}Pu/^{239,240}Pu ratio was 0.200±0.007. The ^{241}Am/^{239,240}Pu ratio ranged between 1.68 and 1.88. Summary data are presented in Table 18.

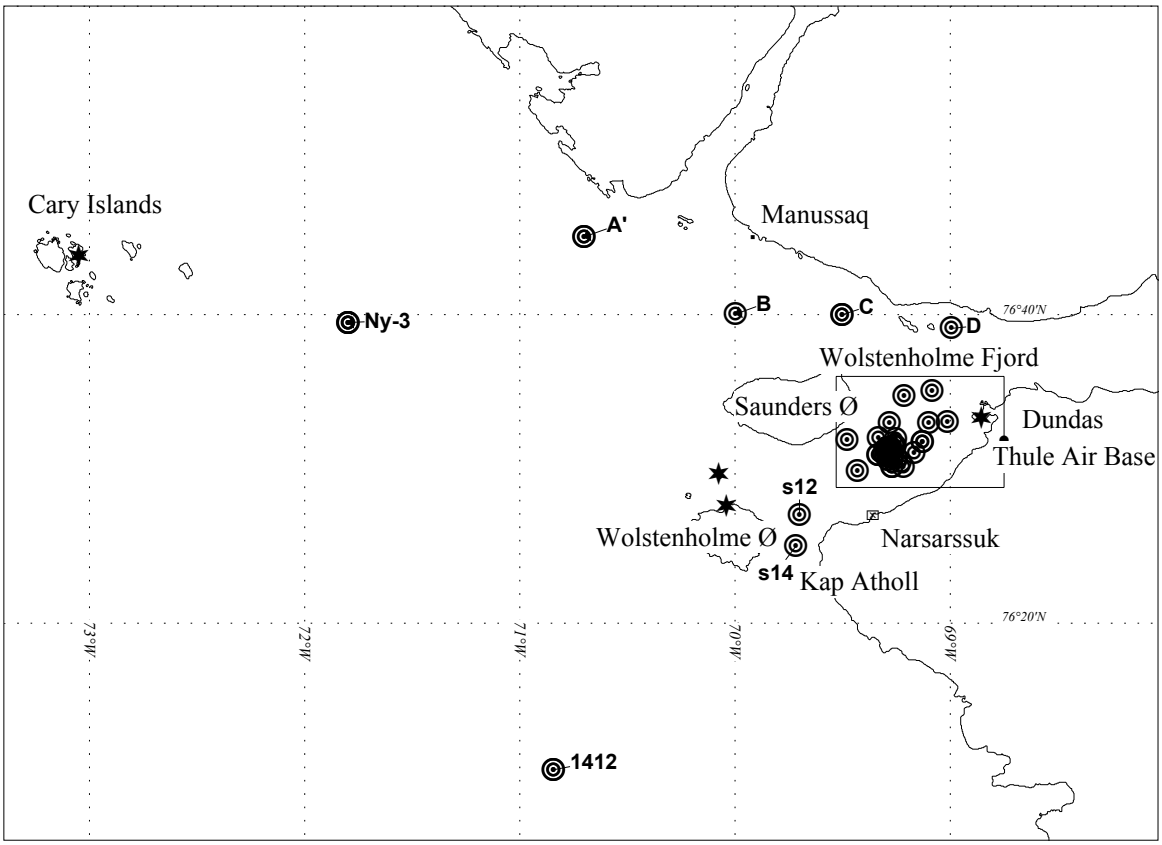

Figure 45a. Thule'97. Sampling locations for sediment (◎) and seaweed (✶). The framed area is enlarged below.

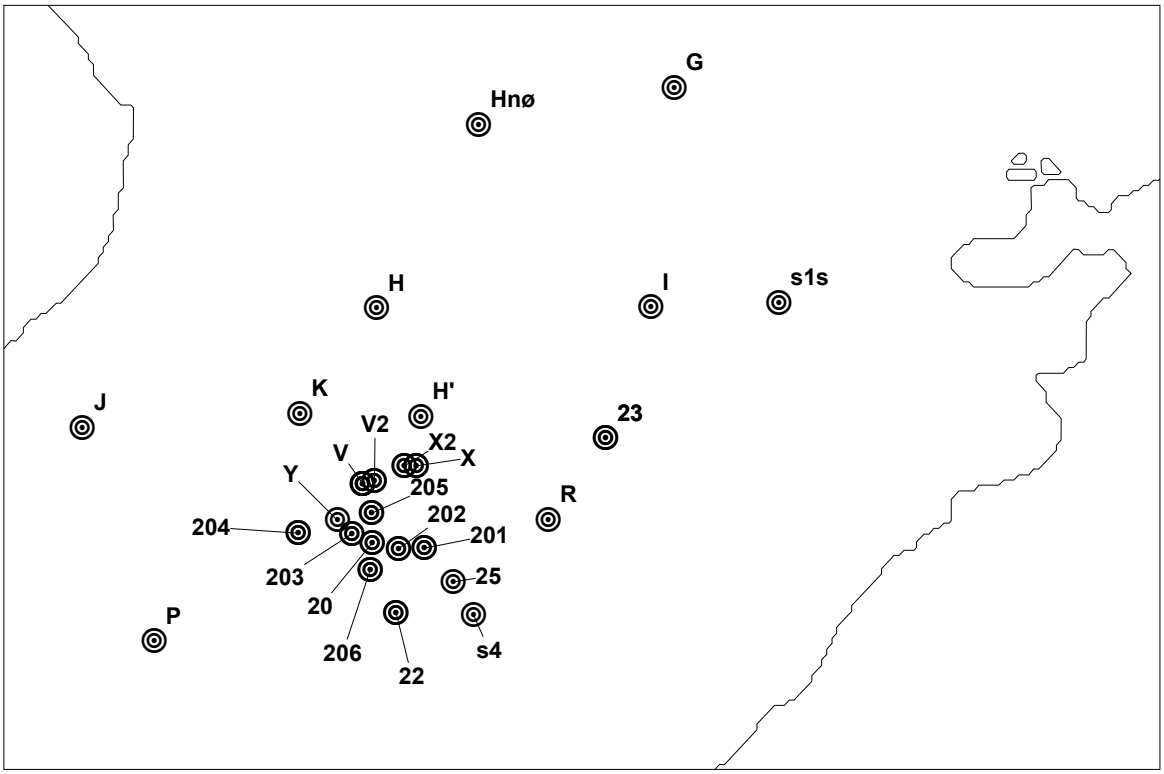

Figure 45b. Thule'97. Sampling locations for sediments (◎). The point of impact for the 1968 accident was at location V

Table 18. Summary activity concentrations and a comparison of plutonium sediment–animal concentration ratios (CR) in Thule and the Irish Sea

Phylum Class	Sub-class	Genus	Location	^{239,240}Pu (mBq kg^{-1}, wet)	CR[a] (Pu)
Echinodermata Stelleroidea					
	Ophiuroidea	*Ophionereis*	Thule	361	0.007
	Ophiuroidea	*Brittle stars*	Thule	385	0.008
	Asteroidea	*Solaster*	Thule	906	0.02
	Asteroidea	*Astropecten*	Thule	252	0.005
				Mean CR=	0.01
	Ophiuroidea	*Brittle stars*	western Irish Sea	221	0.08
	Ophiuroidea	*Brittle stars*	eastern Irish Sea	9240	0.11
				Mean CR=	0.10
Mollusca Bivalvia					
	Herterodonta	*Cardium ciliatum*	Thule	6438	0.13[b]
	Herterodonta	*Macoma calcaria*	Thule	567	0.01[b]
	Herterodonta	*Musculus niger*	Thule	1440	0.03[b]
				Mean CR=	0.05
	Herterodonta	*Tellina & Ensis*	Western Irish Sea	53	0.02[b]
Annelida Polychaeta					
	Errantia	*Nereis*	Thule	438	0.009
		Composite	Thule	250	0.005
	Sedentaria	*Pectinaria (SP)*	Thule	2668	0.055
				Mean CR =	0.023
	Errantia	*Aphrodite*	Western Irish Sea	5380	0.25
		Composite	Western Irish Sea	2670	0.18
		Composite	Eastern Irish Sea	81000	0.19
				Mean CR =	0.21

a: CR is calculated on the basis of ^{239,240}Pu activity concentrations in the animal divided by the activity concentration in the ambient sediment, with both concentrations expressed on a wet weight basis

b: CR in this case refers to the whole animal (including shell or tube); SP: Animal soft parts including inter-valve fluid

6.6.3. Invertebrates at Thule

Plutonium activity concentrations were measured in 17 invertebrate species from Thule with 23 samples analysed in total when appendiculars such as shells and tubes are taken into account. The activity concentrations of ^{239,240}Pu range between <85 mBq kg^{-1} (dry) in the soft parts of a gastropod species (snail) to 53380±2000 mBq kg^{-1} (dry) in a polychaete species. Furthermore it is interesting to note that when species such as the sedentary polychaete *Pectinaria* are divided into soft parts and tube and the ^{239,240}Pu activity concentrations are determined in each fraction and expressed on a wet weight basis, the highest activity concentrations are found in the tube. Another example is the bivalve (sub-class herterodonta) *Macoma calcaria* where the ^{239,240}Pu activity concentrations in the soft parts are 3372±130 mBq kg^{-1} (wet) and in the shell 9503±513 mBq kg^{-1} (wet). This pattern is reflected in other bivalves such as *Musculus niger* and *Cardium ciliatum* as well as the gastropods (Table 19). The ^{238}Pu/^{239,240}Pu activity ratio was determined in 10 samples and excluding one outlier the mean ratio was found to be 0.015±0.003 (1 SD). The ^{241}Am/^{239,240}Pu activity ratio ranged between 0.06 and 7.8, the latter very much an outlier (Table 18). When 3 such outlying values are excluded from the data the ratio was found to be 0.28±0.14 (n=10).

6.6.4. Sediment in the western and eastern Irish Sea

One 12 cm deep core was collected from a site in the western Irish Sea and divided into 1 cm sections. While the core was not particularly deep, much of the benthic activity, though not all, occurs within the top 10 cm. A visual inspection of the core prior to radiometric analysis showed that there was considerable evidence of benthic activity within the core. In the 0–1 cm section there were many shell fragments, polychaetes and small brittle stars. There were bivalves at 2 cm and one *Cucumaria* was found in the 4–5 cm section. There were empty shells found to 10 cm together with obvious signs of burrowing to that depth. The sediment grew considerably darker with depth probably reflecting increasing anoxia, but with no point exhibiting a dramatic change.

Despite an apparent deficit of ^{241}Am in the surface section, plutonium and americium appear to display little variation in activity concentrations in consecutive sections to a depth of 8 cm with activity concentrations decreasing thereafter. This pattern is not observed for caesium which increases steadily in activity down to 9 cm where the activity reaches a plateau of about 45 Bq kg^{-1} (dry). The mean ^{239,240}Pu and ^{241}Am activity concentrations to a depth of 12 cm are 2.82 Bq kg^{-1} (wet) and 2.73 Bq kg^{-1} (wet) respectively. The activity concentrations of ^{239,240}Pu and ^{241}Am in the sediment sampled from the eastern Irish Sea are 86.1 Bq kg^{-1} (wet) and 234 Bq kg^{-1} (wet), respectively, representing significantly higher concentrations than those prevailing in the western Irish Sea. These measurements were used in the determination of the sediment–animal concentration ratios (CR) presented under WP 8.

6.6.5. Sediment from Thule

Caesium-137 was detectable in 10 out of 12 cores to a depth of 10 cm. The cumulative deposition between 0 and 10 cm was found to range between 306 ± 70 Bq m^{-2}and 650 ± 125 Bq m^{-2} with a mean of 517 ± 125 Bq m^{-2} (n=10). The variation is even less pronounced for the cumulative distribution between 0 and 5 cm which has a mean of 261 ± 49 Bq m^{-2}. While some degree of variation would be expected across the cores, due to bio-turbation or smearing during sampling caused by the coarse material in the sediments, the observed variation is relatively small. An examination of cumulative deposition in sections of adjacent cores reveals very close agreement. For example the 0–5 sections of one set of adjacent cores (20-1(1) and 20-1(2)) have ^{137}Cs cumulative depositions of 268 ± 37 Bq m^{-2} and 257 ± 28 Bq m^{-2} respectively which clearly are indistinguishable within the measured uncertainties. Similarly, the 0–5 sections of another set of adjacent cores (20-2 (1) and 20-2 (2)) have cumulative ^{137}Cs depositions of 266 ± 30 Bq m^{-2} and 314 ± 42 Bq m^{-2}, respectively. This pattern is reflected in all of the adjacent cores even when integrated between 0 and 10 cm. This clearly suggests that the practice of bulking corresponding sections of adjacent *Gemini* cores to increase sample mass is vindicated.

The cumulative deposition of ^{239,240}Pu between 0 and 15 cm in the 12 sediment cores was found to range between 3628±360 Bq m^{-2} and 36774±1443 Bq m^{-2} with a mean of 13566 ± 10966 Bq m^{-2}. The variation on the mean contrasts with the tighter distribution of activity concentrations in the 0–5 cm section of the 12 cores which is 3500 ± 1300 Bq m^{-2} (n=12). It is observed from the vertical distribution profiles that the cumulative deposition range is exacerbated by the presence of hot particles. For example, adjacent cores 20-2 (1) and 20-2 (2) exhibit extreme differences in vertical profile. This is principally due to the presence of hot particles in the 5–10 cm section of 20-2 (1) and a hot particle in the 15–20 cm section of 20-2 (2). In general, repeat sample analysis revealed a high degree of sample heterogeneity. The preponderance of the plutonium is found above the 15 cm horizon although in the current study a hot particle in core 20-2 (2) in the 15–20 cm section demonstrates the presence of mixing processes relocating contamination to lower depths. In 7 out of 12 cores a clear sub-surface maximum is observed. Any directional trend in activity concentrations which might be present along the axis of the sampling area is masked by the distortion of the cumulative deposition estimates due to the presence of hot particles.

The ^{241}Am cumulative deposition across the twelve cores and between adjacent cores follows a similar pattern to that of plutonium in that it is highly non-uniform. An examination of the ^{241}Am/^{239,240}Pu ratio shows a wide distribution between 0.0048±0.0003 to 8.5±3.6 with a mean of 0.33 and a median of 0.21. Summary data relevant to the calculation of sediment–animal concentration ratios are given in Table 20.

Table 20. Summary sediment data used in the estimation of sediment–animal CRs

Location	**^{238}Pu** (Bq.kg^{-1}, wet)	**^{239,240}Pu** (Bq.kg^{-1}, wet)	**^{241}Am** (Bq kg^{-1}, wet)	**Dry/ wet ratio**
Western Irish Sea	0.52 ± 0.09	2.8 ± 0.7	2.7 ± 0.7	0.77 ± 0.05
Eastern Irish Sea	17 ± 2	86 ± 7	234 ± 6	0.70 ± 0.07
Stn. 20 Thule	0.73 ± 0.32	49 ± 16	34 ± 29	0.455 ± 0.03

6.6.5. High resolution core profile (Thule, Greenland)

Two adjacent cores at Stn. 20 were sectioned into 1 cm slices and adjacent slices were combined to a depth of 22 cm. The ^{210}Po(^{210}Pb) profile demonstrated a typical sub-surface maximum at the 4–6 cm layer consistent with mixing – probably as a result of invertebrate activity. The concentrations fall off smoothly to levels supported by ^{226}Ra. The latter was determined in the core for consecutive sections and the mean concentration was found to be 29 ± 4 Bq kg^{-1}. The supported fraction of ^{210}Pb down the core was stripped out and the Constant Rate of Supply (CRS) model (Appleby and Oldfield, 1978) was applied to the resulting ^{210}Pb excess profile. The dates derived from the model were in turn plotted against the core's ^{239,240}Pu profile (Figure 46). A broad plutonium peak in the mid 1960s was found, consistent with the timing of the accident at Thule. A further application of the CRS model yields a mean annual sedimentation rate of 0.146 g cm^{-2} y^{-1}, which is in good agreement with the mean value for the area of 0.12 g cm^{-2} y^{-1} reported by Smith *et al.* (1994).

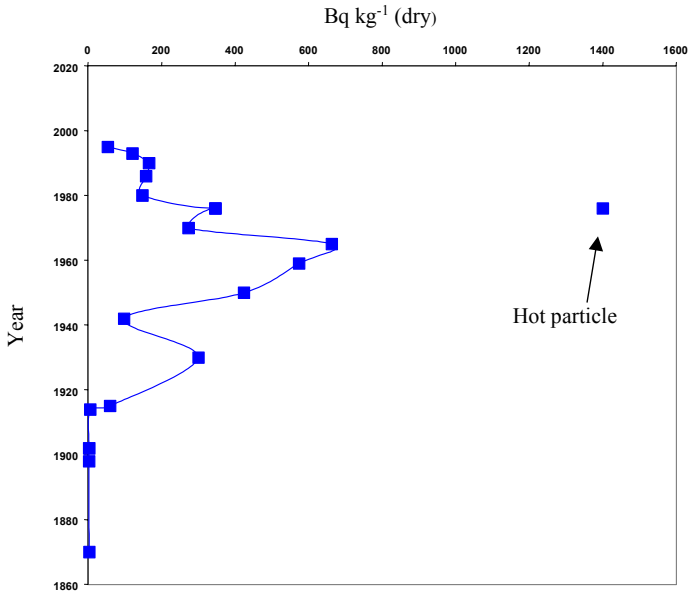

Figure 46. ^{239,240}Pu temporal profile in a core taken at Thule (Stn. 20) in 1997

6.6.6. Plutonium inventories in Thule sediment

In addition to the 12 cores taken around Stn. 20 for CRs calculation, a larger number of cores were collected in the vicinity of Thule (Figure 45) for plutonium inventory determination. Examples of plutonium depth distribution in these sediment cores are shown in Figure 47, where location codes refer to Figure 45.

Plutonium inventories for the cores shown in Figure 47a were found to be quite low, with only two cores (Stns. D and J) from Bylot Sound showing a clear but small effect from the accident. In contrast, the 12 cores from Bylot Sound proper (Figures 47b and 47c) were all clearly affected by the accident, although showed different depth distributions. In four cores (Stns. Hnø, H', V2 and X2), the accident plutonium seems to be well mixed throughout the sediment column, indicating strong biological/physical mixing. In seven other cores (Stns. G, P, 23, Y, 22, 20 and 25), a more classical depth distribution was observed, with a clear biologically mixed layer on the top and a gradual decrease with depth below this layer. If the deeper part of the high concentration layer is assumed to correspond to the date of the accident in 1968, a sedimentation rate of 3–4 mm y^{-1} is derived, in good agreement with the rates determined in previous expedition on the basis of $^{210}Pb_{excess}$ profiles (Smith *et al.*, 1994). The penetration of plutonium to deeper layers and the absence of low concentrations in the top layers are attributed to biological mixing processes by the rich benthic community.

The distribution of $^{239,240}Pu$ concentrations in surface sediments (0–3 cm) at Thule (Figure 48) clearly shows enhanced concentrations around the accident site and an even distribution of the plutonium in the remaining deep part of Bylot Sound (Figure 48b). Outside Bylot Sound, (Figure 48a), concentrations are much lower and compatible with background fallout levels observed in northen latitudes. They are, however, higher to those observed at Shades Øer (0.12 Bq kg^{-1}), far removed from the accident site. Whether this difference is caused by the presence of small amounts of accident plutonium in the vicinity of Thule or if instead can be attributed to difference in sedimentation conditions remains unclear.

The plutonium inventories for the cores analysed are given in Table 21. Integration of these inventories over the seafloor area affected by the accident yields a total inventory of 1.8 TBq(^{239}Pu), which is in good agreement with previous estimates (Aarkrog, 1971; 1977; Aarkrog *et al.*, 1981; 1984; 1988;1997).

Table 21. Inventories of $^{239,240}Pu$ in sediment cores from Thule (August, 1997)

Station Code	Distance from impact (km)	$^{239,240}Pu$ inventory (Bq m^{-2})
V2	0	58940
Y	0.73	45690
20	0.95	12490
X2	0.98	20910
22	2.2	3590
25	2.3	13500
S4	3.07	9440
P	4.07	10320
23	4.2	2300
G	8.7	2654
D	16.1	275
C	17	1140
Ny-3	50	25

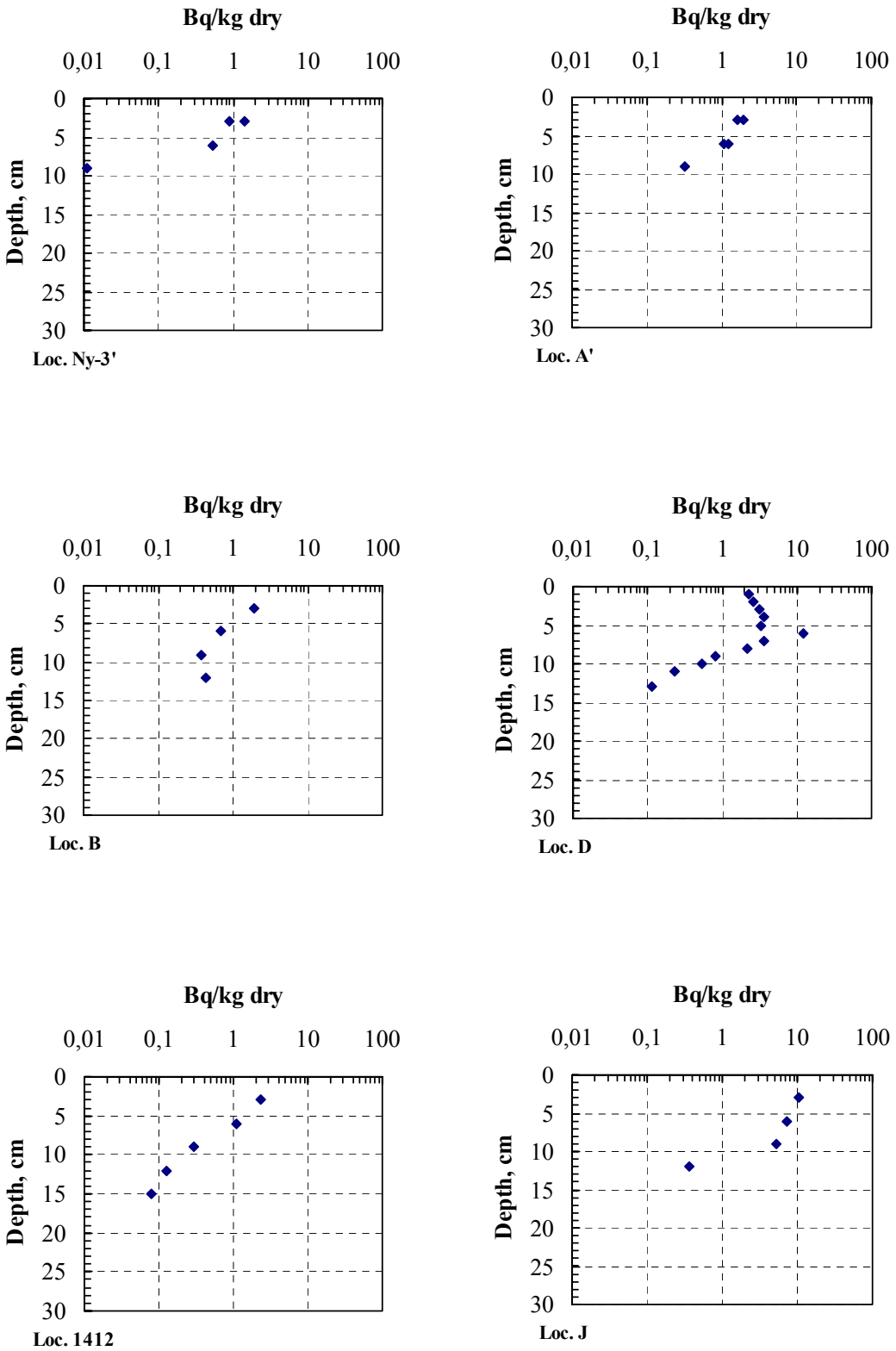

Figure 47a. ^{239,240}Pu depth profiles in cores from Thule (August, 1997)

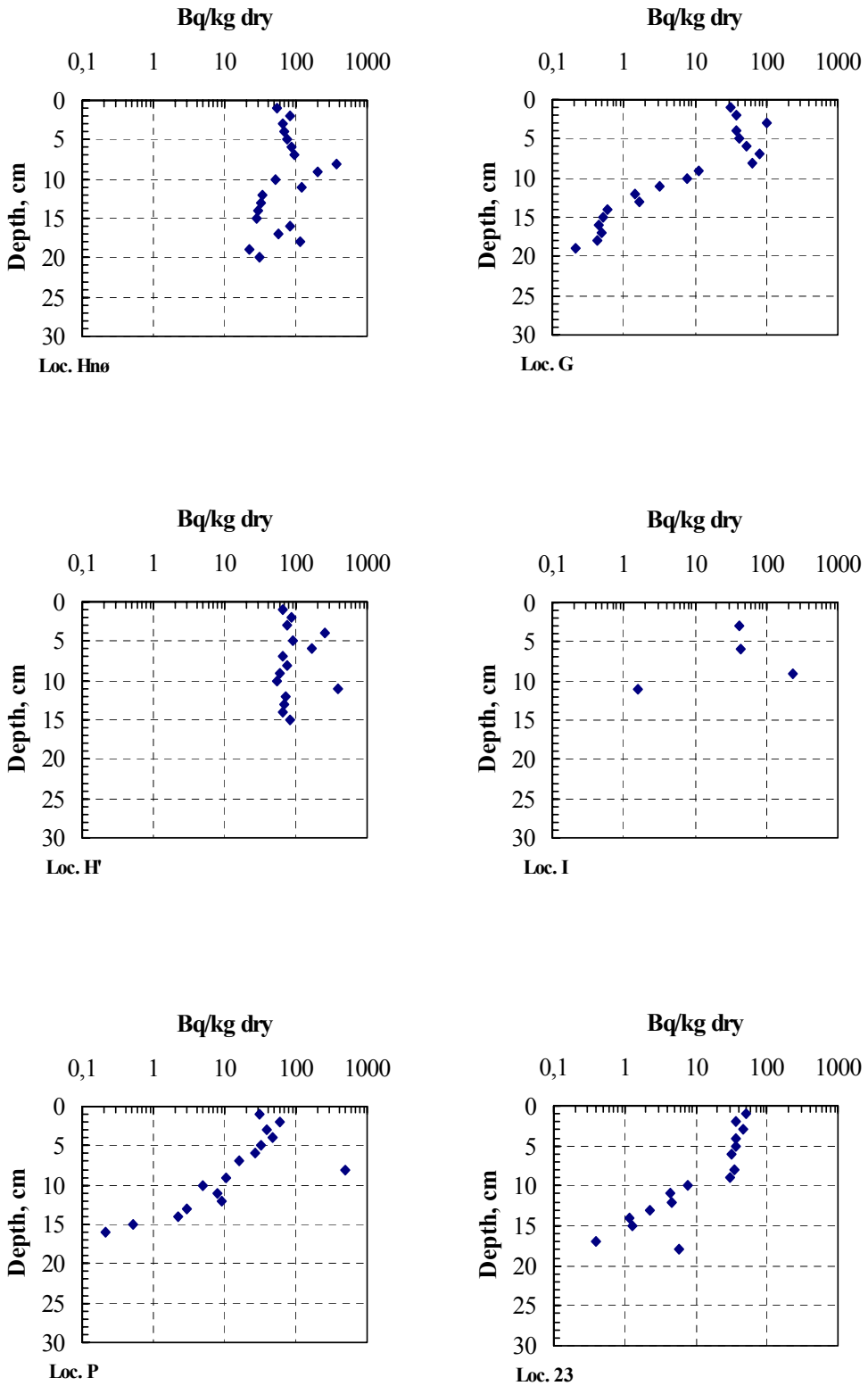

Figure 47b. ^{239,240}Pu depth profiles in cores from Thule (August, 1997)

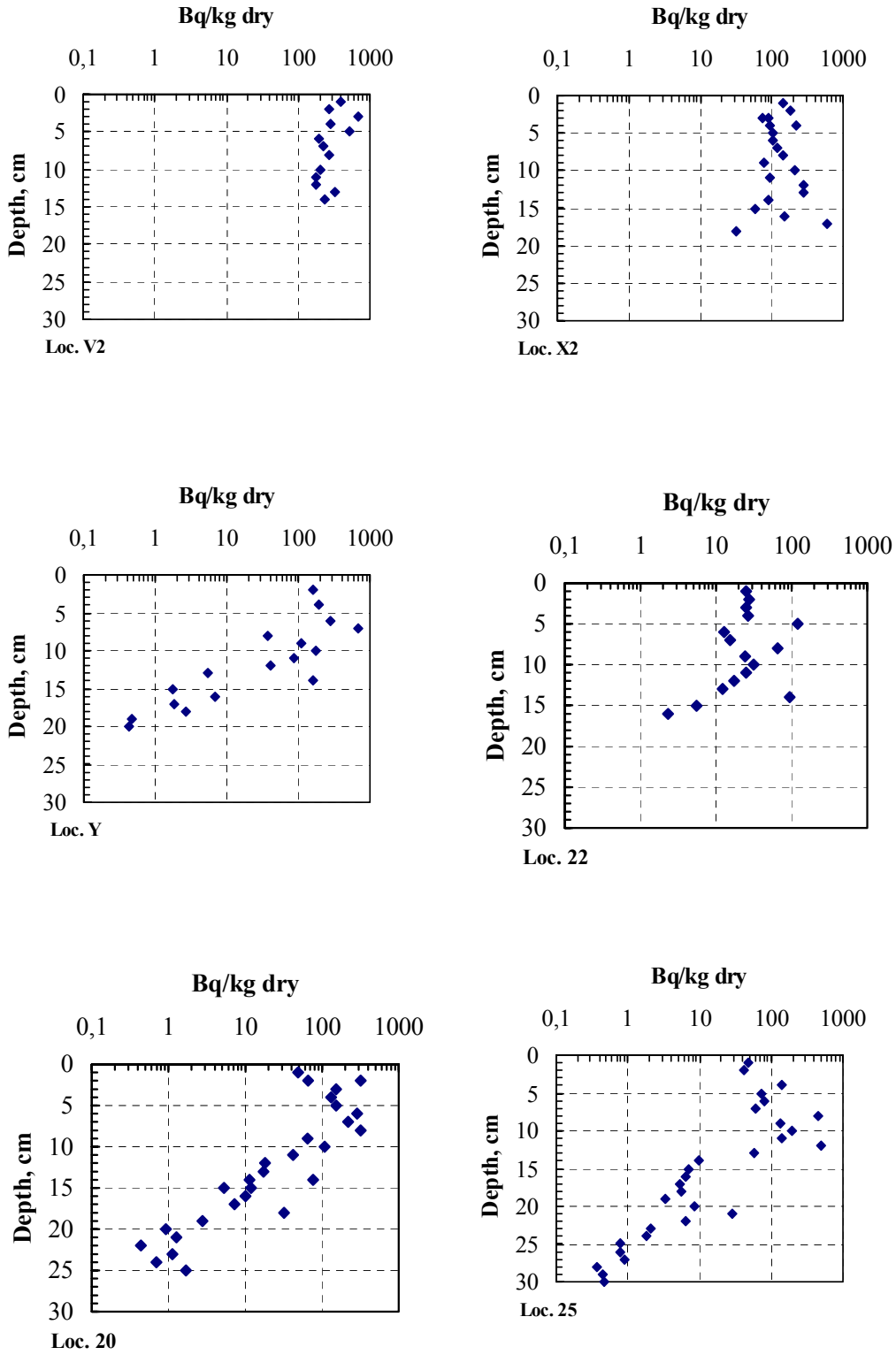

Figure 47c. ^{239,240}Pu depth profiles in cores from Thule (August, 1997)

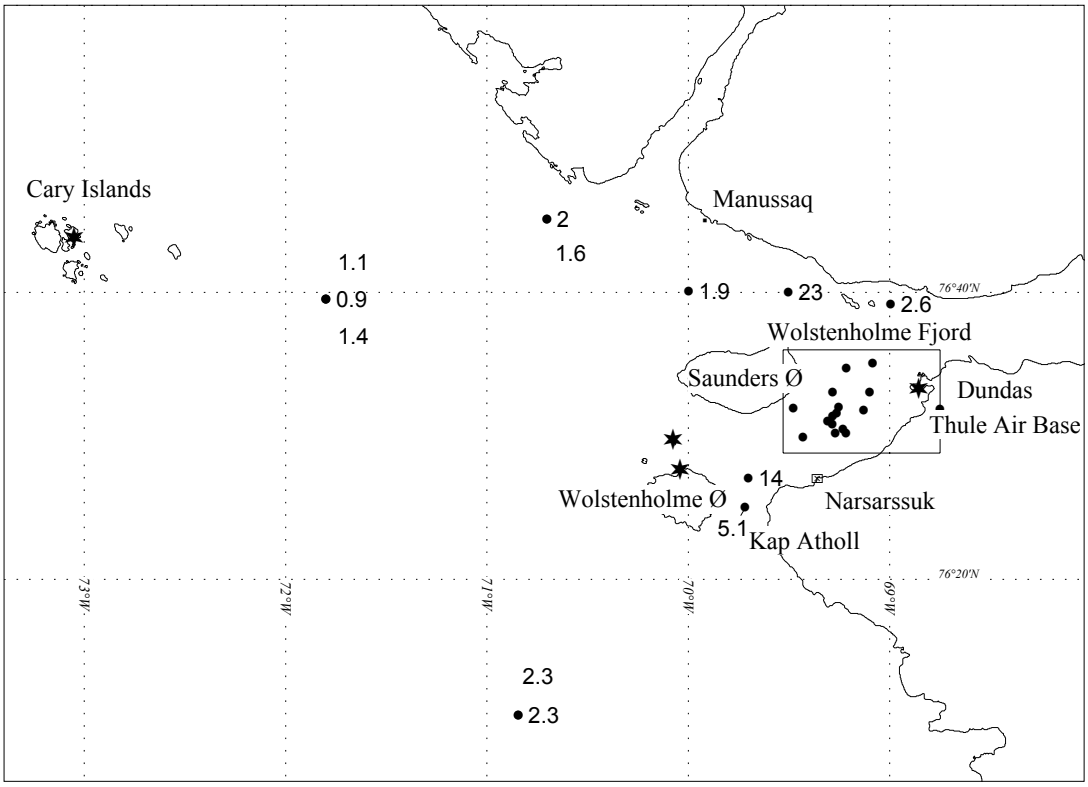

Figure 48a. Plutonium concentrations in surface sediments at Thule (Bq ^{239,240}Pu kg^{-1} dry wt.)

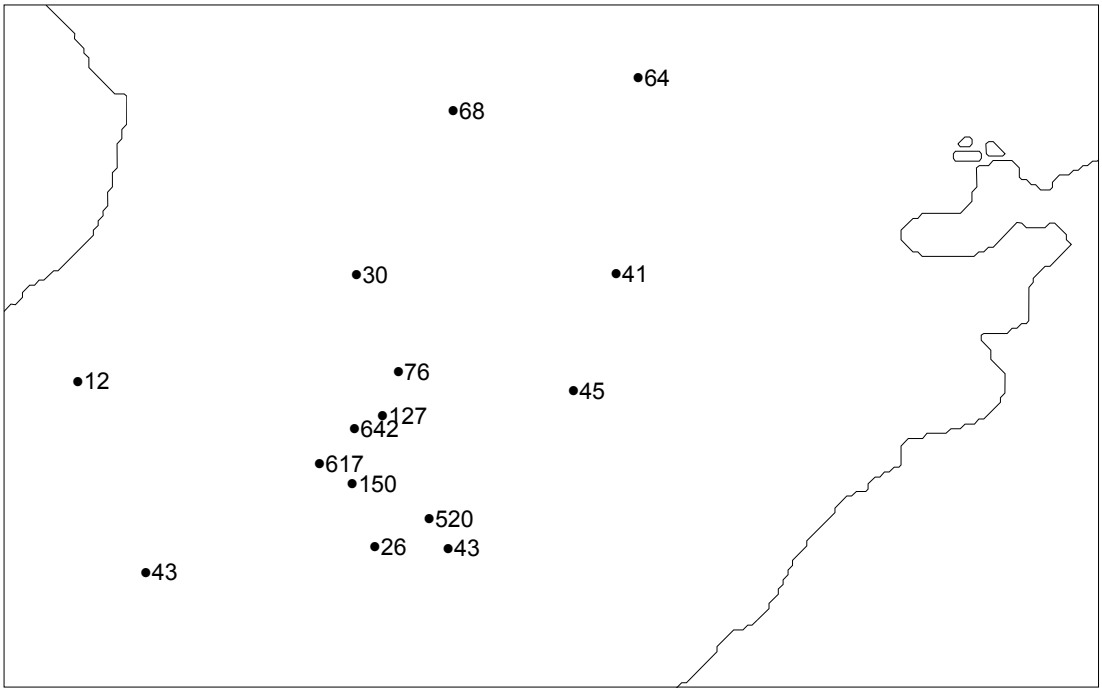

Figure 48b. Plutonium concentrations in surface sediments at Thule (Bq ^{239,240}Pu kg^{-1}, dry wt.)

Surface sediment ^{239,240}Pu concentrations were also employed to estimate CR values for biota sampled at stations throughout Bylot Sound (Figure 49). It is worth noting that although most of the biota sampled live buried in the sediment or on the sediment surface, CR values below 1 indicate that plutonium is not readily transferred to biota. Of all samples, only one single bivalve sample showed a much higher level, most likely due to the presence of a 'hot particle'. In Table 22, average plutonium CRs for different biota groups are given on a dry weight basis. Average plutonium concentrations and radiation doses arising from the consumption of each biota group are given in Table 23.

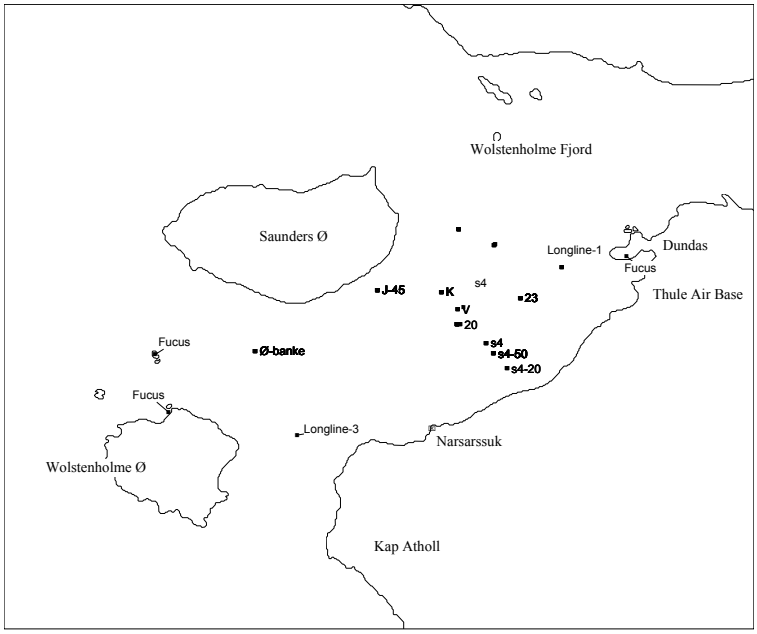

Figure 49. Biota sampling locations at Thule (August, 1997)

Table 22. Plutonium concentration ratios (CR) for biota at Thule (August, 1997)

Class	**Species**	**CR** (Bq kg^{-1} biota / Bq kg^{-1} sediment)		
		Average	SD	n
Mollusc	bivalves	0.025	0.024	13
Mollusc	Macoma calcarea	37*		1
Mollusc	snail	0.0033	0.0018	9
Mollusc	Squid, Rossia sp.	0.00036		1
Echinoderm	Asteroidea	0.0094	0.0139	9
Echinoderm	Ophiuroidea	0.013	0.0159	4
Echinoderm	Crinoidea	0.0070	0.0060	4
Echinoderm	Echinoidea	0.12	0.16	4
Echinoderm	Holothurioidea	0.0080	0.0083	4
Crustacea	shrimp	0.0048	0.0088	4
Crustacea	var.	0.038	0.039	4
Annelida	Pectinaria	0.068	0.05234	4
Annelida	var.	0.023	0.033	10
Annelida	tube	0.28	0.29	6
Fish	Liparis sp.	0.00035		1

* Outlier, likely due to presence of 'hot' particle

Table 23. Average concentration of ^{239,240}Pu in biota samples sampled at Thule, and radiation dose (dose factor = 2.5×10^{-7} Sv Bq^{-1}) expressed as the number of kilograms to be consumed in order to get a 1 mSv dose from ^{239,240}Pu

Sample type	^{239,240}Pu (Bq kg^{-1}, fresh wt.)	SD (%)	n	Dose (kg mSv^{-1})
Fucus	0.08	84	6	5.09E+04
Bivalve	0.29	205	13	1.40E+04
Snail	0.13	97	9	3.17E+04
Seastar	0.94	254	9	4.24E+03
Brittle star	0.29	88	4	1.38E+04
Feather star	0.07	30	4	5.77E+04
Sea Urchin	1.57	114	4	2.54E+03
Sea cucumber	0.05	108	4	7.60E+04
Shrimp	0.06	141	4	6.90E+04
Crustaceans	0.18	47	4	2.17E+04
Pectinaria	4.92	149	4	8.13E+02
Worms	0.34	107	10	1.19E+04
Worm tubes	21.89	50	6	1.83E+02
Bivalve, outlier	83.14		1	4.81E+01
Squid, Rossia sp.	0.0047		1	8.49E+05
Fish, Liparis sp.	0.0363		1	1.10E+05

7. Fluxes, mixing processes and advective transport

7.1. Inputs from reprocessing plants and dumped waste

The detection of radionuclide concentrations arising from dumped wastes in the Kara and Barents Seas requires that these signals be discriminated from other sources, including the contribution from European reprocessing plants (Sellafield and La Hague). Thus, the identification and quantification of past and present contributions from these waste discharges to Arctic waters is considered to be an essential part of this programme. Previously, ^{137}Cs and ^{134}Cs data had been used extensively to evaluate the dispersion of soluble radionuclides from the Irish Sea to adjacent waters such as the North Sea, the Baltic Sea and the North-east Atlantic. Additionally, an extensive sampling programme to determine the distribution of other conservative radionuclides such as ^{99}Tc and ^{90}Sr was carried out in the English Channel, southern North Sea, Skagerrak and Kattegat in the early 1990s, with a view to studying the dispersion of effluent from the La Hague reprocessing plant. However, little information was available at the beginning of the present programme on the distribution of ^{90}Sr and ^{99}Tc concentrations in Irish Sea waters and their contribution to radionuclide fluxes to the Arctic as a result of discharges from Sellafield.

To rectify this, a number of sampling expeditions to the Irish Sea and adjacent waters were undertaken by members of the collaboration in order to (i) evaluate ^{137}Cs, ^{99}Tc and ^{90}Sr concentrations in the Norwegian, Greenland and Barents Seas, (ii) determine ^{90}Sr and ^{137}Cs concentrations in the Irish Sea, and (iii) study the distribution of ^{99}Tc in the Irish Sea and adjacent UK coastal waters following the authorised discharge of elevated quantities of ^{99}Tc arising from the operation of the Enhanced Actinide Removal Plant (EARP) at Sellafield. In addition, results from time-series data on radionuclide concentrations in seaweed collected at Utsira (Norway) over the last two decades have been used to estimate transfer factors and transit times from European reprocessing plants to the Arctic. The results of these studies are summarised below.

7.1.1. Radionuclide concentrations in Norwegian, Greenland and Barents Seas

A survey was carried out in September–October 1994 aboard *R.V. Cirolana* to evaluate ^{137}Cs, ^{99}Tc and ^{90}Sr concentrations in the Norwegian, Greenland and Barents Seas. Results were compared with data from earlier investigations to determine the most recent pattern of contamination from European reprocessing discharges. The ^{137}Cs data have recently been reported in detail elsewhere (Kershaw *et al.*, 1997). Briefly, the distribution pattern in 1994 was similar to that observed on a previous survey in 1989. The highest concentrations were observed in the northern North Sea, decreasing gradually along the Norwegian Coastal Current and into the Barents Sea. Concentrations in the central/western Barents Sea, associated with the incoming Atlantic Water, were lower than in the Norwegian Coastal Current at the same longitude and in the outflowing waters further north. The concentrations along the east Greenland coast, both at 71° N and just north of the Denmark Strait were similar to those in the Norwegian Coastal Current and higher than those in the West Spitsbergen Current. Concentrations between Iceland and Scottish waters could be attributed to global fallout. The net flux of ^{137}Cs into the Barents Sea was estimated to be 300–400 TBq y^{-1}. Of this, only 100–200 TBq y^{-1} was attributable to global fallout (assuming a fallout concentration of 3–5 Bq m^{-3}). A further 120–180 TBq of ^{137}Cs of non-fallout origin, was estimated to have been transported *via* the Fram Strait into the Polar Ocean.

Data for the distribution of dissolved ^{99}Tc and ^{90}Sr are given in Figure 50. The distribution patterns of ^{99}Tc and ^{90}Sr are similar to that observed for ^{137}Cs and show that, despite substantial reductions in discharges from reprocessing operations, the transport of a soluble component to the Arctic is still both detectable and quantifiable. Concentrations in the Barents Sea were relatively uniform, being slightly higher in the incoming Norwegian Coastal Current, but lower in Atlantic Waters. Higher concentrations were observed along the coast of Greenland, especially in waters of polar origin. This is consistent with Sellafield effluent from the higher discharges in the 1970s entering the Arctic and then exiting in the East Greenland Current as a source of radionuclides to the Atlantic Ocean.

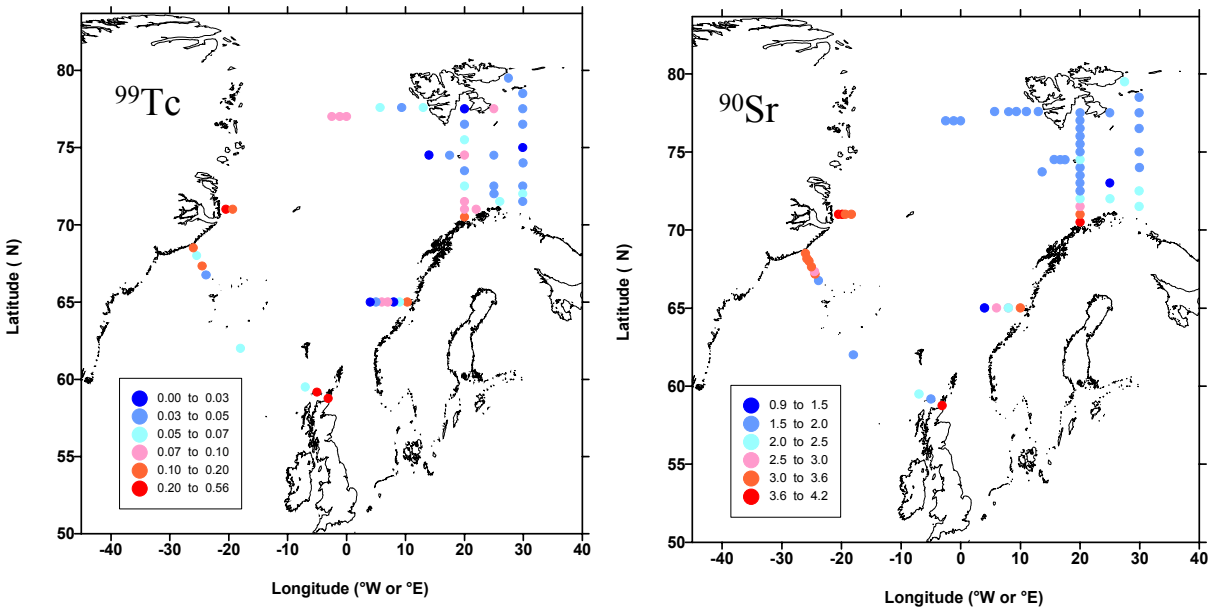

Figure 50. Distribution of ^{99}Tc and ^{90}Sr concentrations (Bq m^{-3}) throughout northern European waters (*R.V. Cirolana*, September 1994)

7.1.2. $^{137}Cs/^{90}Sr$ ratios in the Irish Sea and adjacent waters: an assessment of transport from the Irish Sea en route to the Arctic

In 1995, a collaborative expedition was carried out in the northern Irish Sea to determine ^{90}Sr and ^{137}Cs concentrations in surface sea water samples. Values for the $^{137}Cs/^{90}Sr$ activity ratio were used to evaluate the present contribution from the current Sellafield source-term to the Irish Sea and beyond. ^{137}Cs concentration levels were found to be essentially uniform (15–40 Bq m^{-3}) for a large proportion of the survey area and, given the discharge history, could be considered to reflect residual concentrations of a well-mixed system. Along a large section of the Cumbrian and southern Scottish coastline, extending from Liverpool Bay in the south to the Mull of Galloway in the north, levels were greater by approximately an order of magnitude than those observed along the Irish coastline. The ^{137}Cs contours extended parallel to the Cumbrian coastline with some displacement towards the Mull of Galloway in the north and Liverpool Bay in the south and, overall, confirmed that migration of ^{137}Cs out of the Irish Sea occurs predominantly in a northerly direction through the North Channel.

The overall distribution pattern of ^{90}Sr in the northern Irish Sea was similar to that of ^{137}Cs. However, closer examination of the $^{137}Cs/^{90}Sr$ ratios showed that in close proximity to the Sellafield pipeline (at the discharge point, and immediately to the north and south of the pipeline) ratios were somewhat lower (between 1.5–2.4) than those observed elsewhere in the Irish Sea (range 2.9–4.4). Indeed, the $^{137}Cs/^{90}Sr$ ratio was remarkably uniform throughout the study area with an average value of ~3.8. Ratios were considerably greater than those observed in releases from Sellafield over the preceding two years (0.43–0.47), but less than that for the decay corrected inventory (~6.7) up to the end of 1995.

The difference between the $^{137}Cs/^{90}Sr$ ratios in sea water and releases from Sellafield is not indicative of slow dispersion of effluent since the residence half-time for water in the Irish Sea has been estimated to be about 1 year. Instead, these data indicate the presence of an additional source term of dissolved ^{137}Cs in the Irish Sea, over and above discharges from Sellafield. The secondary source, as already discussed in §6.1, is most likely to be ^{137}Cs remobilised from previously contaminated sediments. A lower limit for the contribution from current Sellafield discharges can be simply derived if it is assumed that only ^{137}Cs was remobilised from the seabed. Then, the difference between the $^{137}Cs/^{90}Sr$ ratio in sea water (~3.8) and Sellafield effluent in 1994 and 1995 (~0.45) implies that discharges from the primary source account for ~12% of the dissolved inventory in the Irish Sea. This value (lower limit) compares very well with that reported in §6.1 using an alternative method of determining the relative contribution of ^{137}Cs from recent discharges.

The annual flux of dissolved ^{137}Cs and ^{90}Sr out of the Irish Sea through the North Channel was estimated using an average value for their respective concentrations in the area, and assuming the flow through the North Channel to be ~5 km^3 per day (Pentreath *et al.*, 1986). Using average values of 44 mBq l^{-1} and 11.5 mBq l^{-1} for the concentrations of ^{137}Cs and ^{90}Sr, respectively, fluxes of 80 TBq and 21 TBq per annum were calculated. These figures provide an estimate of the present source-term of ^{137}Cs and ^{90}Sr to adjacent waters.

7.1.3. Impact of elevated ^{99}Tc discharges from Sellafield

^{99}Tc concentrations throughout the Irish Sea and adjacent UK coastal waters were measured in the course of three major sampling campaigns undertaken after the commissioning of a new treatment plant (EARP) at Sellafield in March 1994. The objective of these campaigns was to assess the impact of elevated ^{99}Tc releases arising from the operation of this new plant. Shortly after the initial discharges from EARP, levels had increased over a relatively wide area, with a marked migration of the effluent towards the southern Scottish coastline and towards the entrance of the North Channel. At this time, discharges appeared to have had minimal influence on the distribution of ^{99}Tc in the southwestern part of the Irish Sea. Concentrations on the Scottish side of the North Channel were found to be over 10 times higher than before the

elevated releases began, and indicated that a portion of the effluent from EARP operations had been transported beyond the Irish Sea within 2–3 months. Tc-99 concentrations as a function of distance from Sellafield along three arbitrarily defined transects, extending north and south along the coastline and a third almost in a west–southwest direction normal to the Cumbrian shore, are shown in Figure 51. It is acknowledged that the distances reported are the shortest between sampling positions and Sellafield, and not necessarily the direct route for ^{99}Tc migration. Also, the release of ^{99}Tc was likely to have occurred continuously over a number of weeks, rather than as a single pulse, further complicating the determination of ^{99}Tc migration. Nevertheless, the ^{99}Tc pulse along the northern transect is remarkably well defined, with a distinct maximum and a drawn out leading edge. Following the initial elevated release, the peak in ^{99}Tc concentrations had migrated some 45 km, nearly half the distance between the release point and the North Channel. Assuming that subsequent transport patterns occurred at the same rate, it is suggested that the mean transit time (as represented by the transport of the maximum concentration of the pulse) to the North Channel on this occasion was of the order of six months

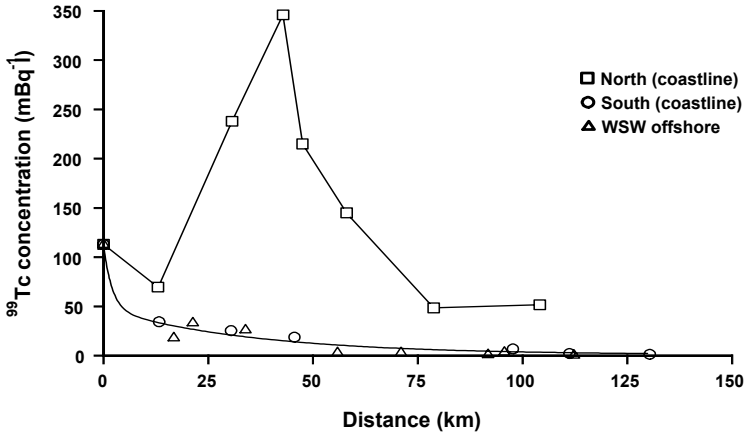

Figure 51. ^{99}Tc concentrations as a function of distance from Sellafield from the first post-EARP survey (*R.V. Cirolana*, May 1994)

Results from a survey carried out before the commencement of the EARP operations indicated the residual levels prior to the elevated ^{99}Tc discharges (Figure 52). There appeared to be no influence from Cap de La Hague discharges in the Celtic Sea, although it is possible that a minor contribution from this source was present in the southern North Sea. The data from the post-EARP survey increased ^{99}Tc concentrations up to the north entrance of the North Channel . Beyond, the signature was temporarily lost due to inflow of Atlantic sea water. However, the ^{99}Tc signal re-emerged, en route to the north Scottish coastline, with concentrations slowly decreasing with distance. No contribution of the elevated discharges was noticeable leaving the southern Irish Sea via St. George's Channel. Thus, it seems reasonable to conclude that ^{99}Tc had migrated to the northern North Sea within some 9 months following the initial elevated discharge.

During 1995 and 1996 the pattern of ^{99}Tc discharges changed in that, although the releases remained elevated, the monthly discharges were relatively constant. The ^{99}Tc distribution in the northern Irish Sea shows that, in comparison to previous surveys, levels were increased over the entire Irish Sea. Although migration occurred predominantly to the north, the impact of the discharges was also significant in the southern Irish Sea. Further afield, it is apparent that the initial plume from 1994 becomes elongated around the north of Scotland and into the North Sea. Additionally, it has been possible, using most recent data and previous surveys, to estimate ^{99}Tc inventories in the water column of the Irish Sea. Overall, the data suggest that in 1995, ≈71% of

the discharge was transported out of the Irish Sea over the twelve month period. In turn, this implies that the residence half time for ^{99}Tc is ≈6–7 months, which is shorter than that of 1 year as previously reported.

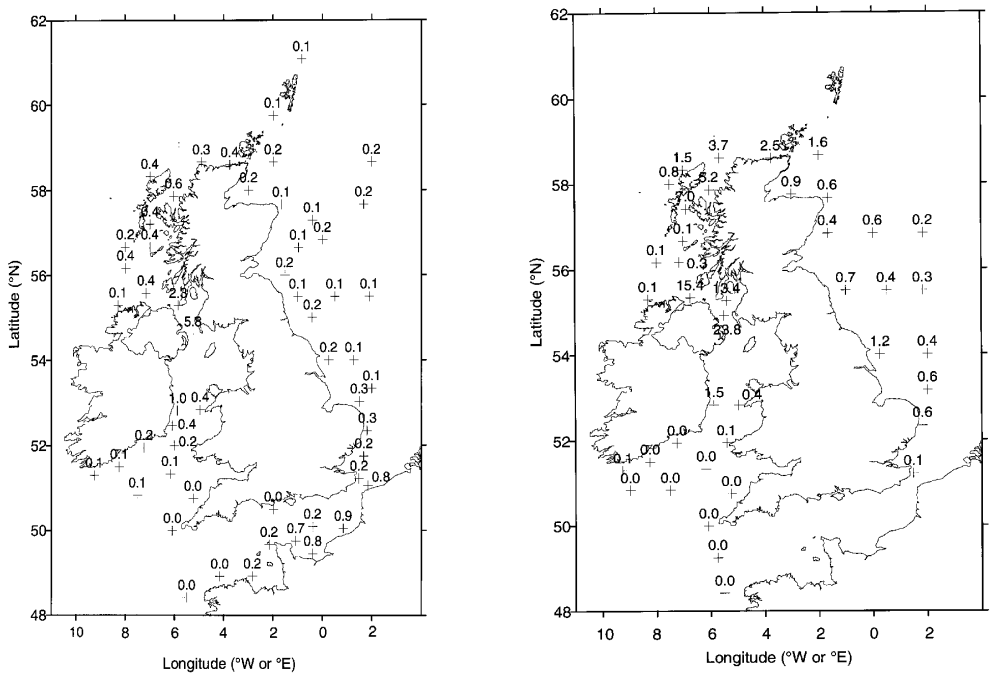

Figure 52. ^{99}Tc concentrations (mBq l^{-1}) outside the northern Irish Sea. (Left) pre–EARP (R.V. *Cirolana* 11/93) and (Right) post–EARP (R.V. *Cirolana* 12/94)

Data from sites lying within a series of arbitrarily defined geographical areas, or boxes, were combined to give a mean and range of concentrations for each sampling period. The areas were selected on the basis of the preferred transport direction of the ^{99}Tc signal and data availability: a 'Sellafield Box', adjacent to the pipeline outfall; a 'Solway Box', across the mouth of the Solway Firth to the north of Sellafield; a 'North Channel Box', across the northern exit of the Irish Sea; a 'Pentlands Box', enclosing the Pentland Firth between the Scottish mainland and Orkney; and, an 'NCC Box' within the NCC between latitudes 59^{o} and 65^{o} N, including data from two published sources (Brown *et al.,* 1998; Herrmann *et al.,* 1995).

The time variation in the concentration of ^{99}Tc (mean and range) in each of the 5 selected boxes is shown in Figure 53. The distribution in June 1994 reflected the preceding pulsed release in March and April, its influence being most apparent in the 'Solway Box'; i.e. the plume of higher activity had been transported out of the immediate vicinity of the outfall within the first three months. Concentrations declined in the next two sampling periods before increasing to a maximum in December 1996. The passage of the initial pulse was also evident in the North Channel, although it had become less distinct. In contrast, the 1994 pulses were not detected in the 'Sellafield Box' and the highest concentrations (up to 1800 Bq m^{-3}) occurred in December 1995, falling significantly by December 1996. The EARP releases were apparent in December 1994 in the 'Pentlands Box' and in the 'NCC Box' in November 1996 (Brown *et al.,* 1998). The highest water concentrations occurred towards the end of 1995 in the Sellafield Box (up to 1800 Bq m^{-3}), coinciding with the annually-averaged maximum discharge in 1995, and were followed by a significant reduction. In contrast, water concentrations in the Solway and North Channel boxes decreased after the 1994 pulses before increasing again. Advection and tidal dispersion within the Irish Sea have reduced concentration variations with distance and time.

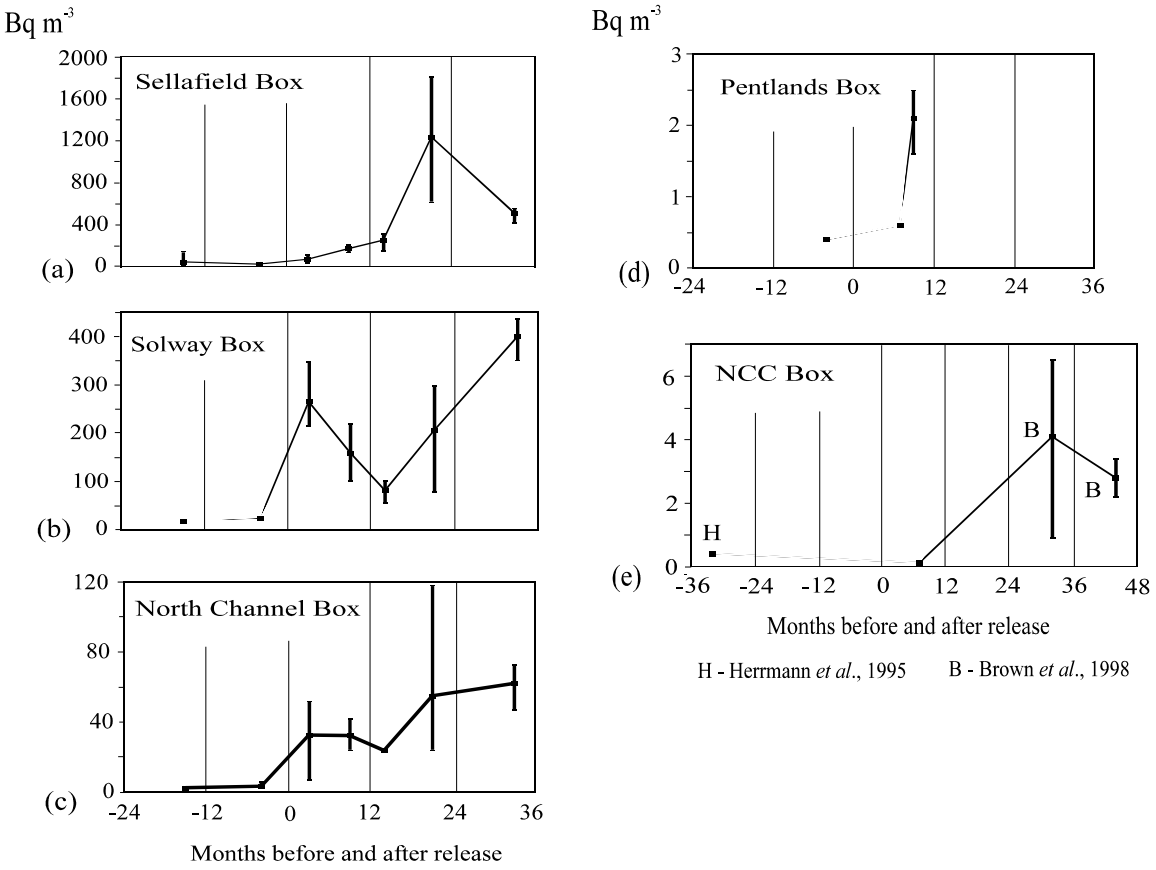

Figure 53. Concentrations of ^{99}Tc (mean and range, Bq m^{-3}) in surface sea water in five regions, plotted against the number of months before or after the start of the EARP-related releases in March 1994

Additional sources of time-series data were identified to augment the offshore studies. Analysis of *Fucus sp.* provides an excellent indicator of concentration trends in the marine environment. In the present study six data sets were selected from sites which provided the optimum spatial and temporal coverage of the time-varying ^{99}Tc signal: Sellafield, adjacent to the pipeline (quarterly); St Bees Head, about 20 km north of Sellafield (quarterly from 1994, previously annual); Port William, on the south coast of Scotland (semi-annual); Cape Wrath, on the northwest tip of mainland Scotland (annual); Sandside Bay to the west of Dounreay in northeast Scotland (quarterly); and, Hartlepool, in northeast England (annual from 1995, previously semi-annual).

The concentrations of ^{99}Tc in *Fucus vesiculosus* increased following the start of the EARP releases. The maximum concentration occurred at the pipeline (over 85 kBq kg^{-1}, wet wt.). On average, there was a decrease of a factor of approximately two at St Bees Head and a further factor of ten reduction at Port William, compared with the Sellafield concentrations. Overall, concentrations at Sellafield and St Bees Head were declining 4 years after the releases commenced. However, a high degree of variability was evident in both data sets, with a periodicity of approximately 12 months. This pattern was repeated at Port William, although it was less well defined. (Kershaw *et al.*, in press).

^{99}Tc is taken up readily by *Fucus* but tends not to be released, in contrast with ^{129}I and ^{137}Cs. Thus, it will tend to integrate short-term (<1 year) variations in water concentrations. This is well illustrated in Figure 54, in which the percentage change in the concentration of ^{99}Tc in *Fucus* from St. Bees Head (within the Solway Box) and in seawater from the Solway Box are compared. Both media registered a rapid response to the increased discharge. However, the water

concentrations revealed the passage of the initial plume, whereas the concentrations in *Fucus* continued to increase after the water concentrations had declined. The variability in the *Fucus* concentrations after the initial uptake had a periodicity of about twelve months. The variability in the monthly releases had a periodicity, presumably for operational reasons, of 3–4 months. Lower concentrations in *Fucus* occur in the spring and summer as a result of increased growth causing dilution. This pattern was overlaid on the variability due to changes in the water concentration. This seasonal effect could also be observed for ^{99}Tc in *Fucus vesiculosus* from the east coast of Ireland (Smith *et al.,* 1997), bringing about a change in the apparent concentration factor. Sampling outside the Irish Sea on an annual basis failed to show this variability, for the obvious reason. It can be appreciated that seawater and *Fucus* analysis may provide complementary information, providing the underlying processes are accounted for. A potential additional factor is the location of the *Fucus* sampling sites. It is conceivable that water transport close to the Norwegian coast is significantly slower than a few kilometres offshore, as has been demonstrated for transport along the coastal boundary of the southern North Sea (Hermann *et al.,* 1995). Utsira is an island within the NCC so *Fucus* concentrations may be expected to respond more rapidly to changes in the NCC water concentrations than at more sheltered fjordic sites. This may result in a disparity between the arrival time of a radionuclide signal detected by water sampling offshore and that obtained by shoreline seaweed sampling on the mainland.

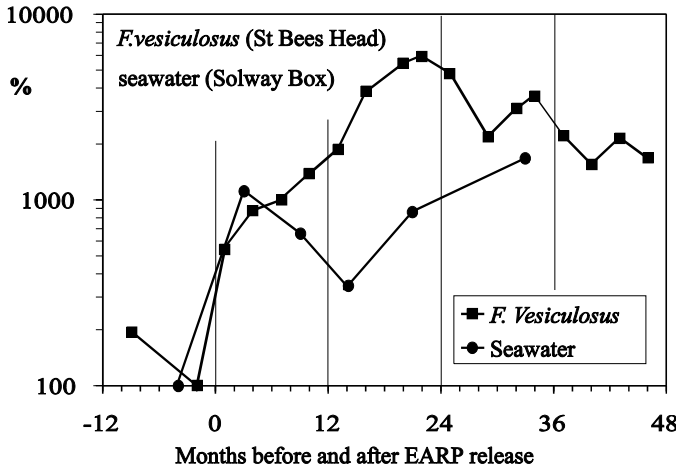

Figure 54. Comparison of the percentage change in the ^{99}Tc concentration in both *Fucus vesiculosus* from St. Bees Head and in sea water from the Solway Box

^{99}Tc transfer factors from Sellafield to the Norwegian south-west coast of 24 Bq m^{-3} per PBq y^{-1} (calculated as the quotient between observed concentrations and the average discharge rate over the transport time) had been reported by Dahlgaard *et al.* (1997) on the basis of pre–EARP measurements. Comparison of more recent ^{99}Tc data (mean concentration of 3.4 Bq m^{-3}on the Norwegian south-west coast in November 1996) with the average discharge from Sellafield in the period 1994–95, yields a transfer factor value of 20 Bq m^{-3} per PBq y^{-1}, in close agreement with the previously estimated value (Brown *et al.*, in press).

7.1.4. ^{99}Tc and ^{137}Cs time-series at the Norwegian coast

Sampling of the algae *Fucus vesiculosus* at three locations on the open Norwegian coast (Figure 55), carried out since the early 1980s, continued in the course of the ARMARA programme with a view to assess past and present contributions from European reprocessing plants to Arctic waters. When a point discharge has been advected by marine currents for 1–5 years, which is the time span for the transport considered here, the effect of a single discharge spreads in time over more than one year. The term *transit time* is used to refer to the maximum

effect (in concentration terms) of the discharge at a given location. This means that the first observation of a particular discharge may be seen somewhat earlier than the estimated transit time, and that the effect of such a discharge may continue to be seen long after this time. The transit times from La Hague and Sellafield to the southernmost sampling station (Utsira) had previously been estimated to be 1–2 years and 3–5 years, respectively (Guegueniat *et al.*, 1994; Dahlgaard, 1995). For a given transit time, t, a transfer factor (TF) can be calculated as the quotient between observed concentrations in water (Bq m^{-3}) at the sampling site and an average discharge rate (PBq y^{-1}) t years earlier. Once the transfer factors are known, concentrations arising from a particular discharge can be readily estimated.

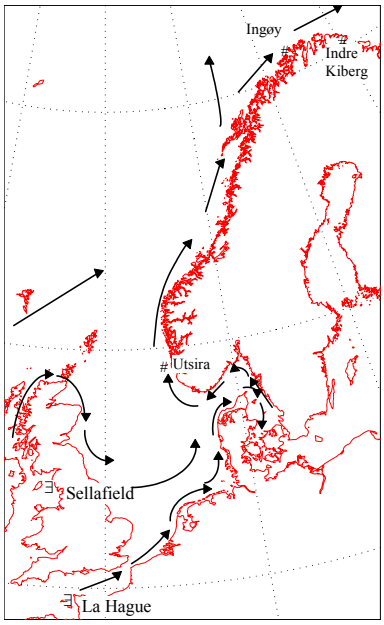

Figure 55. Sampling locations for *Fucus vesiculosus* on the Norwegian coast

In Figure 56, a comparison is made between measured and modelled concentration in *Fucus vesiculosus* at the three Stations along the Norwegian coast. Modelled data were calculated on the basis of transit times, transfer factors and the Sellafield and La Hague discharges. Initially, transfer factors for ^{137}Cs and ^{99}Tc were estimated on the basis of sea water concentrations derived from a numerical compartment model describing the dispersion of European reprocessing wastes to northern waters (Nielsen, 1995), but were then tuned/calibrated to best fit experimental data obtained between 1980–85 (Table 24). For the two sampling sites in northern Norway, an extra year was added to the transport time for calculation purposes. To enable direct comparison with the measured data, radionuclide concentrations in sea water were converted to radionuclide concentrations in *Fucus* by using an appropriate concentration factor (CF).

Table 24. Transfer factors (Bq m^{-3} per PBq y^{-1}) used for modelling ^{137}Cs and ^{99}Tc in *Fucus* along the Norwegian coast

Location	Sellafield		La Hague	
	^{137}Cs	^{99}Tc	^{137}Cs[†]	^{99}Tc
Utsira (Stn. 10)	16.5	24	(47)	55
Northern Norway (Stns. 3 and 4)	7.5	11	(21)	25

[†] Difficult to evaluate, given the weakness of the signal

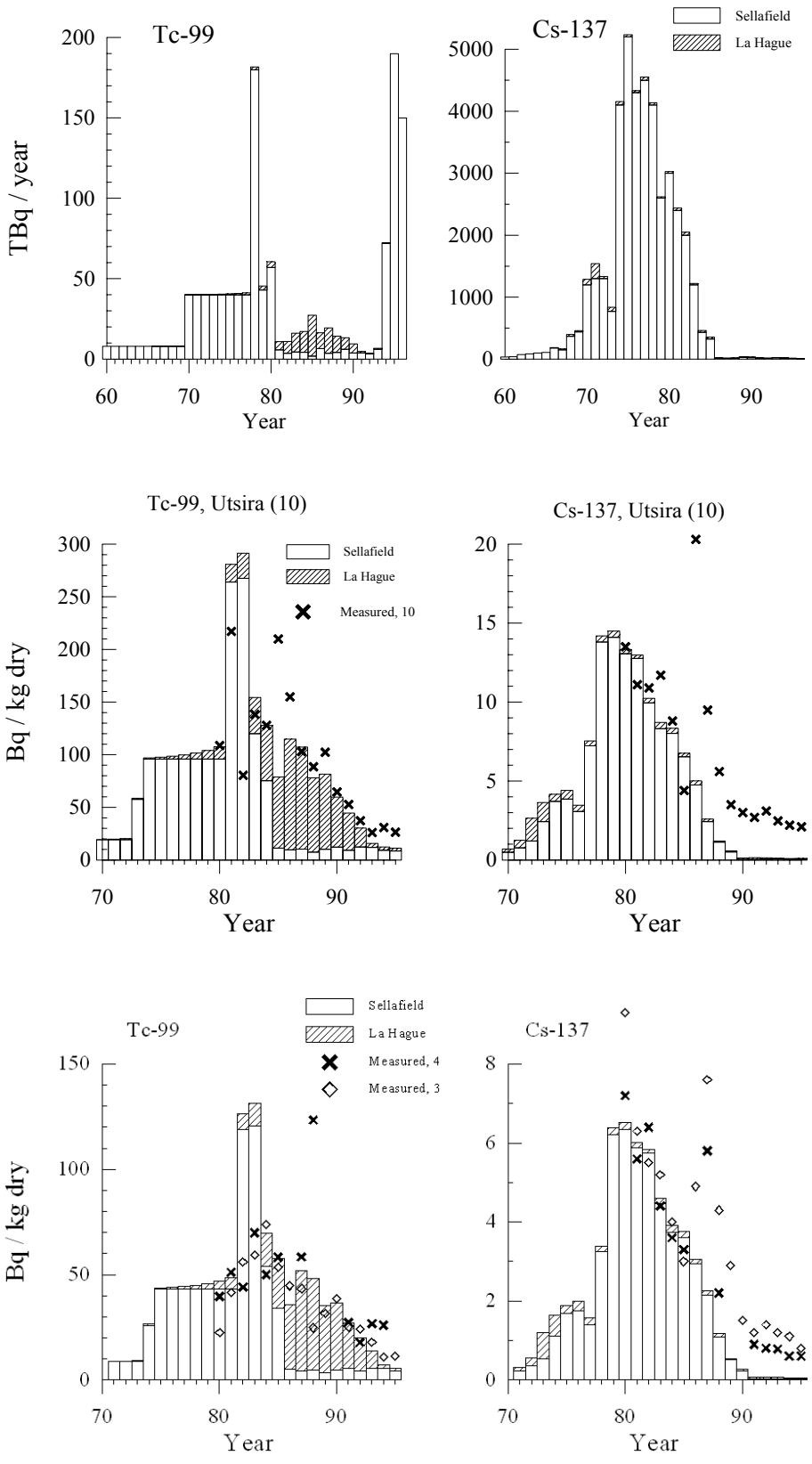

Figure 56. Controlled discharges of ^{99}Tc and ^{137}Cs from Sellafield and La Hague (upper graphs), and measured (marks) and modelled (bars) ^{99}Tc and ^{137}Cs concentrations in *Fucus vesiculosus* from Utsira (Stn. 10), Ingøy (Stn. 4) and Indre Kiberg (Stn. 3)

The effect of the Chernobyl accident in 1986 and the consequent enrichment in ^{137}Cs concentrations from the Baltic outflow are evident at all three stations. For ^{99}Tc, the best agreement is obtained for the period when La Hague discharges were dominant for this nuclide. It must be noted, however, that the modelled data prior to 1978 is based on estimated ^{99}Tc releases only, as discharge values for this nuclide were not reported until that year. Thus, it is possible that historic ^{99}Tc discharges from Sellafield have been overestimated.

7.1.5. Evaluation of the contribution of English Channel waters as a source of artificial radionuclides to Arctic waters

A compilation of radionuclide concentrations in the English Channel, gathered in the course of research campaigns undertaken in 1983, 1986, 1988 and 1994, were employed to assess the impact of controlled releases from the La Hague reprocessing plant in the English Channel (Bailly du Bois *et al.*, in press). The first of the diagrams in Figure 57 (corresponding to the strictly conservative nuclide ^{125}Sb) gives the resulting activities (in Bq m^{-3}) corresponding to a release rate of 1 MBq s^{-1} from the La Hague reprocessing plant. Comparison of this distribution with those for other less conservative elements (^{137}Cs, ^{134}Cs, ^{106}Ru and ^{60}Co) shows the extent of loss for each of these radionuclides in different parts of the Channel (Table 25). Interestingly, an excess in the ^{137}Cs inventory was observed for all the years studied, equivalent to the La Hague signal.

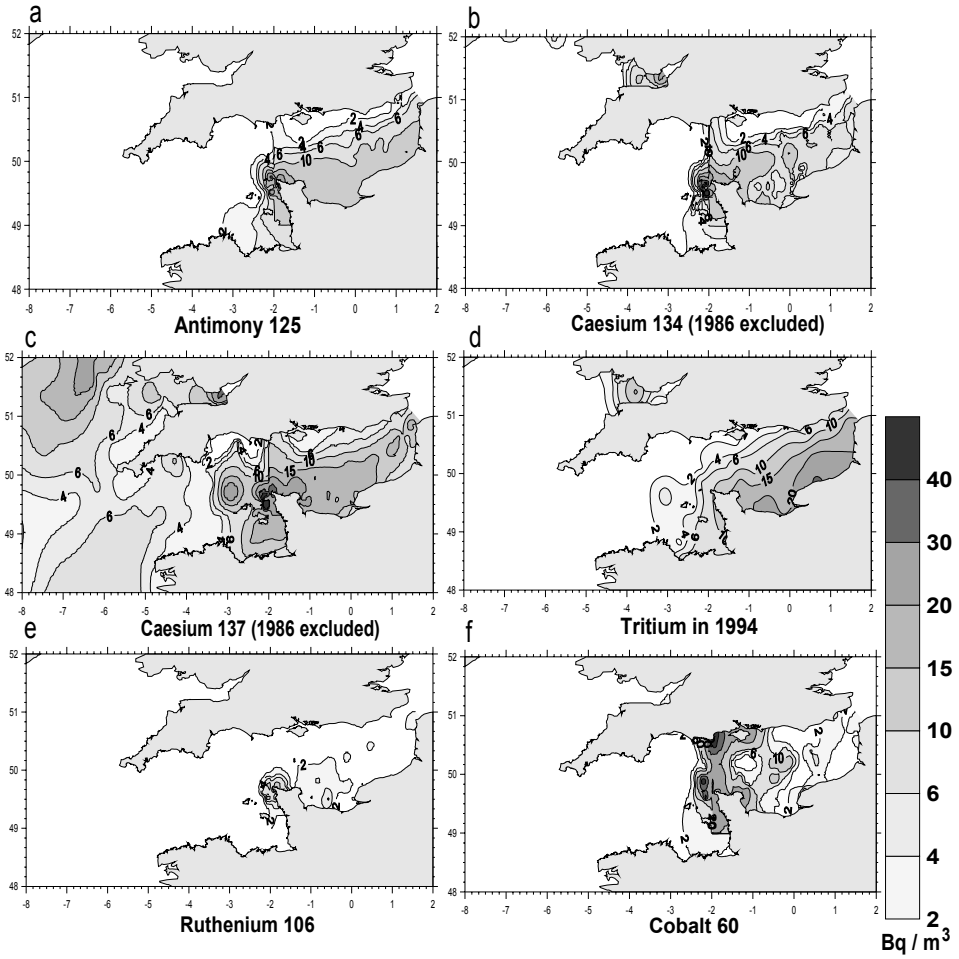

Figure 57. Average distribution of radionuclides in sea water from the English Channel following a constant release of 1 MBq s^{-1} from the La Hague reprocessing plant

Table 25. Comparison of measured radionuclide inventories in the English Channel with corresponding releases from La Hague during 1983–94. ^{125}Sb was used as a reference for the calculations; background levels of Atlantic surface water (^{137}Cs, ^{3}H) and Chernobyl fallout (^{134}Cs, ^{137}Cs) were subtracted before the calculation

	^{137}Cs	^{134}Cs	^{106}Ru	^{125}Sb	^{60}Co	^{3}H
Whole English Channel: 4702 km^3; equivalent release duration: 7.3 months						
Number of campaigns	3	2	3	3	3	1
Fraction of the La Hague release	233%	86%	26%	98%	14%	103%
Eastern English Channel: 1576 km^3; equivalent release duration: 5.7 months						
Number of campaigns	5	3	5	5	2	1
Fraction of the La Hague release	139%	83%	19%	98%	8%	121%

Except for ^{137}Cs, radionuclide inventories in the English Channel could be explained on the basis of the La Hague releases, global weapons and Chernobyl fallout and other nuclear plant controlled releases. Contribution from dumping grounds in the centre of the Channel were not observed in any of the years of study. A local labelling of ^{60}Co was regularly observed west of the Isle of Wight but, given the non-conservative behaviour of this radionuclide in sea water, the effect of this labelling is limited to Channel waters and do not affect concentrations in, for example, the North Sea or the Arctic.

Comparison of the observed ^{137}Cs excess inventory in the Channel between 1983 and 1986 and Sellafield releases during the same period indicate that this excess inventory could be explained if just ~1% of the Sellafield discharge had found its way to the Channel. Numerical modelling gives possible mechanisms to explain this pathway (Garreau and Bailly du Bois, 1997), although other possibilities, such as the return of Arctic waters previously labelled by industrial releases (Sellafield) in the mid–1970s, or leakage from nuclear waste dump sites in the North Atlantic could also account for the observed excess.

In the light of the above considerations, a sampling campaign (ATMARA) was carried out in July 1998 aboard the French research vessel R.V. Surôit within the framework of the ARMARA programme, which aimed to identifying the origin and respective contributions of water masses entering the western approaches of the English Channel. A number of radiotracers were envisaged as possible tools for water mass identification and, accordingly, a large number of surface and sub-surface water samples were collected for ^{134}Cs, ^{137}Cs, ^{60}Co, ^{125}Sb, ^{90}Sr, ^{99}Tc, ^{238}Pu, ^{239,240}Pu and ^{3}H analyses. The resulting data confirm previous observations that ^{137}Cs levels at the entrance of the English Channel (2.0–2.1 Bq m^{-3}) are now very close to the Atlantic background (1.8–1.9 Bq m^{-3}), and show no evidence of North Atlantic water masses labelled with higher ^{137}Cs levels arising from leakage from dump sites or return of historically contaminated Arctic waters. Nevertheless, on average, there is evidence of slightly higher levels in waters from the South Irish Sea. As the ^{3}H data clearly shows the influence of these waters into the Celtic Sea and up to the west of Brittany (Figure 58), it seems reasonable to conclude that it is the contribution from Sellafield discharges, transported via the South Irish Sea and the Celtic Sea, that is responsible for the excess ^{137}Cs inventory in the Channel, although the time scale of this labelling process is not, as yet, known.

Analysis of radionuclide concentrations further afield and comparison with measured concentrations in the Channel indicate that a release of 10 TBq month^{-1} of a conservative radionuclide into the central part of the English Channel (La Hague) gives rise to activities of 4–5 Bq m^{-3} at the entrance of the Norwegian Channel and 1–3 Bq m^{-3} at the entrance of the Barents Sea (Guegueniat *et al.*, 1997). For 1995, the contribution of the La Hague releases to measured ^{125}Sb, ^{90}Sr, ^{137}Cs and ^{99}Tc concentrations in the Barents Sea were estimated to be 0.33, 0.33, 0.06 and 0.002 Bq m^{-3}, respectively. As a comparison, the natural background radioactivity of

Atlantic waters (due mainly to the presence of ^{40}K) is 12000 Bq m^{-3}, while artificial levels due to global weapons fallout in the Barents and Kara Sea are 3–11 Bq m^{-3} for ^{90}Sr, 4–12 Bq m^{-3} for ^{137}Cs and 0.08–0.2 Bq m^{-3} for ^{99}Tc (Strand *et al.*, 1994). It is clear from these figures that the contribution of the La Hague releases to radionuclide concentrations in waters feeding the Arctic is quite low at the present time.

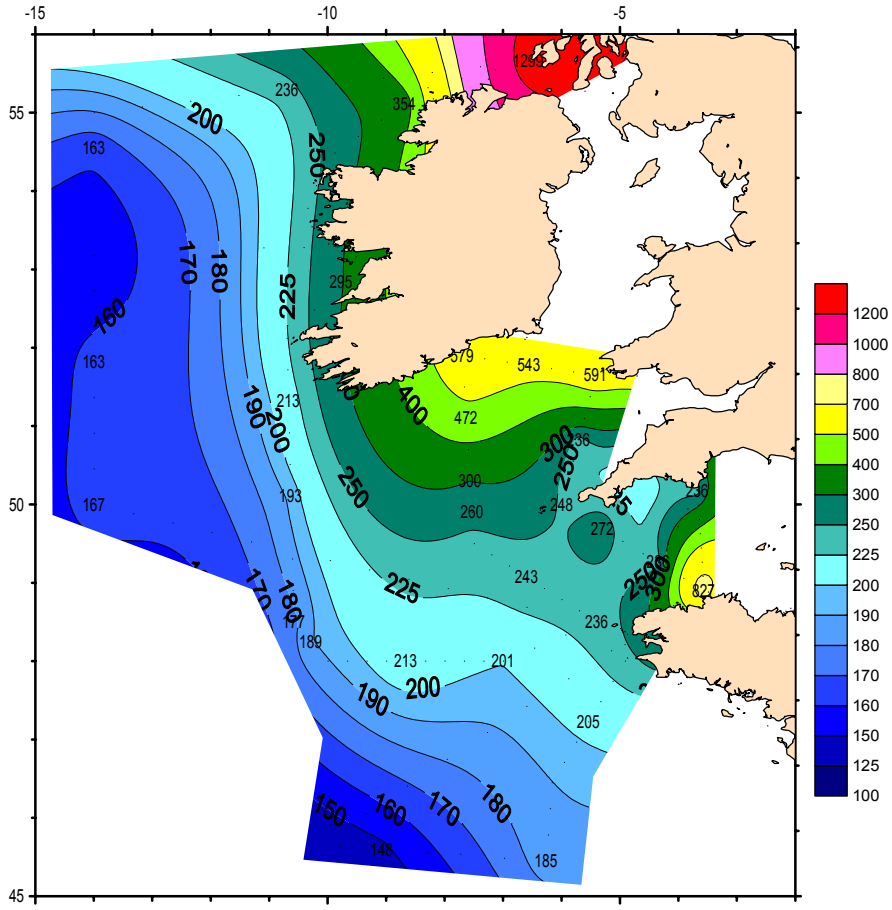

Figure 58. ^{3}H concentrations (mB l^{-1}) in surface Atlantic waters, including the South Irish Sea, the Celtic Sea and the western English Channel (ATMARA expedition, July 1998)

7.2. Radionuclide inputs from Arctic rivers

The Tundra'94 expedition offered the opportunity to sample in different estuaries and rivers along the Eurasian shelf. This allowed an estimation to be made of the riverine contribution to the Arctic Ocean for different radionuclides and facilitated our attempts to identify the presence of river water on the shelf, an exercise that is by not means simple. Measured ^{137}Cs concentrations in fresh water samples from six Siberian rivers in the Kara, Laptev and East Siberian Sea were found to be low, at ~1 Bq m^{-3}, and can be attributed primarily to run-off from global fallout. Indeed, $^{134}Cs/^{137}Cs$ activity ratios measured in low salinity waters outside the mouths of the Ob and Yenisey rivers indicated that only 30% of the measured ^{137}Cs originated from Chernobyl fallout deposition. Although ^{90}Sr was not directly measured in river waters, the lower $^{137}Cs/^{90}Sr$ ratios measured in estuarine waters affected by riverine input compared to those in more saline waters are indicative of excess ^{90}Sr input from the rivers. The lower ratio is not found in the low salinity areas where the fresh water component is derived from ice-melt and suggests that this ratio may serve as a specific tracer for river water.

7.3. Lateral ventilation from the Arctic shelf to the Arctic Ocean interior

Radionuclide concentrations in a large number of surface and sub-surface sea water samples collected along the Eurasian Arctic shelf seas and in a series of latitudinal and longitudinal transects along the Lomonosov Ridge and the Laptev Sea continental break are presented here. The samples were collected during the Tundra '94 and Arctic '96 expeditions with the objective of studying the transport of radionuclides by advection of shelf water and ice into the Central Arctic Ocean.

7.3.1. Transport on the shelf

The ^{137}Cs activity distribution along the Eurasian continental shelf as a function of longitude is illustrated in Figure 59. A clear trend of increasing concentrations from the eastern Barents Sea to the western Laptev Sea was observed in surface and near-bottom waters, with values changing from 5.3 to 15.1 Bq m^{-3}. The lowest ^{137}Cs activities (5.3 and 6.4 Bq m^{-3} in surface and bottom waters, respectively) were measured in the south-eastern Barents Sea, while the highest (12.8 and 15.1 Bq m^{-3} in surface and bottom waters, respectively) were measured in the western Laptev Sea. A sharp gradient was observed at about 150°E, between the Laptev and East Siberian Seas, with ^{137}Cs concentrations falling to 0.8 and 3.0 Bq m^{-3} in surface and near-bottom waters, respectively. These concentrations are similar to those observed in samples exposed only to weapons fallout and suggests that water from the East Siberian shelf originates from the Pacific Ocean.

It is generally accepted that the three dominating radiocaesium sources to the Arctic Ocean are fallout from the Chernobyl accident, marine transport from European reprocessing plants and weapons test fallout, with concentrations of the latter being more or less constant throughout the Arctic. On the other hand, measured ^{134}Cs/^{137}Cs activity ratios were found to be almost constant throughout the Barents, Kara and Laptev Seas both in surface and bottom waters, with mean values of 0.014 ± 0.002 and 0.015 ± 0.002, respectively. Since the ^{134}Cs/^{137}Cs ratio from the Chernobyl accident in 1986 is well known (0.5) and the ^{134}Cs influence from Sellafield releases is small (most of the ^{134}Cs in historic discharges has long decayed to undetectable levels), it was possible to calculate the Chernobyl contribution to the total caesium by assuming that all the ^{134}Cs was Chernobyl-sourced. In all samples, the Chernobyl contribution was found to be ~30%, indicating that the observed longitudinal increase must reflect a parallel increase in both Chernobyl and Sellafield contributions. In the East Siberian Sea, ^{134}Cs/^{137}Cs ratios were different from those in the Barents, Kara and Laptev Sea, with values always below 0.003.

As already mentioned in §7.2 above, ^{137}Cs concentrations in the mouths of the large Siberian rivers, at ~1 Bq m^{-3}, were much lower than those observed in sea water along the shelf. In order to suppress the effect of riverine discharges in the overall ^{137}Cs distribution along the Eurasian shelf, concentrations for low-salinity samples were normalised to a salinity of 34.80 (representative of Atlantic waters) assuming a concentration of 1 Bq m^{-3}for the freshwater end member. This results in a more uniform increase in ^{137}Cs concentrations along the shelf (Figure 59).

The ^{90}Sr (normalised) activity distribution along the Eurasian continental shelf as a function of longitude is shown in Figure 60. As for ^{137}Cs, a clear trend of increasing ^{90}Sr concentrations from the Barents to the Laptev Sea was observed, with a significant decrease east of 150°E. The fact that this decrease is not as sharp as that observed for radiocaesium could reflect the contribution of riverine inputs (enhanced in ^{90}Sr relative to ^{137}Cs) to these waters. In contrast, ^{129}I concentrations were found to decrease in an easterly direction (Figure 60). Of particular interest is the observation that measured ^{129}I/^{137}Cs ratios decreased eastwards from ~300 in the Barents Sea to ~10 in the East Siberian Sea, with a notable exception just outside the mouth of the Yenisey river. From these ratios, after appropriate corrections to account for decay and the contributions from sources other than Sellafield, it was possible to estimate transfer times from Sellafield to different zones along the shelf: 8 years to the south-eastern Barents Sea, 8–9 years

to the Kara Sea and 10–12 years to the Laptev Sea. However, since our determinations of the Sellafield-derived ^{137}Cs concentrations in the shelf seas do not separate directly-transported and older-recirculated contributions, these calculations must be regarded as upper limits.

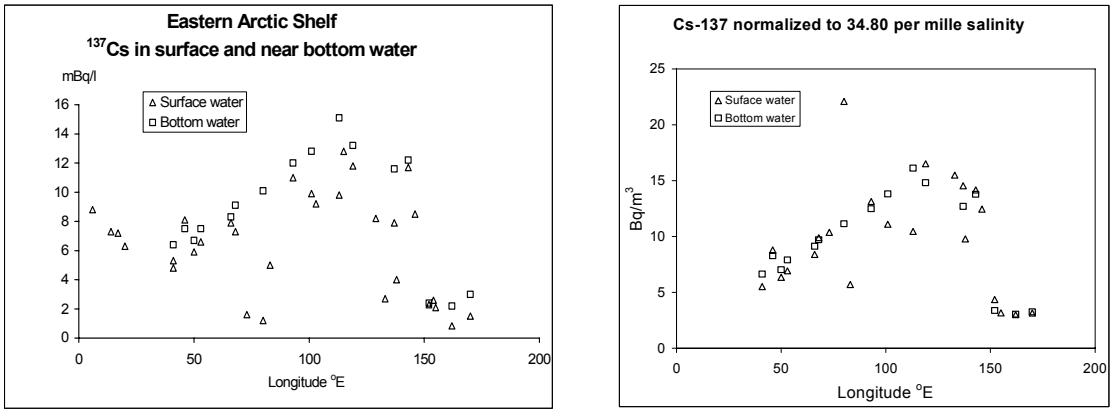

Figure 59. Longitudinal distribution of ^{137}Cs along the Eurasian shelf (Tundra '94 expedition) and normalised distribution to a salinity of 34.80 ‰

The ^{137}Cs and ^{90}Sr longitudinal distributions along the shelf clearly reflect the effect of decreasing reprocessing, Chernobyl and runoff inputs since the early 1990s, while the increase in reprocessed ^{129}I is reflected by the observed decrease in ^{129}I levels along the shelf.

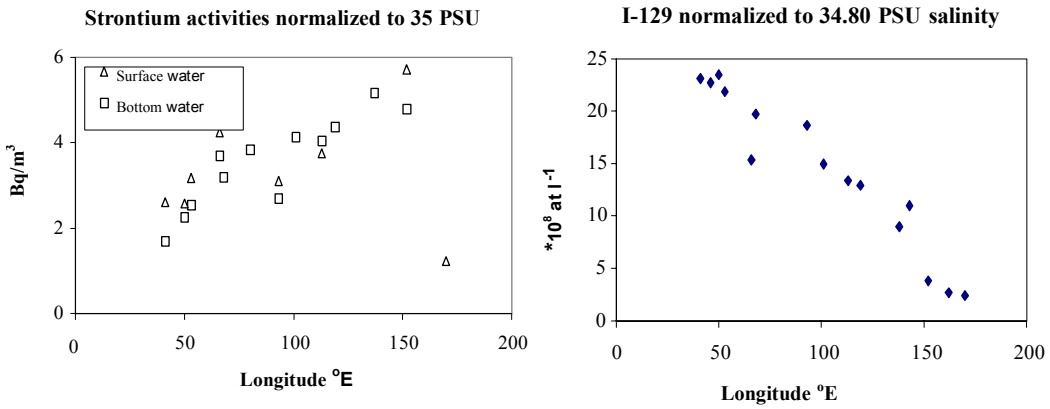

Figure 60. Longitudinal (normalised) distributions of ^{90}Sr and ^{129}I along the Eurasian shelf (Tundra '94 expedition)

In the case of ^{239,240}Pu, concentrations show a general decrease in an easterly direction, with values ranging from a maximum of 11 mBq m^{-3} in the Barents Sea to values well below fallout levels in most samples from the Laptev and East Siberian Seas (Figure 61). This decrease is attributed primarily to losses to sediment along the shallow shelf seas. Measured ^{239,240}Pu/^{137}Cs are highly variable, with maximum values decreasing towards the east. Difference in the average ratios for surface and near-bottom *waters*, at 0.5×10^{-3} and 0.8×10^{-3}, respectively, possibly reflect the higher particle reactivity of plutonium with respect to caesium. These ratios are also considerably lower than the fallout ratio of 2.5×10^{-3} reported for the North Atlantic in 1987 (Holm *et al.*, 1991), and reflect the additional inputs of ^{137}Cs from the Chernobyl accident and from Sellafield discharges.

Excluded from the general eastward decrease in ^{239,240}Pu concentrations are the values observed in samples taken in the mouths of the Ob, Yenisey and Lena rivers, which showed significantly enhanced concentrations. In Figure 62, a plot of ^{239,240}Pu concentrations versus salinity clearly demonstrates the riverine origin of this excess plutonium. Analysis of the particulate fraction in samples outside the Lena and Yenisey rivers showed the increase in particulate activity around the river mouths with respect stations unaffected by riverine discharges to be lower than the corresponding increase in the filtered fraction, suggesting that most of the excess plutonium is in the form of dissolved species or associated to colloidal matter.

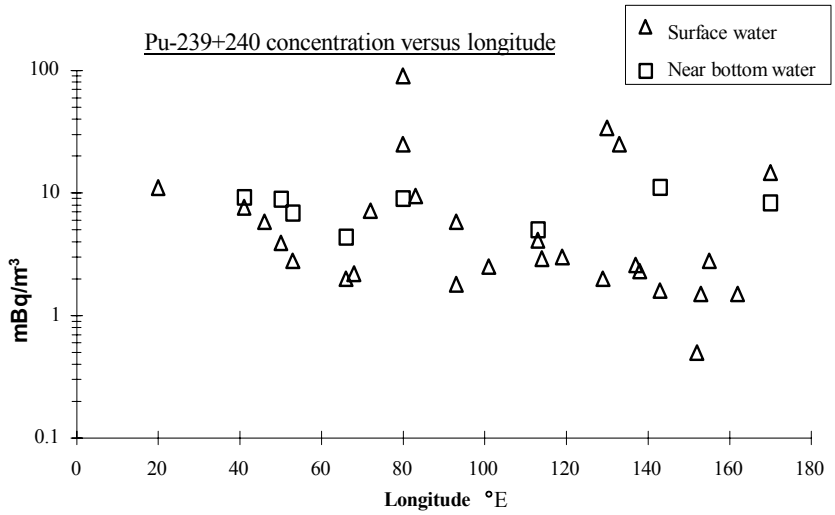

Figure 61. Longitudinal distribution of ^{239,240}Pu along the Eurasian shelf (Tundra '94)

The highest concentrations correspond to samples collected during maximum river flow (which occur in early summer). Repeated sampling under lower discharge regimes, showed a decrease in the ^{239,240}Pu concentration, which suggest a seasonal variation with highest concentrations in periods of maximum water discharge. The higher ^{239,240}Pu activities observed were not associated with increased ^{137}Cs or ^{90}Sr concentrations at the same location. At Stn. 12 (affected by the Yenisey discharge), ^{137}Cs/^{90}Sr ratios were entirely compatible with global fallout. However, ^{238}Pu/^{239,240}Pu and ^{241}Am/^{239,240}Pu at this station, at 0.02 and <0.09, respectively, were somewhat lower than expected from global fallout, while the ^{239,240}Pu/^{137}Cs ratio, at 0.071, was significantly higher than the fallout deposition ratio, at 0.012. No effect of this temporarily high ^{239,240}Pu concentration is reflected in sediments deposited in the river mouth, which show isotopic ratios similar to other Arctic areas (Baskaran *et al.*, 1996).

If the source of seasonally high ^{239,240}Pu concentrations was global fallout, a natural process limiting the runoff of ^{137}Cs, ^{90}Sr and ^{241}Am with respect to ^{239,240}Pu would be required, which seems very unlikely. Instead, the observed isotopic ratios point to a different source of plutonium, such as close fallout from nuclear explosions, debris from safety shots or unfissioned nuclear weapon material.

Despite the (seasonally) higher ^{239,240}Pu concentrations in river waters, the effect of riverine discharges in ^{239,240}Pu concentrations in shelf sea water is quite small. If a 90 mBq(^{239,240}Pu) m^{-3} fresh water pulse, as measured outside the Yenisey river, were to be introduced to sea water of salinity 35‰ to give a typical shelf water with a salinity of 33–34‰, the riverine contribution would be in the order of 3–5 mBq m^{-3}.

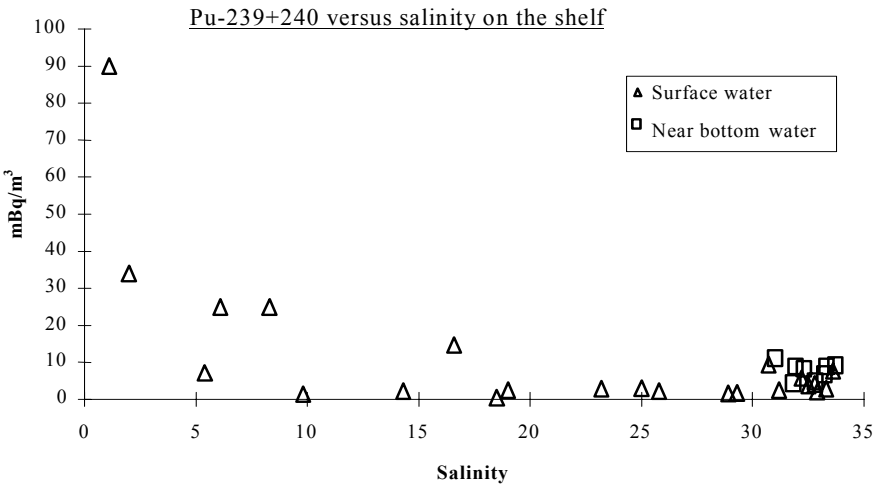

Figure 62. ^{239,240}Pu concentration versus salinity in Eurasian shelf waters (Tundra '94)

7.3.2. The Central Arctic Ocean

In contrast to the Tundra'94 expedition results, samples collected in the Nansen Basin (just north of the St. Anna Trough) in the course of the Arctic'96 expedition were characterised by much lower ^{129}I concentrations, as well as a significantly lower ^{134}Cs/^{137}Cs ratios. This observation is important, confirming as it does that the input of shelf water/modified Atlantic water to the Central Arctic does not take place directly from the Kara Sea. Instead, the major surface shelf activity inflow to the Central Arctic is thought to take place from the Laptev Sea along the Lomonosov Ridge towards the North Pole, where high ^{129}I and ^{134}Cs/^{137}Cs ratios were observed in the course of the Tundra'94 and Arctic'96 expeditions.

The overall ^{137}Cs surface distribution in the Central Arctic in 1996 was found to be similar to that observed in the SWEDARCTIC'91 expedition (Holm *et al.*, 1996), with the highest concentrations (characterised by the highest ^{134}Cs/^{137}Cs ratios) extending in a band stretching from the northern Lomonosov Ridge past the North Pole and then south along 10–15°E to the Gakkel Ridge. A similar trend was observed in the case of ^{90}Sr and ^{129}I.

At the Gakkel Ridge (at about 10°E), a front separated relatively high activities to the north from the significantly lower to the south. The fall-off in ^{137}Cs concentrations (from ≈11 to ≈5 Bq m^{-3}) was accompanied by a decrease in the measured ^{134}Cs/^{137}Cs ratios (from ≈0.005 to ≈0.003). A similar decrease was observed in ^{129}I concentrations, which fell from ≈8 × 10^{8} atoms l^{-1} to the north of the front to ≈5 × 10^{8} atoms l^{-1} to the south. A similar front was observed for ^{137}Cs concentrations in this area during 1994 (Ellis *et al.*, 1994) and, together with other oceanographic information (Anderson and Jones, 1992), supports the view that radioactivity introduced in the Eurasian shelf from the Atlantic enters the Central Arctic well east of the Barents Sea (i.e., at the Laptev Sea).

The observed radionuclide distribution patterns and measured radionuclide ratios are consistent with the transport of surface radioactivity from the Barents Sea along the Eurasian shelf and into the Central Arctic along the Lomonosov Ridge towards the North Pole (with the Transpolar Drift). Transfer time estimates for conservative nuclides from the European shelf (Sellafield) to the Central Arctic yielded values of 5–7 years to the SE Barents Sea, 7–9 years to the Kara Sea, 10–11 years to the Laptev Sea and 12–14 years to the Central Arctic Ocean.

Further confirmation of this transport route was obtained from $^{228}Ra/^{226}Ra$ ratio measurements, which showed consistently higher values along the Transpolar Drift. An elevated $^{228}Ra/^{226}Ra$ ratio with respect to open ocean water values can be regarded as indicatory of the presence of recent shelf contact, as enhanced ^{228}Ra concentrations, arising from riverine inputs and diffusion from sediments, are characteristic of shelf waters. In the western Barents Sea, the low $^{228}Ra/^{226}Ra$ ratios measured indicated the presence of Atlantic water which had not been in recent contact with sediments or received significant riverine discharges. However, further to the east (western Kara Sea), the ratio was found to have doubled as a result of contact with sediment and riverine input. In the southern Eurasian Basin, the ratios were again low, indicating little mixing with shelf water.

In the case of plutonium, surface $^{239,240}Pu$ concentrations in the polar mixed layer (PML) of the Central Arctic, recorded in the course of the Arctic'96 expedition, were found to be very low, never exceeding 13 mBq m^{-3}. Nevertheless, a plot of mean $^{239,240}Pu$ concentrations in the PML across successive latitude and longitude bands along the Siberian shelf and the Lomonosov Ridge towards the North Pole (Figure 63) revealed a clear trend of increasing concentrations as one move to higher latitudes. Sub-surface waters, characterised by higher temperatures and salinities, showed a similar increase, though $^{239,240}Pu$ concentrations were significantly higher (8–20 mBq m^{-3}).

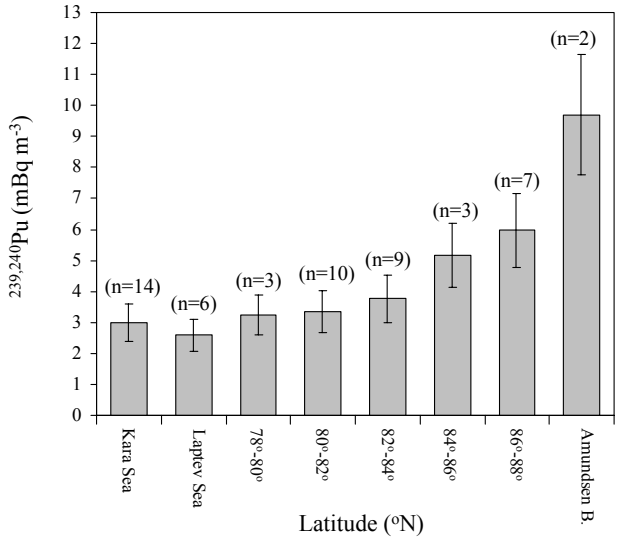

Figure 63. Latitudinal variation in $^{239,240}Pu$ concentration in filtered sea water along the Siberian coast and the Transpolar Drift

That plutonium released from Sellafield could contribute significantly to the enhanced concentrations observed in Central Arctic waters at the present time seems unlikely for the following reasons. A retrospective estimation of the size of the Sellafield signal in Atlantic waters feeding the Barents Sea indicates a maximum contribution from this source of 2–3 mBq m^{-3} in the early 1980s when measured concentrations in this zone were typically 15–18 mBq m^{-3} (n = 7). Further to the east, the Sellafield signal is even weaker and, obviously, can not account for the observed difference of almost 10 mBq m^{-3} between present concentrations in the Laptev Sea and those in the vicinity of the North Pole. Analysis of the $^{238}Pu/^{239,240}Pu$ activity ratio in Central Arctic waters provided further evidence of the limited Sellafield influence on these waters with, at most, ≈15% of the $^{239,240}Pu$ inventory attributable to releases from European reprocessing plants.

Instead, the broad pulse in $^{239,240}Pu$ concentrations, which is moving through the Arctic hydrosphere and is presently centered in the vicinity of the North Pole, is largely attributable to the comparatively high levels of nuclear fallout that labelled mid-latitude waters in the North

Atlantic in the early– to mid–1960s, when the testing of nuclear weapons in the atmosphere was at a peak.

7.3.3. Radionuclide inventories in the Central Arctic Ocean water column

On the basis of the measured radionuclide profiles in the course of the Arctic'96 expedition, estimates were made of radionuclide inventories in the Central Arctic water column (down to 900 m). The calculation assumed a constant concentration in the polar mixed layer (0–50 m) and the halocline (50–200 m). For stations where no samples were taken in the halocline layer, the mean of the polar mixed layer and the Atlantic layer was assumed. In the 200–900 layer, the mean of the Atlantic layer measurements was used. The results for four selected stations are given in Table 26.

Table 26. Water column inventories of ^{137}Cs, ^{129}I and ^{90}Sr in the Central Arctic Ocean (Arctic'96 expedition)

Station	Location	Layer (m)	^{137}Cs (Bq m^{-2})	^{129}I (10^{12} atoms l^{-1})	^{90}Sr (Bq m^{-2})
5	83°47' N 66°13' E	0 – 50	220	38	170
		50 – 200	560	100	420
		200 – 900	1900	240	1200
		0 – 900	2680	380	1800
15	87°09' N 140°47' E	0 – 50	420	43	170
		50 – 200	1300	130	390
		200 – 900	3400	270	1900
		0 – 900	5100	443	2460
34	88°49' N –178°38' E	0 – 50	240	29	200
		50 – 200	1600	87	510
		200 – 900	3200	130	1700
		0 – 900	5000	250	2400
40	85°31' N 12°32' E	0 – 50	540	41	180
		50 – 200	1500	100	540
		200 – 900	4400	200	2100
		0 – 900	6400	340	2800

The data show a progressive increase of ^{137}Cs and ^{90}Sr inventories along from the Laptev Sea along the Lomonosov Ridge past the North Pole. Comparison of Stn. 34 inventories with those at a station in a similar location in 1979 (LOREX) show a two-fold increase in the integrated inventories since that time. ^{129}I show a different spatial distribution, with the lowest inventories at Stn. 34 (close to the North Pole) and the highest at Stn. 25 (86°28' N 132°07' E). Despite the higher concentrations in the surface layers, the Atlantic layer contains 69%, 70% and 58% of the total ^{137}Cs , ^{90}Sr and ^{129}I inventories, respectively. Similar calculations for ^{239,240}Pu and ^{241}Am yield inventories in the range of 14–17 and 0.9–1 Bq m^{-2}, respectively, with 80–90% of the activity in the Atlantic layer.

From the average inventories at six stations and assuming a total area of 1.4 Mkm^2 (Weber, 1989), the estimated total inventories in the upper 900 m of the Eurasian Basin are 6.7 PBq for ^{137}Cs, 3.4 PBq for ^{90}Sr and 5×10^{28} atoms for ^{129}I. From source input data, Aarkrog (1994) had estimated the inventories for the entire Arctic Ocean to be 17–30 PBq for ^{137}Cs and 6–11 PBq for ^{90}Sr.

8. Transfer processes to living species, including man

8.1. Identification of key food chains, critical groups of sea-food consumers and consumption patterns in the Arctic

A review of past and current exploitation of seafood resources in key Arctic regions was used to predict future catches, identify the main food chains and establish consumption patterns in these areas. Current catches of marine organisms in the Barents Sea and Spitsbergen area were obtained from ICES and fishery statistics of Norway and Russia, and are summarised in Table 27 (averaged for 1985–1992).

Table 27. Current annual fish catch (kilotonnes per year) in the Barents Sea and Spitsbergen area (ICES sub-areas I and IIb), averaged for the period 1985–92

Seafood	Current Annual Catch (kt y^{-1})
Fish	588 ± 371
Molluscs	21 ± 15
Deep-water shrimps	73 ± 31

The maximum values of current fish catches (about 1000 kt y^{-1}) are close to the maximum ecologically reasonable catch for these areas. Special efforts will be necessary if present levels of exploitation are to be maintained, as fish resources are steadily decreasing. The development of fish farms could help to maintain the fish catch at a stable level of about 1000 kt y^{-1}. The catch reported for the 1960–70s (2–3 Mt y^{-1}) was abnormally high and led to a depression of the marine ecosystem.

The current catch of molluscs in the Barents and Spitsbergen area is about 3.6% of the fish catch. Although at present this proportion is much lower than the corresponding figure for the North-east Atlantic area (8.2%), it is likely that in the future the proportion between molluscs and fish catches in Arctic fishing grounds will tend to that in the North-east Atlantic. Thus, the future catch of molluscs in the Barents Sea may be estimated to reach a level of 100 kt y^{-1}. This increase in mollusc production may be achieved by the development of specialised mollusc farms. Indeed, there are suitable environmental conditions for common mussel (*Mytilus edulis*) cultivation in the south-western part of the Barents Sea, including the White Sea (Kandalaksha Bay), Murman (Kola Bay) and the Cheskaya Bay. Small-scale experiments on the cultivation of mussels carried out in the 1980s in Kandalaksha Bay and Kola Bay gave harvests of up to 200 t ha^{-1} (live weight). A more realistic harvest of mussels under the conditions of large-scale mariculture may be estimated at a level of 50 t ha^{-1} y^{-1} (taking into account that the climatic conditions in the Barents Sea are more severe than in the more southern areas of the North-east Atlantic). At this rate of production, harvests of 100 kt y^{-1} of molluscs would require 2000 hectares of mollusc farms. The total area which is suitable for mollusc production is much greater than this, but some of these locations will probably be used for fish farming in the future. The cultivation of shrimps in the Barents Sea is not planned and future catches may be estimated at the current level of about 100 kt y^{-1}.

For radiological assessment purposes, the consumption of seafood harvested in the investigated areas was considered to be in the same proportions as in the predicted future catches (i.e., 10:1:1 ratio for fish:molluscs:shrimps). It was also assumed that future diets for populations in these areas will be balanced and include not only seafood as a source of protein, but also meat, milk and other products. The consumption rate of 200 g of fish fillet per day may be used as a basic value (one or two fish meals per day). For a critical group of fish-eaters (if they replace all

meat in their diet by seafood), the consumption rate may increase (up) to 300 g of fish fillet per day.

Using the assumption that 1 kg of fish fillet equals 3 kg of raw fish, the consumption rate in live weight of fish was estimated to be ~600 g day^{-1}. From the above mentioned proportions, the consumption rates of molluscs and crustaceans (in live weight) were estimated as 60 g day^{-1} each (or 90 g day^{-1} for the critical group of fish-eaters). In the above calculations, conversion factors of 1 kg of mollusc meat = 4 kg of molluscs with shells; 1 kg of shrimp meat = 3 kg of shrimps live weight were used. A summary of predicted future seafood consumption rates is given in Table 28.

Table 28. Estimates of future intake of seafood for critical groups located at the Kara Sea

Seafood items	Balanced diet (g d^{-1})	Diet for critical groups (g d^{-1})
Fish fillet	200	300
Mollusc meat	15	22.5
Shrimp meat	20	30

Information provided by Russian scientists (EC/DGXI Kara Sea Project) was used to identify possible critical groups in the Kara Sea area. A map showing the locations of possible developments in the Yamal Peninsula, the Taymur region and the open Kara Sea is given in Figure 64.

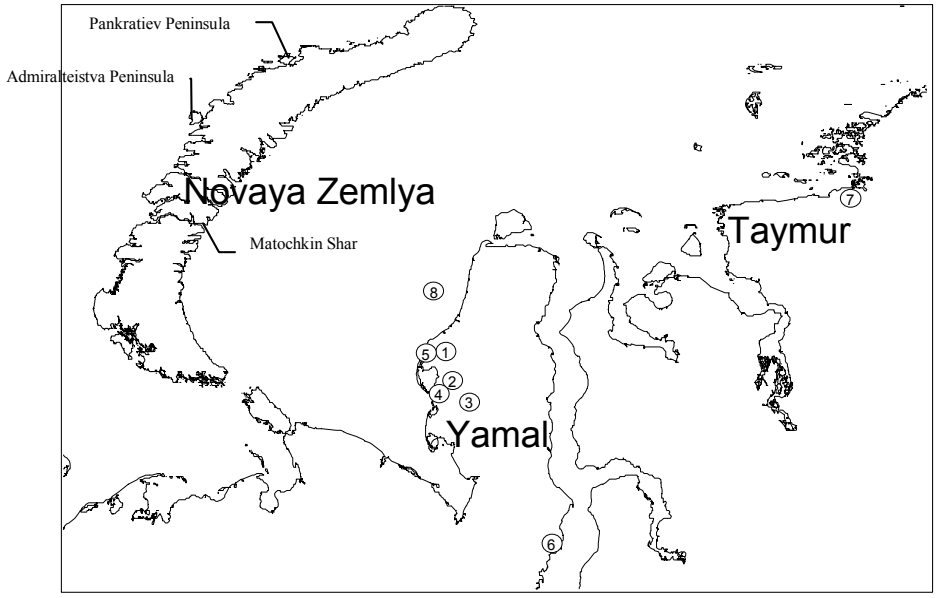

Figure 64. Location of main gas fields and potential locations for future settlements in the Kara Sea region

The Yamal Peninsula is at present the home to 6 oil fields and 15 gas fields. The 3 main gas- and gas-condensate bearing fields are located in the vicinity of the western shore of the Yamal Peninsula (locations 1–3 in Figure 64). Prospects for future development to support this gas industry (Nowagrad I) include the estuary of the River Mordyiakha (location 4 on the map) or the estuary of the River Kharasavey (location 5). Since environmental conditions and type of soil are very sensitive to anthropogenic stress at both locations, the population of this settlement

will be limited in size to about 50000 people or less. For comparison, the present population of the Yamal Peninsula is about 15000 persons. The development of this area is expected within the next 100 years. In addition, some towns are likely to be developed on the eastern shore of the peninsula to support developing gas and fishing industries. One such prospective town is the Novyi Port (location 6), where a small town already exists.

Coal and brown coal basins have been revealed in the Taymur region. The likely site of a new town to support this coal industry (Nowagrad II) is the estuary of the River Pyasina (location 7). However, the development of coal mining in the Taymur region is not likely to occur within the next 100 years.

Two big gas-bearing fields have been revealed recently under the sea bed of the open Kara Sea (Rusanovskoye and Leningradskoye gas-fields). The location of these fields is indicated in Figure 64 (location 8). The gas mining may be organised directly in the sea using floating platforms. The workers of such floating plants will be potentially exposed to radiation from inhalation of seaspray and from contact with deposits raised from the sea bed.

It is assumed that people living on the Yamal Peninsula and the Taymur region will eat molluscs and shrimps from the Barents Sea and fish from the south-western part of the Kara Sea. Based on the information above and previous IAEA assumptions, the following habit assumptions may be recommended for assessing doses to critical groups located in these open coastal areas:

- Ingestion of fish: 110 kg y^{-1};
- Ingestion of crustaceans: 11 kg y^{-1};
- Ingestion of molluscs: 8 kg y^{-1};
- Inhalation of seaspray and resuspended coastal sediment: inhalation rate of 1 m^3 h^{-1} for 1000 h y^{-1} at a loading of 10 g seaspray and 0.25 μg marine sediment per m^3 of air;
- External gamma-ray exposure from coastal beaches: occupancy time 1000 h y^{-1} on coastal sediments with radionuclide concentrations 10 times lower than those in fine-grained marine sediments.

For a hypothetical critical group (military staff) located in the Novaya Zemlya bays, where the nuclear waste has been dumped, the habits may be considered to be identical to those assumed for this group in the IASAP Project. These limit the time of occupancy and inhalation of seaspray and contaminated sediment to just 100 h y^{-1} to take into account the harsher climatic conditions prevailing in this zone.

8.2. Identification of the trophic structure, pathways of radionuclide accumulation and concentration factors in the Barents, Pechora, Kara and White Seas

The Arctic shelf seas are characterised by a rich fauna and flora. More than 2500 species have been identified in the Barents Sea, 1700 species in the Kara Sea and 1600 in the White Sea (Bryasgin *et al.*, 1981). Despite the climatically harsh environment, with long periods without sunlight and extremely low temperatures, these species have developed adaptation features which allow them to survive under these extreme conditions. On the basis of their diet, Arctic fauna can be divided in five main trophic groups (Kuznetsov, 1980):

(1) *Sessile suspension filtrate feeders or sessile filtrate suspensivores* – This group includes stationary animals which collect organic seston by means of active filtration of water through their body (e.g., molluscs, sponges, ascidians) or catch it passively using a tentacle net (e.g., some species of polychaete worms or bryozoans, marine cucumbers) from the water column near the seabed.

(2) *Semi-mobile suspension filtrate feeders or sessile filtrate suspensivores* – This group includes animals which can move from one place to another over short distances. They live on the bottom surface and possess long siphons (molluscs) or tentacles (worms) to obtain their food. They also catch seston (organic particles, small parts of plants and plankton) from the water near the seabed.

(3) *Sessile surface detritivores* – The animals belonging to this trophic group feed from bottom detritus (organic matter occurring in sediments). Detritivores have a large throat/gullet which can be turned inside out to collect sediment detritus by means of special secretions or by absorption after agitation of the sediment bed with special cirrus.

(4) *Semi-mobile subsurface detritivores* – These animals use the organic particles or detritus from the subsurface sediments as foods. They bore into the sediment and catch the organic matter using hard grains of quartz.

(5) *Carnivores* – This group includes active hunters (predators) and species that use the bodies of dead animals as food.

Attached animals belonging to the sessile filtrate suspensivores group inhabit areas with active washing of the bottom sediment, including the mainland slopes, underwater hills, troughs and the continental shelf. The sediments they tend to live in have a large proportion of stones, pebbles and gravel or, alternatively, consist of clean coarse sand. As these animals are not able to leave their biotopes, they are extremely sensitive to pollution and environmental stress situations. Semi-mobile filtrate suspensivores occupy areas with less intense hydrodynamics. The sediments they live in are mainly sand, muddy sand or sandy mud with a low content of gravel. Semi-mobile surface detritivores are present in areas containing accumulated organic matter. These occur in depressions and troughs, in small depressions in bays and inlets and in bays separated from the open sea. Carnivores or predators can change their biotopes very easily according to the amount of food available in an area, being able to travel over long distances.

In Table 29 (Denisenko, 1999), the tropic structure of invertebrate species collected in the Barents, Kara and White Seas and analysed in the course of the ARMARA programme (in collaboration with the Murmansk Marine Biological Institute) is presented, together with the life span of each species. Note that the life span of many species exceeds 10 years, making sessile species an ideal indicator of integrated radionuclide concentrations.

Higher on the food chain are fish species. Most fish correspond to the predator group, feeding on other fish, invertebrates and plankton. The main feature of Arctic fish populations is their instability. Arctic fish migrate from sea to sea and gain weight during these migration periods. Commercial species such as Atlantic cod and haddock occur in large numbers in the Barents Sea in early spring. They appear in areas with high concentrations of zooplankton, or capeline, which develops after the spring bloom. Redfish, plaice and halibut are more stable with regard to their location and population size. They inhabit the deeper western parts of the Barents Sea. Other bottom fish (e.g., wolffish, saithe, ray and sculpin) do not aggregate in big shoal and are caught sporadically in trawling nets. A summary of fish species sampled in the course of the ARMARA programme, together with their main food diet is presented in Table 30. It must be noted that the food spectra presented in the table reflects the main diet for each species under normal conditions. Competition for food between species increases if the quantity of preferred food is not sufficient. It is known, for example, that in addition to their traditional food components, haddock, Atlantic cod, saithe and wolffish can also feed on other fish (capelin, redfish, sculpins) and attached animals with a hard skeleton. In general, animals from the lowest link in the food chain (plankton animals that feed on phytoplankton) are preferably consumed. In this case, radionuclide accumulation is expected to be low, since most of the plankton species live for a short time. In addition to direct ingestion of food, radionuclide uptake in fish feeding from benthic organisms (e.g., halibut, haddock, plaice, ray) can take place by intake of resuspended sediment during the feeding process.

Table 29. Systematic and trophic structure of invertebrates in the Barents, Kara and White Seas (Denisenko, 1999)

Taxa range	Name of taxa	Trophic group	Life span (y)
Phylum	PARAZOA		
	Spongia g.sp.	Sessile suspension filtrate feeder	20
Phylum	COELENTARATA		
Class	*Anthozoa*		
	Gersemia sp.	Sessile filtrate suspensivore	10–15
Phylum	NEMERTEA		
	Nemertini g.sp.	Carnivore	
Phylum	ANNELIDA		
Class	*Polychaeta*		
Subclass	Erranthia		
	Nephthys sp.	Carnivore	2–4
Subclass	Sedentaria		
	Polychaeta g.sp.	Detritivore	2–4
	Pectinaria sp.	Sessile surface detritivore	4–5
	Spiochaetopterus sp.	Sessile surface detritivore	4–5
	Sipunculida	Semi-mobile subsurface detritivore	5–7
	Golfingia margaritaceum	Semi-mobile subsurface detritivore	5–7
Phylum	ARTROPODA		
Class	*Crustacea*		
Order	Cirripedia		
	Balanus crenatus	Sessile filtrate suspensivore	5–7
Order	Amphipoda		
	Amphipoda g.sp.	Mainly mobile detritivore	3–4
	Gammarus sp.	Mainly mobile suspensivore	3–4
Order	Decapoda		
	Pagurus pubescens	Mobile carnivore	5–6
	Hyas araneus	Mobile carnivore	5–6
Class	*Isopoda*		
	Mesidothea entomon	Sessile surface detritivore	3–4
Phylum	MOLLUSCA		
Class	*Gastropoda*		
	Buccinum sp.	Mobile carnivore	
	Buccinum tenue	Mobile carnivore	10–12
	Neptunea sp.	Mobile carnivore	10–12
	Cryptonatica clausa	Mobile carnivore	10
	Margarites sp.	Mobile carnivore	5–6
	Littorina saxatilis	Mobile carnivore	5–6
	Polynices palidus	Mobile carnivore	10
Class	*Bivalvia*		
	Mytilus edulis	Sessile filtrate suspensivore	
	Chlamys islandica	Sessile filtrate suspensivore	8–12
	Ciliatocardium ciliatum	Sessile filtrate suspensivore	15
	Yoldia hyperborea	Semi-mobile surface detritivore	10–15
	Modiolus modiolus	Sessile filtrate suspensivore	40
	Musculus niger	Sessile filtrate suspensivore	15
	Serripes groenlandicus	Semi-mobile filtrate suspensivore	30
	Tridonta borealis	Semi-mobile filtrate suspensivore	20
	Macoma calcarea	Semi-mobile surface detritivore	15–20
	Portlandia arctica	Semi-mobile surface detritivore	30–40
	Hiatella arctica	Sessile filtrate suspensivore	30–40
	Nicania montague	Semi-mobile filtrate suspensivore	15
	Liocyma flexuosa	Semi-mobile surface detritivore	15
	Nuculana pernula	Semi-mobile surface detritivore	20
	Astarte crenata	Semi-mobile filtrate suspensivore	30–40
	Arctica islandica	Semi-mobile filtrate suspensivore	30–40

Table 28. Systematic and trophic structure of invertebrates in the Barents, Kara and White Seas (Contd.)

Taxa range	Name of taxa	Trophic group	Life span (y)
Phylum	TENTACULATA		
Class	*Bryozoa*		
	Alcyonidium disciforme	Sessile filtrate suspensivore	5–6
Phylum	ECHINODERMATA		
Class	*Asteroidea*		
	Asterias rubens	Carnivore (Bivalve mainly)	13
	Crossaster papposus	Carnivore (Bivalve, fish)	13
Class	Ophiuroidea		
	Stegophiura nodosa	Carnivore	2–3
Class	*Echinoidea*		
	Strongylocentrotus sp.	Semi-mobile surface detritivore	8–12
Class	*Holothuroidea*		
	Cucumaria frondosa	Semi-mobile filtrate suspensivore	20
	Myriotrochus rinki	Semi-mobile surface detritivore	5–6
Phylum	TUNICATA		
Class	*Ascidiacea*		
	Ascidiacea g.sp.	Sessile filtrate suspensivore	4–5

Table 30. Trophic characteristics and food diet of fish species from the Barents, Kara and White Seas (Denisenko, 1999)

Name	Latin name	Food diet
Atlantic cod	*Gradus morhua morhua*	Plankton crustaceans: Euphasiida, Amphipoda, Copepoda
Haddock	*Melanogrammus aeglefinus*	Benthic animals: Echinoderms (35%), polychaeta (25%), mollusca (40%)
Saithe	*Polachius viren*	Herring, young cod, capelin, malilotus
Wolffish	*Anarichas lupus*	Benthic animals: Ophiuroidea (37.8%), Echinoidea (25.7%), Decapoda (13.7%), Asteroidea (2.2%), Bivalvia (4.4%), Holothuroidea (0.5%), pisces (10.1%)
Plaice	*Pleurectes sp.*	Benthic animals: Polychaeta and molluscs
Halibut	*Rheinhardtius sp.*	Redfish (70%), cod (25%), shrimps (5%)
Redfish	*Sebaster marinus*	Crustacea, Capelinn Molilotus
Ray	*Raja radiata*	Crustacea (46%), Polychaeta (20%), pisces (32%)
Herring	*Clupea sprottus*	Crustaceans: Euphasia sp., Calanus sp.
Sculpings	*Cottidae sp.*	Sand fish Ammodites tobianus (Linne)
Eelpout	*Zoarcidae sp..*	Small fish

Sea birds represent the next link in the food chain. Specimens of different bird species from the coast of the Kola peninsula were collected by the collaboration in the course of the programme. In total, nine species from the coast of the Kola peninsula were sampled and analysed (Table 31). Two sampling points were in Drosdovskaya Bay and on Nokuev Island, influence by the intense hydrodynamics of the Barents Sea. These areas are intensively washed by a constant tidal current. A third sampling point was along a rather long fjord bay with two high sealing shelves. In this area, water circulation is slow, the tidal cycle irregular and the current weak. Finally, samples birds were also collected near the village of Dalniye Zelentsy in the Dalniye Zelentsy and Yarnishnaya inlets. The conditions in this area are very similar to those in the Drosdovskaya inlet and Nokuev Island.

Table 31. Trophic characteristics and food diet of sea birds from the coastal area of the Kola Peninsula (Denisenko, 1999)

Name	Latin name	Food diet
Great black-back gull	*Larus marinus*	Sand fish Ammodite tobianus (94%), capelin (3%), herring (3%)
Common gull	*Larus canus*	Fish (cod, redfish, haddock, herring) (20%), insects (20%), crustacea (15%) mollusca (19%); Echinoderms (2%), berries (19%)
Great skua	*Stercorarius skua*	Fish (60%), birds (20%), molluscs and plants (20%)
Merganser	*Mergus merganser*	Small littoral fish, Liparis
Black guillemot	*Ceppus grylle*	Cottidae (15%), capelin (2%), Liparis (2%), cod (1%), sand fish (76%)
Eidae	*Somateria mollusina*	Mollusca (65%), sea urchins (35%)
Spotted redshank	*Ceppus*	Littoral polychaeta, crustaceans
Purple sandpipers	*Calidris maritima*	Littoral polychaeta, crustaceans
Endpiper	*Calidris minuta*	Littoral polychaeta, crustaceans

In the next sub-sections, concentration factors for ^{137}Cs and ^{239,240}Pu, resulting from the analysis of the benthic fauna, fish and sea bird species discussed above are presented, together with those in other riverine fish and mammals of importance in the Arctic food chain. The calculations are made on the basis of prevailing ^{137}Cs and ^{239,240}Pu sea water concentrations at the time of sampling.

8.2.1. Concentration factors in benthic fauna

Water-animal concentration factors (CFs) for ^{137}Cs in benthic fauna collected in the Barents, Kara, White and Pechora Seas, calculated as the ratio between the organism activity (Bq kg^{-1}, fresh wt.) and the activity in sea water (Bq kg^{-1}), are summarised in Tables 32 and 33. In almost half of the sampled bivalve, *Gastropoda*, *Echinodermata* and *Decapoda* in the Barents, Pechora and Kara Seas, ^{137}Cs concentrations were below the detection limit of the gamma spectrometer system employed (0.3 Bq kg^{-1}, fresh wt.). Higher concentrations were measured in samples from the White Sea, with the highest values found in *Sipunculida*, *Nephthys* and tubes of *Polychaeta* species belonging to the *Annelida* phylum. Average CFs in molluscs, crustaceans and echinoderms were found to be 63 ± 42, 52 ± 53 and 62 ± 4, respectively.

In soft parts of sessile filtrate molluscs (*Mytilus edulis*, *Chlamys islandica*, *Ciliatocardium ciliatum*), CFs were in the range 21–42; in semi-mobile molluscs (*Tridonta borealis*, *Serripes groenlandicus* and *Arctic islandica*), CFs were in the range 30–37, while for the *Holothuroidea Cucumaria frondosa*, a CF value of 24 ± 6 was found. All these values are compatible with the mean concentration factor of 30 recommended by the IAEA for these benthic organisms, all of which are consumed by man.

In mobile carnivores, CFs were in most cases similar to those in filtrating molluscs. Soft tissue concentrations in *Gastropoda* species (*Buccinum*, *Neptunea* and *Cryptonatica clausa*) yielded CFs of 35 ± 12; in *Decapoda* species, CFs were 30 ± 7 for *Pagurus pubescens* and 29 ± 13 for *Hyas araneus*, while for *Asterias rubens* (feeding mainly on bivalvia), a CF of 37 ± 6 was determined. High concentration factors (1400–1700) were measured in tubes of *Polychaeta Nepthys* in the Kara Sea. In soft parts of the animal, however, the CF was much lower, at 51.

In detritivore species, CFs were found to be 43–51 for the semi-mobile *Echinoidea Strongylocentrotus*, 93 ± 38 for *Macoma calcarea* and 96 ± 47 for sessile *Polychaete*.

Table 32. CFs for ^{137}Cs in benthic fauna in Russian Arctic Seas. All errors quoted are ± 1 S.D. (^{137}Cs concentration in sea water for CF calculation = 5.3×10^{-3} Bq l^{-1})

Phylum class	Species	Sea area	CF (soft)	n	CF (whole)	n	Trophic group
Coelenterata							
Anthozoa	*Gersemia sp.*	K			67	1	SFS
Annelida							
Polychaeta	*Nephtys*	K			1673	1	C
	Nephtys	K			1401	1	C
	Nephtys	K	51	1			C
	Polychaeta	B			96 ± 47	3	SSD
	Polychaeta	P			1178	1	SSD
	Polychaeta	K			451	1	SSD
	Pectinaria	P			148	1	SSD
	Pectinaria	K			1227	1	SSD
	Spiochaetopterus	K			277	1	SSD
	Sipunculida	B, P, K			190 ± 78	3	SMSD
Arthropoda							
Crustacea	*Balanus crenatus*	B, P			36 ± 16	4	SFS
	Gammarus sp.	B, W			53 ± 2	2	SMSD
	Pagarus pubescens	P	30 ± 7	3			MC
	Hyas araneus	P			29 ± 13	3	MC
Isopoda	*Mesidothea entomon*	K			145	1	SSD
Mollusca							
Gastropoda	*Buccinum sp.*	B, P	35 ± 12	5			MC
Bivalvia	*Mytilus edulis*	B	42	1	20 ± 1	3	SFS
	Mytilus edulis	W	21 ± 5	5	11 – 121	2	SFS
	Chlamis islandica	B	22 ± 4	2	32 ± 33	4	SFS
	Ciliatocadium ciliatum	P	31–36	2	78	1	SFS
	Modiolus modiolus	P			6	1	SFS
	Musculus niger	K			179	1	SFS
	Serripes groenlandicus	K	37	1			SMFS
	Tridinta borealis	P	30	1	71± 10	6	SMFS
	Yoldia hyperborea	P			70 – 110	2	SMSD
	Macoma calcarea	P, W			93 ± 39	3	SMSD
	Portlandia arctica	K			46	1	SMSD
	Liocyma flexuosa	P			27	1	SMSD
	Arctica islandica	W	38	1			SMFS
Tentaculata							
Bryozoa	*Alcyonidium disciforme*	P			84	1	SFS
Echinodermata							
Asteroidea	*Asterias rubens*	B, P, W			37 ± 6	3	C
	Stegofiura nodosa	P			57	1	C
Echinoidea	*Strongylocentrotus sp.*	B			47 ± 6	2	SMSD
Holothuroidea	*Cucumaria frondosa*	P, B			24 ± 6	4	SMFS
	Myriotochus rinki	K			118	1	SMSD

B = Barents Sea
K = Kara Sea
P = Pechora Sea
W = White Sea

C = Carnivore
MC = Mobile carnivore
SFS = Sessile filtrate suspensivore
SMFS = Semi-mobile filtrate suspensivore
SMSD = Semi-mobile surface detritivore
SSD = Sessile surface detritivore

Table 33. ^{137}Cs and $^{239,240}Pu$ concentrations (Bq kg^{-1}, fresh wt.), radionuclide ratios and CFs in samples of benthic fauna collected in the Russian Arctic Seas (1993–96). All errors quoted are ± 1 S.D.(Sea water concentration for CF calculation: $^{137}Cs = 5.3 \times 10^{-3}$ Bq l^{-1}; $^{239,240}Pu = 9 \times 10^{-6}$ Bq l^{-1})

Phylum Species	Sea area	^{137}Cs	$^{239,240}Pu$ ($\times 10^{-3}$)	CF ^{137}Cs	CF $^{239,240}Pu$	$^{137}Cs/^{239,240}Pu$
Arthropoda/Crustacea						
Gammarus	White Sea Kuzreka	0.29 ± 0.04	4 ± 1	55	434	581
	Barents Sea Teriberka	0.27 ± 0.03	7 ± 1	51	728	224
Pagurus pubescens	Pechora Sea	0.15± 0.02	16 ± 3	28	1751	10
Mollusca						
Litorina saxatilis	Kola Bay Mitsukovo	<0.2	11 ± 3		1213	
Mytilus edulis	Barents Sea† Ostrov, Nokuyav	0.24 ± 0.02	3.0 ± 0.5	45	388	650
	Barents Sea‡ Ostrov, Nokuyav	0.10 ± 0.02	12 ± 3	19	1360	10
	Barents Sea Ostrov, Nokuyav	0.10 ± 0.02	15 ± 5	19	1636	18
	Barents Sea Teriberka	<0.13	5 ± 1		559	
	Kola Bay Mitsukovo	<0.14	<9			
	White Sea† Kuzreka	0.14 ± 0.01	<2	26		
	White Sea‡ Kuzreka	<0.3	<9			
	White Sea† Kandalaksha	0.08 ± 0.02	1.0 ± 0.3	16	106	1282
	White Sea‡ Kandalaksha	<0.09	<2			
Tridonta borealis	Pechora Sea	0.16 ± 0.04	12 ± 3	30	1338	79
Echinodermata						
Asterias rubens	White Sea Chupa	0.62 ± 0.06	4 ± 1	117	495	168
Stegofiura nodosa	Pechora Sea	<0.14	28 ± 4		3100	
	Pechora Sea	0.30 ± 0.09		57		
	Pechora Sea (benthos drag)	<0.16	19 ± 2		2112	
	Pechora Sea (benthos drag)	<0.17	27 ± 4		3049	
Strongylocentrotus	Pechora Sea	0.23 ± 0.02	<8	43		
Cucumara frondosa	Pechora Sea	0.14 ± 0.02	9 ± 1	26	980	108

† soft parts
‡ shell

CFs values for $^{239,240}Pu$ in samples of Crustacea, Mollusca and Echinodermata collected in the Barents, Pechora and White Seas, as well as in Kola Bay, are summarised in Table 33, together with the corresponding $^{239,240}Pu$ and ^{137}Cs concentrations and radionuclide ratios. The highest CFs values for $^{239,240}Pu$ were found in the carnivore Ophioroidea *Stegofiura nodosa* in the Pechora Sea.

In order to assess the distribution of plutonium within benthic organisms, four *Asteris rubens* sampled near the Polarnyi nuclear submarine yard in Olenaya Bay (Kola Bay) were dissected and the body wall separated from the pyloric caecum, stomach plus rectum. The results, summarised in Table 34, show that plutonium is concentrated in the body wall (mean CF value = 1550 ± 600), with the corresponding value for a pooled pyloric caecum sample being a factor of nearly four lower, at 420.

Table 34. ^{239,240}Pu concentrations (Bq kg^{-1}, fresh wt) in body wall and pyloric caecum in four star-fish *Asterias rubens* collected in Olenaya Bay (Kola Bay) in 1995. For CF calculations, a ^{239,240}Pu water concentration of 9×10^{-6} Bq l^{-1} has been assumed. All errors quoted are ± 1 S.D.

	% dry wt.	^{239,240}Pu ($\times 10^{-3}$)	CF
Body wall			
1	34	13 ± 2	1465
2	26	9 ± 1	1024
3	28	21 ± 2	2381
4	32	12 ± 3	1328
Pyloric caecum			
Pooled (2+4)	32	4	423

8.2.2. Concentration factors in Barents Sea fish

^{137}Cs concentrations and bioconcentration factors in predatory Arctic fish species (arctic cod, haddock, saithe, wolffish, plaice, redfish , halibut and ray) collected by trawling in the main commercial fishing areas of the Barents Sea (Figure 4) during 1993 and 1994, are summarised in Table 35. The stomach contents of the fish analysed varied from partially digested fish to molluscs or big *Hyas araneus* crabs. ^{137}Cs CFs values in fish muscle varied from 75 to 158 which, again, is compatible with the IAEA recommended CF value of 100. ^{239,240}Pu concentrations in all but the ray samples were found to be low, never exceeding 0.002 Bq kg^{-1} (fresh wt.). For ray, the ^{239,240}Pu concentration in a combined sample (n=3) was found to be 0.08 Bq kg^{-1}(fresh wt.), yielding a CF value of 2000. The latter is significantly higher than the IAEA recommended CF value for fish muscle, namely 40. Although the diet of these predatory Arctic fish (Table 30) is highly variable, bioconcentration factors for ^{137}Cs and ^{239,240}Pu are rather even. The ray's diet does not, on its own, explain the high CF value found for ^{239,240}Pu, and could rather have its origin in behavioural differences with respect to the other fish.

Table 35. ^{137}Cs concentrations (Bq kg^{-1}, fresh wt.) in flesh of fish collected in the Barents Sea during 1993–94. ^{137}Cs sea water concentration for CF calculation = 5.3×10^{-3} Bq l^{-1}

Fish	Species	n	^{137}Cs (1993)	CF	n	^{137}Cs (1994)	CF	Mean CF (1993–94)
Atlantic cod	*Gadus morphua morphua*	11	0.67	134	6	0.91	182	158
Haddock	*Melanogrammus aeglefinus*	6	0.51	102	6	0.24	48	75
Saithe	*Pollachius viren*				7	0.44	88	88
Wolffish	*Anarhichas lupus*	3	0.42	84				84
Redfish	*Sebastes marinus*				8	0.46	92	92
Plaice	*Pleuronuctes sp.*	14	0.74	148	4	0.41	82	115
Halibut	*Rheinhardtius sp.*				12	0.50	100	100
Ray	*Raja radiata*	10	0.79	158	3	0.57	114	136
Mean (±1σ)			*0.6 ± 0.2*			*0.5 ± 0.2*		*100 ± 30*

8.2.3. Concentration factors in Arctic salmon

Salmon are migratory fish. After hatching, salmon parr live an average of four years in the spawning river. In their fifth year, 19–cm long smolts leave the river and migrate to the sea, where they spend up to four years, in search for food. After this period, most specimens, now over 1–m long and with a weight in the range15–20 kg, return to the same river they were born in to spawn. There, they remain over winter in the ice-covered river, hardly eating at all and losing more than 50% of their original body weight. In the spring, the starved fish return to the feeding area, where they rapidly regain their weight.

As part of the ARMARA project, radiocaesium and plutonium concentrations in two distinct Arctic salmon populations were compared. Salmon were caught in the river Teno, which drains into the Norwegian Sea, and in the rivers Tornionjoki, Kemijoki and Simojoki, which drain into the northern part of the Gulf of Bothnia (Baltic Sea). The rivers in both areas received approximately the same direct amounts of weapons and Chernobyl fallout. However, the migration pattern of the salmon from the river Teno is completely different from that of the other three rivers. Salmon from the river Leno migrate to a sea area lying between Greenland, the Färc Islands and the Lofoten Islands, where they feed on crustaceans, amphipods and krill. The salmon caught in the other rivers do not leave the Baltic Sea, living mainly on spratt (*Clupea sprattus*) and baltic herring (*Clupea membras*).

^{137}Cs concentrations in 83 salmons (*Salmo salar*) caught in the river Teno and its tributary river Inari during 1988–98 showed a decrease from about 1.0 Bq kg^{-1} to 0.36 ± 0.08 (n=18), yielding a biological half-life of 6 years. No correlation was found between ^{137}Cs concentrations and the weight or sex of the salmon. In salmon from the Baltic rivers, ^{137}Cs concentrations were found to be up to two orders of magnitude higher, reflecting the enhanced ^{137}Cs levels found in the Baltic Sea as a result of the Chernobyl fallout deposition. The Chernobyl origin of this ^{137}Cs was confirmed by the presence in all specimens of small but measurable amounts of ^{134}Cs.

CFs for ^{137}Cs, ^{90}Sr and ^{239,240}Pu in flesh and bone for different weight salmon caught in the river Teno are given in Table 36. A mean ^{137}Cs CF value of 78 ± 15 was obtained for flesh, with no clear variation of CF with weight. This value is only marginally lower than that observed for other Arctic fish caught in the Barents Sea (Table 35). For ^{90}Sr, a mean CF of 2.4 ± 0.8 was found for flesh, compatible with the IAEA–recommended value of 2. In bone, higher ^{90}Sr concentrations were found in starved, low weight specimens. In the case of ^{239,240}Pu, all concentration were found to be below the limits of detection.

Table 36. ^{137}Cs, ^{90}Sr and ^{239,240}Pu concentrations (Bq kg^{-1}, fresh wt.) in flesh and bones of salmon from the river Teno (1994–95). Sea water concentration used for CF calculation: ^{137}Cs = 5 × 10^{-3} Bq l^{-1}; ^{90}Sr = 4 × 10^{-3} Bq l^{-1}; ^{239,240}Pu = 4 × 10^{-6} Bq l^{-1}

Weight	n	Conc. (flesh)			Conc. (bone)		CF (flesh)		
		^{137}Cs	^{90}Sr	^{239,240}Pu	^{90}Sr	^{239,240}Pu	^{137}Cs	^{90}Sr	^{239,240}Pu
1	5	0.35	0.012	<0.001	2.46	<0.007	70	3.0	<250
8	4	0.48	0.012	<0.003	1.55	<0.008	96	3.0	<750
15	3	0.41	0.008	<0.003	1.34	<0.006	82	2.0	<750
18	3	0.31	0.006	<0.003	1.56	<0.005	62	1.5	<750

The total Finnish-Norwegian catch of salmon from the river Teno fluctuated during the 1990s between 90 and 180 tons. The total salmon catch in the Baltic Sea area is estimated to be about 1000 tons, of which 200–300 are caught by sport fisherman in Swedish and Finnish rivers.

8.2.4. Concentration factors in sea birds

^{137}Cs and ^{239,240}Pu concentrations in liver and muscle tissue of nine Arctic sea bird species were examined in the course of the project for CF determination purposes. The birds, caught in the east coast of the Kola peninsula (Figure 4), were kindly provided to the collaboration by the Murmansk Marine Biological Institute. A summary of the measured concentrations, together with the concentration factors, is given in Table 37. The variability observed in CFs for muscle is likely related to the specific diet of each particular type of bird (Table 31) and to the hydrodynamics of the sampling locations. Drosdovskaya Bay, Ostroc Nokuyav, Dalnyie Zelentsy Bay and Yarnishnaya Bay are intensively washed by tidal currents, while Ivanovskaya Bay is a rather long fjord with two ridges, slowing water circulation and favouring particle sedimentation.

Table 37. ^{137}Cs and ^{239,240}Pu concentrations (Bq kg^{-1}; fresh wt.) in muscle and liver of sea birds caught in the Barents Sea coast during 1995–96. Sea water concentration used for CF calculation: ^{137}Cs = 5×10^{-3} Bq l^{-1}; ^{239,240}Pu = 4×10^{-6} Bq l^{-1}

Bird	Location	^{137}Cs				^{239,240}Pu	
		Muscle	CF	Liver	CF liver	Muscle	CF
Great black-back gull	Ivanovskaya B.	5.6	1120	4.4	880		
Great black-back gull	Ivanovskaya B.	2.4	480	2.2	440		
Common gull	Ostrov Nokuyak	1.0	200	1.0	200		
Great skua	Ostrov Nokuyak	3.0	600	2.1	420	<0.001	<250
Merganser	Drosdovskaya B.	0.2	32	<0.2	<40	<0.001	<250
Black gillemot	Yarnishnaya B.	0.4	86	0.9	170		
Eider	Yarnishnaya B.	0.2	30	<0.1	<20	<0.002	<500
Eider	Yarnishnaya B.	0.2	34	0.7	140	0.0023	575
Eider	Yarnishnaya B.	0.3	60	0.3	58	<0.002	<500
Eider	Dalnyie Zelentsy	<0.1	<20	<0.1	<20	<0.001	<300
Spotted redshank	Ivanovskaya B.	4.3	860	4.8	960		
Purple sandpiper	Dalnyie Zelentsy	<0.1	<20	<0.1	<20		
Little stint	Ivanovskaya B.	1.5	300	2.2	960		
Great skua	Drosdovskaya B.	40	8000	22	440		

8.2.5. Concentration factors in seal pups

Seals are an important link in the Arctic food chain, representing part of the diet of several marine predators (e.g., polar bears) and the Arctic indigenous population. The diet of seals consists mainly of fish and benthic fauna. In the course of the project, the organs of two Greenland seal pups hunted near Chapoma (White Sea) in 1995, and those of seven seal pups hunted near Zolotitsa (southern shore of the White Sea) in 1996 were assayed for ^{137}Cs, ^{90}Sr and ^{239,240}Pu, for the purpose of CF determination (Figure 4).

^{137}Cs concentrations in the seal pups from Zolotitsa were found to be low, varying from 0.07 Bq kg^{-1} (fresh wt.) in the stomach content up to 0.95 Bq kg^{-1} (fresh wt.) in cartalaginous ribs. The highest ^{137}Cs concentration (1.6 ± 0.6 Bq kg^{-1}; fresh wt.) was measured in the parathyroid gland from one of the pups. Mean ^{137}Cs concentrations in different organs were found to decrease as follows: 0.59 Bq kg^{-1} (fresh wt.) in cartalaginous ribs and pancreas, 0.56 Bq kg^{-1} (fresh wt.) in ovaries, 0.48 Bq kg^{-1} (fresh wt.) in cartilage and kidney, 0.35 Bq kg^{-1} (fresh wt.) in heart, muscle, brain, spleen cartilaginous coccyx and thyroidal gland, 0.30 Bq kg^{-1} (fresh wt.) in liver, lungs, stomach and testicles, 0.25 Bq kg^{-1} (fresh wt.) in pooled bone samples (limbs, shoulder, pelvis), vertebrae and ribs, and 0.20 Bq kg^{-1} (fresh wt.) in fat. The concentration in stomach contents varied from 0.07 Bq kg^{-1} (fresh wt.) to 0.21 Bq kg^{-1} (fresh wt.), with the higher concentration corresponding to a sample contaminated by blood. An estimate of the ^{137}Cs burden in these pups yielded values below 3 Bq.

For the seal pups from Chapona, ^{137}Cs concentrations in muscle were found to be a factor of 2.5 higher than those from Zolotitsa. For other organs (brain, kidney, spleen, bones and liver), concentrations were also found to be higher, although only by a factor of 1.5. This difference is likely related to differences in ^{137}Cs concentrations in the mother seals feeding areas. In both locations, K, Na and Mg concentrations were found to be relatively constant in different organs, being in the range 1.5–3.2, 0.3–3.0 and 0.14–3.4 mg g^{-1} (fresh wt.), respectively.

^{90}Sr was assayed on a limited number of pooled samples from Zolotitsa. ^{90}Sr mean concentrations in ribs, vertebrae, bones and cartilaginous ribs were 0.18, 0.14, 0.10 and 0.03 Bq kg^{-1} (fresh wt.), respectively. The highest total strontium contents, in the range 130–150 mg g^{-1}, were found in ribs and leg bones. In vertebrae, the corresponding figure was 94 mg g^{-1}, while the concentrations in cartilage, brains, stomach, muscle, spleen, lung, liver, kidney and heart decreased from 5.3 mg $g^{-1}$to 0.05 mg g^{-1}. In the case of ^{239,240}Pu, all samples analysed were below the limits of detection, being always less than 0.03 Bq kg^{-1} (fresh wt.).

Although no adult specimens were analysed in the course of the project, the average ^{137}Cs concentrations in these seal pup muscles, at 0.36 ± 0.12 Bq kg^{-1} (fresh wt.) is identical to that found for adult Greenland seals in the period 1990–94, namely 0.40 ± 0.12 Bq kg^{-1} (fresh wt.). Using a sea water ^{137}Cs concentration of 5×10^{-3} Bq l^{-1}, it was possible to estimate CFs for different organs. In muscle tissue, for example, CFs were found to be in the range 70–170, while for liver, the corresponding figures were in the range 60–90.

8.3. Concentration factors in phytoplankton and zooplankton

From an ecological point of view, phytoplankton and plankton represent the first links in the Arctic marine food chain. In order to assess the transfer processes through this primary producer route, samples of phyto- and zooplankton were collected and assayed for radionuclide content in the course of the programme. The work was carried out in two very different marine zones, namely the Irish Sea and the Greenland continental shelf.

8.3.1. Radiocaesium, plutonium and americium CFs in plankton from the Irish Sea

Transuranic and radiocaesium concentrations in phytoplankton and zooplankton samples collected at 16 stations throughout the Irish Sea in the course of the CIROLANA 6/94 expedition are presented in Tables 38 and 39. Concomitant determination of radionuclide concentrations in filtered (>0.45 μm) sea water enabled the calculation of *in situ* concentration factors (CFs). The results of these calculations for phytoplankton and zooplankton are given in Tables 40 and 41, respectively.

Concentration factors showed high variability, a result not unexpected from (i) the heterogeneous composition of the samples, (ii) the different productivity areas, and (iii) the possible absence of equilibrium due to the presence of the Sellafield source-term. The wide range of values observed and the similarity between both sets of CFs made difficult the assessment of possible bio-magnification or discrimination processes. In any case, a sequence of increasing radionuclide affinity in both planktonic groups from the Irish Sea was clearly established, namely

$$^{241}\text{Am}\ (CF \sim 10^6) > {}^{238}\text{Pu},\ {}^{239,240}\text{Pu}\ (CF \sim 10^5) > {}^{137}\text{Cs}\ (CF \sim 10^3)$$

In Tables 40 and 41, comparison has also been made between our measured concentration factors and those recommended by the International Atomic Energy Agency (IAEA). It is worth noting that these values are based on a limited set of published results and that, therefore, our results should be regarded as a significant expansion of the original database. Based on the IAEA–recommended values, a discrimination between phyto- and zooplankton for plutonium and americium should be manifest. This has not been observed in our experiments.

Table 38. ^{137}Cs, Pu and ^{241}Am concentrations in phytoplankton from the Irish Sea, May 1994

Station	^{137}Cs (kBq kg^{-1})	^{239,240}Pu (Bq kg^{-1})	^{238}Pu (Bq kg^{-1})	^{241}Am (Bq kg^{-1})	^{137}Cs/ ^{239,240}Pu	^{238}Pu/ ^{239,240}Pu	^{241}Am/ ^{239,240}Pu
9	1.2 ± 0.2	772 ± 43*	181 ± 19*	1001 ± 74*	1.5 ± 0.3	0.23 ± 0.06	1.30 ± 0.12
11	0.28 ± 0.04	71 ± 4	15.0 ± 1.5	216 ± 16	4.0 ± 0.5	0.21 ± 0.05	3.1 ± 0.3
13	0.19 ± 0.05	87 ± 5	14.9 ± 1.6	162 ± 14	2.2 ± 0.6	0.17 ± 0.03	1.87 ± 0.19
16	0.6 ± 0.3	106 ± 8	21 ± 3	n.d.	6 ± 3	0.20 ± 0.05	-
20	n.d.	37 ± 4	4.3 ± 1.3	70 ± 17	-	0.12 ± 0.04	1.9 ± 0.5
23	n.d.	44 ± 3	9.4 ± 1.1	n.d.	-	0.21 ± 0.05	-
25	n.d.	11.8 ± 0.6	1.8 ± 0.2	n.d.	-	0.15 ± 0.03	-
27	0.21 ± 0.06	4.9 ± 0.8	0.8 ± 0.3	n.d.	42 ± 14*	0.16 ± 0.07	-
29	n.d.	17.6 ± 1.4	3.0 ± 0.5	n.d.	-	0.17 ± 0.04	-
31	0.23 ± 0.06	40 ± 3	4.8 ± 1.1	n.d.	5.8 ± 1.5	0.12 ± 0.03	-
34	n.d.	9 ± 2	1.4 ± 0.5	138 ± 30	-	0.15 ± 0.06	15 ± 5*
36	n.d.	45 ± 3	10.7 ± 1.1	n.d.	-	0.24 ± 0.06	-
38	0.66 ± 0.17	454 ± 57*	96 ± 14*	733 ± 101	1.5 ± 0.4	0.21 ± 0.05	1.6 ± 0.3
41	0.26 ± 0.04	178 ± 8	39 ± 3	284 ± 14	1.4 ± 0.2	0.22 ± 0.05	1.59 ± 0.11
42	n.d.	83 ± 8	15.4 ± 1.6	105 ± 13	-	0.18 ± 0.04	1.26 ± 0.19
Mean	*0.45 ± 0.12*	*57 ± 14*	*11 ± 3*	*339 ± 120*	*1.7 ± 0.4*	*0.18 ± 0.02*	*1.59 ± 0.18*
σ (n)	*0.34 (8)*	*49 (13)*	*11 (13)*	*340 (8)*	*2.0 (7)*	*0.039 (15)*	*0.61 (7)*
C.V.(%)	*75*	*86*	*99*	*100*	*118*	*22*	*38*
Range	*0.19 – 1.2*	*4.9 – 772*	*0.8 – 181*	*70 – 1001*	*1.4 – 42*	*0.12 – 0.24*	*1.26 – 15*

Reported uncertainties are ±1 S.D.
n.d.: not detected * Outlier.

Table 39. ^{137}Cs, Pu and ^{241}Am concentrations in zooplankton from the Irish Sea, May 1994

Station	^{137}Cs (Bq kg^{-1})	^{239,240}Pu (Bq kg^{-1})	^{238}Pu (Bq kg^{-1})	^{241}Am (Bq kg^{-1})	^{137}Cs/ ^{239,240}Pu	^{238}Pu/ ^{239,240}Pu	^{241}Am/ ^{239,240}Pu
9	355 ± 17	493 ± 14*	114 ± 5*	620 ± 103*	0.72 ± 0.04	0.23 ± 0.05	1.3 ± 0.2
11	323 ± 8	189 ± 7	38 ± 2	235 ± 17	1.71 ± 0.07	0.20 ± 0.04	1.24 ± 0.10
13	180 ± 9	106 ± 3	20.3 ± 1.2	158 ± 14	1.71 ± 0.10	0.19 ± 0.04	1.50 ± 0.14
16	42 ± 3	15.7 ± 0.7	2.8 ± 0.3	23.8 ± 1.9	2.7 ± 0.2	0.18 ± 0.04	1.52 ± 0.14
20	25 ± 2	10.1 ± 0.4	1.89 ± 0.16	16 ± 3	2.5 ± 0.3	0.19 ± 0.04	1.6 ± 0.3
23	n.d.	4.8 ± 0.3	1.06 ± 0.10	5.4 ± 0.9	-	0.22 ± 0.05	1.13 ± 0.21
25	10 ± 3	1.74 ± 0.11	0.22 ± 0.04	n.d.	5.6 ± 1.5*	0.13 ± 0.03*	-
27	55 ± 2	9.6 ± 0.4	1.70 ± 0.15	11.2 ± 1.0	5.7 ± 0.3*	0.18 ± 0.03	1.16 ± 0.11
29	92 ± 6	18.9 ± 0.9	3.2 ± 0.3	33 ± 8	4.9 ± 0.4	0.17 ± 0.03	1.7 ± 0.5
31	179 ± 16	63 ± 3	12.4 ± 1.2	71 ± 12	2.8 ± 0.3	0.20 ± 0.04	1.1 ± 0.2
34	372 ± 22	149 ± 5	30.7 ± 1.9	218 ± 36	2.49 ± 0.17	0.21 ± 0.04	1.5 ± 0.2
36	67 ± 5	21.6 ± 1.0	4.9 ± 0.4	37 ± 6	3.1 ± 0.3	0.22 ± 0.05	1.7 ± 0.3
38	84 ± 6	36.3 ± 1.7	6.8 ± 0.6	62 ± 10	2.33 ± 0.19	0.19 ± 0.04	1.7 ± 0.3
41	345 ± 16	510 ± 15*	119 ± 6*	621 ± 103*	0.68 ± 0.04	0.23 ± 0.06	1.22 ± 0.20
42	328 ± 17	146 ± 6	34 ± 2	202 ± 33	2.25 ± 0.15	0.23 ± 0.06	1.38 ± 0.24
Mean	*176 ± 37*	*59 ± 18*	*12 ± 4*	*89 ± 24*	*2.3 ± 0.3*	*0.20 ± 0.01*	*1.48 ± 0.11*
σ (n)	*140 (14)*	*65 (13)*	*14 (13)*	*88 (12)*	*1.1 (12)*	*0.029 (14)*	*0.22 (14)*
C.V.(%)	*80*	*110*	*113*	*98*	*48*	*15*	*15*
Range	*10 – 372*	*1.74 – 510*	*0.22 – 119*	*5.4 – 621*	*0.68 – 5.7*	*0.13 – 0.23*	*1.13 – 1.7*

Reported uncertainties are ±1 S.D.
n.d.: not detected * Outlier.

Table 40. CFs for ^{137}Cs, ^{239,240}Pu, ^{238}Pu and ^{241}Am in phytoplankton from the Irish Sea

Station code	Concentration factor (l kg^{-1}, dry wt.)			
	^{137}Cs (× 10^{3})	^{239,240}Pu (× 10^{4})	^{238}Pu (× 10^{4})	^{241}Am (× 10^{5})
9	8.1 ± 1.5	49 ± 3*	57 ± 7*	17.1 ± 1.3
11	0.82 ± 0.10	4.6 ± 0.3	4.9 ± 0.5	11.3 ± 0.9
13	1.2 ± 0.3	6.7 ± 0.4	5.8 ± 0.6	7.8 ± 0.7
16	10 ± 4	21.3 ± 1.7	19 ± 3	-
20	-	8.1 ± 0.9	4.9 ± 1.5	12 ± 3
23	-	18.7 ± 1.4	19 ± 2	-
25	-	6.1 ± 0.3	4.2 ± 0.5	-
27	4.8 ± 1.4	2.7 ± 0.5	2.1 ± 0.8	-
29	-	3.4 ± 0.3	2.8 ± 0.5	-
31	1.8 ± 0.4	4.8 ± 0.4	3.0 ± 0.7	-
34	-	1.2 ± 0.3	0.9 ± 0.3	7.4 ± 1.6
36	-	7.4 ± 0.4	8.5 ± 0.9	-
38	6.0 ± 1.6	66 ± 8*	68 ± 10*	63 ± 9*
41	1.5 ± 0.2	9.0 ± 0.4	8.4 ± 0.7	3.9 ± 0.2
42	-	7.4 ± 0.7	7.4 ± 0.9	2.7 ± 0.3
Mean	*4.2 ± 1.2*	*7.8 ± 1.6*	*7.0 ± 1.6*	*8.8 ± 1.9*
σ (n)	*3.4 (8)*	*5.9 (13)*	*5.8 (13)*	*4.9 (7)*
C.V.(%)	*81*	*75*	*83*	*56*
Range	*0.82 – 10*	*1.2 – 66*	*0.9 – 68*	*2.7 – 63*
IAEA value†	*0.1*	*50*	*50*	*10*
IAEA range†	-	*15 – 300*	*15 – 300*	*1.5 – 35*

Table 41. CFs for ^{137}Cs, ^{239,240}Pu, ^{238}Pu and ^{241}Am in zooplankton from the Irish Sea

Station code	Concentration factor (l kg^{-1}, dry wt.)			
	^{137}Cs (× 10^{2})	^{239,240}Pu (× 10^{4})	^{238}Pu (× 10^{4})	^{241}Am (× 10^{5})
9	24.9 ± 1.2	31.0 ± 1.0*	36 ± 2*	10.6 ± 1.8
11	9.4 ± 0.2	12.3 ± 0.5	12.3 ± 0.8	12.3 ± 0.9
13	11.9 ± 0.6	8.1 ± 0.3	7.9 ± 0.5	7.6 ± 0.7
16	6.4 ± 0.4	3.16 ± 0.15	2.6 ± 0.3	3.7 ± 0.3
20	4.2 ± 0.4	2.23 ± 0.10	2.15 ± 0.19	2.6 ± 0.4
23	-	2.03 ± 0.12	2.1 ± 0.2	2.1 ± 0.4
25	2.6 ± 0.7	0.90 ± 0.06	0.51 ± 0.10	-
27	12.7 ± 0.5	5.3 ± 0.2	4.6 ± 0.4	6.5 ± 0.6
29	11.0 ± 0.7	3.66 ± 0.19	3.0 ± 0.4	5.3 ± 1.4
31	13.7 ± 1.2	7.6 ± 0.4	7.8 ± 0.8	5.0 ± 0.8
34	28.8 ± 1.7	19.2 ± 0.8	20.2 ± 1.6	11.7 ± 1.9
36	7.4 ± 0.6	3.50 ± 0.18	3.9 ± 0.4	2.7 ± 0.5
38	7.6 ± 0.5	5.3 ± 0.3	4.8 ± 0.5	5.3 ± 0.9
41	20.5 ± 1.0	25.6 ± 0.9	25.2 ± 1.5	8.5 ± 1.4
42	29.9 ± 1.5	12.9 ± 0.7	16.3 ± 1.4	5.2 ± 0.9
Mean	*14 ± 2*	*8.0 ± 1.9*	*8 ± 2*	*6.4 ± 0.9*
σ (n)	*9 (14)*	*7.2 (14)*	*8 (14)*	*3.4 (14)*
C.V.(%)	*65*	*90*	*94*	*53*
Range	*2.6 – 29.9*	*0.90 – 31.0*	*0.51 – 36*	*2.1 – 12.3*
IAEA value†	*1.5*	*0.5*	*0.5*	*0.1*
IAEA range†	*0.5 – 2.5*	*0.25 – 2.5*	*0.25 – 2.5*	*0.025 – 0.25*

Reported uncertainties are ±1 S.D. * Outlier.

†Value and range recommended by IAEA (IAEA, 1985), converted to dry weight

The distributions of ^{239,240}Pu concentrations in phyto- and zooplankton throughout the Irish Sea are shown in Figure 65. Similar results were obtained for ^{137}Cs and ^{241}Am.

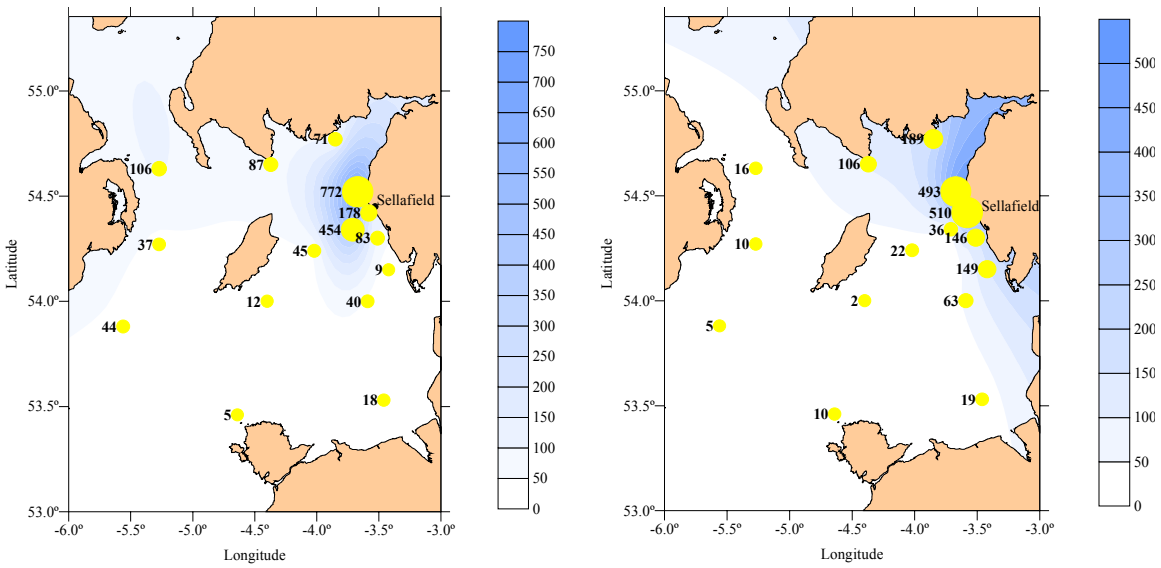

Figure 65. ^{239,240}Pu concentrations in (a) phytoplankton and (b) zooplankton in the Irish Sea

A more limited set of plutonium data was obtained in the course of a research expedition to the western Irish Sea in 1996 aboard the Irish research vessel *Lough Beltra* (Table 42). In general, concentrations were much lower than in the eastern Irish Sea, but similar to those observed in the westernmost stations during the 1994 research expedition. CF values were compatible with those obtained in the previous campaign. Again, a high degree of variability was observed, which is inherent in this kind of biological material.

Table 42. ^{239,240}Pu in plankton from the western Irish Sea (*Lough Beltra'96* expedition)

Station code	**Concentration (Bq kg^{-1})**		**CF (× 10^4 l kg^{-1})**	
	Phytoplankton	**Zooplankton**	**Phytoplankton**	**Zooplankton**
N7	1.9 ± 0.3	0.37 ± 0.04	3.7 ± 0.5	0.74 ± 0.08
N4-N7	0.9 ± 0.2	0.67 ± 0.06	1.9 ± 0.4	1.34 ± 0.12
N4	0.5 ± 0.2	3.4 ± 0.5	1.0 ± 0.4	6.8 ± 1.0
N4-N5	0.4 ± 0.3	0.43 ± 0.03	0.8 ± 0.6	0.85 ± 0.07
N5	8.3 ± 1.1	0.24 ± 0.09	17 ± 2	0.49 ± 0.19
N5-N6	3.1 ± 0.8	0.79 ± 0.05	6 ± 2	1.58 ± 0.11
N6	1.7 ± 0.3	1.38 ± 0.08	3.4 ± 0.5	2.77 ± 0.17
Mean	*2.4 ± 1.0*	*1.0 ± 0.4*	*5 ± 2*	*2.1 ± 0.8*
σ	*2.8*	*1.1*	*6*	*2.2*
C.V. (%)	*115*	*106*	*115*	*106*
Range	*0.4 – 8.3*	*0.2 – 3.4*	*0.8 – 17*	*0.5 – 6.8*

Measurements of the ^{241}Pu/^{239,240}Pu ratio enabled to put an estimate of ~18 years on the 'age' of plutonium released from Sellafield and now attached to both phytoplankton and zooplankton., giving a measure of the hold-up time of plutonium in Irish Sea bottom sediments. A model incorporating the different possible pathways of plutonium accumulation in zooplankton (*via* water, phytoplankton and bottom sediments) has been formulated as part of the programme and is discussed in further detail in WP 9.

8.3.2. Plutonium CFs in plankton from Thule (Greenland)

In the course of the *Thule'97* expedition, samples of phyto- and zooplankton were collected at three stations (P1, P2, 20) located in Bylot Sound, close to the accident site(Figure 45b). In all samples, ^{137}Cs concentrations were found to be below the limits of quantitation of the system used (found to be 2 Bq m^{-3} for phytoplankton and 2–10 Bq m^{-3} for zooplankton). The results of the ^{239,240}Pu analyses in these samples are summarised in Table 43, together with the CF values calculated from concomitant ^{239,240}Pu concentration in sea water at each of the stations. Although the data base is limited, CFs for plutonium in zooplankton were found to be very similar to those found for the Irish Sea (Tables 41 and 42), and also to those found in more temperate environments (e.g., western Mediterranean), suggesting little effect of temperature in CF values. For phytoplankton, the low ^{239,240}Pu concentrations, close to the limits of quantitation, make difficult to draw any comparison with other environments.

Table 43. ^{239,240}Pu in plankton from Thule (*Thule'97* expedition)

Station code	Concentration (Bq kg^{-1})		CF (× 10^4 l kg^{-1})	
	Phytoplankton	**Zooplankton**	**Phytoplankton**	**Zooplankton**
P1	2.4 ± 2.0	0.29 ± 0.03	70 ± 60	8.9 ± 1.0
P2	0.2 ± 0.2	0.104 ± 0.011	5 ± 7	3.2 ± 0.5
20	2.9 ± 2.9	0.143 ± 0.010	30 ± 0.4	1.5 ± 0.2
Mean	*1.8 ± 0.8*	*0.18 ± 0.06*	*40 ± 20*	*5 ± 2*
σ	*1.4*	*0.10*	*30*	*4*
C.V. (%)	*80*	*56*	*95*	*85*
Range	*0.2 – 2.9*	*0.104 – 0.29*	*5 – 70*	*1.5 – 8.9*

8.3.3. ^{210}Pb and ^{210}Po CFs in plankton from Svalbard

Samples of mesozooplankton (>200 μm) were collected at five locations in the course of the 1998 winter campaign to the western continental shelf of Spitsbergen and analysed for the naturally-occurring ^{210}Pb and ^{210}Po. Measured concentrations, as well as the CF values derived from concomitant sea water analyses, are summarised in Tables 44 and 45. A significant difference was observed between the biomasses at three of the stations (ZPNY1, ZPNY2 and ZPNY3), with a mean value of 15 mg m^{-3} (dry wt.), and that at the other two locations (ZPNY4 and ZPNY5), with a mean of 43 mg m^{-3} (dry wt.).

Table 44. ^{210}Po and ^{210}Pb concentrations in mesozooplankton from Svalvard

Location	Biomass	Conc. (Bq kg^{-1}; dry wt.)		
	(mg m^{-3}, dry wt.)	^{210}Po	^{210}Pb	^{210}Po/^{210}Pb
ZPNY1	15	148 ± 6	8.7 ± 0.9	17 ± 2
ZPNY2	17	110 ± 6	6.0 ± 0.5	18 ± 2
ZPNY3	13	176 ± 5	7.8 ± 0.6	23 ± 2
ZPNY4	43	59 ± 3	6.9 ± 0.7	8.5 ± 0.9
ZPNY5	49	76 ± 3	2.3 ± 0.4	34 ± 6
ZPNY5(B)	38	75 ± 3	4.9 ± 0.6	15 ± 2
Mean	*29*	*107 ± 19*	*6.1 ± 0.9*	*19 ± 3*

Po-210 concentrations were also different for both groups of samples (Table 43). For stations ZPNY1, ZPNY2 and ZPNY3, a mean ^{210}Po concentration of 145 ± 19 Bq kg^{-1} was

obtained, which is a factor of 2 higher than that observed for stations ZPNY4 and ZPNY5, namely 70 ± 6 Bq kg^{-1}. For ^{210}Pb, concentrations were about 20 times lower than those for ^{210}Po, also being higher for stations ZPNY1, ZPNY2 and ZPNY3 (mean = 7.5 ± 0.8 Bq kg^{-1}) than for stations ZPNY4 and ZPNY5 (mean = 4.7 ± 1.3 Bq kg^{-1}). The inverse relationship between ^{210}Po and ^{210}Pb concentrations and biomass had been previously reported for zooplankton samples in oligothrophic waters from the French Polynesia (Jeffree *et al.*, 1997).

Table 45. ^{210}Po and ^{210}Pb CFs in mesozooplankton from Svalvard

Location	Biomass	CF (× 10^4)	
	(mg m^{-3}, dry wt.)	^{210}Po	^{210}Pb
ZPNY1	15	-	-
ZPNY2	17	15 ± 2	0.67 ± 0.04
ZPNY3	13	25 ± 2	0.89 ± 0.06
ZPNY4	43	8.9 ± 0.9	0.78 ± 0.04
ZPNY5	49	10.7 ± 1.2	0.22 ± 0.02
ZPNY5(B)	38	10.5 ± 1.2	0.48 ± 0.03
Mean	*29*	*14 ± 3*	*0.61 ± 0.12*

The mean CF factor of ^{210}Po by mesozooplankton, at (14 ± 3) × 10^4 l kg^{-1}, is about an order of magnitude higher than that the corresponding value for ^{210}Pb, at (6.1 ± 1.2) × 10^3 l kg^{-1}, reflecting the higher accumulation of ^{210}Po by marine organisms.

8.4. Concentration ratios and concentration factors in benthic organisms

8.4.1. In situ sediment–animal concentration ratios

In situ sediment-animal concentration ratios (CRs) for plutonium in invertebrates sampled in the Irish Sea and at Thule (Bylot Sound, Greenland) have already been presented in §6.6 above. Sediment-animal CRs for plutonium and americium in the western and eastern Irish Sea are summarised in Table 18. Although the sample numbers are small, there is very good agreement between the CRs determined for plutonium in invertebrates in the eastern Irish sea and those in the western Irish sea, even though the ambient activity concentrations in the sediments are much different. The agreement between the CRs for americium in both zones is good for the polychaete samples but lower americium CRs are observed for brittle stars and for *Cucumaria* in the eastern Irish Sea. The polychaete *Owenia* has a CR of between 0.98–1.4 for plutonium and americium in both sampling zones reflecting the fact that the worm tube is composed mainly of fine sedimentary particles.

Most data found in the literature relating to plutonium or americium CRs are based on laboratory measurements as opposed to *in-situ* field studies. None of the CRs found refer to species examined in this study. The laboratory CRs across the species are generally <0.01. For example, Beasley and Fowler (1976) found that the polychaete *Nereis diversicolor* attained a CR for plutonium of 0.006 and for americium of 0.0043 after 225 days exposure to labelled sediment. Germain *et al* (1984) found similarly low CRs for the polychaete *Arenicola marina* of 0.002 for plutonium and 0.005 for americium after 14 days exposure to labelled sediment. The polychaetes analysed in this study in the Irish Sea all show CRs >0.1 for both plutonium and americium. Miramand *et al* (1982) found a CR for the bivalve *Scrobicularia plana* of 0.01 for plutonium and 0.008 for americium after 14 days exposure to labelled sediment. This compares with CRs of 0.02 for ^{239,240}Pu and 0.04 for ^{241}Am for the bivalves *Tellina* and *Ensis* in this study, both of which are species belonging to the same order (Veneroida) as *Scrobicularia plana*.

Plutonium and americium behaviour in the invertebrates examined appears to be characterised by similar CRs but there are a few exceptions. The scaphopod *Dentalium* appears to exhibit a preference for americium uptake over plutonium. Furthermore, americium CRs for both the brittle stars and the holothurian *Cucumaria* appear to be lower in the eastern Irish Sea than those measured in the western Irish Sea.

In Bylot Sound (Greenland), CRs (excluding appendiculars, i.e., shells/tubes) were found to range between 0.001 for a species of sea urchin to 0.231 for a polychaete species of transparent worm with over 65% of the species measured exhibiting concentration ratios of <0.02. In all cases where species have shells or tube attachments, the concentration ratio to the shell or tube is greater than to the soft parts reflecting the wet weight activity concentrations. A typical example of this is the bivalve *Musculus niger* where the concentration ratio to the soft parts (defined as soft tissue and inter-valve fluid) is 0.014 and to the shell is 0.044. The same pattern is seen in the other bivalves, gastropods and tubulous polychaetes encountered in this study. This pattern was also reflected in americium uptake where data was available (Tables 18 and 19). Estimates of the concentration ratios for americium were confounded by the wider spread on the ^{241}Am activity concentration in the 0–5 cm sections of the sediment cores which was 34 ± 85% (1 SD) Bq kg^{-1} (wet) as compared to 49 ± 33% (1 SD) Bq kg^{-1} (wet) for plutonium.

It has been noticed that there is good agreement between sediment–animal concentration ratios determined for a select number of invertebrates in the eastern and western Irish Sea even though the ambient ^{239,240}Pu activity concentrations in the sediments are very different in the respective locations. However there is very little agreement between the concentration ratios for invertebrates in the Irish sea and those derived for invertebrates collected from station 20 at Thule. For example the concentration ratio for plutonium in the *Brittle stars* in Thule was found to be 0.008 compared with 0.08 in the western Irish Sea and 0.11 in the eastern Irish Sea (Table 18). Similarly, the mean concentration ratio for polychaetes (excluding appendiculars) in Thule was 0.023 compared to a mean of 0.21 in the Irish Sea. There is much better agreement however between the bivalve molluscs *Cardium ciliatum*, *Macoma calcaria* and *Musculus niger* sampled in Thule and the composite bivalve of *Tellina* and *Ensis* sample (same order species) collected in the western Irish Sea. The reason for these differences may lie in a study of the biologically available fractions of plutonium in the sediments of both zones.

8.4.2. In situ sea water–animal concentration factors in the western Irish Sea

In-situ analysis strongly points to the conclusion that the uptake of plutonium and americium by sediment dwelling invertebrates is dominated by transfer from sediment or sediment pore water as opposed to transfer from the water column. However, in the case of the sampling location in the western Irish Sea, sea water–animal concentration factors for plutonium and americium have been calculated and compared with literature data. Plutonium-239,240 and ^{241}Am analyses of total sea water taken from the site in the western Irish Sea yielded total activity concentrations of 278 μBq kg^{-1} and 301 μBq kg^{-1}, respectively. Filtered fraction (<0.45 μm) activity concentrations were found to be 111 μBq kg^{-1} and 77 μBq kg^{-1}, respectively. Using these values, *in-situ* sea water animal concentration factors for plutonium and americium were calculated for the animals collected using both total and filtered sea water.

While no CFs for any of the animals in this particular study were found in the literature, some tentative comparisons were made with similar species. Miramand *et al* (1982) estimated a CF in the laboratory for the mollusc *Scrobicularia plana* and plutonium and americium of 190 and 230 respectively. These values compare with 180 and 332 calculated for the mollusc composite sample of *Tellina* and *Ensis* both of which belong to the same family of bivalves as *Scrobicularia plana*. Noshkin (1972) estimated a CF for plutonium in brittle stars to be 760 and this compares with 791 in this study. IAEA (1985) suggest a general CF for plutonium and americium in crustaceans to be between 100 and 1000 placing the values derived in this study of 827 (Pu) and 930 (Am) at the upper end of the recommended range. However it is well established that CFs vary widely between species and phyla and also that laboratory based

measurements of CFs tend to yield lower values than those determined in the field. This most likely reflects the fact that in the field, other transfer vectors are at work such as sediment–to–animal and food–to–animal pathways.

9. Refinement and validation of a compartmental model for the Arctic and prediction of the likely consequences of Arctic contamination

9.1. Description of the model

The modelling work conducted in the framework of the ARMARA programme focused on the development of an improved version of a compartmental marine dispersion model covering the Arctic and North Atlantic Oceans. Compartmental models have often been used in connection with radiological impact assessments covering marine environments. These models simulate the dispersion of radioactive material between different compartments/regional boxes, the transfer between water and sediments, the uptake of radioactivity in biota, and the transfer to man. This type of modelling assumes instantaneous uniform mixing within each box, with rates of transfer being proportional to the inventories of material in the source boxes. Compartmental models are particularly well suited to describe transport over long distances (>1000 km) and time-scales (up to centuries or millennia), and have been successfully applied to assess the impact of discharges from nuclear facilities to European coastal waters (CEC, 1990), the Mediterranean Sea (CEC, 1994), the Baltic Sea (EC, 1999) and the Arctic (EC, 1997; IAEA, 1999).

9.1.1. The original compartmental model

The model used by the ARMARA collaboration is based on a combination of two models: (1) an adjusted version (Nielsen, 1995) of a regional box model used for radiological assessments in north-west European coastal areas (EC, 1995); and (2) a larger box model covering the Arctic Ocean and the North Atlantic (Chartier, 1993). The larger box model was derived from a world ocean General Circulation Model (Marti, 1992), the results of which were used for the design of a box structure in the Arctic Ocean and surrounding waters.

In its original form, the box model used first order differential equations to describe the transfer of radioactivity between the boxes. These equations are of the form:

$$\frac{dA_i}{dt} = \sum_{j=1}^{n} k_{ji}\, A_j - \sum_{j=1}^{n} k_{ij}\, A_i - k_i\, A_i + Q_i$$

where $k_{ii} = 0$ for all i, A_i and A_j are activities (Bq) at time t in boxes i and j, respectively, k_{ij} and k_{ji} are the rates of transfer (per year) between boxes i and j, and j and i, respectively, k_i is an effective rate of transfer of activity (per year) from box i taking into account loss of material from the compartment without transfer to another (e.g., decay), Q_i is the source input to box i, and n is the total number of boxes in the system.

The rates of transfer between the aquatic boxes, k_{ij} (per year), are related to the volume exchanges, R_{ij} (km^3 per year) according to:

$$R_{ij} = k_{ij}\, V_i$$

where V_i is the volume of water in box i. Figures 66 and 67 show the regions used in the model, and Figure 68 shows the structure of the water boxes and their interconnections.

Each of the water compartments contains associated suspended sediment and the water compartments in contact with the seabed have underlying seabed sediment compartments. The latter are not shown in Figure 68. Details of compartment volumes, depths, suspended sediment loads, sedimentation rates and volume exchange rates may be found in Nielsen *et al.* (1995).

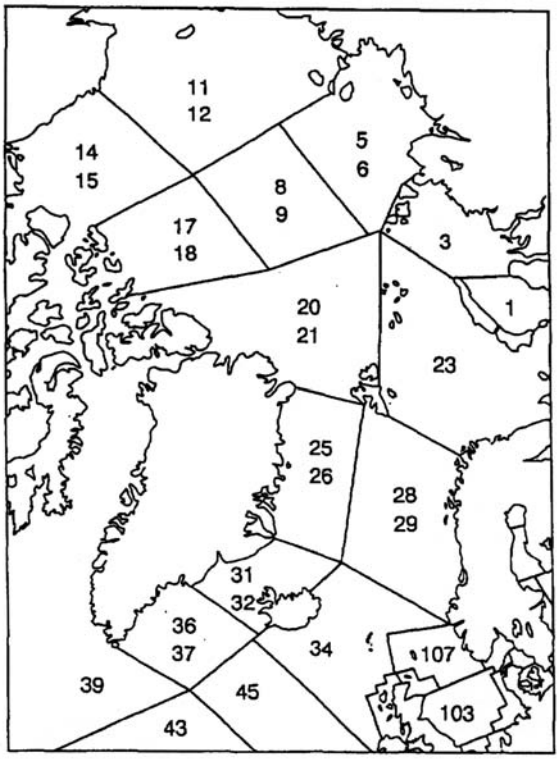

Figure 66. Regions in the Arctic Ocean covered by the compartmental model used in the ARMARA project. The numbers refer to water compartments only.

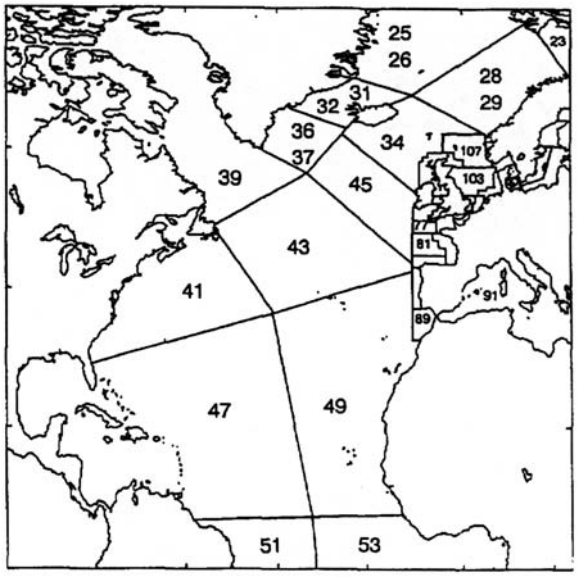

Figure 67. Regions in the North Atlantic covered by the compartmental model used in the ARMARA project. The numbers refer to water compartments only

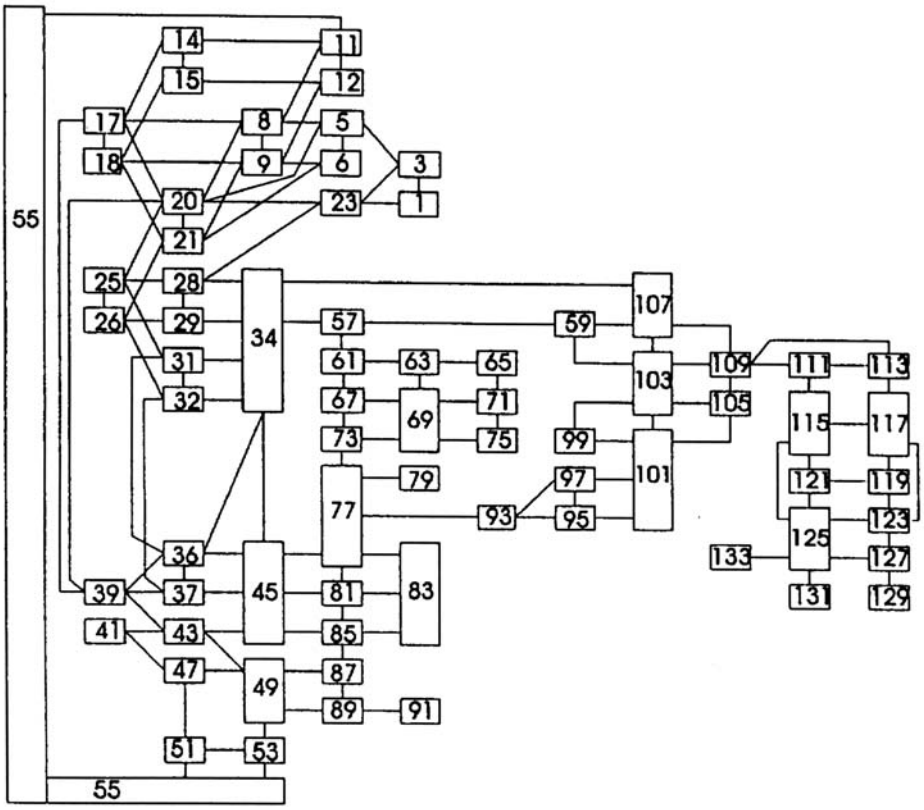

Figure 68. Schematic box structure of the model showing the water boxes only. The lines connecting the boxes indicate water fluxes between adjacent compartments

At any given time, the radioactivity in the water column is partitioned between the water phase and the suspended sediment material. The fraction of the activity (F_W) in the water column which is in solution is given by:

$$F_W = \frac{1}{1 + K_d\, SSL}$$

where K_d is the sediment – water distribution coefficient ($m^2\ t^{-1}$) and SSL the suspended sediment load ($t\ m^{-3}$). Activity on suspended sediment is lost to the underlying boxes when particles settle out. The fractional transfer from a water column compartment (box i) to the sediment compartment (box j) due to sedimentation is given by:

$$k_{ij} = \frac{K_d\, SR_i}{d_i\,(1 + K_d\, SSL_i)}$$

where d_i (m) is the mean water depth of the water column and SR the mass sedimentation rate ($t\ m^{-2}\ year^{-1}$).

The model also includes the transfers of radioactivity between the surface sediment layer and the bottom boundary layer, comprising diffusivity through the pore waters and mixing due to bioturbation modelled as a diffusive process. Furthermore, removal of activity from the top surface sediment to lower sediment layers is taken into account by assuming that the burial rate is equal to the flux of particles which settle from the overlying waters. Radioactive decay is included in all compartments.

Radionuclide concentrations in fish, crustaceans, molluscs and other biota are calculated from the modelled concentrations in the different compartments by using appropriate

concentration factors. Data for the catch of seafood in the various regions (see §8) are used to estimate collective doses by multiplication with the appropriate dose-per-unit-intake factors (IAEA, 1994).

9.1.2. Model refinement

As already mentioned in §1.3, 'traditional' compartmental modelling is based on the assumptions of uniform mixing in each box and instantaneous dispersion throughout the whole modelling space. Although the assumption of uniform mixing may be a realistic approximation in many cases, the assumption of instantaneous dispersion is clearly not correct when the model comprises large water masses (as is the case in the model considered here). Accordingly, a new version of the model was developed which, while maintaining a box structure with uniform mixing in all boxes, also included the dispersion of radionuclides over time.

In mathematical terms, the original differential equations controlling the transfer between boxes were replaced by:

$$\frac{dA_i}{dt} = \sum_{j=1}^{n} k_{ji}\, A_j - \sum_{j=1}^{n} k_{ij}\, A_i\, \gamma(t \geq T_j) - k_i\, A_i + Q_i \qquad \text{for } t \geq T_i$$

$$A_i = 0 \qquad \text{for } t < T_i$$

where γ is an unit function

$$\gamma(t \geq T_j) = \begin{cases} 1, & t \geq T_j \\ 0, & t < T_j \end{cases} .$$

The availability times, T_i,

$$T_i = \min_{\mu_m\,(\nu_0,\nu_i)\in M_i} \sum_{j,k} w_{jk}$$

were calculated as a minimised sum of the weights for all paths $\mu_m = (\nu_0, \nu_i)$ from the initial discharge box (ν_0) to the box i of the oriented graph $G = (V, E)$ with a set V of nodes ν_j corresponding to boxes and a set E of arcs e_{jk} corresponding to the possible transfer paths between boxes j and k. Every arc, e_{jk}, has a weight w_{jk} which is defined as the time required for the immediate transfer of radionuclides from box j to box k (without the intermediate boxes). The weight w_{jk} is considered as a discrete function of the water fluxes between boxes and is based on geographical information. M_i is a set of possible paths from the initial box (ν_0) to box i (ν_i).

In addition, elements of local/regional modelling were incorporated into the original model in order to improve its predictive capability and evaluate the contribution of specific locations (e.g., rivers, estuaries) to estimated doses (Iosjpe *et al.*, 1997).

9.2. Comparison between traditional box modelling and the improved version of the model

To illustrate the differences between traditional box modelling and the present approach, modelled ^{239}Pu concentrations in Arctic waters six months after an hypothetical 1 TBq (^{239}Pu) discharge into Obskaya Guba, as determined by the original and improved models, are shown in Figure 69. With the new version of the model, only boxes close to the discharge point are affected during the initial phase of dispersion. This is in contrast to the traditional approach, where distant boxes are affected immediately. Clearly, the output of the refined model gives a

more realistic description of radionuclide dispersion, leading to higher initial concentrations close to the source, and delayed effect in distant boxes.

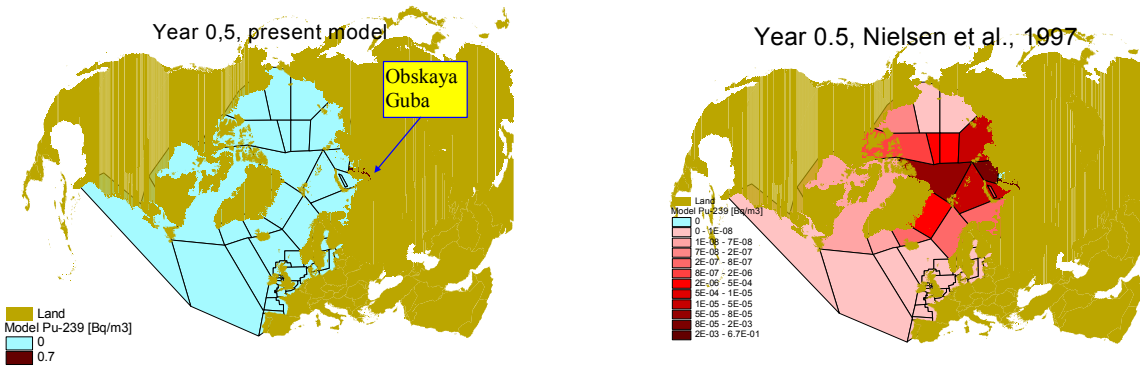

Figure 69. Estimated ^{239}Pu concentrations in Arctic waters six months after the release of 1 TBq (^{239}Pu) in Obskaya Guba. (Left) Improved model; (Right) original model

A comparison between modelled ^{239}Pu concentrations in waters of the Greenland Sea using both models is shown in Figure 70. Notice the significant differences during the initial phase of dispersion.

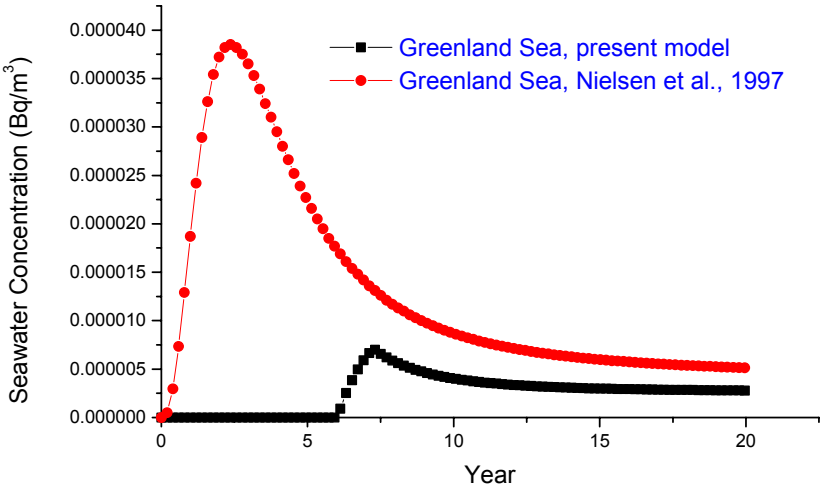

Figure 70. Comparison of modelled ^{239}Pu concentrations in the Greenland Sea following a release of 1 TBq (^{239}Pu) in Obskaya Guba

Calculations of world collective doses to man using the improved version of the model indicate significant differences in comparison with those obtained with the original version of the model. To illustrate, the ratios of calculated doses for a 1 TBq discharge of different radionuclides in different boxes are shown in Figure 71. The plots show that, for some radionuclides and scenarios, the differences in estimated dose can be up to an order of magnitude in the initial phase of dispersion. It is interesting to note that the higher radionuclide concentrations in the initial phase of the dispersion obtained with the refined model do not necessarily translate into higher estimated doses. A comparison of the long-term doses arising from a 1 TBq discharge of different radionuclides into Obskaya Guba, as determined by both versions of the model, are given in Tables 46 and 47.

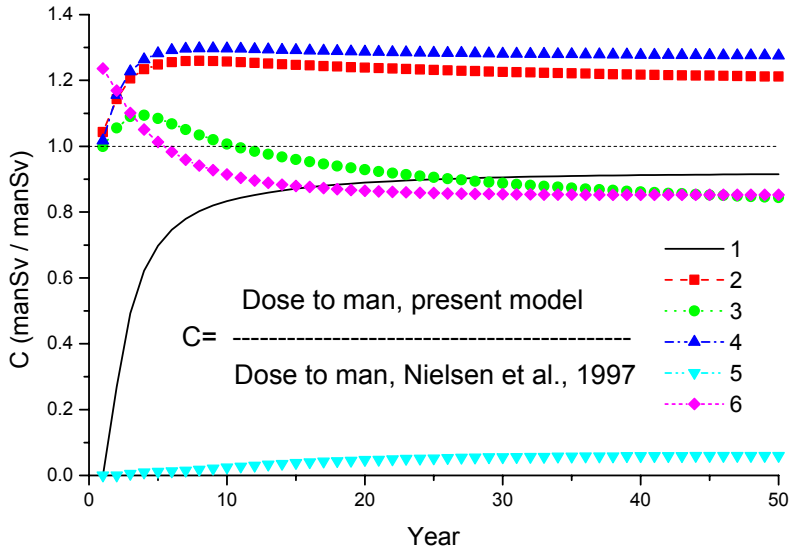

Figure 71. Comparison of doses to man calculated by the refined and original models for 1 TBq discharges to different boxes for some radionuclides: (1) Novaya Zemlya Bay, ^{137}Cs; (2) Barents Sea, ^{137}Cs; (3) Barents Sea, ^{239}Pu; (4) Cumbrian waters, ^{90}Sr; (5) Obskaya Guba without account of fisheries in this area, ^{60}Co; (6) Obskaya Guba with account of fisheries in this area, ^{60}Co

Table 46. Comparison of world collective doses (man-Sv) for 1000 years arising from 1 TBq discharges of radionuclides to the Barents Sea and Obskaya Guba. Scenarios 1 and 2 correspond to calculations without and with account being taken of the fisheries in Obskaya Guba, respectively. The scenarios with a * sign correspond to calculations with a high sedimentation rate in Obskaya Guba. Calculations for ^{236}Pu(III,IV) were carried out with a dynamic K_d value during the initial phase of the dispersion (see §6.5)

Radionuclide	**Scenario 1**		**Scenario 2**	
	Refined model	**Original model**	**Refined model**	**Original model**
^{60}Co	5.3×10^{-6}	8.8×10^{-5}	2.1×10^{-4}	2.4×10^{-4}
^{137}Cs	1.3×10^{-3}	1.8×10^{-3}	4.8×10^{-3}	4.3×10^{-3}
^{90}Sr	1.8×10^{-4}	2.2×10^{-4}	6.7×10^{-4}	5.5×10^{-4}
^{239}Pu	2.3×10^{-1}	4.3×10^{-1}	2.4×10^{-1}	4.4×10^{-1}
^{239}Pu	1.1×10^{-4}	9.5×10^{-3}	2.6×10^{-4}	9.6×10^{-3}
^{236}Pu(III,IV)*	4.2×10^{-9}	8.9×10^{-6}	2.2×10^{-5}	3.0×10^{-5}

Despite the differences between calculated doses using both versions of the model during the initial phase of the dispersion, results in Table 46 suggest good agreement between calculated world collective doses in the long term (1000 years). There are, however, important differences in the contribution of different sea areas (boxes) to the total dose, which arise from the assumption of non-instantaneous mixing of radionuclides in the improved version of the model. To illustrate, modelled ^{239}Pu water concentrations in the Labrador Sea using both versions of the model are shown in Figure 72. Note the effect of the availability time of 7 years imposed in the improved version of the model. For scenarios with a high sedimentation rate and radionuclides with high water–sediment distribution coefficients, a significant part of the initial discharge is removed from the water column by sedimentation and burial processes during the initial phase of the dispersion. This process is more significant for the improved version of the model (Figure 73).

Table 47. Comparison between the doses arising from a 1 TBq discharge in Obskaya Bay (Scenario 2) using the refined and original versions of the model. Doses are given in percent of collective dose

Region (Box)	Time (y)	Improved model [original model]					
		^{236}Pu(III,IV)	^{60}Co	^{90}Sr	^{137}Cs	^{239}Pu	^{239}Pu*
Labrador Sea (43)	1	0 [0.2]	0 [0.09]	0 [0.003]	0 [0.004]	0 [0.2]	0 [0.3]
	5	0 [5]	0 [3]	0 [0.3]	0 [0.4]	0 [8]	0 [10]
	10	0.0005 [9]	0.03 [6]	0.07 [1]	0.06 [1]	0.4 [21]	0.03 [22]
	50	0.003 [10]	0.5 [9]	2 [4]	2 [5]	21 [36]	2 [37]
Ob Estuary (141)	1000	0.003 [10]	0.5 [9]	3 [5]	3 [5]	16 [16]	7 [16]
	1	100 [95]	100 [96]	100 [99.5]	100 [99]	100 [96]	100 [95]
	5	100 [79]	99.6 [77]	96 [87]	95 [90]	98 [69]	99 [66]
	10	100 [72]	99 [69]	90 [82]	92 [82]	95 [48]	99 [46]
	50	100 [70]	98[63]	79 [66]	84 [66]	51 [17]	96 [15]
	1000	100 [70]	97 [63]	73 [60]	79 [60]	4 [1]	58 [0.02]

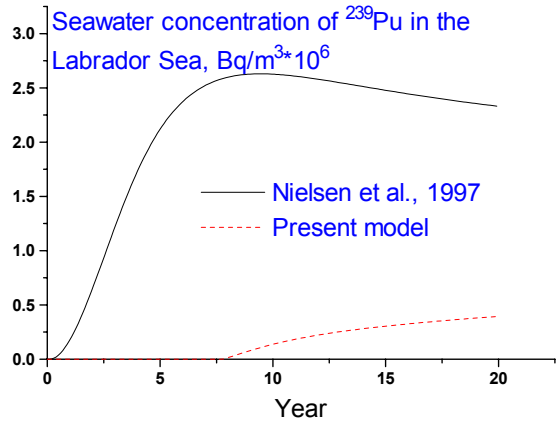

Figure 72. Comparison of ^{239}Pu sea water concentrations in the Labrador Sea arising from a 1 TBq discharge in Obskaya Guba as determined by the improved and original compartmental models

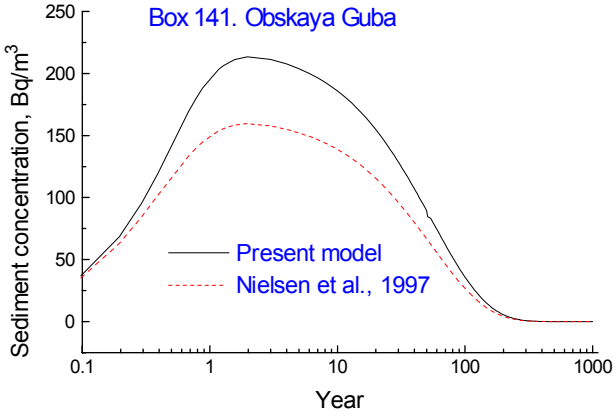

Figure 73. Comparison of ^{239}Pu concentrations in sediments from Obsaya Guba following a 1 TBq discharge as determined by the improved and original compartmental models

In summary, the modelling approach adopted keeps all features of traditional box modelling (the original model is a particular case of the improved version for which all availability times are zero), while providing a more realistic description of radionuclide dispersion.

9.3. Validation of the model

The compartmental model was validated by comparison with independent sets of data obtained in the course of the programme. As an example, a comparison between measured and modelled ^{99}Tc concentrations in Cumbrian waters (Box 75) is shown in Figure 74.

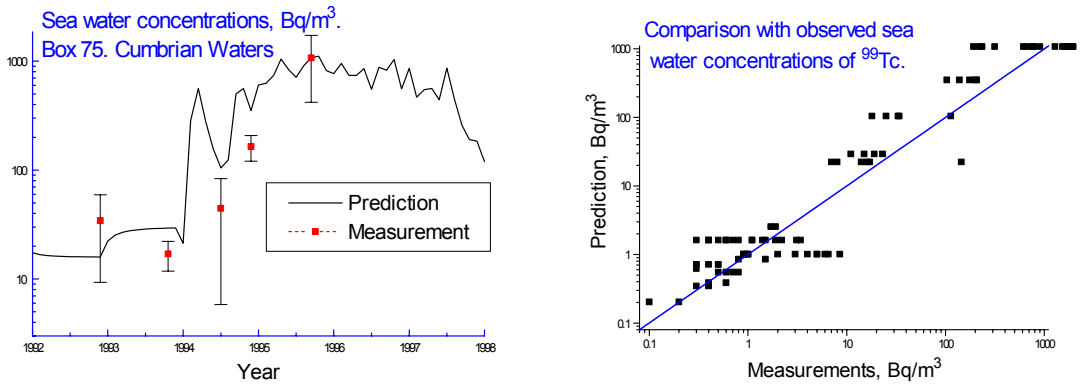

Figure 74. Comparison of measured and modelled ^{99}Tc concentrations in Cumbrian waters

9.4. Calculation of doses

The models described in the previous sections were used for the calculation of individual and collective doses to man from potential discharges of radioactivity from dumped nuclear waste in the Arctic Seas. The source terms considered were those defined by the EC/DG–XI Kara Sea project, and included reactors with spent nuclear fuel dumped by the former Soviet Union at Novaya Zemlya during 1965–81. The radionuclide inventories employed were estimated on the basis of the operational histories of the reactors. The rates of release were based on estimates of corrosion by sea water of the protective (steel) barrier containing the fuel. Releases were predicted to peak shortly after dumping due to corrosion of steel (^{55}Fe and ^{60}Co), and much later (around the year 3500) due to the delayed corrosion of the nuclear fuel (mainly transuranic elements).

A range of locations were considered for critical groups (Tsivolki Bay on Novaya Zemlya, Yamal Peninsula and Taymur coast in the Kara Sea, Kola Peninsula in the Barents Sea, northern Norway, Iceland and Alaska). The calculations included the following exposure pathways: ingestion of seafood (fish, crustaceans and molluscs), inhalation (seaspray and coastal sediment particles) and external exposure due to beach occupancy. The peak annual doses were found to be less than 1 μSv for all the critical groups. The annual dose rate to individuals from a critical group located in the western Kara Sea is shown in Figure 75. The break down of the maximum dose rates in years 1970 and 3700 by nuclide and exposure pathway are given in Figures 76 and 77, which show the percentage contributions to the maximum dose rates. The maximum annual dose occurs in year 1970 at a value of 2×10^{-8} Sv y^{-1}, with contributions from ^{55}Fe and ^{60}Co at 99.2% and 0.8%, respectively. Figure 77 shows that the dominating exposure pathways are the ingestion of fish for ^{55}Fe and external exposure for ^{60}Co. The overall pathway contributions to the maximum annual dose are ingestion of fish (52%), ingestion of molluscs (38%), ingestion of crustaceans (9%), external exposure (0.7%) and inhalation (0.005%). The peak annual dose in year 3700 has a value of 2×10^{-9} Sv y^{-1} and is dominated by the plutonium isotopes (Figure 78).

The pathway contributions to the latter peak annual dose are ingestion of molluscs (64%), inhalation (16%), ingestion of fish (11%), ingestion of crustaceans (9%) and external exposure (0.07%).

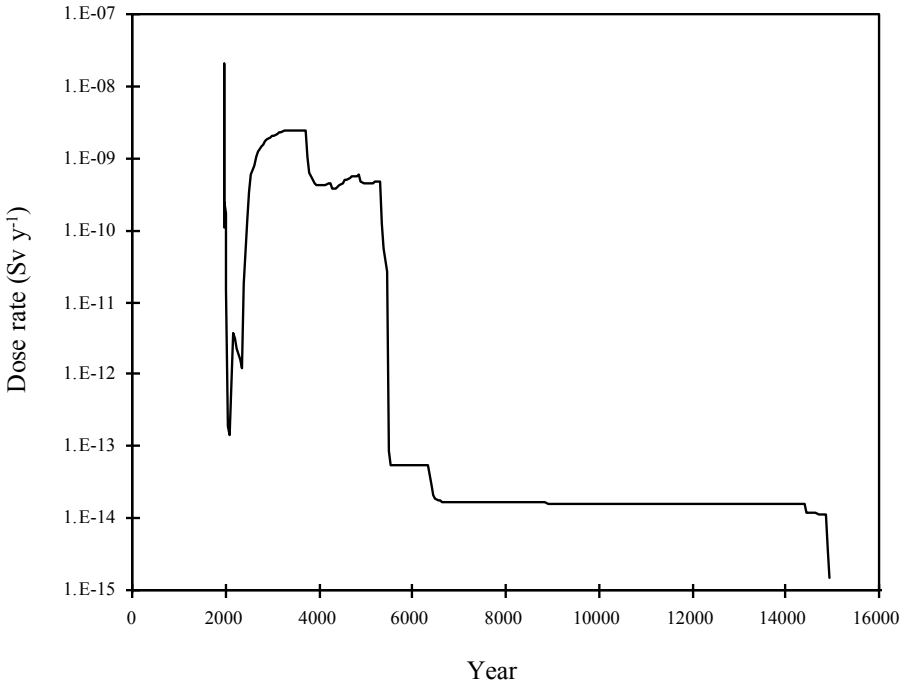

Figure 75. Annual dose to the critical group on the Yamal Peninsula, western Kara Sea (for the next 13000 years)

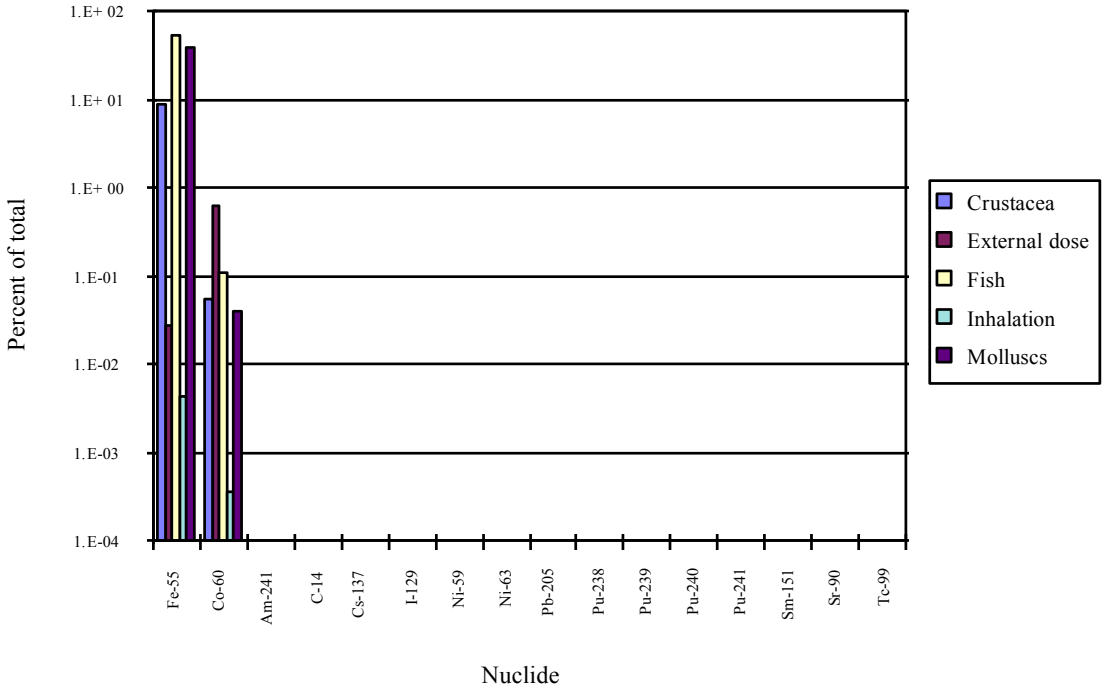

Figure 76. Relative contributions (percent) by nuclide and exposure pathway to the peak annual dose in the year 1970 to the critical group on the Yamal Peninsula

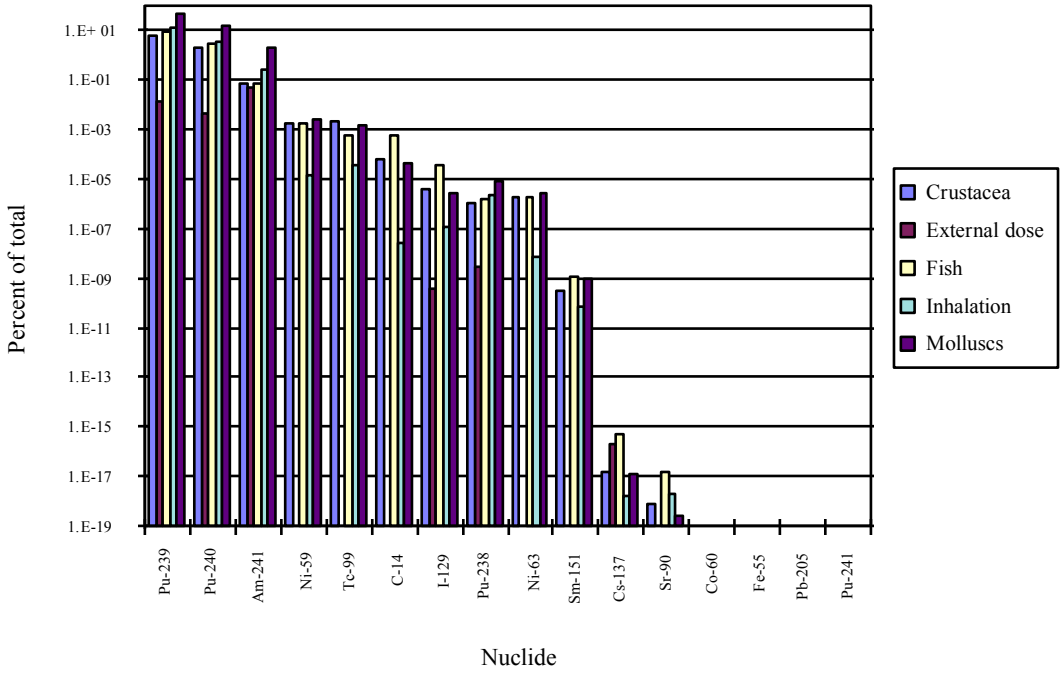

Figure 77. Relative contributions (percent) by nuclide and exposure pathway to the peak annual dose in the year 3700 to the critical group on the Yamal Peninsula

9.5. Parameter sensitivity analysis

The parameter sensitivity of the doses to individuals and populations was investigated with respect to three main processes: water movement and mixing, sediment–water interaction and biological transfer. For the hydrodynamic processes, four parameters were investigated, namely the advection and mixing between the Kara Sea and the Laptev Sea to the east, the advection and mixing between the Kara Sea and the Barents Sea to the west, the vertical mixing between surface and deep waters over the Novaya Zemlya Trough and the rates of exchange of water between the bays containing the dumped waste and the open Kara Sea. The sediment-related parameters considered were sedimentation rates, sediment distribution coefficients (K_d), suspended sediment loads, depth of the mixed surface sediment layer, and the mixing rates in the surface sediments. For the biological transfer processes, parameters representing biological concentration factors for fish, crustaceans and molluscs were included.

The parameter sensitivity analysis was carried out by assigning identical variabilities of 10% to all the above-mentioned parameters and running the model repeatedly (about 500 times). Correlation coefficients were calculated between parameter values and dose values, and the square of the correlation coefficients (r^2) were interpreted as a measure of how much of the variation in doses is accounted for by a linear relationship with the parameters in question. Parameter sensitivities are thus expressed in percent of the total variability.

The results of the parameter sensitivity analysis for the collective doses are shown in Table 48, which summarises the integrated releases (source term from IASAP Project), the collective doses and the main parameter sensitivities (>1%). The total collective dose is calculated to 0.4 man-Sv (truncated at 1000 y) with dominating contributions from plutonium isotopes (57%) and from ^{137}Cs (37%). The parameter sensitivities are seen to vary across the radionuclides from ^{90}Sr, which has a low K_d compared to the transuranics and activation products, which have higher K_ds. For the total collective dose, the main parameter sensitivities are due to sedimentation processes (sedimentation rate, K_d, suspended sediment load) and biological transfer processes (concentration factor for fish).

Table 48. Integrated releases (TBq), collective doses (man-Sv) and main parameter sensitivities

Nuclide	^{137}Cs	^{90}Sr	^{239}Pu	^{240}Pu	^{60}Co	^{241}Am	^{63}Ni	^{59}Ni
Total release (TBq)	49	42	6	2.4	3	0.5	480	150
Collective dose (man-Sv)	0.14	0.02	0.16	0.06	7E–05	0.001	0.002	0.001
Collective dose (%)	37	5	41	16	0.02	0.4	0.6	0.3
Sedimentation rate, (%)	19		66	66	54	61	53	53
Conc. Factor, fish (%)	65	90			13		4	4
K_d (%)	11		13	13	25	7	24	24
Susp. Sediment load, (%)			16	16	4	14	1	1
Conc. Factor, molluscs (%)			9	9		5	1	1
Advection, W. Kara Sea (%)	4	1					4	4

9.6. Parameter uncertainty analysis

Variabilities were assigned to the most sensitive parameters identified above. The variabilities take into account current observed variability and estimated future variability. The variabilities are expressed as ranges around the central values (c), so that for each parameter the same factor (f) determines the high value (c·f) and the low value (c/f). The factors of variability for the sediment related parameters were 2 for the sedimentation rate, 2 for the suspended sediment load and 10 for the sediment distribution coefficient, K_d. A factor of 3 was used for the variability of each of the biological concentration factors for fish, crustaceans and molluscs. A factor of 2 was used for the variability of the rate of exchange of the water between the Novaya Zemlya bays and the Kara Sea. Finally, a factor of 2 was used for variability of the depth of the surface sediment layer in the Novaya Zemlya bays. There was no specific information available on suitable probability distributions for the different parameter values, for which reason it was decided to sample (Monte Carlo technique) the values from log-uniform distributions with upper and lower values as specified above. The factors of variability were applied globally for each parameter across the model in each simulation. One hundred simulations were carried out for each model endpoint involving collective doses and doses to critical groups from the dominating nuclides (^{55}Fe, ^{60}Co, ^{137}Cs and ^{239}Pu) and source locations, in order to determine the ranges on the model output values. This number of simulations was considered adequate for the purpose, a decision confirmed by carrying out 500 simulations for one of the above combinations.

9.6.1. Uncertainties of maximum annual doses to critical groups

The results of the parameter uncertainty calculations on the peak annual doses to the critical groups are shown in graphical form in Figure 78. Correlation analysis was carried out using rank correlation coefficients to identify and quantify the main components of variability. Only correlation coefficients numerically greater than 0.5 are mentioned. The peak annual doses to the critical groups show negative correlation coefficients with the sediment distribution coefficients, K_ds, of –0.8 for ^{55}Fe and –0.6 for ^{239}Pu, while the sedimentation rates and the peak annual doses give negative correlation coefficients (–0.5) for both radionuclides. This means that high doses are associated with low values of the two parameters. Both radionuclides have high K_d values and are, therefore, particularly sensitive to sedimentation processes that transfer the radionuclides from the water column to the sediments and reduce the wider dispersion of the nuclides in the marine environment.

For the critical group located in Tsivolki Bay on Novaya Zemlya, the analysis yields different results due to the different exposure pathways that apply here. The peak annual dose from ^{60}Co shows a negative correlation coefficient of –0.8 with the depth of the surface sediment layer (mixing layer). This is due to the dominant exposure pathway, which in this case is external exposure from ^{60}Co in coastal sediments and in which the concentration is inversely related to the

depth of the mixing layer. The peak annual dose from ^{239}Pu shows a negative correlation coefficient of –0.7 with the bay flushing rate. In this case inhalation is the dominant exposure pathway (controlled by the concentration of ^{239}Pu in the waters of the bay) and the peak concentration is inversely related to the bay flushing rate.

The predicted variabilities of the peak annual doses to the critical groups around the mean values increase with distance from the Kara Sea. For the doses dominated by long-lived plutonium isotopes, the variability is nearly symmetrical around the mean value on a log-scale. The predicted variabilities on the doses from Pu-isotopes range from a factor of about 4 in Tsivolki Bay to a factor of about 40 in Norway. For the doses dominated by the short-lived isotope ^{55}Fe, the variability is non-symmetrical around the mean value on a log-scale due to the low values associated with delayed transfer and physical decay. The variabilities for ^{55}Fe of the maximum values relative to the mean values range from a factor of 6 in the Kara Sea to a factor of 10 in Norway, and the variabilities of the minimum values relative to the mean values range from a factor of about 80 in the Kara Sea to a factor of about 250 in Norway.

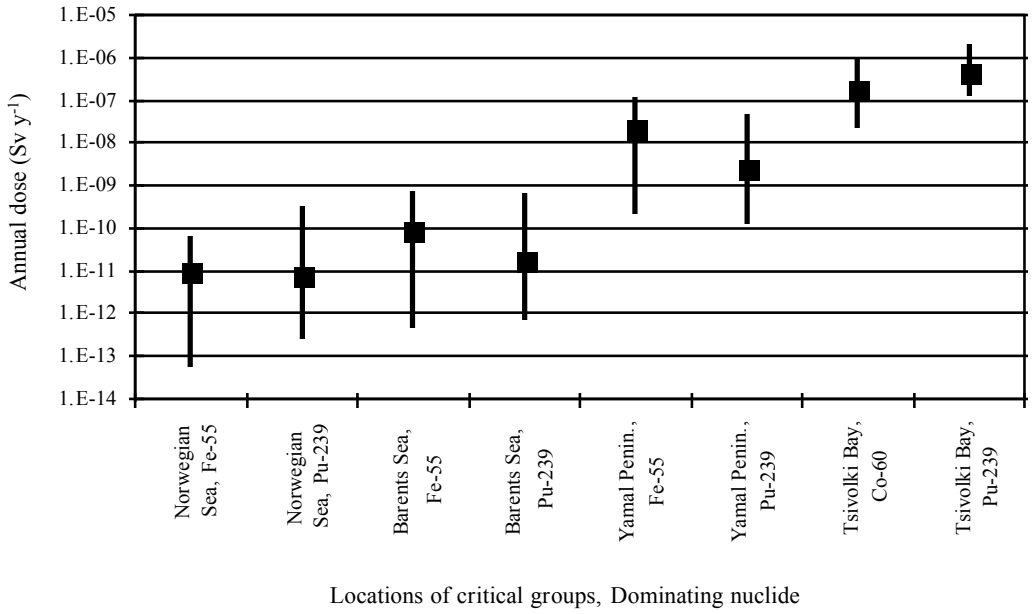

Figure 78. Peak annual doses to critical groups (Sv y^{-1}) with ranges of variability estimated from parameter uncertainty analysis

9.6.2. Uncertainties of collective doses

The predicted variability of the collective dose to the world population is based on the variability predicted for the plutonium isotopes. Correlation analysis shows that the collective dose is negatively correlated with the sediment related parameters, yielding a correlation coefficient of –0.7 for the sediment distribution coefficient and a correlation coefficient of –0.5 for the sedimentation rate.

The predicted variability of the collective dose is about two orders of magnitude up and down around the mean value of about 1 man-Sv. The collective dose is thus predicted at a level of about 1 man-Sv and not to exceed 100 man-Sv. The annual doses to individuals are significantly below the value of 10 μSv yr^{-1}, which is the lower dose limit considered to be of regulatory concern by both the IAEA and EURATOM.

9.7. Development of sub-models

Modelling efforts were also directed at the development of an ecological sub-model with a view to elucidating the behaviour of plutonium and other radionuclides in the lower levels of the marine food-chain. The conceptual basis of this sub-model, tested and calibrated using phytoplankton and zooplankton data from the Irish Sea (see §8.3), is shown in Figure 79.

The mathematical structure of the sub-model is based on the box-model formalism, where each compartment (or box) represents a functional unit of the real system. The radioactivity flows between compartments as a result of the different processes involved. Assuming first order kinetics, the time evolution of radionuclide concentrations in a particular box *i* is given by

$$\frac{dN_i}{dt} = \sum_{j \neq i} k_{j,i} N_j - \sum_{j \neq i} k_{i,j} N_i + F_i(t) - S_i(t) - \lambda N_i$$

where
- N_i = number of atoms in the i^{th} compartment at a given time.
- $k_{j,i}$ = transfer coefficient of matter from the j^{th} compartment to the i^{th} compartment (resulting in a positive flux).
- $k_{i,j}$ = transfer coefficient of matter from the i^{th} compartment to the j^{th} compartment (resulting in a negative flux).
- $F_i(t)$ = source term of the i^{th} compartment.
- $S_i(t)$ = sink of the i^{th} compartment.
- l = radionuclide decay constant.

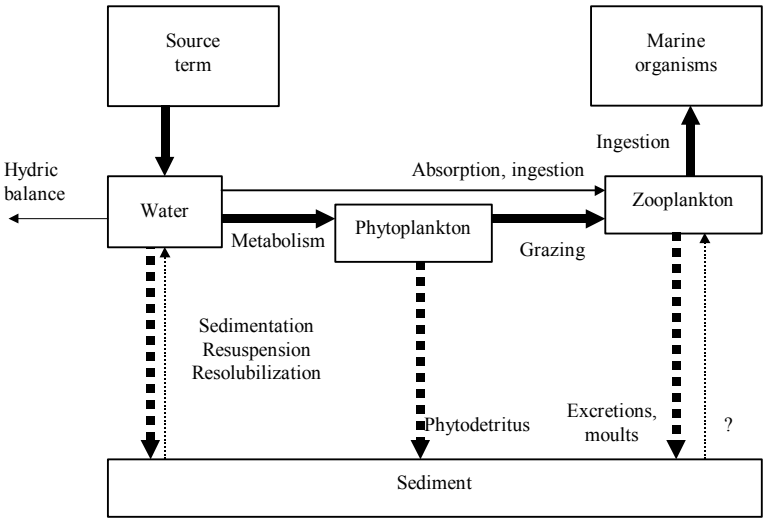

Figure 79. Conceptual model of the marine trophic chain in the Irish Sea

Transfer rates between compartments were defined by appropriate equations and realistic values for the parameters describing each process were obtained from values published in the literature. The model calibration was performed by varying these free parameters in order to predict measured ^{239,240}Pu concentrations in water, phytoplankton and zooplankton in the Irish Sea (§8.3) using the Sellafield ^{239,240}Pu discharge as the input source. The results of this exercise are presented in Table 49. Sensitivity analysis indicated that the most sensitive parameters of the model are the immobilisation time in sediments, the sedimentation rate, the fraction of phytoplankton biomass to the total suspended matter, the K_d, the transfer coefficient from water to phytoplankton, the particle uptake rate by zooplankton, the production rate of faecal pellets by zooplankton, and the enrichment factor of faecal pellets.

Table 49. Comparison between observed and predicted ^{239,240}Pu concentrations for 1994

	Observed mean value	Confidence interval of the mean	Predicted value
Concentration in water (Bq m^{-3})	1.0 ± 0.3[a]	[0.3, 1.7]	1.3
Concentration in phytoplankton (Bq kg^{-1})	57 ± 14	[21, 93]	84
Concentration in zooplankton (Bq kg^{-1})	59 ± 18	[11, 107]	54
CF in phytoplankton (m^3 kg^{-1})	78 ± 16	[34, 122]	65
CF in zooplankton (m^3 kg^{-1})	80 ± 19	[29, 131]	42
Sediment inventory (TBq)[b]	>320[d]		494
Annual hydrological loss (TBq y^{-1})[c]	1.3[d]		1.3

[a] Mean value in the CIR 6/94 campaign
[b] Values related to 1980
[c] Values related to 1992
[d] Cook *et al.*, 1997

Finally, the time evolution of mean plutonium concentrations in water, plankton and sediments were simulated assuming that releases will remain constant at present–day values. The results are shown in Figure 80. Plankton concentrations followed closely water concentrations (and therefore Sellafield releases) in the 1960s and 1970s. As already discussed, during the 1980s and 1990s, sediments started to act as a source of radioactivity to the overlying sea water. As a consequence, plankton concentrations have remained at a rather constant level since then, and are predicted to do so in the future. It must be emphasised that these predictions only represent an average of the behaviour of plutonium in the whole Irish Sea.

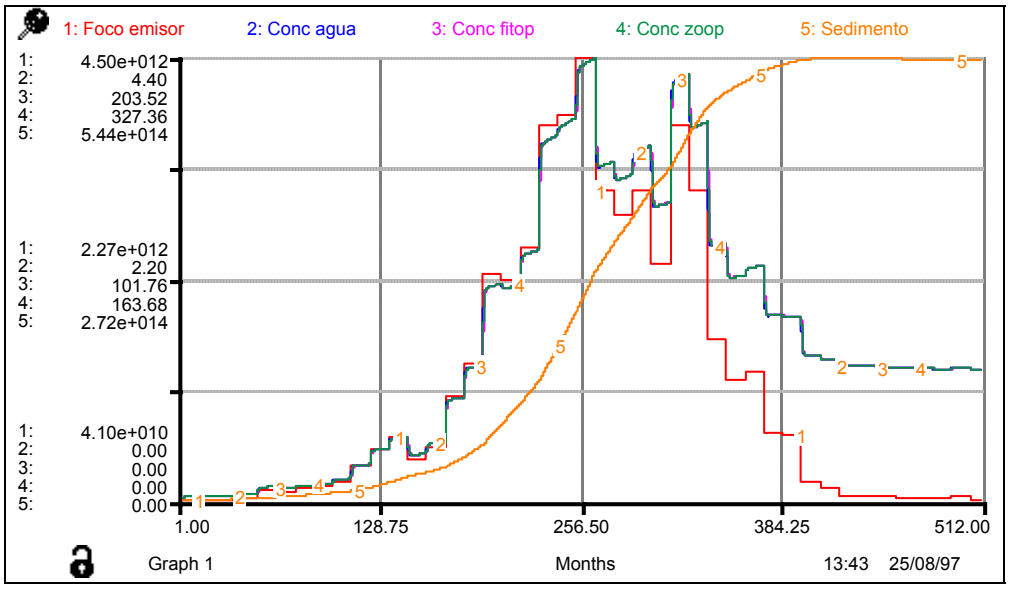

Figure 80. Simulation of the time evolution of ^{239,240}Pu mean sea water and plankton concentrations and sediment inventory in the Irish Sea

10. Publication of results and archiving of data

No serious programme of research can be considered complete without the widest possible dissemination of the research findings and results, as well as the archiving of all raw and derived data acquired during the project in a readily accessible database. Throughout the ARMARA programme, the participants took the necessary steps to ensure that the results were published in the open, refereed, scientific literature and promulgated at appropriate symposia and conferences. As evidenced by the many individual and joint publications listed in Appendix A below, this important process of publication has been actively and systematically pursued by the members of the collaboration. We count at least 30 joint publications and over 80 individual publications relating directly or indirectly to the Arctic, which have either been published by the ARMARA groupor have been accepted for publication.

Further, the collaboration was strongly represented in the programmes of two international symposia on *Radionuclides in the Oceans* held at Cherbourg (RADOC–1; October 1996) and Norwich (RADOC–2; April 1997), and an international symposium on *Marine Pollution* held at Monaco (October 1998), as well as at the *Third International Conference on Environmental Radioactivity in the Arctic*, held at Tromsø in June 1997, where an overview of the ARMARA project was presented. More recently, at the *Fourth International Conference on Environmental Radioactivity in the Arctic* held at Edinburgh in September 1999, a full session was dedicated to the dissemination of the results of the ARMARA programme to the scientific community.

The publications referred to above have been complemented by the annual and mid-term reports submitted to the Commission, which described the operations and progress of the ARMARA group, backed-up by annual reports from the individual laboratories, research expedition reports, tec-docs on modelling and analytical techniques, and articles in other more general publications, including in-house magazines and national newspapers.

11. Summary of main achievements

The main achievements of the ARMARA group can be summarised conveniently under the following headings: the planning and successful execution of major collaborative field campaigns in the Central Arctic Ocean and surrounding shelf seas (including Svalbard and Thule), supported by campaigns of more limited scope in other marine and estuarine zones considered relevant in the context of Arctic studies; laboratory-based experiments to simulate various mechanisms of key importance from the radioecological perspective; laboratory-based analyses of a wide range of environmental samples (e.g., sea water, suspended particulate, shelf and ocean sediments, biota of various description, etc.) for their radionuclide content, with emphasis on those nuclides of greatest radiological significance in the intermediate- to long-term; group endeavours to achieve high standards in quality assurance and quality control, as well as standardisation in certain types of analyses; identification and quantification for modelling purposes of key parameters controlling radionuclide behaviour under extreme conditions, including the use of state-of-the-art techniques to examine radionuclide speciation *in situ*; re-evaluation of the conceptual basis of an advanced compartmental model for use in the Arctic, refinement and calibration of same, and application to the determination of long-term doses to individuals and critical groups within Arctic populations; and publication and, finally, dissemination of the results of these studies and dose projections.

11.1. Field operations in the Arctic and other marine/estuarine zones

Eight major expeditions in Arctic waters were undertaken by the ARMARA group during the 1996–99 campaigning seasons. This was a splendid achievement as it required the most careful advanced planning on both the logistic and scientific fronts. Intensive and physically demanding operations were carried out in this remote and hostile environment, which involved extensive environmental sampling, *in situ* radiochemistry and a variety of other onboard experiments. In each case the campaigns were designed to satisfy the most pressing needs of the modellers by filling gaps in the existing Arctic database (e.g., the absence of concentration values for specific boxes and compartments, uncertainties in the values of key parameters such as sediment-water distribution coefficients, transfer coefficients, poorly understood mechanisms, etc.).

Attainment of most of the key objectives of the ARMARA project was predicated on the success of expeditions such as these. It is, therefore, gratifying to report that each of these expeditions was extremely successful, having achieved all their main objectives. None of this would have been possible without the goodwill and the generosity of those institutions which have provided berths and facilities for our people aboard the research vessels involved. We can but express our gratitude.

For the record, the major expeditions undertaken in the Arctic in the course of the programme were: • F.S. *Polarstern*, Central Arctic Ocean (July–September 1996); • I.B. *Oden,* Central Arctic Ocean (July–September 1996); • R.V. *Håkon Mosby*, Svalbard zone (August 1996); • F.S. *Adolf Jensen*, North-west Greenland, including Thule (August 1997); • R.V. *Håkon Mosby*, Svalbard zone (August 1997); • R.V. *Håkon Mosby*, Svalbard zone (September 1998); • Svalbard zone, land-based (winter 1998); • Svalbard zone, land based (winter 1999). In addition, a number of related joint operations took place in non-Arctic regions, including the estuaries of the Seine and the Rhône, the details of which are given elsewhere in this report. Suffice that the studies undertaken in these estuaries have provided important insight into the mechanisms at play in the fresh water/sea water interface, mechanisms which, by virtue of their universal character, are also operative in Arctic estuaries.

All of the major campaigns referred to above have produced a wealth of new data on radionuclide levels across the full spectrum of marine compartments in the Arctic, as well as on key mechanisms controlling the transfer of radionuclides between compartments. This accomplishment should be recognised as a major achievement of the ARMARA programme.

11.2. Laboratory-based experiments and simulations

Laboratory experiments were carried out to examine the influence of speciation and solid partition of radiocaesium on biological uptake. Both filtering and non-filtering organisms were exposed to ^{134}Cs in ionic and particulate form and the results show that in both cases there are clear differences in the initial concentration factors for both forms. Other experiments were carried out to study the behaviour of ^{137}Cs and ^{90}Sr in riverine sediments when these sediments come in contact with sea water; these have demonstrated a pronounced desorption in the case of both nuclides, leading to enhanced levels in the dissolved phase. Similar experiments with contaminated marine sediments from the Irish Sea showed an initial rapid desorption, probably of a labile form of caesium, followed by a much slower desorption of caesium tightly bound to inter-lattice sites.

Separate experiments were also carried out to examine the effects of two key environmental variables (light and temperature) upon the sorption/desorption behaviour of $^{239,240}Pu$ and ^{241}Am. These indicate that the rate and extent of Pu(V) remobilisation from, and uptake of dissolved Pu(V) by, suspended particulate matter are concurrently enhanced by increases in temperature and light irradiation. On the other hand, the behaviour of Pu(IV) and ^{241}Am appears to be largely unaffected by these parameters. Thus, in the natural environment, processes other than surface chemistry may be equally important in governing the rate and extent of remobilisation.

Other important experiments by members of the group have highlighted the need to adopt the most stringent precautions when investigating radionuclide solid partitioning in anoxic sediments. For example, it has been shown how artifacts introduced during chemical leaching procedures following contact with air can seriously distort the results of such experiments.

11.3. Laboratory-based analyses of Arctic samples

Collectively, the group committed very significant human and financial resources to the analysis of a wide range of environmental samples from the Arctic in order to develop a comprehensive database for the modellers. Some of this material was retrieved from sample banks assembled by members of the present collaboration following expeditions to the Arctic in 1994 and 1995. Although a considerable number of these analyses can be carried out using non-destructive techniques (i.e., gamma spectrometry), a large number can only be processed with the aid of radiochemistry. In the case of radionuclides such as ^{90}Sr, ^{99}Tc and the transuranics, this requires particular expertise and dedication, not least because these nuclides are present in extremely low concentrations in the Arctic. All of the laboratories in the collaboration participated actively in this work and it is satisfying to report that the analysis of the samples painstakingly collected in the course of the above-mentioned campaigns has resulted in a significant expansion of the existing Arctic database, particularly for nuclides such as ^{99}Tc and the transuranics, where existing information prior to the commencement of this programme was scarce.

11.4. Quality assurance and quality control

The group achieved considerable standardisation in the analytical procedures employed by the participating laboratories. For example, agreed (and sometimes complementary) procedures were used to separate plutonium, technetium, strontium, etc. from sea water, while internationally-accepted techniques were used to study the physico-chemical speciation (including solid partitioning) of a number of radionuclides. Moreover, the group undertook the analysis of a large water sample from the North Sea for internal intercomparison purposes. The agreement between the results submitted by the participants was considered to be very satisfactory, demonstrating that the data reported by collaborating laboratories within the framework of the ARMARA project are consistent and that an appropriate level of intra-laboratory quality control is in place.

11.5. Determination of key parameters controlling radionuclide behaviour under extreme conditions

In the course of the programme, site-specific values for a large number of key parameters were determined. These included sediment–water distribution coefficients, concentration factors for phytoplankton, zooplankton, invertebrates, fish, sea birds and mammals, radionuclide residence times and scavenging rates in the water column, sedimentation and mixing rates, etc. The results obtained were compared with representative parameter values from other marine zones and, where possible, with values for the Arctic in the rather scant literature that existed prior to this project. The partition of various radionuclides between the solid and dissolved phases (including the colloidal phase) in both shelf and Central Arctic waters was examined in detail, as was the chemical speciation of strontium and plutonium. This was the first occasion on which such chemical speciation studies had been conducted in an Arctic environment.

11.6. Modelling and dose prediction

The above data on transfer processes in the Arctic were incorporated into the RISØ–NRPA model and the model was run in order to estimate doses to man from the source terms defined in the EC/DGXI Kara Sea project. A refined version of the model was also developed which, while maintaining a box structure with uniform mixing in all boxes, also includes the dispersion of radionuclides over time. Comparison of the calculations based on the more traditional approach with those obtained using the refined version showed that the latter gives a more realistic description of the dispersion of radionuclides within boxes. Results obtained by the new version of the model yield radionuclide concentrations which are up to an order of magnitude higher in the initial phase of dispersion than those obtained using traditional modelling. Calculations of world collective doses to man indicate significant local differences (up to 30%) in comparison with the original model. It is interesting to note that the higher radionuclide concentrations in the initial phase of the dispersion obtained with the refined model do not necessarily translate into higher estimated doses.

Our models predict that the collective dose (truncated at 10000 years) to the world population will be in the order of 1 man-Sv. The parameter sensitivity of the doses to individuals and populations was investigated with respect to the following processes: water movement and mixing, sediment–water interaction, and biological transfer, all of which were represented in the model by appropriate parameter values (the best currently available). The parameter sensitivity analysis was carried out by assigning identical variabilities of 10% to all of these parameters and running the model repeatedly. The results of the parameter sensitivity analysis for the collective doses are summarised in Table 48 (§ 9.6). Suffice, that for the total collective dose, the main parameter sensitivities were shown to be due to sedimentation processes (i.e., sedimentation rate, K_d, suspended sediment load) and biological transfer processes (i.e., concentration factors). Accordingly, determination of site-specific values for these parameters constituted one of the main objectives of the experimental work.

The models were also run to test the uncertainty in dose estimation arising from variability in parameter values. Correlation analysis was carried out using rank correlation coefficients to identify and quantify the main components of variability. It was found that the peak annual doses to the critical groups show significant negative correlation coefficients with the sediment distribution coefficients for ^{55}Fe and ^{239}Pu, while the sedimentation rates and the peak annual doses give negative correlation coefficients for both radionuclides. This means that high doses are associated with low values of the two parameters. Both radionuclides have high K_d values and are, therefore, particularly sensitive to sedimentation processes that transfer the radionuclides from the water column to the sediments and reduce the wider dispersion of the nuclides in the marine environment.

11.7. Publication and dissemination of data and results

As previously mentioned, the group was committed to the necessary actions to ensure the widest possible dissemination of its findings and conclusions, and the archiving of all raw and derived data acquired during the project. To this end, we can report at least 30 joint publications and over 80 individual publications based on the results of studies within the framework of the ARMARA project. Members of the group also took every opportunity to present aspects of the work at various international conferences and symposia, the details of which are given in §10. These publications and presentations on the group's Arctic studies have been underpinned by a series of annual reports from the individual laboratories, research expedition reports, tec-docs on modelling and analytical techniques, articles in other more general publications and a limited number of technical brochures, all of which have been well ventilated within the collaboration as well as circulated to other interested parties. Regarding the archiving of data, the group has agreed that all data will be submitted to the NRPA, after an appropriate period, for inclusion in the AMAP database. This, it is felt, is the most satisfactory way to preserve the data for future use by the widest possible scientific constituency.

12. Conclusions and recommendations

12.1. Conclusions

The following main conclusions are based on knowledge gained in each of the above work packages in the course of the programme:

12.1.1. Radionuclide distributions

- Present anthropogenic radionuclide concentrations in the Arctic Seas are dominated by three main sources, namely (i) fallout from nuclear weapons testing, riverine discharges and land run-off of radionuclides originating from global fallout; (ii) marine transport of radionuclides discharged from European reprocessing plants; and (iii) fallout from the Chernobyl accident and run-off from land areas contaminated by this accident.
- The distributions of the most radiologically-important nuclides (^{90}Sr, ^{99}Tc, ^{137}Cs, ^{239,240}Pu) reflect the evolution of the above-mentioned source-terms when coupled to water circulation patterns and transport processes.
- ^{137}Cs and ^{90}Sr distributions clearly reflect the effect of decreasing reprocessing, Chernobyl and run-off inputs since the mid–1970s, while the increase in reprocessed ^{129}I is reflected by the observed decrease in ^{129}I levels along the shelf. The observed radionuclide distribution patterns and measured radionuclide ratios are consistent with the transport of radioactivity from the Barents Sea along the Eurasian shelf and into the Central Arctic along the Lomonosov Ridge towards the North Pole (with the Transpolar Drift). Transfer estimates for conservative nuclides from the European shelf (Sellafield) to the Central Arctic yielded values of 5–7 years to the SE Barents Sea, 7–9 years to the Kara Sea, 10–11 years to the Laptev Sea and 12–14 years to the Central Arctic Ocean.
- Measured ^{239,240}Pu (and ^{238}Pu) concentrations in surface and sub-surface sea water samples throughout the Central Arctic and the Arctic shelf seas are extremely low, being in the range 2.0–20 mBq m^{-3}. Along the shelf, ^{239,240}Pu concentrations show a general decrease in an easterly direction, which can be attributed primarily to losses to sediment along the shallow Eurasian shelf. Along the Lomonosov Ridge, ^{239,240}Pu concentrations show a clear trend of increasing concentrations towards the North Pole (and beyond, into the Amundsen Basin). This broad pulse in ^{239,240}Pu concentrations is largely attributable to the comparatively high levels of nuclear fallout that labelled mid-latitude waters in the North Atlantic in the early– to mid–1960s, when the testing of nuclear weapons in the atmosphere was at a peak.
- Excluded from the general eastward decrease of ^{239,240}Pu concentrations along the shelf are the seasonally high values observed in the mouths of the Ob, Yenisey and Lena rivers, which correspond to periods of maximum river flow. The higher ^{239,240}Pu concentrations are not accompanied by a concomitant increase in ^{137}Cs and ^{90}Sr concentrations. The observed isotopic ratios point to a different source of plutonium to global fallout, such as close fallout from nuclear explosions, debris from safety shots or unfissioned nuclear weapon material. Despite these (seasonal) higher ^{239,240}Pu concentrations, the effect of these discharges on shelf water concentrations is quite small.
- To date, there is no evidence that anthropogenic radionuclide concentrations in general Arctic waters are elevated as a result of dumping practices by the former Soviet Union. Although enhanced radionuclide levels have been detected at specific locations (e.g., Kola Bay) or near dumped objects, the impact of these releases and the contribution to present radionuclide concentrations appear to be negligible. This is supported by the observations in Thule (Greenland), where 30 years after an accident involving the dispersion of weapons-

grade plutonium over the seabed, there is no evidence of any significant remobilisation of the deposited inventory into the water column.

12.1.2. Radionuclide speciation

- Measurements on the chemical speciation of plutonium and its physical partitioning between dissolved and solid phases in Arctic waters suggest that, under field conditions, at least after long equilibration periods, the physico–chemical speciation of plutonium is rather similar to that observed in more temperate environments. Specifically, the oxidation–state distribution of plutonium between oxidised and reduced species, the proportion of plutonium associated to suspended particulate matter and the sediment–water distribution coefficient (K_d) is within the ranges reported for North Atlantic, Irish Sea or western Mediterranean waters.
- Analyses carried out in order to determine the extent and size fractionation of colloidal plutonium in Arctic surface waters reveal that in the Laptev Sea and the Lomonosov Ridge, a significant fraction (24 ± 9%; n = 5) of the plutonium in the operationally-defined dissolved phase is actually in a colloidal form. In contrast, no retention is observed in the Kara Sea continental shelf or at Thule (Greenland). As the colloidal particles/aggregates involved appear to be of high molecular weight, it is not unreasonable to suggest that some of this colloidal matter may be of riverine origin. If this is the case, riverine colloidal material could play an important role in the transport of particle-reactive contaminants from the shelves to the Arctic interior.
- Experiments conducted at the fresh water/sea water interface (Seine Estuary, France) confirm the non-conservative behaviour of plutonium under estuarine conditions, with low-salinity waters being substantially enriched in plutonium and intermediate-salinity waters being depleted in plutonium relative to the theoretical dilution line. The partitioning of plutonium between colloidal and dissolved phases in the micro-filtered (<0.45 μm) fraction along the salinity gradient shows that while dissolved plutonium is progressively removed towards lower salinities as a result of dilution and removal by particles, the colloidal component increases at low salinities, being responsible for most of the observed plutonium excess at these low salinities.

12.1.3. Scavenging and sedimentation processes

- Data based on the disequilibrium between ^{238}U and ^{234}Th in the water column of the W-Spitsbergen coastal environment (fjords and continental shelf) have provided accurate values for scavenging rates and residence times of particles in this area. Our results indicate that scavenging processes are more intense in fjords than on the continental shelf. In the upper 60 m of the water column, the residence time for dissolved thorium is estimated to be 10–20 days in fjord areas and 60–100 days on the shelf and open sea. This is related to the presence in fjord area (during the summer) of considerable amounts of terrigenous particles originating from ice melt. On the shelf and in open sea, scavenging of dissolved thorium is mainly related to the cycling of biogenic particles in the photic zone. Once thorium becomes associated to particles, its residence time in the water is much shorter, 5–10 days in the fjords and 15–30 days in the shelf and open water.
- Radionuclide deposition inventories in the Kara, Laptev and East Siberian Seas are estimated to be in the range 100–800 Bq m^{-2} and 5–35 Bq m^{-2} for ^{137}Cs and $^{239,240}Pu$, respectively. In contrast, the corresponding figures for the Central Arctic Ocean are much smaller, at 15–100 Bq m^{-2} and 0.2–1.3 Bq m^{-2}, respectively. The larger deposition on the shelf reflects the higher sedimentation rates prevailing in these shallow zones. Comparison of sediment column inventories with time-integrated water column inventories estimated from reported sea water profiles indicate that approximately 10% of the ^{137}Cs and 75% of the $^{239,240}Pu$ which have entered the shelf seas have been deposited on the shelf sediment, while the

corresponding figures in the Central Arctic are 0.3% and 0.9%. These figures indicate that while the Arctic shelf acts as a sink for particle-reactive elements, only a very small fraction of the total inventory is deposited on the sea-floor of the Central Arctic during the time it takes the water to pass through the basin.

12.1.4. Remobilisation and post-depositional behaviour of radionuclides

- Laboratory experiments have shown that a significant desorption of both ^{90}Sr and ^{137}Cs can take place upon contact of contaminated estuarine sediments with sea water, with sediment–water distribution coefficients (K_ds) decreasing by factors of ~50 and ~100 for ^{90}Sr and ^{137}Cs, respectively.
- Information and data obtained from our laboratory studies indicate that the rate and extent of Pu(V) remobilisation from, and uptake of dissolved Pu(V) by, suspended particulate/sediment are concurrently enhanced by increases in temperature and light irradiation. The behaviour of ^{137}Cs and ^{241}Am appear to be largely unaffected by these parameters. In the environment, processes other than surface chemical reactions may be equally important in governing the rate and extent of remobilisation/uptake. These include diffusion of radionuclides from pore waters into the overlying water column, physical resuspension of contaminated sediment and biological mixing. Physical resuspension processes are enhanced during storms, which are episodic events whose frequency is likely to be greatest in the winter. Conversely, the rate of chemical reactions at the particle surface are likely to be least during this season because of low water temperature and light irradiation.
- Laboratory experiments have demonstrated the importance of the nature of the mileau (oxic/anoxic) in the solid speciation and sorption/desorption behaviour of radionuclides associated to anoxic sediments. They have also highlighted the need to adopt the most stringent precautions when applying any chemical leaching technique to anoxic sediments or when extrapolating results from radionuclide post-depositional behaviour under laboratory conditions to environmental systems.
- Sequential leaching experiment in oxic and anoxic sediments have indicated that plutonium and americium are associated to stable phases, with little if any of the transuranium inventory in a readily available, exchangeable form.

12.1.5. Transfer processes to living species

- The large number of *in situ* concentration factors for Arctic plankton, invertebrates, fish, sea birds and mammals obtained in the course of the programme, and the comparison of the resulting data with those obtained in other more temperate environments or with recommended values in the published literature, highlights the need for carrying out site specific determinations for dose estimation purposes. This is particularly the case for the Arctic, where the trophic structure and the extreme conditions under which organisms grow differ dramatically from those in other regions.

12.1.6. Modelling and prediction of the likely consequences of Arctic contamination

- A new compartmental model covering the Arctic and North Atlantic regions has been developed in the course of the programme for the assessment of the short- and long-term consequences of past and potential radionuclide releases of radioactivity to the Arctic. The improved model, while maintaining the assumption of uniform mixing in all boxes, also includes the dispersion of radionuclides with time. This is in contrast to the original model, which essentially required that radionuclides be instantaneously dispersed through the whole modelling space.

- The new modelling approach adopted here retains all the features of traditional box modelling, while providing a more realistic description of radionuclide dispersion. This is important.
- In addition, elements of local/regional modelling have been incorporated in order to improve its predictive capability and evaluate the contribution of specific locations (e.g., rivers, estuaries) to estimated doses.
- Comparison of the new version of the model with the original version indicate significant differences in estimated doses during the initial phase of dispersion.
- Sensitivity analysis show that the main parameter sensitivities are due to sedimentation processes (i.e., sedimentation rate, K_d, suspended sediment load) and biological transfer processes (i.e., concentration factors).
- The models have been used to estimate individual and collective doses to man from potential discharges of radioactivity from dumped nuclear waste in the Arctic Seas by the former Soviet Union. The models predict a collective dose in the order of 1 man-Sv. Given the uncertainty in the parameters, the predicted variability in the collective dose is about two orders of magnitude up and down on this value. The collective dose is thus predicted at a level of about 1 man-Sv and not to exceed 100 man-Sv. The resulting annual doses to individual members of the public (even for those in critical groups) are significantly below the value of 10 $\mu Sv\ yr^{-1}$, which is the lower dose limit considered to be of regulatory concern by both the IAEA and EURATOM. These potential doses are also significantly below those arising from natural radioactivity in the Arctic.
- The potential health risks associated with the consumption of Arctic seafood containing radionuclides derived from hypothetical releases from dumped waste by the former Soviet Union are negligible, and do not pose any threat to the Arctic population and, by extention, to populations further afield.

12.2. Recommendations

12.2.1. Radioactive waste dumping

- The practice of dumping radioactive material in the Barents and Kara Sea by the former Soviet Union, which triggered international concerns in the early 1990s, has now ceased, so there is no practical need to recommend its discontinuance. Although one of the main conclusions to be extracted from the experimental and modelling work carried out in the course of the ARMARA programme is that the potential radioecological risks to human and marine life arising from the dumping of these radioactive materials are very small, it is the view of the collaboration that such practice is highly undesirable and that any attempt to renew the practice should be strenuously opposed by the European Commission at international level.
- The collaboration does not consider justifiable or practical at this stage to attempt remediation measures in the case of radiactive material dumped in the Kara and Barents Seas. Such retrieval is likely to be problematic, given the large number of items (including nuclear reactors, vessels, barges and containers) spread over a relatively large area. The radiological hazards associated with the deliberate movement of dumped material are likely to be greater than those estimated were no action to be taken.

12.2.2. Monitoring

- Although the Arctic radioactivity database has been expanded very considerably as a direct result of the ARMARA programme, the group recognises the value of ongoing monitoring programmes by northern countries and would encourage their continuation as a valuable tool

of surveillance and detection of potential releases from dumped materials and nuclear installations.

- To maximise the efficacy of these monitoring programmes, the group recommends the development of an harmonised monitoring system to allow for an effective assessment of human exposure pathways and resulting doses. This would require a critical review of present monitoring programmes and a possible expansion on the type of samples analysed.

12.2.3. Research

- As highlighted by the findings of this programme, future research in the Arctic should focus on the determination of site-specificic values for the more sensitive parameters for modelling purposes (K_d values, sedimentation rates, concentration factors, etc.). Determination of radionuclide concentrations in marine biota should be accompanied by concurrent sea water/sediment measurements in order to improve the accuracy and site-specificity of calculated concentration values.
- Remobilisation of radionuclides from historically-contaminated sediments has been shown to play an important role in the rate of dispersion and ultimate fate of particle-reactive radionuclides. The complex dynamics of remobilisation processes and the influence of environmental conditions on these processes warrant further high-quality research.
- The contributions of global fallout, discharges from European reprocessing plants and Chernobyl fallout to present concentrations in Arctic waters are now well understood. It is, however, appropriate to flag that the role of the large Siberian rivers is not yet fully clarified. Although it is clear that they are acting as an important source of water, sediment and organic matter, their significance as a source of anthropogenic radionuclides has not been fully quantified. The former Soviet Union's nuclear programme has been operating for the last 50 years, with most of its facilities in the western Siberian Basin. These nuclear facilities include three major reprocessing plants (Mayak, Tomsk-7 and Zheleznogorsk), which represent the main source of radioactive contamination to the Ob and Yenisey rivers, feeding into the Arctic Ocean through the Kara Sea. Clearly, it is desirable that field investigations be carried out in order to determine actual radionuclide fluxes from these sources and to establish the fate of these radionuclides at the freshwater/sea water interface under Arctic conditions. The first action must be achieved at a political level, given the present reluctance of the Russian authorities to permit access to these important zones.
- Further research should be carried out on the dietary habits of Arctic populations in order to enable more precise estimates of radiological exposures and associated health risks.

12.2.4. Modelling

- The new compartmental modelling approach adopted in the course of the programme has proved to give a better representation of the dispersion of radionuclides upon release to the marine environment and yields more accurate dose estimates, particularly in the initial phase of the dispersion. It is thus recommended that this approach be employed for future radiological assessments of the impact of radionuclide releases in the marine environment.
- As recommended by the Arctic Nuclear Waste Assessment Program (ANWAP), collaboration between assessment modellers and scientific groups developing ocean circulation models or performing tracer studies should be fostered and encouraged. The various groups involved in Arctic contamination research should continue to work together in order to provide the most efficient integration of experimental data and results into the modelling, not least for calibration and validation purposes.

12.2.5. Potential risks

- The greatest threat to the Arctic marine environment is associated with potential releases from decommissioned nuclear submarines moored in NW Russia, nuclear-powered ice-breakers and the large amounts of spent fuel and liquid radioactive wastes stored in floating vessels under poor conditions. Other potential sources include accidental releases from nuclear plants and reprocessing facilities sited in the Arctic, accidents in military operations involving nuclear weapons, accidents in civilian vessel operations including refuelling, and accidents in the handling and disposal of radioactive material stored on land. It is recommended that all these sources are systematically reviewed and that the potential radiological consequences and health risks to human and marine life evaluated.

Acknowledgements

This study was made possible by the generous financial support provided under the European Commission's Nuclear Fission Safety Programme, 1995–99 (Contract No. F14P–CT95–0035).

The group would also like to express its more sincere thanks to the following institutions and individuals, who have contributed to the overall success of the ARMARA programme:

- The *Alfred Wegener Institute for Polar and Marine Research* (Bremerhaven) and, in particular, Prof. E. Augstein, for his generous invitation to participate in the ARK–XII expedition aboard the F.S. *Polarstern* in 1996.
- The *Swedish Polar Research Secretariat* (Stockholm) for their kind invitation to participate in the Arctic'96 expedition to the Central Arctic Ocean aboard the I.B. *Oden* in 1996.
- The *Arctic Monitoring and Assessment Programme*, who provided the marine platform for the Thule '97 research expedition.
- The *University of Bergen*, for their many invitations to participate in research expeditions to the Svalvard continental shelf.
- Dr. Nina V. Denisenko, for the preparation of a report entitled '*Identification of the trophic structure of Arctic invertebrates, fish and birds, and pathways of radionuclide accumulation in the Barents, Kara and White Seas*', which was of great help in the design of sampling strategies for the determination of *in situ* CF values in Arctic biota.
- The captains and crews of the following research vessels, for their support while on station: R.V. *Academic Fedorov* (Russia), F.S. *Adolf Jensen* (Greenland), R.V. *Celtic Voyager* (Ireland), R.V. *Cirolana* (United Kingdom), R.V. *Dalnie Zelenski* (Russia), R.V. *Golitsyn* (Russia), R.V. *Håkon Mosby* (Norway), R.V. *Lough Beltra* (Ireland), I/B *Oden* (Sweden), F.S. *Polarstern* (Germany), R.V. *Suroît* (France) and R.V. *Thalia* (France), R.V. *Vsevolod Berjozkin* (Russia) and R.V. *Yasnogorsk* (Russia).
- The Finnish Institute of Marine Research.
- The Finnish Game and Fisheries Research Institute.
- Dr. Gilbert Desmet (CEC) and his successor, Dr. Ernst Schulte (CEC), for their valuable support and assistance throughout the period of the project.

References

Aarkrog, A. (1971), 'Radioecological investigations of plutonium in an Arctic marine environment', *Health Phys.* **20**, 31–47.

Aarkrog, A. (1977), 'Environmental behaviour of plutonium accidentally released at Thule, Greenland', *Health Phys.* **32**, 271–284.

Aarkrog, A. (1994), 'Radioactivity in Polar regions – Main sources', *J. Environ. Radioactivity* **25**, 21–35.

Aarkrog, A. (1996), '*Radionuclides in the Greenland Marine Environment*', National Assessment Report, Risø National Laboratory.

Aarkrog, A., Dahlgaard, H., Nilsson, K. and Holm, E. (1984), 'Further studies of plutonium and americium at Thule, Greenland', *Health Phys.* **46**, 29–44.

Aarkrog, A., Boelskifte, S., Dahlgaard, H., Duniec, S., Holm, E. and Smith, J.E. (1987), 'Studies of transuranics in an Arctic marine environment', *J. Radioanal. Nucl. Chem. Art.* **115**(1), 39–50.

Aarkrog, A., Dahlgaard, H., Holm, E., Hansen, H., Lippert, J. and Nilsson, K. (1981), '*Environmental Radioactivity in Greenland in 1980*', Risø National Laboratory Report RISØ–R–449, Roskilde, Denmark, 55 pp.

Aarkrog, A., Buch, E., Chen, Q.J., Christensen, G., Dahlgaard, H., Hansen, H., Holm, E. and Nielsen, S.P. (1988), '*Environmental Radioactivity in the North Atlantic Region including the Faroe Islands and Greenland, 1986*', Risø National Laboratory Report RISØ–R–550, Roskilde, Denmark, 69 pp.

Aarkrog, A., Chen, Q.J., Clausen, J., Christensen, G., Dahlgaard, H., Ellis, K., Hansen, H., Holm, E., Joensen, H.P, Nielsen, S.P. and Strandberg, M. (1997), '*Environmental Radioactivity in the North Atlantic Region including the Faroe Islands and Greenland, 1982 and 1993*', Risø National Laboratory Report RISØ–R–757, Roskilde, Denmark, 132 pp.

Anderson, L.G. and Jones, E.P. (1992), 'Tracing upper waters of the Nansen Basin in the Arctic Ocean', *Deep Sea Res.* **39(2A)**, 425–433.

AMAP (1998), '*AMAP Assessment Report: Arctic Pollution issues*', Arctic Monitoring and Assessment Programme (AMAP), Oslo, Norway, 859 pp.

Assinder, D.J., Kelly, M. and Aston, S.R. (1984), 'Conservative and non-conservative behaviour of radionuclides in an estuarine environment, with particular respect to the behaviour of plutonium species', *Environ. Technol. Lett.* **5**, 23–30.

Bailly du Bois, P. and Guegueniat, P. (in press), 'Quantitative assessment of dissolved radiotracers in the English Channel: sources, average impact of the La Hague reprocessing plant and conservative behaviour (1983, 1986, 1988 and 1994)', *Cont. Shelf Res.*

Baskaran, M., Asbill, S., Santschi, P., Brooks, J., Champ, M., Adkinson, D., Kolmer, M.R. and Makeyev, V. (1996), 'Pu, ^{137}Cs and excess ^{210}Pb in Russian Arctic sediments', *Earth Planet. Sci. Lett.* **140**(1–4), 243–257.

Beasley, T.M. and Fowler, S.W. (1976), 'Plutonium isotope ratios in Polychaete worms', *Nature* **262**, 813–814.

Boust D., Mitchell P.I., Garcia K., Condren O., León Vintró L. and Leclerc, C.G. (1996), 'A comparative study of the speciation and behaviour of plutonium in the marine environment of two reprocessing plants', Radiochim. Acta, 74, 203–210.

Brown, J., Kolstad, A.K., Lind, B., Rudjord, A.L. and Strand, P. (1998), '*Technetium-99 contamination in the North Sea and in Norwegian coastal areas1996 and 1997*', Stralevern Report 1998:3, Statens Stravelern, Osteras, 21 pp.

Bryazgin, V.F., Denisenko, N.V., Denisenko, S.G., Kalyuzdiy, E.E. and Ryzov, V.M. (1981), 'Animals and plants of the Barents Sea', Kola Branch Academy of Science of the USSR, 189 pp.

Buesseler, K.O., Bacon, M.P., Cochran, J.K. and Livingston, H.D. (1992), 'Carbon and Nitrogen export during the JGOFS North Atlantic Bloom Experiment estimated from ^{234}Th:^{238}U disequilibria', *Deep Sea Res.* **39**, 1115–1137.

CEC (1990), 'The radiological exposure of the population of the European Community from radioactivity in North European marine waters', EUR 12483, Commission of the European Communities.

CEC (1994), 'The radiological exposure of the population of the European Community from radioactivity in the Mediterranean Sea', CEC Report XI–094/93, Commission of the European Communities.

Chartier, M. (1993), 'Radiological assessment of dumping in the Kara and Barents Seas: Design of a compartmental structure for the Arctic Ocean and surrounding oceans', CETIIS, Ivry sur Seine, France.

Chester, R. and Aston, S.R. (1981), 'The partitioning of trace metals and transuranics in sediments', In: *Techniques for Identifying Transuranic Speciation in Aquatic Environment*, International Atomic Energy Agency, Vienna, STI/PUB/613, pp. 173–193.

Cochran, J.K., Hirschberg, D.J., Livingston, H.D., Buesseler, K.O. and Key, R.M. (1995), 'Natural and anthropogenic radionuclide distributions in the Nansen Basin, Arctic Ocean: Scavenging rates and circulation timescales', *Deep Sea Res. II* **42**, 1495–1517.

Cook, G.T., Baxter, M.S., Duncan, H.J., Toole, J. and Malcomson, R. (1984), 'Geochemical association of plutonium in the Caithness environment', *Nucl. Inst. Meth. Phys. Res.* **223**, 517–522.

Cook, G.T., MacKenzie, A.B., McDonald, P. and Jones, S.R. (1997), 'Remobilization of Sellafield-derived radionuclides and transport from the North-east Irish Sea', *J. Environ. Radioactivity* **35**, 227–241.

Dahlgaard, H. (1995), 'Transfer of European coastal pollution to the Arctic: Radioactive tracers', *Mar. Poll. Bull.* **31**, 3–7.

Dahlgaard, H., Bergen, T.D.S. and Christensen, G. (1997), 'Technetium-99 and caesium-137 time series at the Norwegian coast monitored by the brown algae *Fucus vesiculosus*', *Radioprotection-Colloques* **32(C2)**, 353–358.

Dahlgaard, H., Chen, Q.J., Stürup, S., Eriksson, M., Nielsen, S.P. and Aarkrog, A. (1999), 'Plutonium isotopic ratios in environmental samples from Thule (Greenland) and the Techa River (Russia) measured by ICPMS and α spectrometry', In: *Proc. International Symposium on Marine Pollution*, Monaco, 5–9 October 1998, IAEA–TECDOC–1094, International Atomic Energy Agency, Vienna, pp. 254–259.

Eakins, J.D., Burton, P.J., Humphreys, D.G. and Lally, A.E. (1985), 'The remobilisation of actinides from contaminated intertidal sediments in the Ravenglass Estuary', In: *Proc. CEC Seminar*, Renesse, Netherlands, CEC Publ. XII/380/85EN, pp. 107–122.

EC (1995), 'Methodology for assessing the radiological consequences of routine releases of radionuclides to the environment', EUR 15760–EN, European Commission.

EC (1997), 'Evolution of the radiological situation around the nuclear reactors with spent fuel which have been scuttled in the Kara Sea', EUR 17634–EN, European Commission.

EC (1999), 'The radiological exposure of the population of the European Community to radioactivity in the Baltic Sea, Marina-Balt project', European Commission.

Ellis, K.M., Smith, J.N., Nelson, R.P., Kilius, L., MacDonald, R., Carmack, E., and Moran, S.B. (1995), 'Distribution of artificial radionuclides in the Arctic Ocean from the 1994 Arctic Ocean Section', In: *Proc. Second Int. Conference on Environmental Radioactivity in the Arctic*, Oslo, Norway, pp. 204–207.

Garcia (1996), '*Distribution et comportament du plutonium dans les eaux de la Manche et de l'estuarie de la Seine*', PhD Thesis, Universite de Paris Sud U.F.R. Scientifique d'Orsay, Paris, 323 pp.

Garcia, K., Boust, D., Moulin, V., Douville, E., Fourest, B. and Guillamont, R. (1996), 'Multiparametric investigation of the reactivity of plutonium under estuarine conditions', *Radiochim. Acta* **74**, 165–170.

Garreau, P. and Bailly du Bois, P. (1997), 'Transportation of radionuclides in Celtic Sea, a possible mechanism', *Radioprotection–Colloques* **32(C2)**, 381–385.

Germain, P., Miramand, P. and Masson, M. (1984), 'Experimental study of long-lived radionuclides transfers (americium, plutonium, technetium) between labelled sediments and Annelidae (*Nereis Diversicolor*, *Arenicola Marina*)', In: *International Symposium on the Behaviour of Long-Lived Radionuclides in the Marine Environment*, A. Cigna and Myttenaere (Eds.), Commission of the European Communities, Luxembourg, pp. 327–341.

Guéguéniat, P., Bailly du Bois, P., Gandon, R., Salomon, J.C., Baron, Y. and Leon, R. (1994), 'Spatial and temporal distribution (1987–1991) of ^{125}Sb used to trace pathways and transit times of waters entering the North Sea from the English Channel', *Estuarine Coastal Shelf Sci.* **39**, 59–74.

Guéguéniat, P., Hermann, J., Kershaw, P.J., Bailly du Bois, P. and Baron, Y. (1997), 'Artificial radioactivity in the English Channel and the North Sea', In: *Radionuclides in the Oceans: Inputs and Inventories*, P. Guéguéniat *et al.* (Eds.), Les Editions de Physique, Les Ulis Cedex A, France, Chapter 6, pp.121–154.

Hamilton, E.I., Williams, R. and Kershaw, P.J. (1991), 'The total alpha particle radioactivity for some components of marine ecosystems', In: *Radionuclides in the Study of Marine Processes*, P.K. Kershaw and D.S. Woodhead (Eds.), Elsevier, London, pp. 234–244.

Herrmann, J., Kershaw, P.J., Bailly du Bois, P. and Guegueniat, P. (1995), 'The distribution of artificial radionuclides in the English Channel, southern North Sea, Skagerrak and Kattegat, 1990–1993', *J. Mar. Sys.* **6**(5/6), 427–456.

Herrmann, J., Nies, H. and Goroncy, I. (1998), 'Plutonium in the deep layers of the Norwegian and Greenland Seas', *Rad. Prot. Dosim.* **75**, 237–245.

Holm, E., Roos, P. and Persson, R.B.R. (1991), 'Radiocaesium and plutonium in Atlantic surface waters from 73^{o}N to 72^{o}S', In: *Radionuclides in the Study of Marine Processes*, P.J. Kershaw and D.S. Woodhead (Eds.), Elsevier Science, pp. 3–11.

IAEA (1994), '*International Basic Safety Standards for Protection Against Ionizing Radiation and for the Safety of Radiation Sources*', Safety Series No. 115–I, International Atomic Energy Agency, Vienna.

IAEA (1985), 'Behaviour of radionuclides released into coastal waters', IAEA–TECDOC–329, International Atomic Energy Agency.

IAEA (1999), 'Radioactivity in the Arctic Seas', Report for the International Arctic Seas Assessment Project (IASAP), International Atomic Energy Agency, Vienna, TECDOC–1075.

Iosjpe, M., Strand, P. and Salbu, B. (1997), 'Estimations of significance of some processes for modelling of consequences from releases in the Arctic Ocean', In: *Proc. Third Int. Conf. on Environmental Radioactivity in the Arctic*, Tromsø, 1–5 June 1997, pp. 74–75.

Jefree, R.A., Carvalho, F., Fowler, S.W. and Faber-Lorda, J. (1997), 'Mechanisms for enhanced uptake of radionuclides by zooplankton in French Polynesian oligothrophic waters', *Environ. Sci. Technol.* **31**, 2584–2588.

Josefsson, D., Holm, E., Persson, B.R., Roos, P., Smith, J.N. and Kilius, L. (1995), 'Radiocaesium and ^{129}I along the Russian coast. Preliminary results from the Swedish Russian Tundra ecology expedition, 1994', In: *Proc. Second Int. Conference on Environmental Radioactivity in the Arctic*, Oslo, Norway, pp. 273–275.

Kershaw, P.J., Gurbutt, P.A., Woodhead, D.S., Leonard, K.S. and Rees, J.M. (1997), 'Estimates of fluxes of ^{137}Cs in northern waters from recent measurements', *Sci. Total Environ.* **202**, 211–223.

Kershaw, P.J., McCubbin, D. and Leonard (1999), 'Continuing contamination of North Atlantic and Arctic waters by Sellafield radionuclides', *Sci. Tot. Environ*. **237**–**8**, 119–132.

Knapinska-Skiba, D., Bojanowski, R. and Radecki, Z. (1994), 'Sorption and release of radiocaesium from particulate matter of the Baltic coastal zone', *Neth. J. Aquat. Ecol.* **28**(3–4), 413–419.

Kuznetsov, A.P. (1980), 'Bottom communities ecology of shelf zones of the World (trophic structure of sea bottom fauna)', Nauka, 244 pp.

Ledgerwood, F.K., Larmour, R.A. Mitchell, P.I., León Vintró, L. and Ryan, R.W. (1999), 'Radiocaesium, plutonium and americium partitioning and solid speciation in sized, intertidal sediments from Strangford Lough', In: *Proc. International Symposium on Marine Pollution*, Monaco, 5–9 October 1998, IAEA–TECDOC–1094, International Atomic Energy Agency, Vienna, pp. 509–510.

León Vintró, L. (1997), '*The Determination of Transuranium Isotopic Signatures in Environmental Materials and Their Application to the Study of Marine Processes*', PhD Thesis, National University of Ireland, 184 pp.

Leonard, K.S., McCubbin, D. and Lovett, M.B. (1995), 'Physico-chemical characterisation of radionuclides discharged from a nuclear establishment', *Sci. Tot. Environ.* **175**, 9–24.

Lynn, N., Timms, S, Warden, J., Mount, M., Sivintsev, Y., Yefimov, E., Gussgard, K., Dyer, R. and Sjoeblom, K.L. (1995), 'Scenarios for potential radionuclide release from marine reactors dumped in the Kara Sea', In: *Proc. International Conference on Environmental Radioactivity in the Arctic*, P. Strand and A. Cooke (Eds.), Østerås, pp. 135–138.

Nelson, D.M. and Lovett, M.B. (1981), 'Measurements of the oxidation states and concentration of plutonium in interstitial waters of the Irish Sea', In: *Impacts of Radionuclide Releases into the Marine Environment*, International Atomic Energy Agency, Vienna, pp. 105–108.

Nielsen, S.P., Iosjpe, M. and Strand, P. (1995), '*A Preliminary Assessment of Potential Doses to Man from Radioactive Waste Dumped in the Arctic Sea*', Strålevern Rapport 1995:8, Østerås, Norwegian Radiation Protection Authority, ISSN 0804–4910.

Nielsen, S.P., Iosjpe, M. and Strand, P. (1997), 'Collective doses to man from dumping of radioactive waste in the Arctic Seas', *Sci. Tot. Environ.* **202**, 135–146.

Marti, O. (1992), 'Etude de l'Ocean Mondial: modélisation de la circulation et du transport des traceurs anthropiques', PhD Thesis, University Pierre and Marie Curie, Paris.

Mitchell, P.I., Vives i Batlle, J., Downes, A.B., Condren, O.M., León Vintró, L. and Sánchez-Cabeza, J.A. (1995), 'Recent observations on the physico-chemical speciation of plutonium in the Irish Sea and the western Mediterranean', *J. Appl. Radiat. Isot.* **46**, 1175–1190.

Mitchell, P.I., León Vintró, L., Dahlgaard, H., Gascó, C. and Sánchez-Cabeza, J.A. (1997), 'Perturbation in the ^{240}Pu/^{239}Pu global fallout ratio in local sediments following the nuclear accidents at Thule and Palomares', *Sci. Total Environ*. **202**, 147–153.

Mitchell, P.I., Downes, A.B., León Vintró, L and McMahon, C.A. (in press), 'Studies of the speciation, colloidal association and remobilisation of plutonium in the marine environment', In: *2nd International Conference on Plutonium in the Environment*, Osaka, October 1999.

Miramand, P., Germain, P., and Camus, N. (1982), 'Uptake of americium and plutonium from contaminated sediments by three benthic species: *Arenicola marina*, *Corophium volutator* and *Scrobicularia plana*', *Mar. Ecol. Prog. Ser.* **7**, 59–65.

Moran, S.B., Ellis, K.M. and Smith, J.N. (1997), '^{234}Th/^{238}U disequilibrium in the Central Arctic Ocean', *Radioprotection–Colloques* **32(C2)**, 169–175.

Nielsen, S.P. (1995), 'A box model for North-East Atlantic coastal waters compared with radioactive tracers', *J. Marine Systems* **6**, 545–560.

Nielsen, S.P., Iosjpe, M. and Strand, P. (1997), 'Collective doses to man from dumping of radioactive waste in the Arctic seas', *Sci. Tot. Environ.* **202**, 135–146.

Noshkin, V.E. (1972), 'Ecological aspects of plutonium dissemination in aquatic environments', *Health Phys.* **22**, 537–549.

Noshkin, V.E. and Wong, K.M. (1981), 'Plutonium mobilization from sedimentary sources to solution in the marine environment', In: *Proc. Marine Radioecology*, 3rd Nuclear Energy Agency Meeting, Paris, 1979, pp. 165–178.

Östlund, G. (1993), 'Transport pattern of Siberian river water in the Arctic Basin', In: *Proc. International Conference on Environmental Radioactivity in the Arctic and Antarctic*, P. Strand and E. Holm (Eds.), Østeras, pp. 151–155.

Oughton, D., Børretzen, P., Mathisen, B., Salbu, B. and Tronstad, E. (1995), 'Mobilization of radionuclides from sediments: potential sources to Arctic waters', In: *Proc. International Conference on Environmental Radioactivity in the Arctic*, P. Strand and A. Cooke (Eds.), Østerås, pp. 186–190.

Persson, B.R., Holm, E., Carlsson, K.A., Josefsson, D. and Roos, P. (1995), 'The Russian–Swedish Tundra radioecology expedition, 1994', In: *Proc. Second Int. Conference on Environmental Radioactivity in the Arctic*, Oslo, Norway, pp. 266–272.

Penthreath, R.J., Harvey, B.R. and Lovett, M.B. (1986), 'Chemical speciation of transuranium nuclides discharged into the marine environment', In: *Seminar on Speciation of Fission and Activation Products in the Environment*, R.A. Bulman and J.R. Cooper (Eds.), Elsevier Applied Science, pp. 1582–1585.

Schauer, U., Muench, R., Rudels, B. and Timokhov, L. (1997), 'Impact of eastern Arctic shelf waters on the Nansen Basin intermediate layers', *J. Geophys. Res.* **102(C2)**, 3371–3382.

Shanbag, P.M. and Morse, J.W. (1982), 'Americium interaction with calcite and aragonite surfaces in seawater', *Geochim. Cosmochim. Acta* **46**, 241–246.

Smith, J.N., Ellis, K.M., Aarkrog, A., Dahlgaard, H. and Holm, E. (1994), 'Sediment mixing and burial of the ^{239,240}Pu pulse from the 1968 Thule, Greenland nuclear weapons accident', *J. Environ. Radioactivity* **25**, 135–159.

Smith, V., Ryan, R.W., Pollard, D., Mitchell, P.I. and Ryan, T.P. (1997), 'Temporal and geographical distributions of ^{99}Tc in inshore waters around Ireland following increased discharges from Sellafield', *Radioprotection–Colloques* **32(C2)**, 71–77.

Somayajulu, B.L.K., Sharma, P. and Herman, Y. (1989), 'Thorium and uranium isotopes in Arctic sediments', In: *The Arctic Seas: Climatology, Oceanography, Geology and Biology*, Y. Herman (Ed.), Van Nostrand Reinhold Co., New York, pp. 571–580.

Schultz, M.K., Burnett, W., Inn, K.G.W. and Smith, G. (1998), 'Geochemical partitioning of actinides using sequential chemical extractions: comparison to stable elements', *J. Radioanal. Nucl. Chem.* **234**(1–2), 251–256.

Strand, P., Nikitin, A., Rudjord, A.L., Salbu, B., Christensen, G., Føyn, L., Kryshev, I.I., Chumichev, V.B., Dahlgaard, H. and Holm, E. (1994), 'Survey of artificial radionuclides in the Barents Sea and the Kara Sea', *J. Environ. Radioactivity* **25**, 99–112.

Strand, P., Sickel, M., Aarkrog, A., Bewers, J.M., Tsaturov, Y. and Magnusson, S. (1996), 'Radioactive contamination of the Arctic marine environment', In: *Radionuclides in the Oceans: Inputs and Inventories*, P. Guéguéniat *et al.* (Eds.), Les Editions de Physique, Les Ulis Cedex A, France, Chapter 5, pp.95–119.

Appendix A: Publications by the ARMARA collaboration

A.1. Joint publications

Boust D., Mitchell P.I., Garcia K., Condren O., León Vintró L. and Leclerc, C.G. (1996), 'A comparative study of the speciation and behaviour of plutonium in the marine environment of two reprocessing plants', Radiochim. Acta, 74, 203–210.

Dahlgaard, H., Bergan, T.D.S. and Christensen, G.C. (1997), 'Technetium-99 and Caesium-137 time series at the Norwegian coast monitored by the brown alga *Fucus vesiculosus*', In: *Radioprotection – Colloques* **32**, C2, 353–358.

Dahlgaard, H., Eriksson, M., Ilus, E., Ryan, T.P, McMahon, C.A. and Nielsen, S.P. (1999), 'Plutonium in the marine environment at Thule, NW-Greenland, after a nuclear weapons accident', In: *Proc. 2nd Int. Symp. on Plutonium in the Environment*, Osaka, Japan, November 1999.

Dahlgaard, H., Eriksson, M., Ilus, E., Ryan, T.P., McMahon, C.A. and Nielsen, S.P. (1999), 'Plutonium in an Arctic marine environment 29 years after the Thule accident', In: 12th Meeting of the Nordic Society for Radiation Protection, Skaken, Denmark, August 1999.

Eriksson, M., Dahlgaard, H., Ilus, E., Ryan, T.P., Chen, Q.J., Holm, E. and Nielsen, S.P. (in press), 'Plutonium in the marine environment off Thule Air Base, N.W. Greenland: Inventories and distribution in sediments 29 years after the accident', In: *Proc. 4th International Conference on Environmental Radioactivity in the Arctic*, Edinburgh, September 1999.

Eyrolle, F., Arnaud, M., Delfanti, R., Papucci, C. and Salvi, S. (in press), 'Gamma-emitting radionuclide reactivity within the Rhône river mouth waters (North Western Mediterranean Sea)', In: *Proc. 4th International Conference on Environmental Radioactivity in the Arctic*, Edinburgh, September 1999.

Fisher, N.S., Fowler, S.W., Boisson, F., Carrol, J.L., Rissanen, K., Salbu, B., Sazykima, T.G. and Sjöblom, K.L. (1998), 'Radionuclide bioconcentration factors and sediment partition coefficients in Arctic Seas subject to contamination from dumped nuclear wastes'**,** *Environ. Sci. Tech.* **33**, 1979–1982.

Guéguéniat, P., Hermann, J., Kershaw, P., Bailly du Bois, P. and Baron, Y. (1996), 'Artificial radioactivity in the English Channel and the North Sea', In: *Radionuclides in the Oceans: Inputs and Inventories*, P. Guéguéniat *et al.* (Eds.), Les Editions de Physique, Les Ulis Cedex A, France, Chapter 6, pp. 121–154.

Holm, E., Carlsson, K.C., Eriksson, M., Josefsson, D., Persson, B., Roos, P., Mitchell, P.I., León Vintró, L. and McMahon, C. (1997), 'Radionuclides in the study of marine processes in the Arctic Sea', In: *Polarforsknings-sekretariatets årsbok*, E. Grönlund (Ed.), Swedish Research Polar Secretariat, Stockholm, Sweden, 96 pp.

Iosjpe, M., Strand, P. and Salbu, B. (1997), 'Estimations of significance of some processes for modelling of consequences from releases in the Arctic Ocean', In: *Proc. Third Int. Conf. on Environmental Radioactivity in the Arctic*, Tromsø, 1–5 June 1997, pp. 74–75.

Josefsson, D., Holm, E., Roos, P., Eriksson, M., Persson, B. and Smith, J.N. (submitted), 'Distribution and circulation of Chernobyl and reprocessing radioactivity in the central Arctic Ocean'.

Josefsson, D., Holm, E., Roos, P., Eriksson, M. and Aarkrog, A. (submitted), 'Transuranic elements in the waters of the Arctic Ocean shelf and interior'.

León Vintró, L., McMahon. C.A., Mitchell, P.I., Josefsson, D., Holm, E. and Roos, P. (in press), 'Transport of plutonium in surface and sub-surface waters from the Laptev Sea to the North Pole via the Lomonosov Ridge', *J. Environ. Radioactivity*.

Leonard, K.S., McCubbin, D., McMahon, C.A., Mitchell, P.I. and Bonfield, R. (1998) '^{137}Cs/^{90}Sr in the Irish Sea and adjacent waters: a source term for the Arctic', *Rad. Prot. Dosim.* **75**, 207–212.

Malyshev, S.V., Westerlund, E.A., Amundsen, I., Christensen, G.C., Drozhkon, E.G., Salbu, B., Oughton, D.H., Mokrov, Y.G., Strand, P., Bergan, T.D.S. and Romanov, G.N. (1997), 'Waste handling, releases and accidents at 'Mayak' PA – a description of sources contaminating the Techa River', In: *Proc. Third Int. Conf. on Environmental Radioactivity in the Arctic*, Tromsø, 1–5 June 1997, pp. 16–17.

McMahon, C.A., León Vintró, L., Mitchell, P.I. and Dahlgaard, H. (1999), 'Physico-chemical speciation of plutonium in Arctic shelf waters at Thule, NW Greenland'. In: *Proc. International Symposium on Marine Pollution*, Monaco, 5–9 October 1998, IAEA-TECDOC-1094, International Atomic Energy Agency, Vienna, pp. 303–304.

McMahon, C.A., León Vintró, L., Mitchell, P.I. and Dahlgaard, H. (2000), 'Oxidation state distribution of plutonium in surface and sub-surface waters at Thule, NW Greenland', *Appl. Radiat. Isot.* **52**, 697–703.

Mitchell, P.I., Vives i Batlle, J., Downes, A.B., Condren, O.M., León Vintró, L. and Sánchez-Cabeza, J.A. (1995), 'Recent observations on the physico-chemical speciation of plutonium in the Irish Sea and the Western Mediterranean', *Appl. Radiat. Isot.* **46/11**, 1175–1190.

Mitchell, P.I., Kershaw, P.J. and León Vintró, L. (1996), 'Radioactivity in the Irish Sea: Past Practices, Present Status and Future Perspectives', In: *Radionuclides in the Oceans: Inputs and Inventories*, P. Guéguéniat *et al.* (Eds.), Les Editions de Physique, Les Ulis Cedex A, France, Chapter 7, pp.155–175.

Mitchell, P.I., León Vintró, L., Dahlgaard, H., Gascó, C. and Sánchez-Cabeza, J.A. (1997), 'Perturbation in the ^{240}Pu/^{239}Pu global fallout ratio in local sediments following the nuclear accidents at Thule and Palomares', *Sci. Total Environ*. **202**, 147–153.

Mitchell, P.I., Holm, E., Papucci, C., León Vintró, L. and McMahon, C.A. (1997), 'Radioecological assessment of the consequences of contamination of Arctic waters – European Commission research update on the ARMARA project', In: *Proc. Third Int. Conf. on Environmental Radioactivity in the Arctic*, Tromsø, 1–5 June 1997.

Mitchell, P.I., Holm, E., León Vintró, L., Condren, O.M. and Roos, P. (1998), 'Determination of the ^{243}Cm/^{244}Cm ratio, by alpha spectrometry and spectral deconvolution, in environmental samples exposed to discharges from the nuclear fuel cycle', *J. Appl. Radiat. Isot.* **49**, 1283–1288.

Mitchell, P.I., Holm. E., Dahlgaard, H., Nielsen, S.P., Boust, D., Leonard, K.S., Papucci, C., Salbu, B., Strand, P., Sánchez-Cabeza, J.A., Rissanen, K., Pollard, D., Gascó, C., Christensen, G., León Vintró, L., McMahon, C.A., Herrmann, J. and Nies, H. (1999), 'Results and analysis of the ARMARA sea water intercomparison for ^{137}Cs, ^{238}Pu and ^{239,240}Pu'. In: *Proc. International Symposium on Marine Pollution*, Monaco, 5–9 October 1998, IAEA–TECDOC–1094, International Atomic Energy Agency, Vienna, pp. 530–531.

Nielsen, S.P., Iosjpe, M. and Strand, P. (1995), '*A Preliminary Assessment of Potential Doses to Man from Radioactive Waste Dumped in the Arctic Sea*', Strålevern Rapport 1995:8, Østerås, Norwegian Radiation Protection Authority, ISSN 0804–4910.

Nielsen, S.P., Iosjpe, M. and Strand, P. (1997), 'Collective doses to man from dumping of radioactive waste in the Arctic seas', *Sci. Tot. Environ.* **202**, 135–146.

Rissanen, K., Ikaheimonen, T.K., Nielsen, S.P., Matishov, D.G. and Matishov, G.G. (1997), 'Gammanuclide and plutonium concentrations in the White Sea', In: *Proc. Third Int. Conf. on Environmental Radioactivity in the Arctic*, Tromsø, 1–5 June 1997, pp. 222–224.

Ryan, T.P., Dahlgaard, H., Ilus, E., Brogan, C. Rafferty, B. and Eriksson, M. (submitted), 'Some observations on the horizontal and vertical distribution of plutonium, americium and caesium in sediment at a contaminated zone in Bylot Sound, Thule (Greenland)'.

Ryan, T.P., Dahlgaard, H., Dowdall, A.M., Pollard, D., Ilus, E., Eriksson, M. and Cunningham, J.D. (1999), 'The uptake of plutonium by some marine invertebrates in a contaminated zone of Bylot Sound, Thule, northern Greenland', In*: Proc. Fourth Int. Conf. On Environmental Radioactivity in the Arctic*, Edinburgh, September 1999.

Salbu, B., Malyshev, S.V., Westerlund, E.A., Romanov, G.N., Strand, P., Christensen, G.C., Amundsen, I., Oughton, D.H., Bergan, T.D.S., Drozhko, E.G., Mokrov, Y.G. and Glagolenko, Y.V. (1997), 'Radioactive contamination in the Mayak PA area – Results from the joint Russian–Norwegian field work in 1994', In: *Proc. Third Int. Conf. on Environmental Radioactivity in the Arctic*, Tromsø, 1–5 June 1997, pp. 18–20.

Salbu, B., Bjørnstad, H.E., Sværen, I., Prosser, S.L., Bulman, R.A., Harvey, B.R. and Lovett, M.B. (1997), 'Size distribution of radionuclides in nuclear fuel reprocessing liquids after mixing with seawater', Sci. Tot. Environ. **130/131**, 51–63.

Sánchez-Cabeza, J.A., Merino, J., Schell, W.R. and Mitchell, P.I. (1995), 'Transuranic accumulation in plankton from the Spanish Mediterranean coastal environment', *Rapp. Comm. int. Mer Médit.*, **34**, 231.

Sánchez-Cabeza, J.A., Merino, Mitchell, P.I., León Vintró, L., Cross, Ll. and Calbet, A. (submitted), 'Transuranic uptake by marine plankton in the western Mediterranean Sea', *Environ. Sci. Technol.*

Smith, V., Ryan, R. W., Pollard, D., Mitchell, P.I. and Ryan, T.P. (1997), 'Temporal and geographical distributions of ^{99}Tc in inshore waters around Ireland following increased discharges from Sellafield', *Radioprotection – Colloques* **32**(C2), 71–78.

Strand, P., Sickel, Aarkrog, A., Bewers, J.M., Tsaturov, Y. and Magnusson, S. (1996), 'Radioactive contamination of the Arctic marine environment', In: *Radionuclides in the Oceans: Inputs and Inventories*, P. Guéguéniat *et al.* (Eds.), Les Editions de Physique, Les Ulis Cedex A, France, Chapter 5, pp. 95–119.

Strand, P., Balonov, M., Aarkrog, A, Bewer, M., Howard, B., Salo, A. and Tsaturov, Y. (1997), 'Radioactive contamination in the Arctic', In: *Proc. Third Int. Conf. on Environmental Radioactivity in the Arctic*, Tromsø, 1–5 June 1997, pp. 5–9.

A.2. Other publications by contractors/associated contractors

Aarkrog, A. (1997), 'Doses to the Arctic population', In: *Proc. Third Int. Conf. on Environmental Radioactivity in the Arctic*, Tromsø, 1–5 June 1997, pp. 113–114.

Antón Mateos, Ma. Paz (1998), '*Dinámica sedimentaria de radionucleidos de vida larga en el litoral Mediterráneo Español*', PhD Thesis, Universidad Complutense de Madrid, 272 pp.

Antón M.P., Gascó, C. and Pozuelo, M. (1995). 'Chemical partitioning of plutonium and americium in sediments from the Palomares marine ecosystem', *Rapp. Comm. Int. Mer Med.* **34**, 223.

Bailly du Bois, P. (1996), 'Mapping of water masses in the North Sea using radioactive tracers', *Endeavour* **20**(1), 2–7.

Bailly du Bois, P. (1996), 'Quantitative assessment of dissolved radiotracers in the English Channel: sources, average impact of La Hague reprocessing plant and conservative behaviour (1983, 1986, 1988 and 1994)', *Fluxmanche II Final Report*.

Bailly du Bois, P., Rozet, M., Thoral, K. and Salomon, J.C. (1997), 'Improving knowledge of water-mass circulation in the English Channel using radioactive tracers', *Radioprotection – Colloques* **32** (C2), 63–69.

Balonov, M. and Strand, P. (1997), 'Contamination of the Arctic and local population exposure caused by major accidents', In: *Proc. Third Int. Conf. on Environmental Radioactivity in the Arctic*, Tromsø, 1–5 June 1997, pp. 115–117.

Børretzen P., Salbu, B. and Oughton, D.H. (1997), 'Speciation and binding of radionuclides in Abrosimov and Stepovogo Fjord sediments', In: *Proc. Third Int. Conf. on Environmental Radioactivity in the Arctic*, Tromsø, 1–5 June 1997, pp. 76–80.

Bohrmann, H. (1991), 'Radioisotopenstratigraphie, sedimentologie ind geochemie jungquartärer sedimente des östlichen Arktishen Ozeans', *Berichte zur Polarforschung*, Alfred Wegener Institute, Bremerhaven.

Boust, D., Bailly du Bois, P., Leclerc, G., Quillard, R.J., Rozet, M. and Solier, L. (1996), 'Distribution and inventory of some naturally-occurring and artificial radionuclides in coarse-grained sediments of the Channel', *Fluxmanche II Final Report*.

Boust, D., Bailly du Bois, P., Leclerc, G. and Solier, L. (in preparation), 'Distribution and inventory of some naturally-occurring and artificial radionuclides in coarse-grained sediments of the Channel', *Continental and Shelf Science Special Issue*.

Brown, J.E., Kolstad, A.K., Lind, B., Rudjord, A.L. and Strand, P. (1998), 'Technetium-99 contamination in the North Sea and in Norwegian coastal areas, 1996 and 1997', Strålevern Rapport 1998:3, Østerås, Norway.

Brown, J.E., Kolstad, A.K., Brungot, A.L., Lind, B., Rudjord, A.L. and Strand, P. (1999), 'Levels of ^{99}Tc in seawater and biota samples from Norwegian coastal waters and adjacent seas', *Mar. Poll. Bull*. **28**(7), 560–571.

Christensen, G. C., Bergan, T.D.S., Berge, D., Bækken, T. and Varskog, P. (1997), 'A study of fresh water sediments in marine environment', In: *Proc. Third Int. Conf. on Environmental Radioactivity in the Arctic*, Tromsø, 1–5 June 1997, pp. 186–188.

Christensen, G. C. and Selnaes, T. D. (1995), 'Study of marine radioactivity along the Norwegian Coast, 1980–1994', In: *Environmental Impact of Radioactive Releases*, International Atomic Energy Agency, Vienna, pp. 618–622.

Condren, O.M. (1998), '*Plutonium, Americium and Radiocaesium in the Western Irish Sea: Origin, Bioavailability and Ultimate Fate*', PhD Thesis, National University of Ireland, 157 pp.

Dahlgaard, H., Chen, Q.J., Stürup, S., Eriksson, M., Nielsen, S.P. and Aarkrog, A. (1999), 'Plutonium isotopic ratios in environmental samples from Thule (Greenland) and the Techa River (Russia) measured by ICPMS and α spectrometry', In: *Proc. International Symposium on Marine Pollution*, Monaco, 5–9 October 1998, IAEA–TECDOC–1094, International Atomic Energy Agency, Vienna, pp. 254–259.

Delfanti, R., Papucci, C., Cedrola, P. and Gheddou, A. (1997), 'Scavenging rates and residence times of particles in the continental shelf of W-Svalbard, estimated from the disequilibrium ^{234}Th/^{238}U', In: *Proc. Third Int. Conf. on Environmental Radioactivity in the Arctic*, Tromsø, 1–5 June 1997.

Delfanti R., Frignani, M., Langone, L., Papucci, C. and Ravaioli, M.A. (1997), 'The role of the rivers in Chernobyl radiocaesium delivery: distribution and accumulation in coastal sediments

of the Northern Adriatic Sea', In: *Freshwater and Estuarine Radioecology*, Desmet *et al.* (Eds.), Elsevier, Amsterdam, pp. 235–240.

Dethleff, D., Nies, H., Harms, I.H., Karcher, M.J. and Strand, P. (1997), 'Sea-ice as transport agent for potentially radioactively contaminated sediment from Kara Sea dumping sites to the North Atlantic', In: *Proc. Third Int. Conf. on Environmental Radioactivity in the Arctic*, Tromsø, 1–5 June 1997, pp. 197–199.

Emerson, H.S., McCubbin, D. and Leonard, K.S. (1999), 'Influence of photochemical reactions upon the redox cycling of Pu between the solid and liquid phases in seawater', In: 8th Int. Symp. on Environmental Radiochemical Analysis, Blackpool, U.K., G.W.A. Newton (Ed.), Royal Society of Chemistry, pp. 88–96.

Gascó C., Antón M.P., Espinosa A., Aragón A., Alvarez A., Navarro N. and García-Toraño E. (1997). 'Procedures to define Pu isotopic ratios characterizing a contaminated area in Palomares (Spain)', *J. Radioanal. Nucl. Chem.* **222**(1–2), 81–86.

Garreau, H. and Bailly du Bois, P. (in press), 'Transportation of radionuclides in the Celtic Sea : a possible mechanism', *Radioprotection – Colloques* **32** (C2), 381–385.

Holm, E., Carlsson, K.-C., Josefsson, D. and Persson, B. (1995), 'Tundra Radioecology –94', In: *Swedish-Russian Tundra Ecology-Expedition –94, A Cruise Report*, E Grönlund and Olle Melander, Swedish Research Polar Secretariat, Stockholm, Sweden.

Holm, E., Roos, P., Josefsson, D., and Persson, B. (1996), 'Radioactivity from the North Pole to the Antarctic', In: *Radionuclides in the Oceans: Inputs and Inventories*, P. Guéguéniat *et al.* (Eds.), Les Editions de Physique, Les Ulis Cedex A, France, Chapter 3, pp. 59–74.

Howard, B. and Strand, P. (1997), 'Radiological vulnerability in the Arctic', In: *Proc. Third Int. Conf. on Environmental Radioactivity in the Arctic*, Tromsø, 1–5 June 1997, pp. 36–37.

Ikäheimonen, T.K., Rissanen, K., Matishov, D., Matishov, G. (1997), 'Plutonium in fish, algae and sediments in the Barents, Petshora and Kara Seas', *Sci. Tot. Environ*. **202**, 79–87.

Iosjpe, M. and Strand, P. (1998), 'Some aspects of modelling of radiological consequences from releases into the marine environment. The state and use of science and predictive models', In: First Int. Symp. on the State and Use of Science and Predictive Models, Denver, USA, August 1998, ISA.

Iosjpe, M. and Strand, P. (1999), 'Influence of time and space resolution on dispersion of radionuclides and radiological assessment in the marine environment', In: *Proc. International Symposium on Marine Pollution*, Monaco, 5–9 October 1998, IAEA–TECDOC–1094, International Atomic Energy Agency, Vienna, pp. 366–367.

Josefsson, D. (1998), '*Anthropogenic Radionuclides in the Arctic Ocean – Distribution and Pathways*', PhD Thesis, University of Lund, 159 pp.

Josefsson, D., Holm, E., Persson, B., Roos, P., Smith, J.N. and Kilius, L. (1995), 'Radiocaesium and ^{129}I along the Russian coast. Preliminary results from the Swedish Russian Tundra Ecology expedition 1994', In: *Environmental Radioactivity in the Arctic*, P. Strand and A. Cooke (Eds.), Oslo, 21–25 August 1995, Norwegian Radiation Protection Authority, pp. 273–275.

Josefsson, D., Holm, E., Persson, B. and Roos, P. (1995), 'Anthropogenic radioactivity along the Russian coast. Preliminary results from the Swedish Russian Tundra Ecology expedition 1994', In: *Proc. Arctic Nuclear Waste Assessment Program Workshop*, Woods Hole, Massachusetts, 1–4 May 1995.

Josefsson, D., Holm, E., Persson, B., Roos, P. and Eriksson, M. (1997), '^{137}Cs and ^{134}Cs in the Arctic Ocean. Preliminary Results from the Swedish Arctic Ocean '96 Expedition', In: *Proc. Third Int. Conf. on Environmental Radioactivity in the Arctic*, Tromsø, 1–5 June 1997, pp. 208–210.

Josefsson, D., Holm, E., Roos, P., Persson, B. and Smith, J.N. (submitted), 'Radiocaesium,, ^{90}Sr and ^{129}I in the eastern Arctic shelf seas'.

Kershaw, P.J., Gurbutt, P. A., Woodhead, D. S, Leonard, K. S. and Rees, J. M. (1997), 'Estimates of fluxes of ^{137}Cs in northern waters from recent measurements', *Sci. Total Environ.* **202**, 211–223.

Kershaw, P.J., Leonard, K.S. and McCubbin, D. (1997), 'Continuing contamination of Arctic waters by European reprocessing wastes?', In: *Proc. Third Int. Conf. on Environmental Radioactivity in the Arctic*, Tromsø, 1–5 June 1997, pp. 106–107.

Kershaw, P.J., McCubbin, D. and Leonard, K.S. (in press), 'Continuing contamination of North Atlantic and Arctic waters by Sellafield radionuclides', *Sci. Tot. Environ.*

Ledgerwood, F.K., Larmour, R.A., Mitchell, P.I., León Vintró, L. and Ryan, R.W. (1999), 'Radiocaesium, plutonium and americium partitioning and leachability in size-fractionated, inter-tidal sediments from Strangford Lough'. In: *Proc. International Symposium on Marine Pollution*, Monaco, 5–9 October 1998, IAEA–TECDOC–1094, International Atomic Energy Agency, Vienna, pp. 509–510.

León Vintró, L. (1997), '*The Determination of Transuranium Isotopic Signatures in Environmental Materials and Their Application to the Study of Marine Processes*', PhD Thesis, National University of Ireland, 184 pp.

León Vintró, L., McMahon, C.A. and Mitchell, P.I. (1997), 'Assessing the long-term consequences of nuclear dumping in the Arctic', The Irish Scientist **5**, p. 113.

Leonard, K. S., McCubbin, D., Brown, J., Bonfield , R. and Brooks, T. (1997), 'A summary report of the distributions of ^{99}Tc in UK coastal waters', *Radioprotection – Colloques* **32**(C2), 109–114.

Leonard, K. S., McCubbin, D., Brown, J., Bonfield , R. and Brooks, T. (1997), 'Distribution of Technetium-99 in UK coastal waters', *Mar. Pollut. Bull.* **34**(8), 628–636.

Leonard, K.S., McCubbin, D., Emerson, H.S. and Bonfield, R. (1999), 'The behaviour of ^{99}Tc in UK waters, 1995–1996', In: *Proc. International Symposium on Marine Pollution*, Monaco, 5–9 October 1998, IAEA–TECDOC–1094, International Atomic Energy Agency, Vienna, pp. 389–390.

Leonard, K.S., McCubbin, D., Blowers, P. and Taylor, B.R. (1999), 'Dissolved plutonium and americium in surface waters of the Irish Sea, 1973–1996', J. Environ. Radioactivity **44**, 129–158.

Long, S., Pollard, S., Hayden, E., Smith, V., Fegan, M., Ryan, T.P., Dowdall, A. and Cunningham, J.D. (1998), 'Radioactivity monitoring of the Irish marine environment, 1996 and 1997', RPII–98/2, Radiological Protection Institute of Ireland, 43 pp.

McCubbin, D. and Leonard, K.S. (1996), 'Photochemical dissolution of radionuclides from marine sediment', *Mar. Chem.* **55**(3–4), 399–408.

McCubbin, D. and Leonard, K.S. (1997), 'Temporal variations and behaviour of radionuclides in a shoreline location', *Radioprotection – Colloques* **32**(C2), 197–204.

McCubbin, D., Emerson, H.S. and Leonard, K.S. (1999), 'The role of thermal and photochemical reactions upon the remobilisation of Pu from an Irish sediment', *J. Environ. Radioactivity* **44**, 253, 273.

Merino J. (1997), '*Estudios sobre el ciclo del plutonio en ecosistemas acuáticos*', PhD Thesis, Universitat Autònoma de Barcelona, 355 pp.

Merino, J., Sánchez-Cabeza, J.A., Molero, J. and Masqué, P. (1998), 'Estudio sobre el ciclo del plutonio en ecosistemas marinos', *Radioproteccion* **18**, 83–91.

Mitchell, P.I. (1999), 'Radiological assessment of the consequences of contamination of Arctic waters – Update on the progress of the EC–supported ARMARA project', In: *Proc. International Symposium on Marine Pollution*, Monaco, 5–9 October 1998, IAEA–TECDOC–1094, International Atomic Energy Agency, Vienna, pp. 260–261.

Mitchell, P.I. (1999), 'Arctic marine radioecology', In: *Proc. 11th International Congress on Radiation Research*, Dublin, July 1999.

Mitchell, P.I., McMahon, C.A., León Vintró, L. and Ryan, R.W. (1998) 'Plutonium in Arctic surface and sub-surface waters at the St. Anna/Voronin Trough', *Rad. Prot. Dosim.* **75**, 247–252.

Mitchell, P.I., Condren, O.M., León Vintró, L. and McMahon, C.A. (1999), 'Trends in plutonium, americium and radiocaesium accumulation and long-term bioavailability in the western Irish Sea mud basin', *J. Environ. Radioactivity* **44**, 223–251.

Mitchell, P.I., Downes, A.B., León Vintró, L and McMahon, C.A. (in press), 'Studies of the speciation, colloidal association and remobilisation of plutonium in the marine environment', In: *2nd International Conference on Plutonium in the Environment*, Osaka, October 1999.

Mordeglia, B. (1998), '*Ciclo dei radionuclidi in ambiente marino: applicazione allo studio della dinamics delle particelle nell'Oceano Artico*', Tesi di Laurea, University of Milan, 92 pp.

Nielsen, S.P. (1998), 'A sensitivity analysis of a radiological assessment model for Arctic waters', *Rad. Prot. Dosim*. **75**, 213–218.

Nies, H. and Nielsen, S.P. (1996), 'Radioactivity in the Baltic Sea', In: *Radionuclides in the Oceans: Inputs and Inventories*, P. Guéguéniat *et al.* (Eds.), Les Editions de Physique, Les Ulis Cedex A, France, Chapter 10, pp. 219–231.

Nyffeler, F., Cigna, A.A., Dahlgaard, H. and Livingston, H.D. (1996), 'Radionuclides in the Atlantic Ocean: a survey', In: *Radionuclides in the Oceans: Inputs and Inventories*, P. Guéguéniat *et al.* (Eds.), Les Editions de Physique, Les Ulis Cedex A, France, Chapter 1, pp.1–28.

Oughton, D.H., Salbu, B., Skipperud and Tronstad, E. (1997) 'Source term influence on the mobility of radionuclides in soil', In: *Proc. Third Int. Conf. on Environmental Radioactivity in the Arctic*, Tromsø, 1–5 June 1997, pp. 68–70.

Oughton, D.H., Børrezen, P., Salbu, B. and Tronstad, E. (1997), 'Mobilization of ^{137}Cs and ^{90}Sr from sediments: potential sources for Arctic waters', Sci. Tot. Environ. **202**, 155–165.

Oughton, D.H., Skipperud, L., Salbu, B., Fifield, K., Cresswell, R.C. and Day, J.P. (1999), 'Determination of ^{240}Pu/^{239}Pu isotope ratios in Kara Sea and Novaya Zemlya sediments using accelerator mass spectrometry', In: *Proc. International Symposium on Marine Pollution*, Monaco, 5–9 October 1998, IAEA–TECDOC–1094, International Atomic Energy Agency, Vienna, pp. 123–128.

Papucci, C., Delfanti, R. and Mordeglia, B. (1998), 'Radionuclides as tracers of particle dynamics in the W-Svalvard marine environment', In: *The Arctic and Global Change*, NySMAC Publication No. 007, pp. 185–192.

Papucci, C., Delfanti, R. and Torricelli, L. (in press), 'Scavenging and sedimentation processes in the marine environment of the Svalvard islands', In: *Proc. Fourth International Conference on Radioactivity in the Arctic*, Edinburgh, September 1999.

Pöllänen, R., Klemola, S., Ikäheimonen, T.K., Rissanen, K., Juhanoja, J., Paavolainen, S. and Likonen, J. (submitted), 'Analysis of radioactive particles from Kola Bay', *J. Appl. Radiat. Isot.*

Pollard, D., Long, S., Hayden, E., Smith, V., Ryan, T.P., Dowdall, A., Cunningham, J.D. and McGarry, A. (1996), '*Radioactivity Monitoring of the Irish Marine Environment, 1993–1995*', Radiological Protection Institute of Ireland, Dublin, 41 pp.

Pollard, D., Ryan T.P. and Dowdall, A. (1998), 'The dose to Irish seafood consumers from ^{210}Po', *Radiat. Prot. Dosim.* **75** (1–4), 139–142.

Rissanen, K. and Ikäheimonen, T.K. (in press), 'Caesium and plutonium concentrations in salmon caught in River Teno (Norwegian Sea) and in River Tornionjoki (Gulf of Bothnia)', Proc. Marina-Balt Seminar, June 1998, Stockholm, Sweden.

Rissanen, K., Ikäheimonen, T.K., Matishov, D.G. and Matishov, G.G. (1997), 'Radioactivity levels in fish, benthic fauna, seals and sea bird collected in the northwest Arctic of Russia', *Radioprotection – Colloques* **32** (C2), 323–331.

Rissanen, K., Ikäheimonen, T.K., Matishov, D.G. and Matishov, G.G. (1998), 'Radioactivity levels in Kola Bay', *Rad. Prot. Dosim*. **75**, 223–228.

Rissanen, K., Ikäheimonen, T.K., Matishov, D.G. and Matishov, G.G. (1998), 'Plutonium concentrations in Russian Arctic Seas', In: *Proc. Int. Seminar Afterword to the White Book (Yablokov Commission)*, January 1998, Nizhny Novgorod, Russia, International Science and Technology Center, pp. 160–171.

Rissanen, K., Ikäheimonen, T.K., Matishov, D.G. and Matishov, G.G. (1999), 'Radioactive caesium, cobalt and plutonium in biota, algae and sediments in the nonrestricted areas of the Russian Arctic Seas', In: *Proc. International Symposium on Marine Pollution*, Monaco, 5–9 October 1998, IAEA–TECDOC–1094, International Atomic Energy Agency, Vienna, pp. 311–312.

Rissanen, K., Ikäheimonen, T.K., Matishov, D.G. and Matishov, G.G. (1999), 'Radionuclide concentrations in sediment, soil and plant samples from the archipelago of Franz Joseph Land, an area affected by the Chernobyl fallout', In: *Proc. 4th International Conference on Environmental Radioactivity in the Arctic*, Edinburgh, September 1999.

Rissanen, K., Pempkowiak, J., Ikäheimonen, T.K., Matishov, D.G. and Matishov, G.G. (1999), '^{137}Cs, ^{239,240}Pu, ^{90}Sr and selected metal concentrations in organs of Greenland seal pups in the White Sea area', In: *Proc. 4th International Conference on Environmental Radioactivity in the Arctic*, Edinburgh, September 1999.

Rissanen, K., Ikäheimonen, T.K., Matishov, D.G. and Matishov, G.G. (submitted), 'Radioactivity levels in Kola Bay', *Radiat. Prot. Dosim.* **75** (1–4), 223–228.

Roos, P., Holm, E., Josefsson, D., Hulth, S. and Hall, P. (1995), 'Distribution and inventories of ^{239,240}Pu, ^{241}Am, ^{210}Pb and ^{137}Cs in sediments around Svalbard', In: *Environmental Radioactivity in the Arctic*, P. Strand and A. Cooke (Eds.), Oslo, 21–25 August 1995, Norwegian Radiation Protection Authority, pp. 250–253.

Ryan, T.P. (1996), '*Actinide Bio-kinetics in Marine Invertebrates - A Review*', Radiological Protection Institute of Ireland, Technical Document submitted to the EC as part of the ARMARA programme.

Ryan, T.P. (1999), 'Transuranic bio-kinetic parameters for marine invertebrates – a review', *Environment International* (accepted for publication).

Ryan, T.P., Dowdall, A.M. and McGarry, A.T. (1997), 'Polonium-210 uptake by *Mytilus edulis* (l.) in Irish estuarine and inshore waters', In: *Freshwater and Estuarine Radioecology.* G. Desmet *et al.* (Eds.), Elsevier Science, pp. 419–424.

Ryan, T.P., Dowdall, A.M., McGarry, A.T., Pollard, D. and Cunningham, J.D. (1999), 'Polonium-210 in *Mytilus edulis* in the Irish marine environment', *J. Environ. Radioactivity* **43**, 325–342.

Ryan, T.P., Dowdall, A.M., Long, S., Smith, V., Pollard, D. and Cunningham, J.D. (1999), 'Plutonium and americium in fish, shellfish and seaweed in the Irish environment and their contribution to dose', *J. Environ. Radioactivity* **44**, 349–369.

Ryan, T.P., Long, S., Smith, V., Dowdall, A.M., Pollard, D. and Cunningham, J.D. (1999), 'Plutonium-241 and its progeny in Sellafield discharges to the Irish Sea and their impact on the Irish environment', In: *Proc. 11th International Congress on Radiation Research*, Dublin, July 1999.

Ryan, T.P., Dowdall, A.M., Long, S., Rafferty, B., Pollard, D. and Cunningham, J.D. (submitted), 'Uptake of plutonium and americium by some sediment dwelling marine invertebrates in the Irish Sea', *J. Radiol. Prot.*

Salbu, B. and Børretzen, P. (1997), 'Marine sediments as a sink, and contaminated sediments as a diffuse source of radionuclides', *Radioprotection – Colloques* **32**, C2, p. 56 (Abstract).

Salomon, J.C., Breton, M., Guéguéniat, P. (1996), 'A 2D long term advection-dispersion model for the Channel and southern North Sea. Part B: Transit and transfer function from Cap de La Hague', *J. Mar. Systems* **6**, 515–527.

Scott, E.M., Gurbutt, P., Harms, I., Heling, R., Kinehara, Y., Nielsen, S.P., Osvath, I., Sazykina, T., Wada, A. and Sjoeblom, K.L. (1997), 'Radiological assessment of dumped waste in the Kara Sea', In: *Proc. Third Int. Conf. on Environmental Radioactivity in the Arctic*, Tromsø, 1–5 June 1997, pp. 26–27.

Trapeznikov, A., Pozolotina, V., Aarkrog, A., Nielsen, S.P., Yushkov, P., Trapeznikova, V., Chebotina, M., Molchanova, I., and Karavaeva, E. (1997), 'Up-to-date radioecological studies of the Techa and Iset Rivers (Ob-Irtysh Basin) contaminated form 'MAYAK' Plant', In: *Proc. Third Int. Conf. on Environmental Radioactivity in the Arctic*, Tromsø, 1–5 June 1997, pp. 233–234.

Varskog, P., Christensen, G.C. and Bergan, T.D. (1997), 'Potential transport of radionuclides from the Mayak Region', In: *Proc. Third Int. Conf. on Environmental Radioactivity in the Arctic*, Tromsø, 1–5 June 1997, pp. 71.